Performance and Feasibility Assessment of Porous Radiant Burner Aided Cook-stoves for LPG, Biogas and Waste Cooking Oil Fuels

A thesis submitted in partial fulfillment of the requirements for the degree of

Doctor of Philosophy

by

Lav Kumar Kaushik

(Roll No: 146103031)

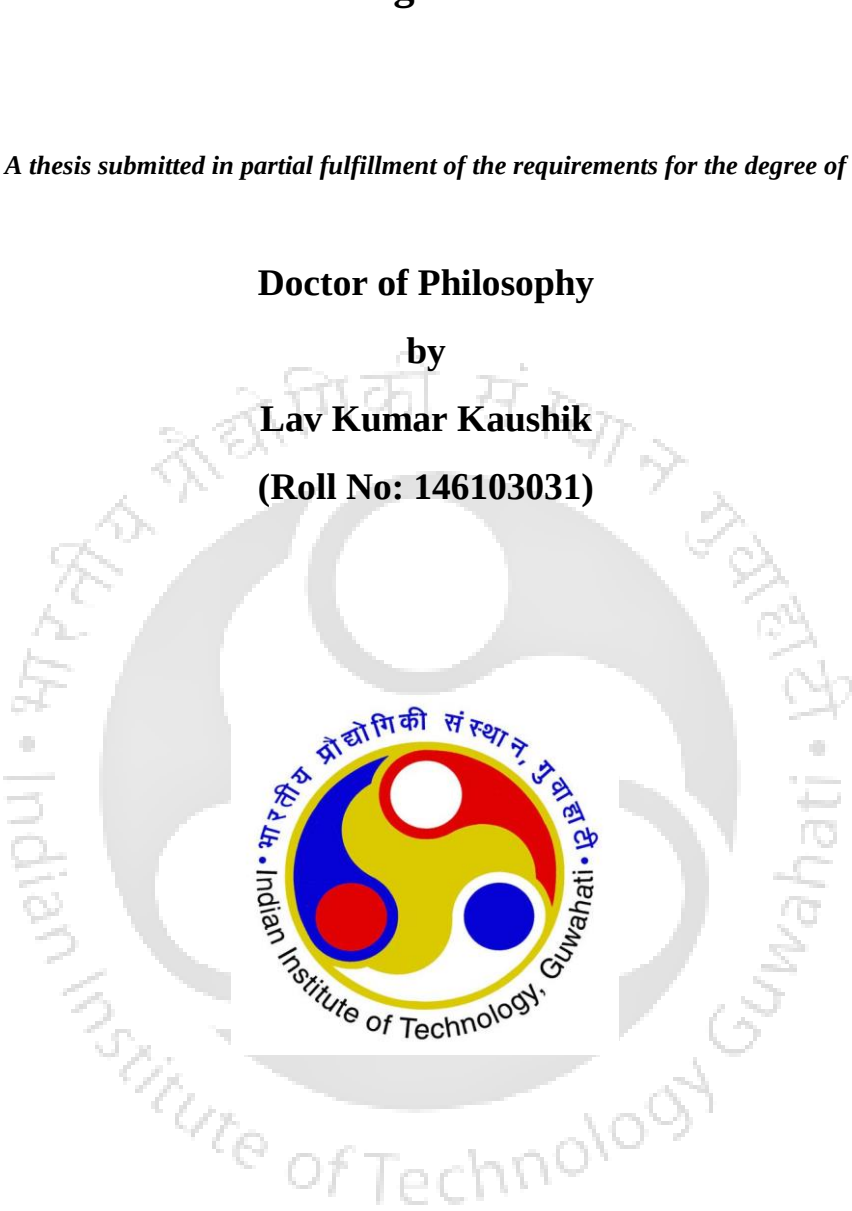

Department of Mechanical Engineering

Indian Institute of Technology Guwahati

Guwahati – 781039, India

September, 2019

Department of Mechanical Engineering

Indian Institute of Technology Guwahati

Guwahati – 781039, India

THESIS CERTIFICATE

It is certified that the work contained in the thesis entitled **Performance and Feasibility Assessment of Porous Radiant Burner Aided Cook-stoves for LPG, Biogas and Waste Cooking Oil Fuels** by **Lav Kumar Kaushik**, a student in the Department of Mechanical Engineering, Indian Institute of Technology Guwahati, India, for the award of the degree of the **Doctor of Philosophy** has been carried out under my supervision and that this work has not been submitted elsewhere for the degree.

Dr. P. Muthukumar

Professor

Department of Mechanical Engineering

Indian Institute of Technology Guwahati

Guwahati – 781039, Assam, India.

Dedicated to

My Family and friend

Acknowledgement

I am deeply indebted to my thesis supervisor, **Prof. P. Muthukumar**, for his invaluable guidance and steady encouragement throughout my Ph.D. program. The vigor and attention bestowed by him in taking my research ahead in difficult times will never be forgotten. Starting from framing the problems to the final experimental results and their physical interpretations, he remained deeply involved in my thesis work. He provided me with the most innovative ideas that were very helpful in completing the present thesis. I have immensely benefited from every moment of my association with him. I am highly inspired by his intellectual prowess and exemplary professionalism. I enjoyed every moment working under his supervision and learned a lot of things from him, which will be an asset for my future research.

I wish to express my deep gratitude to ***(Late) Dr. Subhash C. Mishra***, who provided opportunity to work on this topic. On critical personal decisions his "***Dharmic way of life***" provided clarity and encouraged me throughout my Ph.D. program. I will try to keep that in all my life.

I wish to express my deep gratitude to all those who have helped me in various ways during the tenure of my Ph.D. work at IIT Guwahati. I have been supported and accompanied by many people, and each one has played an indispensable role during my work. I am grateful to all of them.

I am thankful to my Doctoral Committee members, Prof. Niranjan Sahoo, Dr. Amaresh Dalal and and Dr, V Prabu for their valuable suggestions and encouragement during the period of my research work.

I specially thank Mr. D. Chetri, Mr. M. Sarma, Mr. J. Basumatary and Mr. G. Das for their help during the course of fabrication of the setup and also their assistance when needed during my experimental studies.

I am thankful to Sangjukta Devi, Saiparneeth Gauravaraju, and Vishal Agrawal, with whom I had healthy discussions and they made my stay memorable one at IIT Guwahati.

I also extend my gratefulness to my lab mates Sunita Deb, R. Nithin Narmada, J. Sunku Prasad, Alok Kumar, Sureandhar Gunasekaran, Jasinta P. Ekka, Pratibha Maurya, Arunkumar Mahalingam, Pratap Chandra Das, Najrul Haque.

The authors are thankful to the MHRD for their financial help vide IMPRINT project No. 6727.

I venerate my parent's patience, wishes and enormous trust repose in my abilities at all times.

Lav Kumar Kaushik

Abstract

Currently, 3 billion people lack access to clean-cooking and are exposed to dangerous levels of air pollution. In highly populated and energy deficit nations, the cooking sector plays a decisive role in achieving Sustainable Development Goals (SDGs). One vital goal in Sustainable Development Goals (SDG) 7 is to ensure the usage of clean cooking fuel to 100% households by 2030. India's cooking scenario indicates that only 43.8% of households use clean cooking fuel. In the case of cooking, availability of fuel, access to modern infrastructure, household location, education, and income are the key factors that influence the choice of fuel. Fuel stacking is a common practice in India, where the households depend on more than one fuel for cooking. Therefore, it is important to emphasize that new clean cooking solutions need to focus on more than one cooking fuel and technology combinations. Also, new development towards cleaner cook-stove has to resemble the existing cooking practices, for example, a natural draft improved cook-stove along with cooking fuels viz., LPG, biogas, CNG, etc. This has thus necessitated the need to search for alternative sources for cooking energy, and also design modifications in the existing cook-stoves.

Commercially available gaseous and liquid fuel cook-stoves in India are characterized by Free Flame Combustion (FFC) in which the combustion takes place in open air environment, and convection is the main mode of heat transfer. In conventional cook-stoves, contributions of conduction and radiation, from the post flame to pre-flame zone is insignificant. Thus, due to poor heat transport, these cook-stoves are less efficient, and they have undesirable features such as low flammability limits, low power density, high level of pollutant emissions, etc.

Research works reported on the development of energy efficient cook-stoves can be broadly categorised in two categories. The first one, in which the combustion technology remains the same (i.e. FFC), but the design of cook-stoves is modified to get improved efficiency and cleaner combustion. The other includes the use of Porous Media Combustion (PMC) technology, in which instead of combustion in the gaseous environment, like in the FFC, fuel is made to combust in a highly conducting and radiating porous matrix. Owing to enhanced heat transfer, thermal efficiency goes up, and emissions of CO and NO_x comes down. PMC utilizes the principle of excess

enthalpy combustion in which the preheating of fuel-air mixture enables even lean mixture and low calorific value fuel to be combusted. This preheating in the porous matrix is realized due to the manifestation of the volumetric thermal radiation. Apart from preheating of the incoming fuel-air mixture, PMC elongates reaction zone and homogenizes the temperature. All these lead to higher thermal efficiency and reduced emissions.

Considerable experimental and numerical studies have been performed for analysing the performance of the various combustion systems by employing different ceramic materials, fuels, and operating conditions. Recently naturally aspirated cook-stoves with Porous Radiant Burners (PRBs) were developed using LPG and kerosene for domestic as well as medium scale cooking applications. It was observed that the commercial applicability and detailed cooking performance assessment of these developed cook-stoves were lacking. It was also observed from the literature that no research works were carried out on the development of naturally aspirated cook-stove with PRBs for alternate cooking fuels viz., biogas, and waste cooking oil. This necessitated the need to search for design modifications in the developed LPG cook-stoves with PRB for its commercialization, and also to develop cook-stoves for biogas and waste cooking oil as alternative options.

In view of the above, the following core objectives are chosen for this thesis work;

- To demonstrate PRB based cook-stove as potential alternative to their conventional counterpart's.
    - To analyze the impact of PRB on daily heat energy requirement per household by performing Control Cooking Test (CCT).
    - To investigate PRBs ability to reduce environmental burden of a typical life cycle of LPG by performing a Life Cycle Assessment (LCA) using "SimaPro v.8.2.0.0" (Pre-Consultants 2016) software.
    - To examine PRBs ability to impact the overall cost of cooking.
- To identify the shortcomings in the PRB based LPG cook-stove developed at IIT Guwahati (Mishra, 2015) for its commercialization and propose a new cook-stove design. Also, to perform detailed performance assessment of the newly developed cook-stoves.

- To design and develop a naturally aspirated porous radiant burner for domestic biogas cook-stove and carryout detailed performance assessments.
- To perform experimental investigation to analyze waste cooking oil (WCO) as an alternative cooking source, and design and test a domestic cook-stove for its application.

In the present study, the performance investigation of LPG operated PRB based cook-stoves developed at IIT Guwahati for domestic as well as medium scale cooking applications were carried out in view of their feasibility for commercialization. Control Cooking Test (CCT) on domestic scale PRB cook-stove shows a fuel savings of approximately 93.27 g per day per household. The average heat energy requirement per household for daily cooking activities is estimated as 9283 kJ and 13306 kJ for stoves with Conventional Burner (CB) and PRB, respectively. Cooking time saving of approximately 51 min explains the extent to which time budgets can be affected by cook-stove with PRB.

Investigation on medium scale LPG operated PRB based cook-stoves shows that it has a surplus of 7% Life Cycle Energy Efficiency for input power of 5 kW which further rises to 11.6% for 10 kW. With reference to the functional unit tested at IIT Guwahati, the life cycle cost can be reduced to a great extent with an annual saving of ₹43,192 /- and ₹73,831 /- when compared to CB at 5 and 10 kW, respectively. Study concludes that PRB shows better performance as compared to CB at all three fronts of energy saving, emissions and overall cost. But, PRBs operation with 1.2 and 1.5 bar pressure regulator for domestic and medium scale cooking application, respectively, hinders its commercialization. Investigation were focused on overcoming the shortcomings of existing PRB designed for medium scale LPG cook stove. Newly designed burner works with unreduced pressure regulator (commercially feasible) and results in maximum thermal efficiency of 64.49%. With the improved design, significant amount of LPG was saved (30-45 %) and the measured emissions were found lower than the conventional burner. Newly developed burner with PRB showed a steady-state operation without any flashback and blow off for more than four-hour continuous operation and start up time of the burner is found as 5-6 min. As the developed stove works on the natural draft, it is ideally suited for replacement of conventional medium scale LPG cook-stove.

The work contained in the development of biogas cook-stove has been carried out in two parts. In the first part, the performance analyses have been carried out for the domestic scale biogas cooking stove with a PRB. Though working on external air supply, the objective of the first study is to understand the stability range of the burner, and to fix the geometric and operating parameters. The second part of the study was dedicated to the development of naturally aspirated domestic biogas cooking stove with a PRB. To compare the improvements in terms of thermal efficiency and emissions, experiments were also performed on the conventional biogas cooking stove for the same power input available in the market. First, from forced air supply the range of biogas flame stability limit (equivalence ratio) in two-layer PRB is found as 0.75-0.95 for domestic power range. Further, with self-aspirated PRB design about 22% improvement in thermal efficiency was observed. CO emissions are found as 36-48 ppm with self-aspirated PRB, whereas same is 235-276 ppm in case of CB. Similarly, NOx emissions are always found lower than 2 ppm in PRB whereas the same is 15 ppm in case of CB.

Present investigation also demonstrates a comparative study of combustion characteristics of WCO in a conventional kerosene pressure stove (CKPS) and a newly developed pressure stove with PRB (PKPS), with the following specific objectives. The first objective is to investigate the maximum % of the WCO, which can be blended with kerosene in domestic operational power range. The second objective is to measure the temperature distribution, thermal efficiency and emission with the obtained blending %. Third is to carry out CCT and TEA to get a proper understanding of cooking energy requirement and economic benefit of the newly developed stove with PRB. Maximum of 50% WCO and kerosene blend combustion can be sustained in both the test stoves. At condition of maximum blending (50% WCO), maximum ~9% improvement of thermal efficiency is found in case of PKPS. The newly developed PKPS reduces CO and NOx emission by 50-60% and 74-83%, respectively. From CCT it has been found that, on per day basis, PKPS results in 49 minutes and ~59% saving in cooking time and fuel consumption, respectively, as compared to CKPS. Techno-economic Assessment (TEA) indicates that, in a span of 10 years, PKPS can offer a sum of ₹16,817 as net present worth of savings.

Nomenclature

Symbols	*Comments*
S_L	Laminar flame speed, m/s
d_m	Equivalent pore diameter, m
c_P	Specific heat, J/kg-K
$c_{fuel-air}$	Specific heat of fuel air mixture, J/kg-K
$\rho_{fuel-air}$	Density of fuel air mixture (kg/m^3)
$k_{fuel-air}$	Thermal conductivity of fuel air mixture, W/m-K
$h_{fuel-air}$	Convective heat transfer coefficient (W/m^2-K)
$k_{ceramic}$	Thermal conductivity of ceramic, W/m-K
ε	Surface emissivity (-)
ϕ	Equivalence ratio (-)
η_{th}	Thermal efficiency (%)
P_i	Input power (kW)
η_{rad}	Radiation efficiency (%)
$T_{ceramic}$	Ceramic temperature (^{o}C)
$T_{fuel-air}$	Temperature of fuel air mixture, (°C)
$\dot{q}_{cond}$	Conductive heat flux (W/m^2)
$\dot{q}_{rad}$	Radiative heat flux (W/m^2)
$\dot{q}_{conv}$	Convective heat flux (W/m^2)
S_{PIM}	Burning velocity of fuel/air mixture in PIM (Porous Inert Media), m/s
v_o	Gas mixture velocity, m/s
D	Burner diameter (mm)
$\dot{m}_f$	Mass flow rate (kg/s)
σ	Stefan-Boltzmann constant, (5.67051x10^{-8} W/m^{2}K^4)
₹	Indian rupee

Abbreviations

CB	Conventional burner
CCT	Controlled Cooking Test
CZ	Combustion zone
ELU	Environmental Loading Unit
FCC	Free Flame Combustion
HCV	High calorific value
ICS	Improved cook stove
LCA	Life Cycle Assessment
LCV	Low calorific value
LCEA	Life Cycle Energy Analysis
PB	Porous burner
PM	Porous matrix
PMB	Porous medium burner
PMC	Porous medium combustion
PRB	Porous radiant burner
ppm	part per million
ppi	Pores per inch
ppc	Pores per inch
PRB	Porous radiant burner
PZ	Preheat zone
NPV	Net Present Value
NSS	National Sample Survey
RZ	Reaction zone
TEA	Techno-economic Assessment
WCO	waste cooking oil

Contents

List of Figures

List of Tables

Chapter 1

Introduction

1.1 Overview of India's Energy Situation

Developing countries like India are not only going through challenges associated with climate crisis but also tackling with the development and the poverty mitigation. For the sustainable economic growth of a nation, readily available energy resources and its consistent supply are the most essential requirements. The economy of a country is dependent on secure, sufficient and efficient energy facilities. Presently, India tops the energy consumer's list in the whole world. However, per capita final energy consumption in India is very low and there is a wide disparity between urban and rural areas. Energy balance of India for 2017-18, showed the total primary energy supplies summed up to ~8,37.37 million tonnes of oil equivalent (Mtoe) and the national energy consumption was ~5,53.9 Mtoe. But, at the same time, out of total primary energy supplies approximately 4,19.1 Mtoe of primary energy has been imported (Energy Statistics, 2019). The creeping growth of the share of imported energy in demand, threatens the energy security of the nation. India's population as well as GDP are likely to grow in the future, so, the demand for energy will also experience a substantial rise and consequently there will be increase in greenhouse gas (GHG) emissions as well. Recently, National Institution for Transforming India (NITI) Aayog, adopted a bottom-up energy system model and analyzed the future development of India's complex energy system (Thambi et al., 2018). On the demand side, five broad demand sectors viz., industry, agriculture, transport, cooking and buildings, were consider. The grouping of end use demand and sub-parts of cooking demand are shown in the Fig. 1.1.

Their assessment for the period 2017 to 2042, showed that the major consumer of final energy will be the industry sector and the second largest will be the growing transport sector of the country. In the cooking sector, energy consumption will come down significantly. This will be mainly due to efficiency improvement, as a result of less use of non-commercial biomass, which has an extremely low conversion efficiency. Hence, the overall efficiency of the cooking sector will improve and energy consumption will

decrease despite rising population. The use of electric stoves continues to be negligible as they are costly relative to other options. The share of gas gradually increases, this could be due to improved access in urban and rural areas, a result of existing government policies. The decrease in unclean fuels like biomass and cleaner fuels like LPG, natural gas and biogas, will have a positive effect on the emission reduction probability of the country. Cooking sector energy demand for India is depicted in Fig 1. 2.

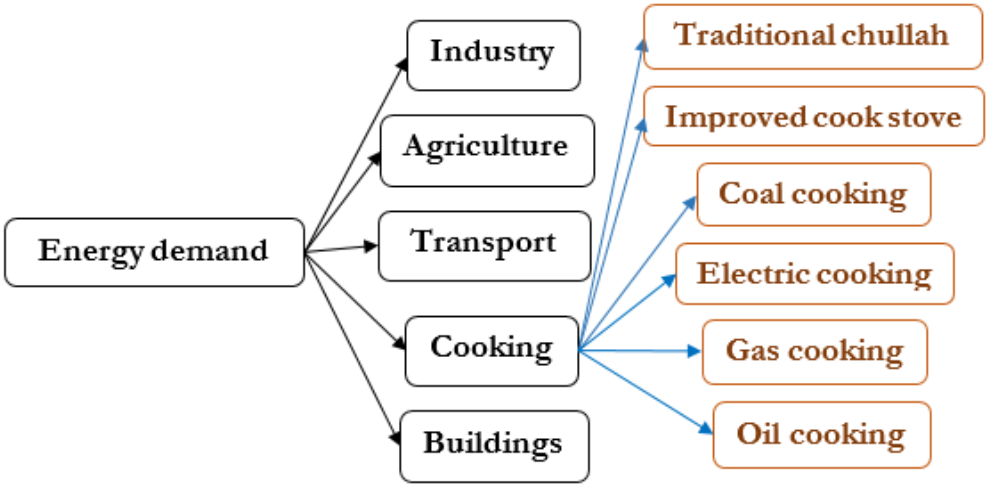

Fig. 1.1: Detailed of end user demand sectors.

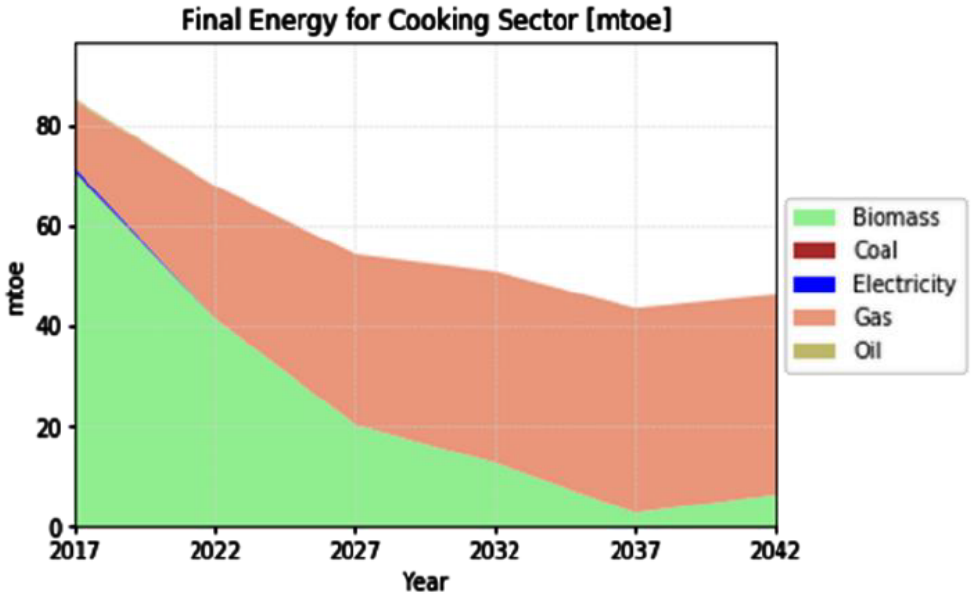

Fig. 1.2: Detailed of end user demand in cooking sectors (Thambi et al., 2018).

Under Sustainable Development Goals (SDGs) India sets targets to ensure access to affordable, reliable, sustainable and modern energy for all by 2030. However, the SDGs India dashboard indicates that only 43.8% households use clean cooking fuel (Electricity, LPG/natural gas, biogas), i.e., India needs to cover around 56% households in next coming years (NFHS-4, 2015-16). Majority of the households lacking clean cooking fuel are located in rural India. Four SDGs which profit from investments in clean cooking energy are mentioned below:

1. ***SDG 3-Good health and well-being:*** With the availability of clean cooking, the number of annual deaths due to household air pollution (HAP) can be reduced to a great extent. In maximum cases, women and children are the highly affected ones because of extended hours of exposure to HAP.
2. ***SDG 5- Gender equality:*** In India, women spend ten times more time on unpaid work than men, as compared to the global women's record of three times. Subsequently, women can contribute only a very less amount of 17% towards the country's GDP. This is quite inferior than the average in the corresponding developing nations like China (41 per cent) and Sub-Saharan Africa (39 per cent) (Woetzel et al., 2015). Availability of clean cooking energy helps in the reduction of time poverty, i.e., the hour invested by women for unpaid work such as collecting fuelwood and cooking for prolonged hours on inefficient stoves.
3. ***SDG 7-Affordable and clean energy:*** Almost 50% of households in India are dependent on the conventional biomass for cooking. Venture into clean cooking energy and technology will help in speeding up the advancement towards minimizing the count of households relying on the conventional use of biomass for cooking.
4. ***SDG 13- Climate action:*** Significant reduction in conventional cook stoves usage will offer positive outcomes in case of climate change too. This will be possible because of sharp reduction in black carbon emissions from the incomplete combustion of biomass. Contribution of India towards the global anthropogenic black carbon emissions is 12%, out of which 60% is emitted from the residential sector (Anenberg et al., 2011).

The cook stove sector in India can be mapped in six dimensions with respect to overall trend in supply and demand, and emerging opportunities and challenges. Each dimension deals with a specific aspect of Indian cooking sector as shown in Table 1.1 (Global Alliance for Clean Cook stoves, 2013).

Table 1.1: Sector mapping of the Indian cook stove industry across six dimensions (Global Alliance for Clean Cook stoves, 2013).

Fuel usage and trends	What kind of fuels do Indian consumers use, how much do they use and what are the effects of this on the cook stove sector?
Health, social & environmental impact	What are the impacts of inefficient and polluting cook stoves on health, society and environment in India?
Consumer assessment	Who are the major customers for cook stoves and what are the chances and challenges of addressing their preferences?
Cook stove industry	What is the technology landscape for cook stoves in India, who are the major players and what are the challenges they face?
Cook stove policy environment	How have governments agencies, multilaterals and donors approached cook stoves and what are their likely future policy priorities?
Macro environment	What are the overall economic, social, demographic and environmental trends shaping India?

In the next section some of the dimensions related to the present thesis work particularly fuel usage and trend, and cook stove industry are analyzed.

1.1.1 Fuel usage trend in Indian household

In India, the major part of the energy requirements in cooking applications is still fulfilled via fossil fuels. India derives the bulk of its cooking energy needs from solid fuels, such as firewood and cattle dung in rural areas and from LPG and kerosene in urban areas (Parikh et al., 2016). LPG and kerosene are the two cheap clean cooking fuels used in India. Natural gas and electricity are not generally used due to the shortage of common availability for household use. Biogas, which is a biomass-based clean fuel,

is not quite used because it has not yet been commercialized (India Clean Cooking Forum, 2018).

The detailed information related to cooking sources for Indian household in urban and rural areas are available in National Sample Survey, 68th round report (NSS, 2011-12). After 2012 due to change in government policies, some improvement in these figures are plausible, but the overall trend remains same. According to NSS, the rural households, generally used firewood and chips as the main source of energy for cooking. All over India, firewood and chips have been used by more than two-third (67.3%) of the rural households, followed by LPG, which has been used by 15.0% households. Only 9.6% and 1.1% of the rural households have been using dung cake and coke & coal, respectively as the primary source. The remaining 4.9% households use other sources, i.e. gobar gas, charcoal, electricity and others. The left out 1.3% rural households did not have any arrangement for cooking (Fig 1.3a). However, in the urban areas, most of the households used LPG as primary source of energy for cooking. LPG was used by 68.4% of the households in urban India, and 14% households used firewood and chips. Also, 5.7% of the homes used kerosene, 2.1% used coke & coal and only a meagre amount of 1.3% of the urban houses used dung cake as their main source for cooking. The remaining 1.5% houses used other sources. It is to be noted that, 6.9% of the households in urban area did not have any arrangement for cooking (Fig. 1.3b).

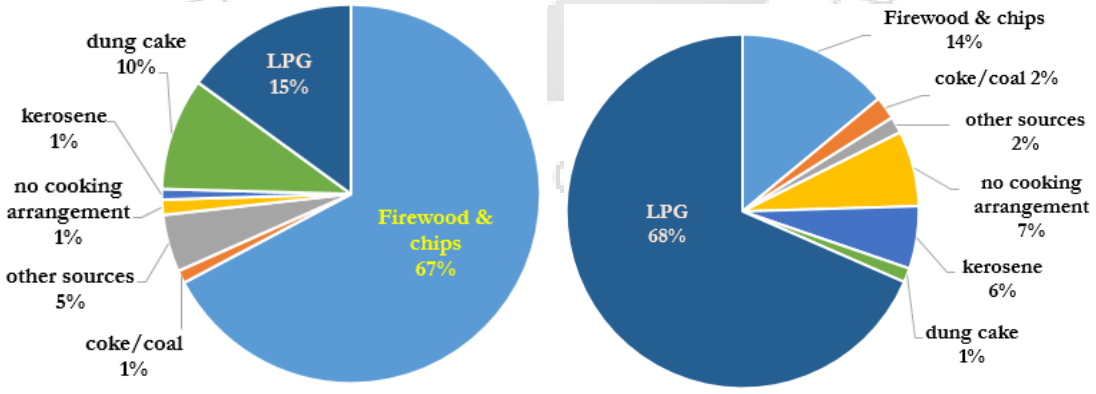

(a) (b)

Fig. 1.3: Percentage distribution of households by primary source of energy used for cooking: (a) rural and (b) urban India, 2011-12.

However, in recent years, India has acquired improved access to use of cleaner cooking devices/arrangements. The access to LPG has expanded all over India in a short duration. The count of registered LPG consumers has increased beyond double from 106 million connections in the fiscal year (FY) 2008/09 to 263 million in the FY 2017/18 (PPAC, 2019). The total consumption of LPG in domestic (household) sector has nearly doubled in the last ten years, increasing from 10.6 million tonnes (MT) in FY 2008/09 to 20.4 MT in FY 2017/18 (Indian petroleum natural gas statistics, 2017-18). As the consumption has raised significantly, the ratio between domestic and commercial consumption has remained stable, with domestic consumption accounting for approximately 86–88% of total LPG consumption. In spite of the expansion in total LPG connections, the Ministry of Petroleum and Natural Gas assesses that nearly one fifth of the households (over 50 million) still did not have access to clean cooking fuel as of the end of FY 2017/18.

1.1.2 Current status of cooking technology

The technological options, which could potentially provide clean cooking energy to significant proportion of population, are several and diverse. The cook stoves available in Indian market can be broadly classified in six categories as shown in Table 1.2. Further this technology can be grouped in to conventional cooking, enhanced cooking solutions and clean cooking energy.

Table 1.2: Cook-stoves available in Indian market.

Traditional cooking	*Traditional stove* (Three stone fires, basic non-improved chulhas, and unvented coal stoves)	
Improved cooking solutions (ICS)	*Basic ICS* (Basic improved chimney chulhas, basic biomass portable stoves, and basic vented coal stoves)	 

	Enhanced ICS (Rocket stoves, highly improved charcoal stoves and highly efficient coal stoves)		
Clean cooking energy	*Advanced ICS* (Natural draft gasifier (TLUD or side load and fan gasifiers)	 	
	Modern fuel solutions (LPG, electricity, kerosene and natural gas)		
	Renewable energy solutions (Biogas, biofuels/ethanol/ methanol, solar/ retained heat cookers)		

The above combustion-based cook stoves are categorized by a Free Flame (FF). These cook-stoves confirm its operation through the occurrence of the flame and assesses the heat output by the size of the flame. The flame size, shape and color can be changed by adjusting the fuel and air quantity. The flame is a region where all required component of combustion viz., fuel, air and ignition heat, meet to yield visible light and also hot combustion products that provide heat to the cooking vessel. Fuel-air mixture enters into the mixing chamber, combustion takes place on the surface of the burner and the burnt products exit through the flame (Fig. 1.4). The location of the flame in a traditional cook stove is controlled by a number of factors, which includes:

1. The composition, amount, and speed of the air and combustible gases;
2. Geometry in the combustion zone that the flame can “attach” to;
3. Flow constrictions at the exit of the combustion zone.

The combustion process in Free Flame Combustion (FFC) based cook-stove is illustrated in Fig. 1.4. Such kind of combustion occurs in an environment of bare air where the primary method of heat transfer is convection. Gases are characterized by low thermal conductivity and emissivity, because of which contributions of radiation and conduction heat transport from combustion products to reactants for preheating of the unburnt air-fuel mixture are negligible. Consequently, owing to poor heat transfer, the FF combustion-based devices are less efficient, and they possess unwanted characteristics such as high emission of toxic pollutants, inferior stable flame limits, low power density, etc. Majority of the commercial cook-stoves are designed for FF combustion, due to which they have the above-mentioned inherent drawbacks.

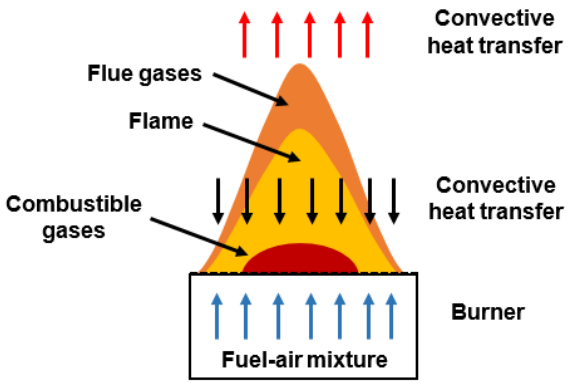

Fig. 1.4: Schematic of FFC based cook-stove: convection dominated FF.

1.1.3 Existing policies and efforts to improve access to clean cooking energy

For over a period of three decades, both central and state governments in India have made immense efforts to increase the clean cooking energy solutions like LPG stoves, improved biomass cook-stoves (ICS), biogas plants and piped natural gas (PNG) based stoves (Patnaik et al., 2018). These policies have strived towards the awareness of the negative health effects of conventional cook-stoves. Also, policies speak about the subsidies on clean fuels or technologies to improve affordability, enhance the amount of investment in research and development to turn down the existing market prices. Most of the recent efforts have been concentrated in supplying LPG in rural areas and PNG in densely-populated urban centers. Some of the landmark policies (Fuel or Technology) undertaken by the government have been summarized below:

Liquefied Petroleum Gas: LPG has been chosen as clean cooking energy for domestic cooking by the government. It is to be noted that an increase in the coverage of LPG beneficiaries is necessary to reduce their dependence on kerosene. This will result in the usage of cleaner fuel, promote the health of users, and address the problem of adulteration. For address these issues, government initiatives are mainly focused on increasing coverage of LPG by making available it at reasonable cost. The Ministry of Petroleum and Natural Gas provides subsidy on LPG cylinders. Subsidies on LPG in India were introduced in late 1960s. Indian Government has provided ₹23,464 crores as subsidy in year 2017-18 for LPG (Khullar, 2018). The amount of subsidy provided by government and oil companies on domestic LPG in last decades is shown in Fig. 1.5. In June 2013, Government had launched a scheme, Direct Benefit Transfer for LPG (DBTL), in which the amount of LPG subsidies was credited to directly to bank accounts of the consumers. Later (March 2015), the government had proposed an initiative where the households were encouraged to voluntarily surrender their access to the subsidized rate LPG and buy cylinders at the market rates (a program known as GiveItUp). The count of LPG connections has increased very fast in the last ten years, partly because of government-directed investments in generating additional LPG supply infrastructure. In spite of this, the bulk of budgetary expenditure on LPG subsidies by the central government has been directed to price subsidies, with very few expenditures on extending its access. The scheme (known as Pradhan Mantri Ujjwala Yojana or Ujjwala) was launched in May 2016 with an aim of arranging 50 million connections to below poverty line (BPL) classified households by 2019. In the budget of February 2018, the government had announced an increment in the target connections under Ujjwala from 50 million to 80 million, with a commensurate increase in the budget allocation of ₹4,800 crores and an expansion of the relevant eligibility criteria (Lok Sabha, 2018). Alongside increased expenditure on access, the central government spent an equivalent amount on the implementation of the DBTL program, primarily through advance payments to households. To expand the network of rural LPG distributors, the government has also relaxed the eligibility and financial criteria to get licenses.

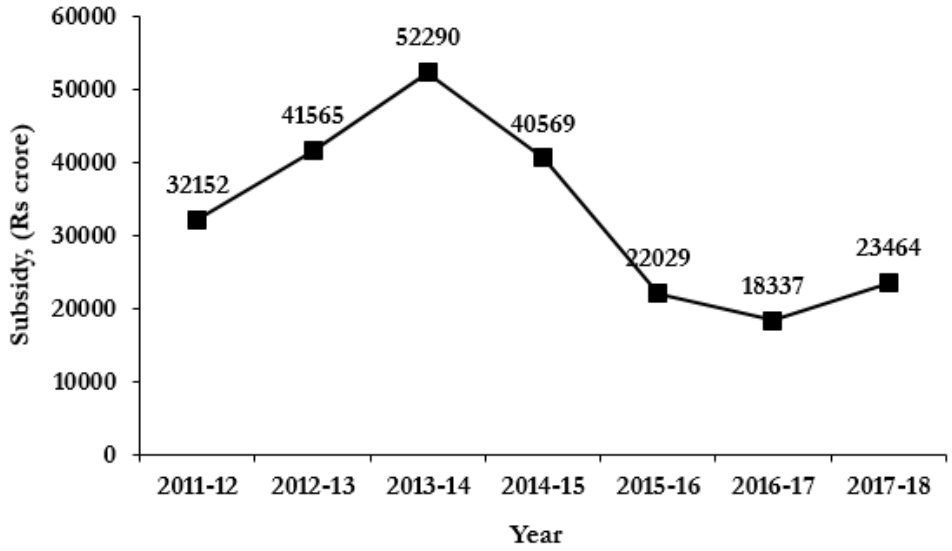

Fig. 1.5: Subsidy provided by government and oil companies on domestic LPG.

Improved Biomass Cook stoves: Solid fuels (a collective term used for firewood, crop residues and dung cakes) are generally available free of cost although the users need to make efforts in terms of collection and storage. Inefficient burning of solid fuels in traditional mud-stoves leads to household air pollution posing adverse impact on health of the cook especially in enclosed spaces. To overcome this drawback, concerted efforts to introduce improved cook-stove technologies began during 1980s by the Ministry of New and Renewable Energy (MNRE). The first scheme by government in support of ICS was the National Programme on Improved Chulhas (NPIC), which distributed 35 million chulhas in 16 years since its launch in 1986 (Venkataraman et al., 2010). After its termination in 2002, much of the public investment into ICS has been in research and development to upgrade the product design. The government's recent Unnat Chulha Abhiyan (UCA) scheme could meet just one per cent of its ICS deployment target of 2.75 million between 2014 and 2017 (Patnaik and Tripathi, 2017).

Biogas: Clean cooking programmes based on biogas was introduced during 1990s at various pockets of the country. A family type biogas plant produces biogas from organic matters like cattle-dung, and other bio-degradable constituents such as biomass from farms, gardens, kitchens, etc. The issue of feed and maintenance remained the major challenge for adoption of household biogas plants for cooking. The nodal scheme for biogas since 1981 has been the National Biogas and Manure Management Programme (NBMMP). Ministry of New and Renewable Energy has been

implementing the NBMMP in all the States and UTs of the country. It provides financial aid for a family-type biogas plant and also train the users and staff on the maintenance requirements of the plants. About 47.5 Lakh biogas plants have already been installed in the country up to 31st March, 2014. During the year 2014-15, setting up 1,10,000 biogas plants had been targeted. The Biogas plant is the best option for households having feed material, to become self- dependent for cooking gas and highly organic enriched bio-manure. In recent years, the annual NBMM deployment target has not been met, with only 55 per cent of the target met in 2016-17 (MNRE, 2017).

Piped Natural Gas: The government has also initiated provision of domestically produced natural gas to city gas distributors (CGDs) to meet the urban demand for clean energy. Since 2014, CGDs have been prioritized to receive domestic PNG, helping them keep prices low for urban consumers.

In keeping with these developments, numerous policy measures have also been taken, which focused on increasing access to energy, also aim to keep emissions in check. Considerable progress has been made in improving energy access in the country in the past few years.

1.1.4 Lesson learned and way forward

In spite of the rapid uptake of LPG for domestic cooking, nearly 500 million people in India remain unprivileged to clean cooking fuel (Jain et al., 2018). They are utilizing biomass or kerosene as their cooking fuel, both of which cause harmful air pollution. Also, nearly half of the total houses with LPG connection were not using it as their main cooking fuel. Most of the houses practice “fuel stacking,” using a range of fuels depending on price, availability and what is being cooked (Parikh et al., 2016). Learning from the past, one need to re-look at initiatives and assessment criteria of the clean cooking programmes. The programmes need to focus on more than one cooking fuel and technology combinations. One among the technology has to be resemble to the existing cooking practices and the other has to be the cleaner cooking technology. The combinations may be introduced based on the cooking technologies used in the area, economic status of the households, affordability of the clean cooking fuel, availability of solid fuels, connectivity to the LPG refilling stations, and electricity access scenario of the area. It is, therefore, critical to scale other clean cooking energy solutions such

as ICS, biogas and induction so that households stack between LPG and traditional stoves. Currently, LPG subsidies absorb a large share of resources-mostly because they remain largely untargeted-and as such are the principal pillar of India's efforts on clean cooking. Attaining access to clean cooking in a universal scale will require a range of organized policies, clean fuels and technologies. No part of energy problem is ever sorted by one fuel alone. One way to promote alternative fuels and reduce subsidy costs is to encourage higher-income households to shift to alternative modern sources of energy, such as biogas or electric cooking with induction stoves. To expand LPG use in the non-subsidized market, the government needs to remove restrictions on sales and distribution (except those that ensure health and safety). Improved participation of the private sector in the market would bring in competition and innovation, as well as improve distribution.

1.2 Porous Medium Combustion (PMC)

As discussed earlier, in order to achieve clean cooking solutions for all, development of efficient cook stoves is very important. Available combustion-based cook stoves have the inherited disadvantage of FFC. Recently, a new concept of combustion, namely Porous Media Combustion (PMC), has gained increased attention as it delivers numerous benefits, in particular high thermal efficiency, low pollutant emission, homogeneous heat flux, etc., as compared to the existing technology working on the principle of FFC.

1.2.1 Heat transfer mechanism in PMC

The concept of heat recirculating combustion or excess enthalpy flame prevails in PMC, which means that a part of enthalpy contained in the combustion gases is transferred back to the upstream, into fresh incoming mixture, via radiation and conduction heat transfer (Fig. 1.6) (Weinberg, 1971).

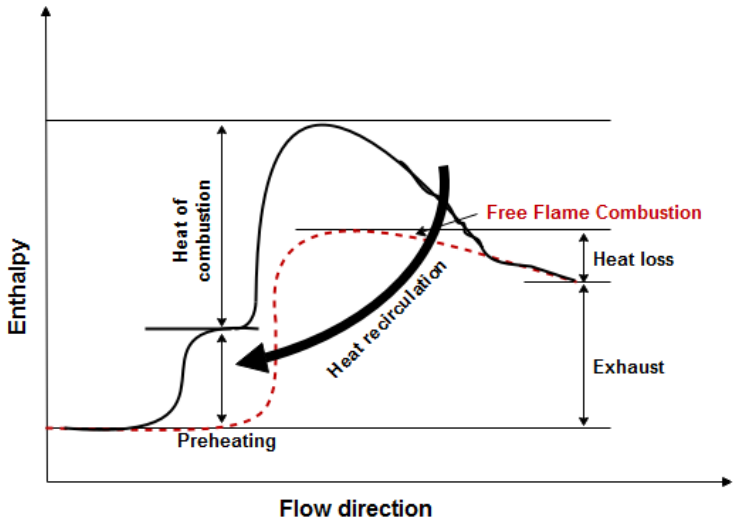

Fig. 1.6: Concept of heat recirculation (Weinberg, 1971).

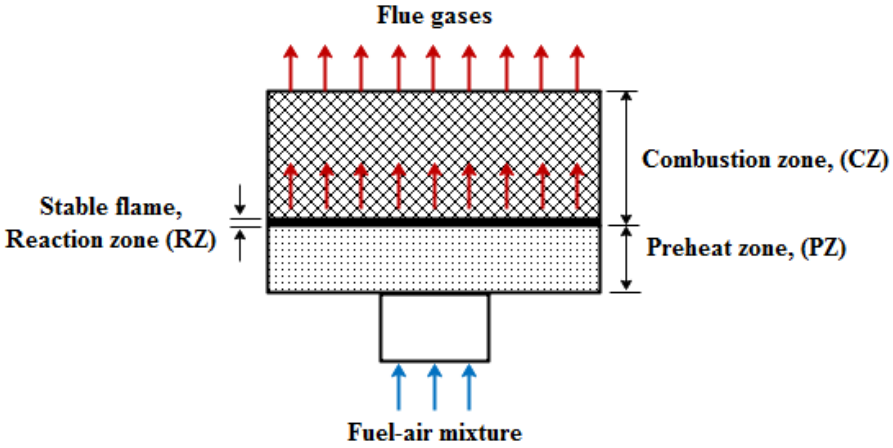

(a)

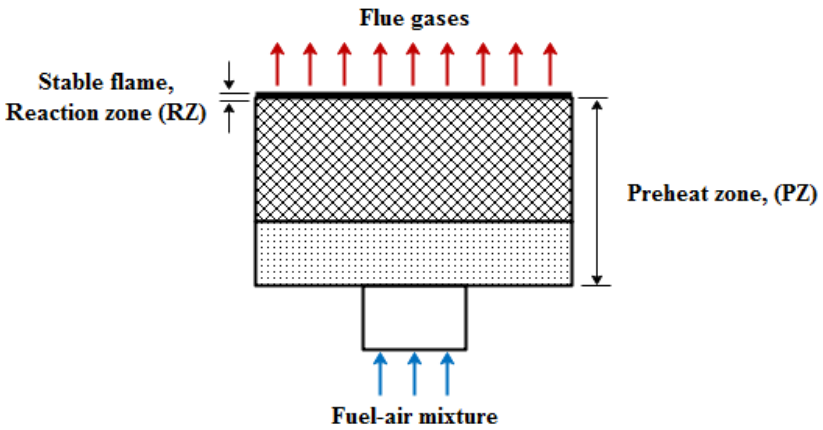

(b)

Fig. 1.7: Schematic of (a) matrix-stabilized and (b) surface-stabilized PRB.

This type of combustion is characterized by highly conducting and radiating porous matrices, and the flame is either submerged (matrix-stabilized-combustion) or floats at the surface (surface-stabilized-combustion) depending on the burner operating conditions (Fig. 1.7a and b). In a matrix stabilized two-layer Porous Radiant Burner (PRB), bottom layer is the Preheat Zone (PZ) and upper layer is Combustion Zone (CZ) (Fig. 1.7a). In such a case, the stable flame (Reaction Zone (RZ) is trapped in the upper layer (CZ). But, in case of surface-stabilized double layered PRB, the RZ is anchored on the top surface and both the layer act as PZ (Fig. 1.7b). The heat propagation in the PRB is entirely different from the FF based Conventional Burner (CB). Figure 1.8 illustrates the heat transfer in a two-layer matrix-stabilized PRB.

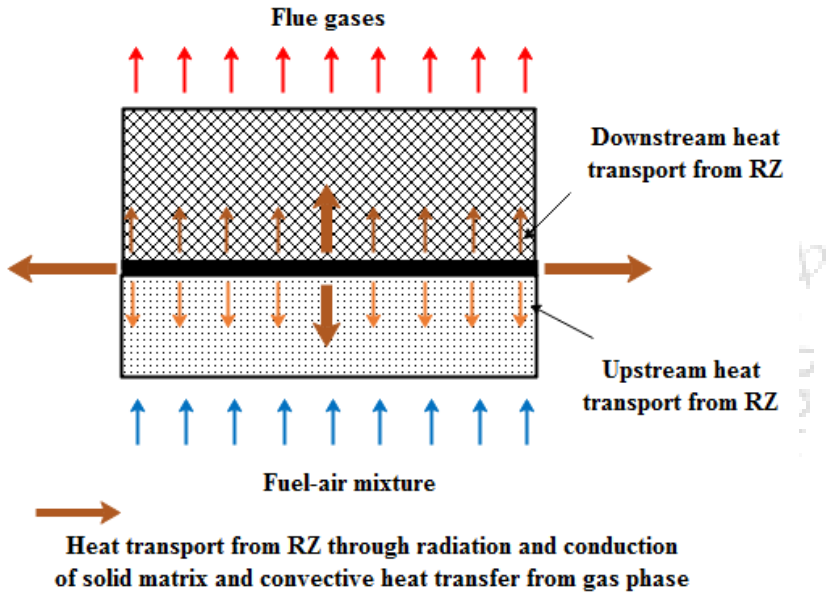

Fig. 1.8: Schematic of PRB: radiation dominated submerged flame.

As shown in Fig. 1.8, the three forms of heat transfer viz. conduction, convection and radiation, are present in a PMC. Conduction heat transfer can be estimated by Fourier law, using Eq. 1.1 (x is in direction of ceramic thickness) and convective heat transfer by Eq. 1.2. Convection heat transfer is more prevalent in PMC than in FF combustion. The coefficient of convective heat transfer can be deduced from the Nusselt number (Nu) by Eq. 1.3. Radiation, which dominates the heat transfer in PMC, due to highly radiant property of porous media, can be calculated by Stefan-Boltzmann law using Eq. 1.4.

$$\dot{q}_{cond} = -k_{ceramic}\frac{dT_{ceramic}}{dx} \quad \ldots\ldots\ldots (1.1)$$

$$\dot{q}_{conv} = -h_{fuel-air}(T_{fuel-air} - T_{ceramic}) \quad \ldots\ldots\ldots (1.2)$$

$$Nu = \frac{h_{fuel-air} \times l}{k_{fuel-air}} = f(Re, Pr, Geometry) \quad \ldots\ldots\ldots (1.3)$$

$$\dot{q}_{rad} = \varepsilon\sigma(T_{ceramic})^4 \quad \ldots\ldots\ldots (1.4)$$

Part of the heat produced in the flame zone is transferred to the solid matrix via convection heat transfer. Heat transfer from the CZ to PZ takes place by solid-to-solid conduction and radiation. Consequently, the PZ, preheats the incoming air fuel mixture. This process of heat transfer is called heat recirculation, specializing the combustion heat through the porous media. To quantify and compare the convective, conductive and radiative heat transfer between the gas and solid phases in the burner, the following parameters are used.

$$Convective\ recirculation\ efficiecncy = \frac{Solid - to - gas\ convection\ rate\ in\ Preheat\ zone}{Thermal\ power} \quad \ldots\ldots\ldots (1.5)$$

$$Conductive\ recirculation\ efficiecncy = \frac{Solid - to - solid\ conduction\ rate\ into\ Preheat\ zone}{Thermal\ power} \quad \ldots\ldots\ldots (1.6)$$

$$Radiative\ recirculation\ efficiecncy = \frac{Solid - to - solid\ radiation\ rate\ into\ Preheat\ zone}{Thermal\ power} \quad \ldots\ldots\ldots (1.7)$$

1.2.2 Combustion stability in PMC

In PMC, stabilization of flame at desired location is of prime concern. Un-stable flame may lead to the adverse conditions of lift-off or flash back, which ultimately extinguish the combustion process and shut down the burner. “Flashback” prevails when the

incoming mixture velocity (v_o) is not sufficient to resist the burning velocity (S_{PIM}) and allows the flame to propagate upstream in to the incoming reactants. Similarly, when the v_o is higher than the S_{PIM}, the flame travels downstream (out of the burner surface) and this phenomenon is termed "Blow-off". In the case of stable flame, v_o equals S_{PIM} and for PRB, it can be quantified by using Eq. 1.8. Another term used for burner stability in PRB is flame velocity ratio (FVR), given in Eq. 1.9.

$$v_o = S_{PIM} = \frac{\frac{P_i}{LCV}\left(\frac{AFR_{stoic}}{\phi\rho_{air}(p,T)} + \frac{1}{\rho_{fuel}(p,T)}\right)}{\frac{\pi \times D^4}{4}} \quad \ldots\ldots\ldots (1.8)$$

$$FVR = \frac{S_{PIM}}{S_L} \quad \ldots\ldots\ldots (1.9)$$

In steady state, flame propagation regimes for gaseous fuel combustion in porous media are given in Table 1.3 (Babkin et al., 1991).

Table 1.3: Steady state flame propagation mechanism and regimes for gaseous fuels combustion in Porous Media (Babkin et al., 1991).

Regimes	S_{PIM} (m/s)	Flame propagation mechanism
Low velocities	0-10^{-4}	heat conductivity, interphase heat exchange
High velocities	0.1-10	Convective, uniform pressure
Sound velocities	100-300	Convective, pressure gradient
Low velocities detonation	500-1000	Self-ignition under shock wave interaction
Normal detonation	1500-2000	Detonation under heat and pulse losses

Due to internal heat recirculation mechanism, the flame speed in porous media is much higher than the laminar flame speed of the same mixture combusted in an open environment. This supports the stable combustion for an extended range of equivalence ratios (ϕ) (Eq. 1.10) and firing rates (Khanna et al., 1994).

$$\phi = \frac{AFR_{stoic}}{AFR_{actual}} = \frac{\left(\frac{m_{air}}{m_{fuel}}\right)_{stoic}}{\left(\frac{m_{air}}{m_{fuel}}\right)_{actual}} \quad \ldots\ldots\ldots (1.10)$$

In a double-layered PRB, flame stabilizes at the transition zone between two regions (viz. PZ and CZ) with different pore sizes. Babkin et al. (1991) presented the stabilization criteria of the hydrocarbon flame based on Peclet number (Pe), which is the ratio of convective to conductive heat flow. They introduced a limiting condition as $Pe \geq 65$ for flame propagation (Eq. 1.11). According to Bakin et al. (1991), any porous burner having $Pe \geq 65$ allows the hydrocarbon flame to propagate, while Dillon (1999) found the same limit for hydrogen flame to be 37. For other flames, however, no such study has been reported.

$$Pe = \frac{S_L d_m c_{fuel-air} \rho_{fuel-air}}{K_{fuel-air}} \quad \ldots\ldots (1.11)$$

1.2.3 Materials used in PMC

Ceramics such as Aluminium oxide (Al_2O_3), Zirconium dioxide/Zirconia (ZrO_2), Silicon carbide (SiC), Mullite, Cordierite, etc. and some metallic materials such as stainless steel, Fecralloy (iron-chromium-nickel), etc. are used for the construction of PRB (Fig. 1.9). Ceramics are largely preferred over metals due to their adequate thermal stability at high temperature and low thermal inertia. Considerable progress has been made on the development of ceramics that particularly suit in PMC, exhibit high oxidation and offer high creep resistance. The basic material such as SiC is now available in the form of SSiC (sintered silicon carbide), SiSiC (silicon infiltrated silicon carbide), and HPSiC (hot pressed infiltrated silicon carbide). Another suitable material, ZrO_2 bonded with yttria or magnesia, known as partially stabilized zirconia (PSZ), was also used. Long term testing is however needed to prove the structural stability of the PM and the ability to sustain heat cycle (cooling and heating) before disintegration. Table 1.4 provides the thermal and radiative properties of the ceramics reported in earlier studies.

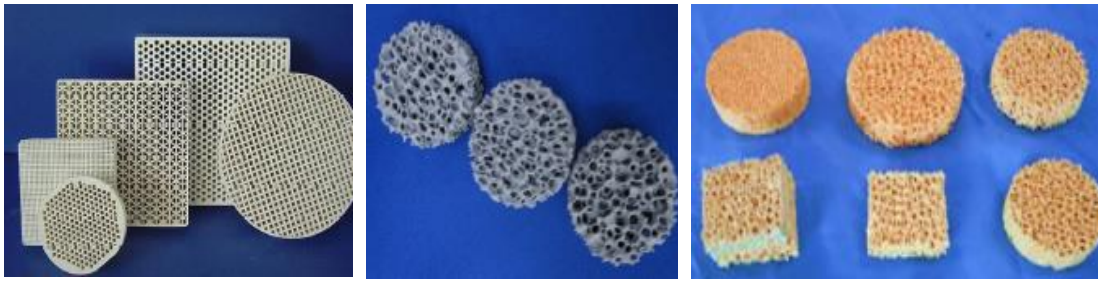

(a) (b) (c)

Fig. 1.9: Different types of ceramics.

Table 1.4: Ceramic material properties (Hsu et al. (1993), Leonardi et al. (2002), Fuse et al. (2003), Pickenacker et al. (1999), Gao et al. (2014), Hale and Bohn (1993), Avdic et al. (2010), Mujeebu et al. (2009a)).

Material		**A**	**B**	**C**	**D**	**E**	**F**	**G**	**H**	**I**
T_{max}		1600	1900	1800	1400-1750	1380	1700			
$k_{ceramic}$		20-50	5-6	2-4	40-120	110-160	80-145	2.6	0.37	0.13
		at (1000°C)			at (20-100°C)					
ε at 2000K		0.9	0.28	0.31	-	-	-			0.65
$\alpha_{th,ex}$ 20-1000°C (10^{-6} K^{-1})		4-5	7.2	10-13	-		-			
C_p at 25-800°C		-	1.05	0.59	0.84	0.84	0.84	0.80		0.432
τ	10 ppi 65 ppi			28.2 300						
ω	10 ppi	0.55-0.88		0.87-0.99		0.7		0.76	0.84	
β	10 ppi 20 ppi 25 ppi 30 ppi	234.1 468.1 585.2 702.2	210 300	234.1	100	178 244		270	202	234.1

(A) SiC, (B) Al_2O_3, (C) ZrO_2, (D) SSiC, (E) SiSiC, (F) HPSiC, (G) Cordierite, (H) Mullite, (I) FeCrAl

1.2.4 Advantages of PMC

The main advantages of PMC are given below;

- Better heat transfer properties keep the surface temperature of the burner lower which consequently lowers NO_x emissions.

- Owing to increased residence time, the formation of CO emission is low.
- It can operate at low equivalence ratios.
- It is featured by wide range of power modulation.
- Complex combustion chambers geometries are possible with PMC in porous radiant burners.
- This technique improves the heat transfer process because of good radiation and conduction properties of porous medium resulting in higher thermal efficiencies.

1.2.5 Applications of PMC

Some of the featured applications of PMC based porous burner are as follows:

- Household, i.e., porous burners for cooking and heating systems
- Burner for automobiles.
- Burner for gas turbine and propulsion.
- Burners for heat exchangers.
- Miscellaneous applications like thermoelectric conversion, steam generation etc.

1.3 Motivation of the Thesis Work

Over a decade, Government of India has been focusing to increase the coverage of clean cooking fuels, mainly LPG to a large rural population. As the government is providing huge subsidy in LPG price, the economic feasibility is the main factor for success of the such programs. In order to provide clean and economic cooking energy to large population of India, there is a need for R&D efforts to develop energy efficient and less polluting cook stoves. The available cook-stoves are designed on FFC, which works on rich fuel-air combustion. These cook-stoves provide only lower efficiency (less than 68%) and higher emissions. Another combustion technology, Porous Media Combustion, offers improved and clean combustion and can be utilized for numerous applications. Recently, it has been found that PMC is very efficient particularly in cooking applications. Recent self-aspirated LPG cook-stove development by Mishra et al. (2015) showed encouraging results, but their commercial viability has not been investigated. The porous radiant burner assisted LPG cook-stoves developed for domestic as well as medium scale cooking showed large energy saving potential. In the

case of domestic stove maximum improvement in the thermal efficiency of ~10% was observed. Whereas, in the case of medium scale, cook-stove maximum improvement moved to ~28%. Similarly, for kerosene application porous radiant burner assisted cook-stoves developed by Sinha (2017), showed maximum thermal efficiency improvement of ~16%. As the consumer base in India is large, efficiency improvement by porous radiant burner assisted cook-stoves could result in large energy saving. As discussed earlier, fuel stacking is also a major hindrance towards the clean cooking energy expansion in rural areas, therefore, alternative fuels for cook stoves (viz., biogas, waste cooking oil, etc.) are also needed to be explored. It has been also observed that no researchers have studied the use of PMC for development of cook stoves operating on biogas and waste cooking oil. Hence, this thesis work is devoted to investigate the commercial feasibility of the PRBs developed by Mishra et al. (2015) and make necessary modifications to make them commercially viable. Also, this study has been dedicated to investigate the use of biogas and waste cooking oil particularly, for domestic scale cooking applications. This thesis contains of seven chapters and the contents presented in each chapter are discussed in the next section.

1.4 Organization of thesis

In the second chapter, first, an overall view on porous medium combustion is presented. Research carried out on PMC for cook-stove developments have been critically analyzed. Chapter two is mainly focused on three cooking fuels viz., LPG, Biogas and Plant oil. Latest cook-stoves available for these three fuels are also examined. The chapter ends with concluding remarks on the literature review and then presents the objectives of the present thesis.

Chapter 3 deals with the performance and feasibility assessments of PRB assisted cook stove developed by Mishra et al. (2015). Three performance tests viz., Control Cooking Test (CCT), life Cycle Assessment (LCA) and Techno-economic Assessment (TEA) have been performed. Each test method is explained in detail. These studies concluded that PRB showed better performance as compared to CB at all three fronts of energy saving, emissions and overall cost.

Above mentioned medium-scale PRB cook-stove is critically analyzed for its commercial viability and based on the shortcomings of the design, modifications have

been presented in chapter 4. The use of 1.5 bar pressure regulator was found as main hindrance and the design has been modified with an unreduced pressure regulator. Detailed stability analysis for long hours of operation (5-6 hours) showed submerged mode of operation as main problem in the developed PRB. Further modification with a partially submerged mode operation has been proposed. Detailed comparative performance studies on the newly developed PRB, PRB developed by Mishra (2015) and CB are presented. Overall performance of the newly designed PRB shows that for cooking application, partially submerged mode is more favorable than submerged mode operation.

The next two Chapters (Chapters 5 and 6) deals with the development of PRBs for biogas and waste cooking oil, respectively. Chapter 5, deals with the experimental investigation of biogas combustion in a double layer PRB. The combustion behavior within the burner has been studied using the temperature distribution at different positions of the burner. After determining the stability range for domestic cooking application using forced air supply, the burner was then re-designed to work natural drat.

Chapter 6 deals with the combustion behavior waste cooking oil in PRB. The maximum % of waste cooking oil blending with kerosene that can work in a pressurized kerosene cook-stove with a PRB has been found. A vaporizer has been designed and detailed performance assessment viz., thermal efficiency, emission (CO and NO_x), for different blend samples has been carried out.

Conclusions and future work are presented in Chapter 7.

Chapter 2

State-of-the-Art

2.1 History of porous media combustion (PMC)

The initial study on Porous Media Combustion (PMC) was devoted to the understanding of excess enthalpy flame that gets generated because of heat recirculation in porous matrix (Hardesty and weinberg, 1973; Takeno et al., 1979, 1981, 1983; Deshaies and Joulin, 1980). In the early 1980s and late 1990s, researchers put more focus on understanding the heat transfer and combustion mechanisms within porous matrix (Echigo et al., 1982, 1986; Yoshiazwa et al. 1988; Sathe et al., 1991; Hanamura et al., 1993; Viskanta, 1995; Norbury and Byrne, 1996; Mital et al., 1997). Several studies have been dedicated to understanding the flame behavior in both surface and submerged modes. With the aid of a few fundamental studies (Takeno and Murayama, 1986; Chen et al., 1987; Echigo, 1991; Min and Shin, 1991) matrix-stabilized-combustion was more or less understood. In the beginning of the twenty-first century, focus was shifted towards the understanding of flame stabilization process of burners developed for various practical applications (Koseki and Sato, 2002; Mathis and Ellzey, 2003; Leonardi et al., 2003; Avdic, 2004; Hayashi et al., 2004; Barra and Ellzey, 2004). Combustion of liquid fuel in PM has also been studied by some researchers (Jugjai et al., 2002, 2003, 2007; Vijaykant and Agrawal, 2007) using domestic and industrial scale burners. Few researchers have studied the potential application of PMC for hydrogen production using different fuels like methanol (CH_3OH), methane (CH_4), octane (C_8H_{18}) and automotive-grade petrol, etc. (Bingue et al., 2002; Mjaanes et al., 2005). The latest trend of research in PMC technology focuses on the development of burners for LPG (Mujeebu et al., 2011a; Pantangi et al., 2011; Muthukumar et al., 2011; Mishra et al., 2015, 2018; Panigrahy et al., 2016a, 2016b) and kerosene (Kakati et al., 2007; Sharma et al., 2009, 2011, 2016a, 2016b; Sinha, 2017) used in the domestic as well commercial sectors. The progress of the PMC technology has been documented in various review papers. Howell et al. (1996) were the first to discuss the experimental findings on the nature of combustion of liquid as well as gaseous fuels used in different porous media and the challenges in modeling. Wood and Harris (2008) outlined the research works carried out on lean CH_4 combustion in PRB. Mujeebu and co-workers

(Mujeebu et al., 2009a, 2009b, 2010) presented the state-of-the-art on materials, configurations, and performance of PRB operated with various liquid and gaseous fuels, etc. It can be seen that until 2010, there has been a good track of the various developments in PMC technologies. However, beyond this period, there is no report, except the article by Malico and Mujeebu (2015), where the performance of domestic burners was discussed.

2.2 State of Art on LPG Cook-stove with Porous Radiant Burner (PRB)

The first PRB development for the cooking application can be found in work by Jugjai and Sanitjai (1996). They proposed a new burner design, i.e., Porous Radiant Recirculated Burner (PRRB) to improve the thermal efficiency. Unlike PRB, the PRRB is not characterized by flame inside the porous medium. Instead, it has a FF, and the porous medium only fosters the recirculation of heat from the exhaust gas to the unburnt fuel and air mixture. But in their work, the performance of PRB assisted cook-stove has also been compared with its conventional counterpart, Standard Burner (SB) (Fig. 2.1).

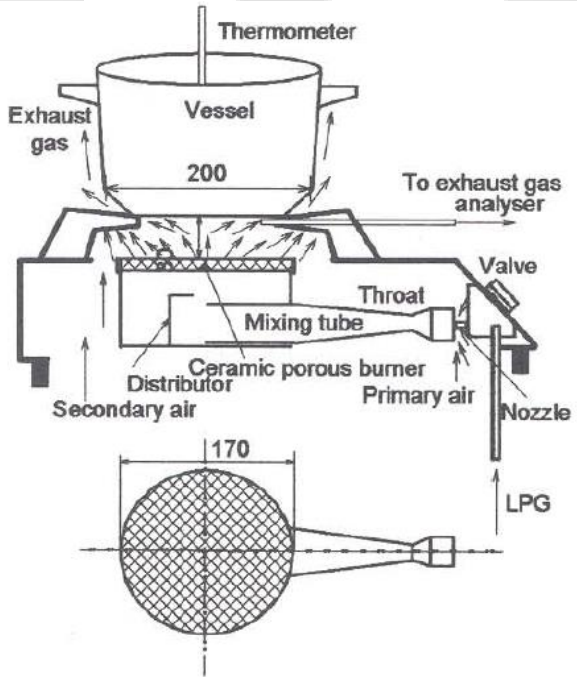

Fig. 2.1: PRB assisted LPG domestic cook-stove tested by Jugjai and Sanitjai (1996).

The PRB was made of ceramic and operated with LPG at a pressure of 0.14 bar for combustion rate of 1 to 3.5 kW. The thermal efficiency of SB varied between 52 to 56%, whereas PRB showed efficiency in the range of 59-65%. Emissions of CO and NO_x showed the opposite trend between SB and PRB. In SB, for lower combustion rate, CO was found to be

very low ~4-5 ppm, but after 2.5 kW, large increase of 153 to 2980 ppm was observed. Whereas, in case of PRB nearly constant emissions ~3000-3500 ppm was observed over the range of combustion rate examined in the experiment. So, it was assumed that, in the case of the PRB, the mixing process between the combustion flame and secondary air was not very proper. This might have adversely affected the performance of the PRB. The NO_x from PRB has limited to 4 to 22 ppm, and for SB these value was found as 22 to 102 ppm. Lower NO_x emissions in case of PRB might be associated with the reduced flame temperature and lower excess air.

Using PRRB design Jugjai and Sanitjai (1996) found that at 4 kW combustion rate, primary air has a maximum value of temperature ~210ºC, leading to a significant increase in burner efficiency compared to PRB design (Fig. 2.2). But in PRRB, at certain combustion rates, CO emission increases, whereas, in PRB, these values were nearly constant. Also, because PRRB operates at a higher flame temperature, it resulted in a sharp increase in NO_x emission as the combustion rate increased.

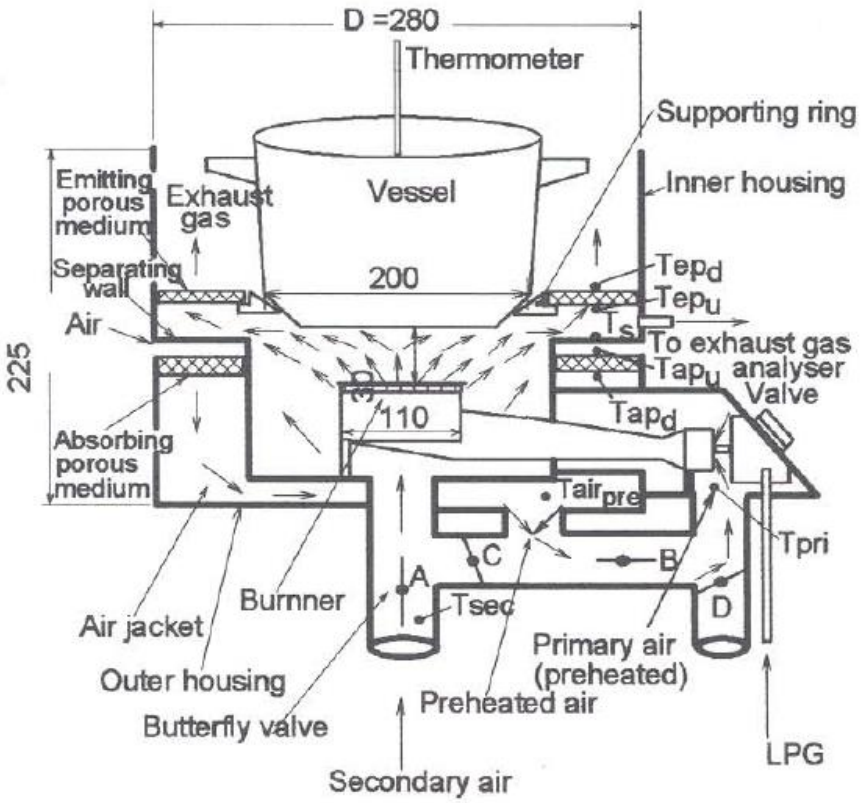

Fig. 2.2: PRRB assisted LPG domestic cook-stove developed by Jugjai and Sanitjai (1996).

Further using the same concept of PRRB, Jugjai and Rungsimuntuchart (2002) developed a semi-confined PRRB (Fig. 2.3) by using same ring burner as those in the Conventional Burner (CB), i.e., PRRB(CB). Compared to their previous design (Jugjai and

Sanitjai, 1996), they also scaled up the capacity of the burner from 5 kW to 30 kW, making it suitable for realistic applications, specially, to small-scale food processing industries. Throughout the tested capacity, the proposed PRRB(CB) was found to be about 12% higher efficient than that of the CB. The maximum thermal efficiency of 44% was observed with PRRB(CB). They further improved the thermal efficiency by replacing ring burner (CB) with the swirling central flame ring burner (SB), i.e., PRRB(SB). The PRRB(SB) yielded a maximum thermal efficiency of about 60%. The joint effect of efficient heat-recirculation and the swirling central flame was the reason behind the significant improvement in case of PRRB(SB). Over the studied range of burner capacity, CO and NO_x emissions were found to be higher for PRRB(SB). The relatively smaller port area and thus less amount of primary air leads to incomplete combustion, which becomes the main cause behind higher emissions.

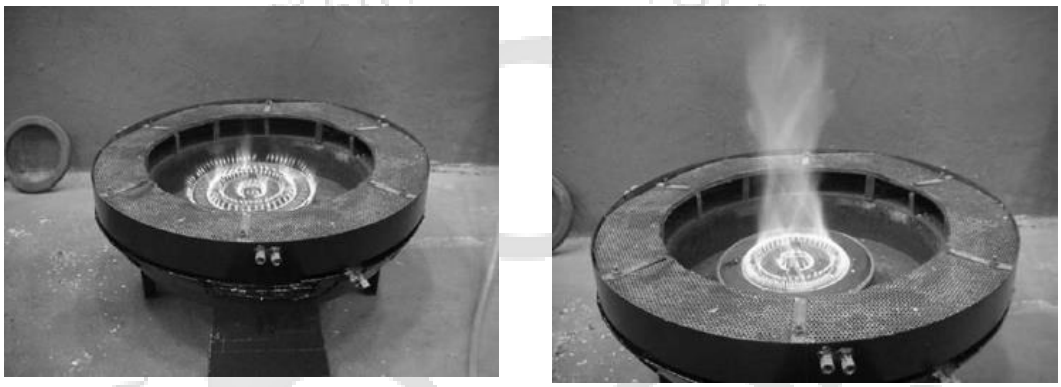

(a) (b)

Fig. 2.3: (a) Conventional radial flow flame (CB) and (b) Swirling central flame (SB) in the PRRB housing, developed by Jugjai and Rungsimuntuchart (2002).

Fig. 2.4: Cook-stove with PRB tested by Makmool et al. (2006).

Makmool et al. (2006) experimentally investigated the performance of 400 LPG domestic cooking burners with less than 5 kW capacity, in Thailand. The PRBs was also among the several types of burners analyzed (Fig. 2.4). Details of the burner are not mentioned in the paper. The PRB yielded relatively high average value of thermal

efficiency of about 47% but with relatively large average CO emissions of about 1,800 ppm.

In the above-discussed PRRBs, the porous media was only added to recirculate heat from exhaust gases to the fresh fuel-air mixture, but combustion inside porous media was not considered. Concept of submerged combustion in porous media was later used by Yoksenakul and Jugjai (2011). They developed a Self-aspirating Porous Media Burner (SPMB) for 23 to 61 kW by replacing CB, which are broadly used in the heating process in SMEs (small and medium scale enterprises). The packed bed in SPMB was formed with alumina spheres of a particle diameter of 15 mm, and LPG fuel was used in the experiment (Fig. 2.5). The SPMB required about 1-hour time to shift from the original diffusion free flame to the final steady-state submerged flame. Within the firing range (23-61 kW) equivalence ratio was ranged from 2.5 to 2.08. The radiation efficiency was found as high as 23%. The comparative emission performance highlights the ability of cleaner combustion of SPMB. Throughout the firing range, CO values were always found less than 200 ppm in SPMB. Whereas, in case of CB the CO was lower than 1000 ppm for firing rate lower than 38 kW and then sharply increased to 3800 ppm at a firing rate of 54 kW. For more than 32 kW firing rate, SPMB yields higher NO_x emission when compared to the CB. The highest NO_x yielded by SPMB was about 98 ppm, whereas, same was only 70 ppm in case of CB. Such behavior could be due to better combustion with comparatively high flame temperature in SPMB as compared to the CB.

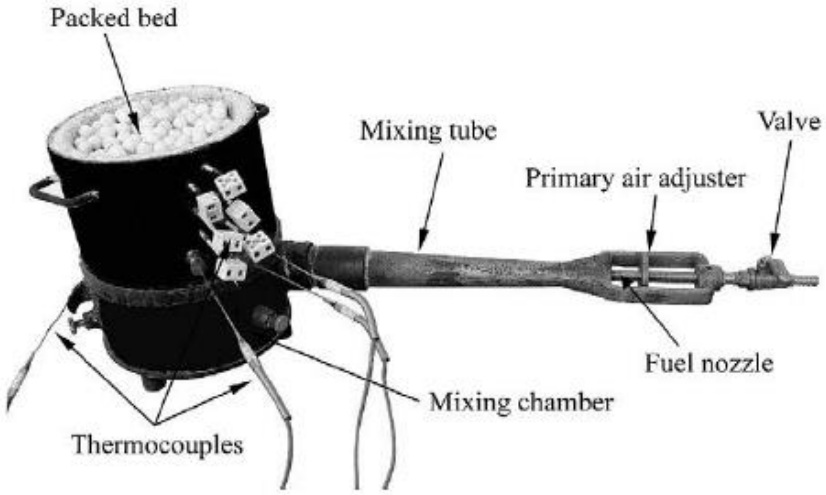

Fig. 2.5: The self-aspirating porous medium burner developed by Yoksenakul and Jugjai (2011).

Recently, Chaelek et al. (2019) coupled the concept of Jugjai and Sanitjai (1996) and Yoksenakul and Jugjai (2011) and developed a self-aspirating Annular Porous Medium Burner

(APMB) with Porous Radiant Recirculated Heater (PRRH) as shown in Fig. 2.6. The APMB was packed with alumina spheres of 10 mm diameter. The burner when operated between firing rates from 21 to 44 kW resulted in elevated preheated air, with temperatures of 136-252°C. The thermal efficiency of the APMB with PRRH attained a highest value of ~51%, and decreases the energy consumption by ~28.6% compared to the CB. Performance of the APMB with and without PRRH (Fig. 2.7), and CB are given in Table 7.

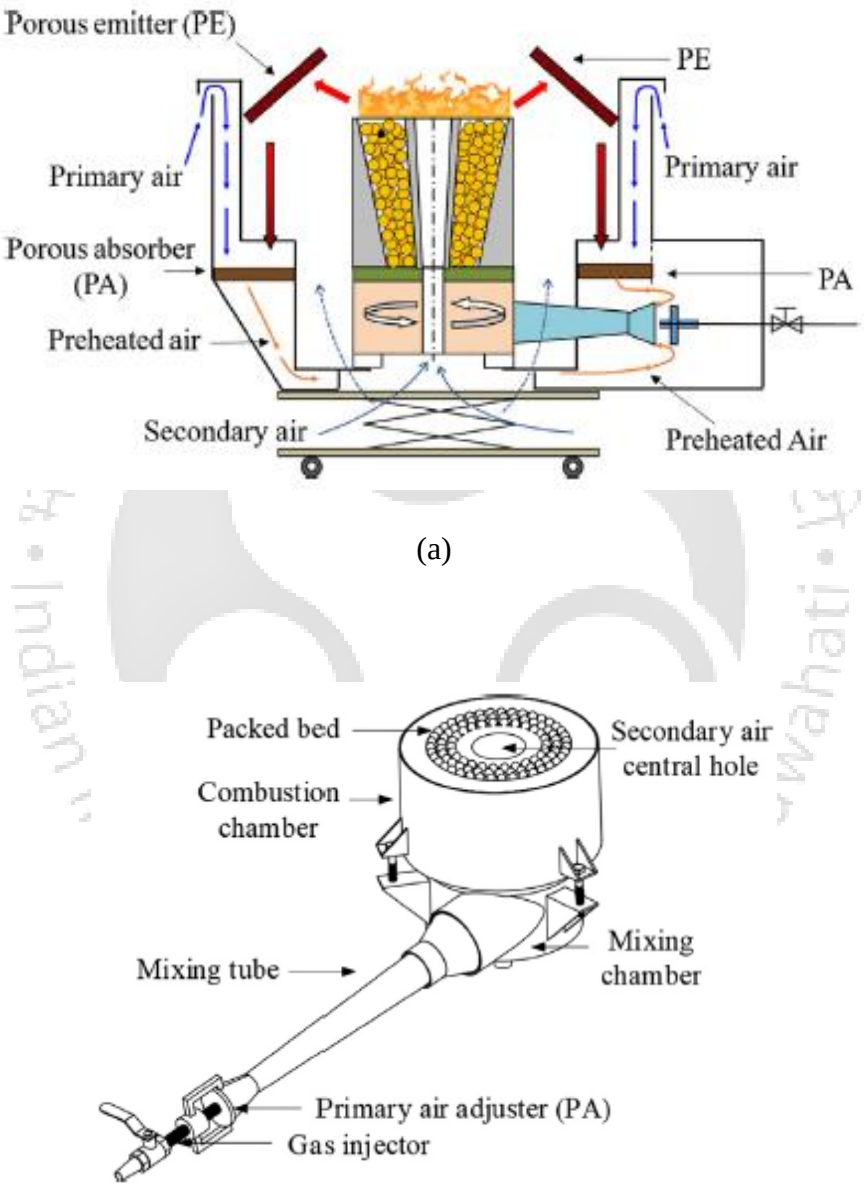

Fig. 2.6: Proposed structure of APMB (a) with PRRH and (b) without (PRRH), Chaelek et al. (2019).

Table 2.1: Thermal efficiency, CO and NO_x for firing rate of 21 to 44 kW, Chaelek et al. (2019).

Burner types	Thermal efficiency (%)	CO (ppm)	NO_x (ppm)
APMB with PRRH	50.8-44	5714-1177	24-46
APMB without PRRH	44-38	2103-942	38-51
CB	36.4-33.6	94-376	102-116

(a) (b)

Fig. 2.7: Flames: APMB impinging flame (a) without PRRH and (b) with PRRH, Chaelek et al. (2019).

An LPG operated compact PRB for cooking application has been extensively studied at Universiti Sains Malaysia (Mujeebu et al., 2011a, 2011b, 2011c, 2013). Mujeebu et al. (2011a, 2011b) developed two-layer PRBs for matrix (MSB) and surface (SSB) mode combustion. The SSB consisted of two layers of alumina foam, forming PZ (26 ppcm, 12.7 mm thick, porosity 86%) and CZ (8 ppcm, 12.7 mm thick, porosity 84%). Whereas, these layers in case of MSB was made up of porcelain foam (18 ppcm and 15 mm thickness) and solid Alumina balls of 30 mm size, respectively. The developed PRB (Fig. 2.8) was suitable for both surface and submerged combustion.

At 0.62 kW thermal load, the thermal efficiencies of MSB, SSB, and CB were found as 59%, 71%, and 47%, respectively. The CO and NO_x emission values for MSB was found as 21 ppm and 7 ppm, respectively. Whereas these values were 36 and 10 ppm, and 118 and 5 ppm for SSB and CB, respectively. The overall performance of SSB proved that it was as a suitable alternative to CB for cooking application. The loss of heat through radiation from the outer surface of the burner housing was calculated as 6.3% in the case of MSB and 8.0% in case of

SSB, which showed the scope for performance enhancement by design modification of the burner. Mujeebu et al. (2011c) also studied the impact of CZ thickness and alumina ball size (10, 20 and 30 mm) on MSB performance and found that the combination of porcelain foam (preheat layer) and one combustion layer made of 30-mm-size alumina balls provided the best performance. The radiation loss from these burner design was tackled by Ismail et al. (2013) with a micro-cogeneration system (Fig. 2.9). The developed design can simultaneously function as a cook stove and can also generate a voltage of 9.3 V through a thermoelectric cell.

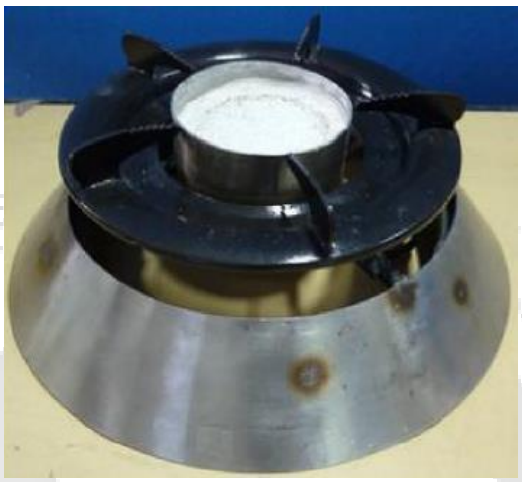

Fig. 2.8: The PRB developed by Mujeebu et al. (2011a).

Fig. 2.9: The micro-cogeneration system developed by Ismail et al. (2013).

A group of researchers from Indian Institute of Technology, Guwahati, India (Pantangi et al., 2007, 2011; Muthukumar et al., 2011, 2013; Mishra et al., 2015, 2018; Panigrahy et al.,

2016a, 2016b) had used the concept of PMC for domestic cook-stoves development, and following that, several prototypes have been designed and successfully demonstrated. They have been involved in performance improvement of the LPG cook-stoves over a decade. LPG has received higher prominence as it is used by a larger population. Several studies on LPG with PRBs have been conducted, and the usability of PRBs has been proved. The history of their various developments and the important findings are highlighted below. To begin, Pantangi et al. (2007) induced porous media (metal balls, pebbles, and metal chips) in the mixing chamber of a conventional cook-stove, fueled by LPG (Fig. 2.10). They removed the head of the CB and filled its mixing chamber with different combinations of PM. To minimize the heat losses, they insulated both the base of the bottom and the sides of the mixing chambers by employing ceramic wool. Thermal efficiencies of the PM incorporated LPG cook-stoves without insulation yielded comparable values with the conventional cook-stoves. Lesser CO concentration in the exhaust gas signified better combustion in case of PRB. The thermal efficiency raised to 72% when the side of the mixing chamber was covered by insulation and pebbles and metal balls were used as PM. A maximum thermal efficiency of 73% was resulted when pebbles were induced in the PZ and mild steel chips in the CZ. However, these burners have failed to provide the stable operation.

Fig. 2.10: Conventional cook-stove burner filled with (a) metal balls and (b) metal chips as porous media, Pantangi et al. (2007).

In the work explained above, only preliminary experimentations were performed, and retrofitting of the CB was undertaken. Later, Pantangi et al. (2011) developed a two-layer PRB consisting of SiC foam (CZ) and Al_2O_3 balls (PZ), working in power input range of 0.8-1.8 kW and equivalence ratio of 0.3-0.7 (Fig. 2.11). Their group found that the thermal efficiency of the burner was strongly dependent on the equivalence ratio and diameter of the burner. Maximum 68% thermal efficiency was achieved for a burner with diameter 80 mm, which was 3% higher than that of a conventional LPG cook-stove. Unlike the conventional LPG cook-stoves, where the CO and NO_x emissions ranged between 400-1050

mg/m^3 and 162-216 mg/m^3, respectively, for the one with PRB, the same were in the ranges of 25-350 mg/m^3 and 12-25 mg/m^3.

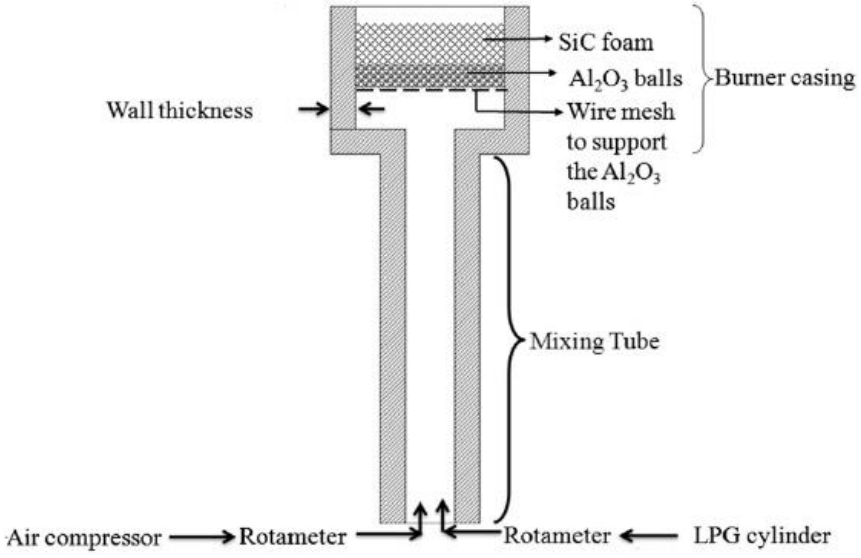

Fig. 2.11: Schematics of the PRB developed by Pantangi et al. (2011).

Later, Muthukumar et al. (2011) tested a similar LPG based PRB but employed a perforated ceramic plate in place of Al_2O_3 balls in the PZ and showed that the thermal efficiency of the stove could be improved to 71%. The burner diameter was equal to the one that yielded better efficiency in Pantangi et al.'s (2011) work. This efficiency was acquired for an equivalence ratio of 0.68, 1.24 kW power intensity, and 31ºC ambient temperature. The CO and NO_x emissions were found to be always below 16 ppm and 0.2 ppm, respectively. Whereas, the respective values for the CB were in the range of 50 to 225 ppm and 2 to 7 ppm, respectively. From the comparison of Pantangi et al.'s (2011) results with those of Muthukumar et al. (2011), it can be concluded that use of ceramic block as PZ is better than alumina balls forming a PZ. The stable range of equivalence ratio was also found to be shifted slightly (ϕ = 0.5-0.8 against ϕ = 0.3-0.7 in the former, Pantangi et al.'s (2011)) and the peak thermal efficiency was achieved at an equivalence ratio of 0.68. Another noteworthy observation regarding influence of the surrounding temperature on the thermal efficiency of PRB was also made by Muthukumar et al. (2011). At similar operating conditions, a 10% improvement in efficiency was achieved with varying surrounding temperature from 18.5ºC to 31ºC. Results suggested that for comparison of thermal efficiency of burners, the effect of surrounding temperature has to be taken into consideration. Further, Muthukumar and Shyamkumar (2013) extended Muthukumar et al.'s (2011) works (Fig. 2.12) and studied the effect of porosity of CZ of the same burner. In this case, the porous matrices of 90 mm diameter were chosen. Like in Muthukumar et al. (2011), the PZ is composed of a ceramic matrix with 40% porosity and thickness of 10 mm and the CZ

is formed with a SiC foam having thickness of 20 mm. However, in this investigation, the porosity of the SiC varied from 80 to 90%. The thermal efficiency and CO and NO_x emissions were experimentally determined for equivalence ratios and powers ranging from 0.54 to 0.7 and 1.3 to 1.7 kW, respectively. They observed that with porosity of 90%, the burner delivered maximum thermal efficiency of 75%, at equivalence ratio of 0.54 and input power of 1.3 kW. For the SiC foam with 90% porosity, NO_x emissions ranged from 0 to 0.75 mg/m^3 and CO emissions from 12 to 124 mg/m^3. Conventional LPG cooking stoves emit 4 to 7 mg/m^3 of NO_x and 250 to 650 mg/m^3 of CO, for same input power range.

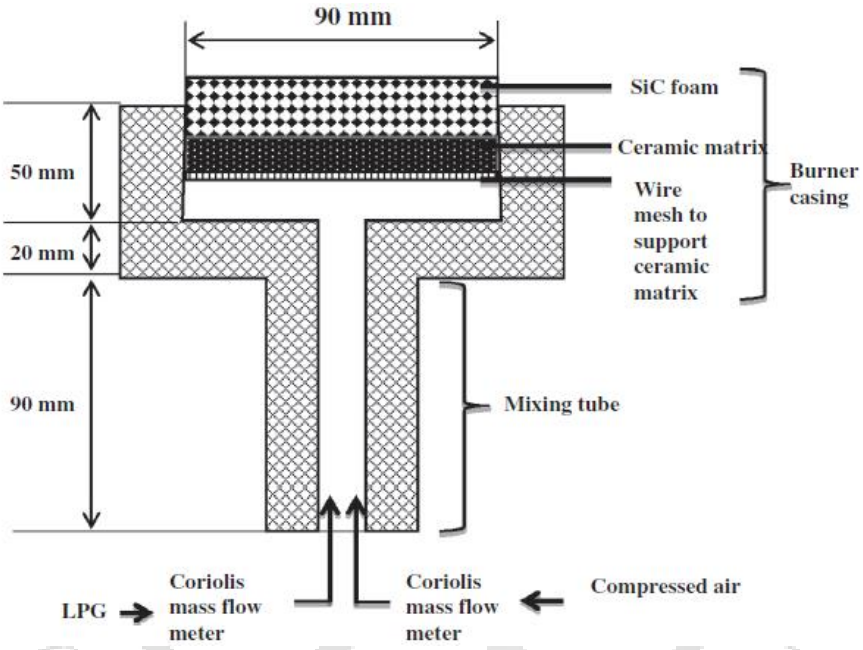

Fig. 2.12: Schematic of PRB used by Muthukumar et al. (2013).

Mishra et al. (2015) scaled up the previously developed two-layer PRBs by Muthukumar and Shyamkumar (2013) to a power range of 5-10 kW for medium-scale LPG cooking applications (Fig. 2.13). For this new burner, the diameter of the porous media was chosen as 120 mm. They concluded that the burner provided submerged combustion within the equivalence ratio range of 0.54-0.72. At an input power of 5 kW and equivalence ratio of 0.58, the reported thermal efficiency was 58% which was 28% more than that of the CB with the same input power. With an increase in the thermal load decreasing trend of thermal efficiency was observed. They also observed that the loading height (viz., the distance between the top surface of the PRB and the vessel) of 30 mm results as optimum. Below this height, the quantity of diffusion air required for combustion is partly mitigated and beyond this distance, the losses by radiation and

convection through the gap between the radiation shield and bottom surface of the utensil increases. Exhaust emission comparison of CB and PRB highlights the potential of cleaner combustion of PRBs. In CB, they found that with increase in power input, both CO and NO_x concentrations increases. Similarly, in PRB also the CO and NO_x emission is found to rise with increase in both equivalence ratio and thermal load.

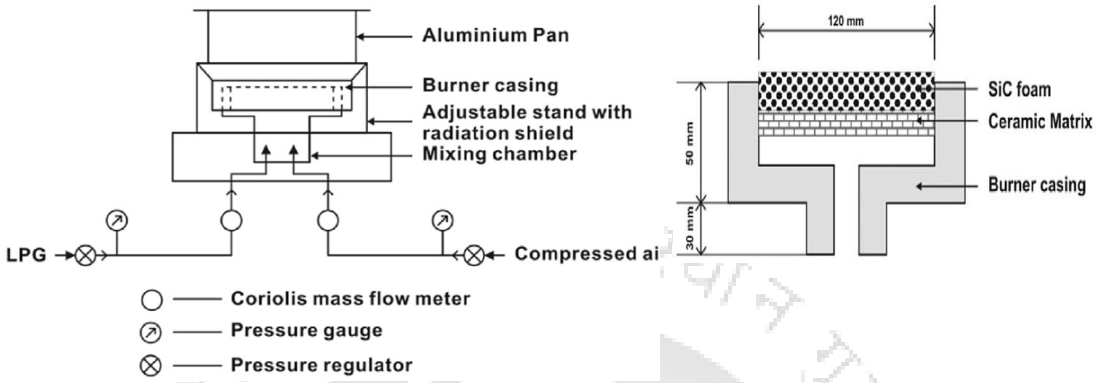

(a) (b)

Fig. 2.13: Schematic of (a) the experimental set-up and (b) the PRB (Mishra et al. (2015)).

Above porous media based cooking stoves (Pantangi et al., 2007, 2011; Muthukumar et al., 2011, 2013; Mishra et al., 2015) were not guided by numerical studies, and so, it required a number of experimental trials for stable combustion. To overcome the above problem, computational modeling of LPG combustion inside porous media was done by Panigrahy et al. (2016a, 2016b) by using the same burner as Pantangi et al.'s study (2007). The studied burner (dia. 80 mm) comprised of CZ of SiC matrix with 90% porosity, and the PZ was made of 3 mm diameter alumina balls. In the numerical analysis (finite volume method) temperature distributions, flammability limits and pollutant emissions for various equivalence ratios and thermal power have been analyzed. Effect of SiC matrix thickness, preheater thickness, solid-phase conductivity and scattering albedo on CO emissions and radiative flux have also been studied. They examined the impact of varying thickness (15 to 40 mm) of CZ and found that for the similar condition of equivalence ratio (0.5) and input power (3-5 kW), the burner with CZ of thickness 15 mm resulted in greater thermal efficiency than the one with a thickness of 30 mm. This is because, with increase in CZ thickness, the radiative heat flux increases, and consequently, the preheating temperature also increases.

Table 2.2. Specifications, operating range (kW) of investigated cooking burners, Panigrahy et al. (2016a).

Designation	Thickness, mm		Equivalence ratio				
			0.4	0.5	0.6	0.7	0.8
	PZ	CZ	Operating range (kW)				
CB1	12	15	0.62-1.65	0.77-5.15	5.13-8.31	8.47-11.70	12.10-15.63
CB2	12	20	0.68-2.27	0.85-6.01	5.64-9.24	8.95-12.77	12.91-16.59
CB3	12	30	0.55-3.23	3.0-6.18	6.16-9.44	8.95-12.77	12.91-16.59
CB4	12	40	0.55-3.23	3.26-5.75	6.16-9.75	9.55-13.49	13.19-16.99
CB5	20	15	0.55-3.10	2.57-4.29	4.92-8.41	8.47-11.70	12.23-15.63

Table 2.3. Range of CO emission as a function of thermal input and equivalence ratio, Panigrahy et al. (2016a).

Designation	CO emission (ppm)			
	0.4	0.6	0.7	0.8
CB1	3.24-5	19.14-68.23	78.27-255.53	478.85-881.49
CB2	1.4-1.72	16.06-56.86	51.69-174.02	310.48-693.98
CB3	0.25-1.38	7.22-35.74	26.44-107.35	163.36-427.08
CB4	0.12-1.69	4.33-35.19	18.66-111.74	154.65-357.73

Further, Al_2O_3 balls of 3 mm diameter used by Panigrahy et al. (2016a, 2016b) in preheat zone resulted in lower temperature fluctuations than 5 mm diameter balls used by Pantangi et al. (2007). Various results found from Panigrahy et al.'s (2016a, 2016b) studies which show the impact of various parameters on PRB performance are given in Table 2.2-2.5.

Table 2.4. Thermal efficiency, Panigrahy et al. (2016a).

Power (kW)	Thermal efficiency (%)	
	CB1	CB3
1	71.15	-
2	70.21	-
3	67.43	65.97
4	64.32	63.22
5	61.59	60.8

Table 2.5. Effect of scattering albedo and burner conductivity on CO emission and radiative flux, Panigrahy et al. (2016a).

Power (kW)	CO emission (ppm) and radiative flux (MW/m^3), (CB3 and equivalence ratio 0.7)							
	Scattering albedo				Thermal conductivity (W/m-K)			
	0.8		0.4		2.721		27.21	
	ppm	MW/m^3	ppm	MW/m^3	ppm	MW/m^3	ppm	MW/m^3
9	27.22	17.42	19.08	27.02	25.76	17.42	20.03	36.87
10	41.95	20.63	32.93	31.03	41.22	20.55	34.92	38.66
11	92.45	31.94	52.02	34.24	92.16	31.75	64.12	40.19
12	110.08	32.84	62.66	36.66	109.91	32.66	78.99	42.52

It is to be stated that in the above studies, the air supply to the burner was given through a compressor and therefore research activities were intensified to eliminate this component to make the device less complicated or more user-friendly. In this attempt, the same group of authors was able to unveil a new design that works on self-aspiration mode, which was achieved by changing fuel supply pressure, and modifying orifice, mixing chamber, PZ and burner casing dimensions. The details of the constructions are available in the authors' recently filed patents (Mishra et al., 2013, 2015, 2015a). They developed LPG operated cook-stoves for domestic (1-3 kW) as well as medium scale cooking operation (5-15 kW). The developed domestic PRB (Mishra and Muthukumar, 2018) consists of two layers of ceramic matrix of 80 mm diameter (PZ: Al_2O_3 thickness 10 mm with porosity 30% and CZ: SiC thickness 20 mm with porosity 90%). Details of the burner are shown in Fig. 2.14.

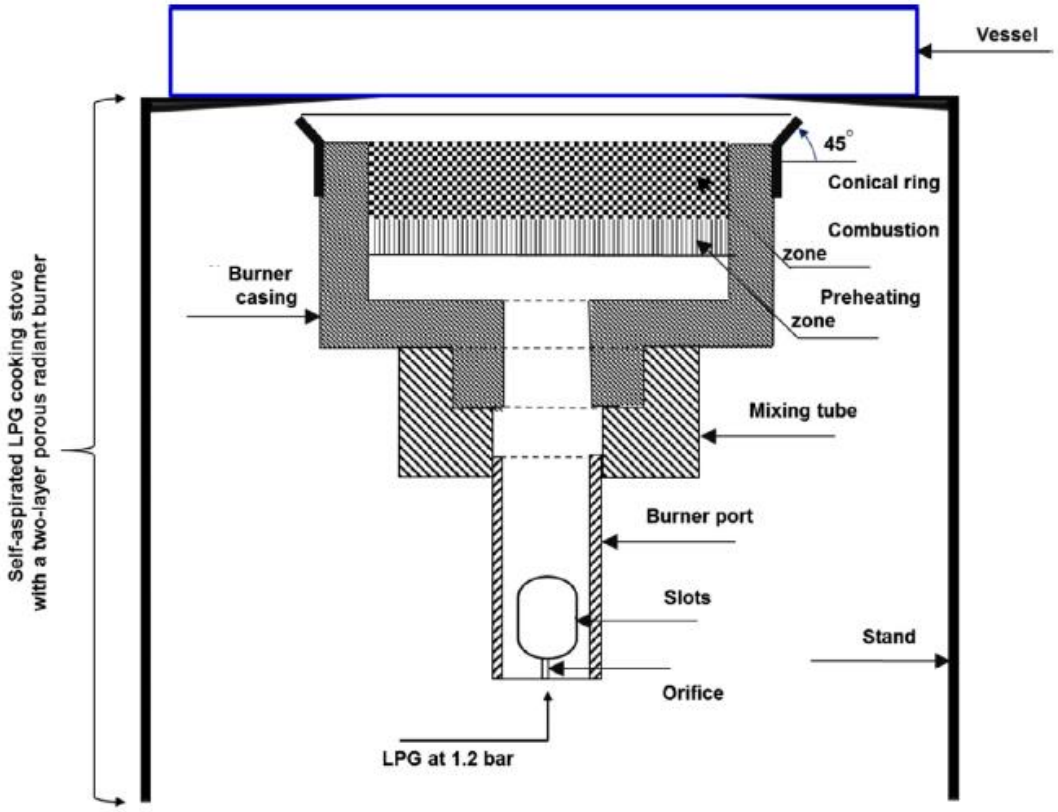

Fig. 2.14: Details of the PRB developed by Mishra and Muthukumar, 2018.

For input power range of 1-3 kW, stable burner operation (without flash-back (FB) and flame lift-off (FL)) has been tested for a combination of orifice and port diameter. From the tested combination, for all port diameters, orifice of 0.35 mm shows most stable operation (Table 2.6). With enlargement of port diameter or decrease in orifice diameter, entrainment of air has been improved, but, the flexibility in change of port and orifice diameters are limited because it affects the stability of the burner. The axial and radial temperature profile, thermal efficiency and emission (CO and NO_x) performance for all the stable cases (Table 2.6) have been experimentally analyzed and compared with its conventional counterpart. The temperature measurement indicates that unlike conventional LPG burner, where the heat is more concentrated at the center of the flame, the distribution of heat flux in PRB is quite uniform. The maximum thermal efficiency has been found as 75.1%, which is about 12-15% higher than the CB. Similarly, for PRB, the maximum values of CO and NO_x emissions have been measured as 140 ppm and 3.5 ppm, respectively. Whereas, the same is as high as 550 ppm and 25 ppm for CB.

Table 2.6. Stability analysis of PRB for different orifice and port diameters, Mishra and Muthukumar, 2018.

S. No.	Port internal diameter in mm	Orifice diameter in mm		
		0.25	0.35	0.50
1	17	FL	Stable	FB
2	19	FL	Stable	Stable
3	21	FL	Stable	Stable

Similarly, a comprehensive experimental analysis has been carried out for investigation of stability and performance of PRB based medium-scale LPG cooking stove (Mishra, 2015). Schematic of self-aspirated medium-scale LPG cooking stove with PRB is shown in Fig. 2.15.

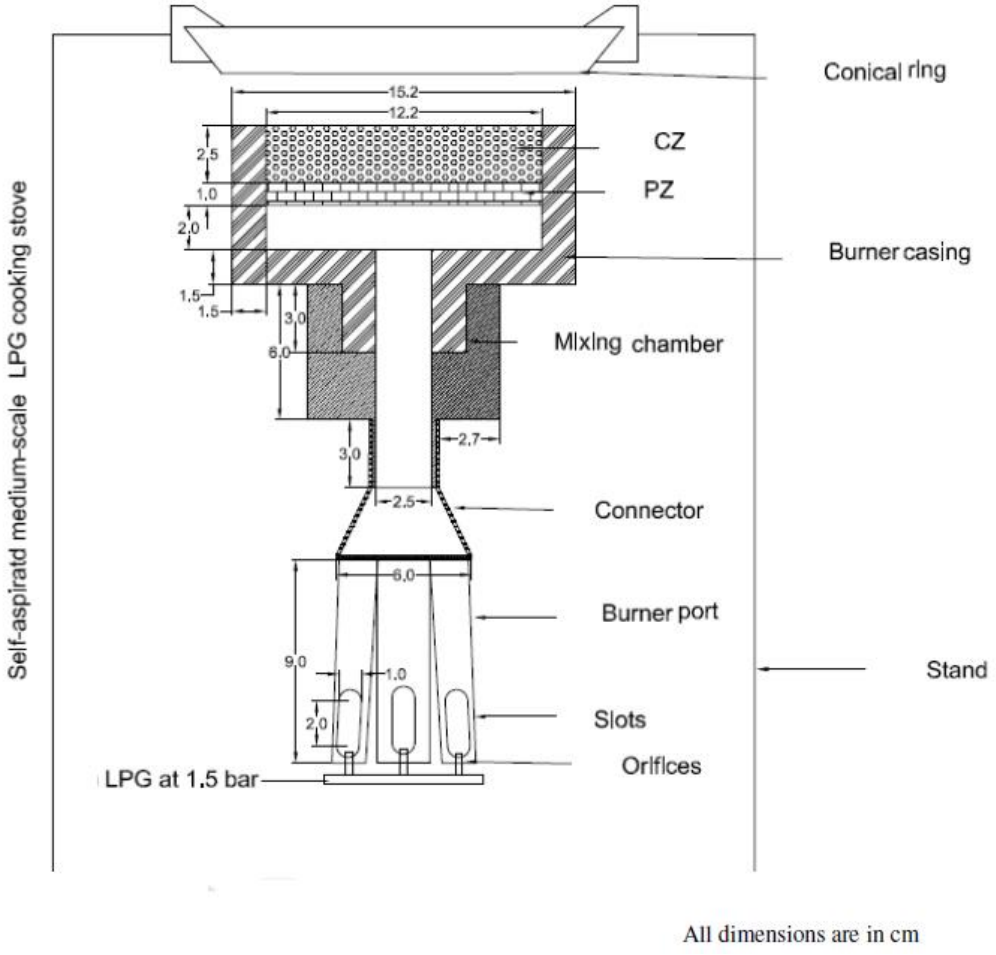

Fig. 2.15: Schematic of self-aspirated medium-scale LPG cooking stove with PRB developed by Mishra, 2015.

In case of domestic PRB, the best thermal performance was achieved with a port diameter of 21 mm and therefore, with same port diameter stability analysis was carried out for orifice diameter of 0.25, 0.35, 0.5 mm. For the power range of 5-15 kW, orifice diameters of 0.25 and 0.35 mm showed stable operation, whereas, in 1-3 kW (Mishra and Muthukumar, 2018) the same was 0.35 and 0.5 mm. For getting higher power rating of 5-15 kW, burner diameter was increased to 120 mm, the porosity of PZ was reduced to around 7-8 %, and thickness of CZ was increased to 25 mm. Similarly, LPG supply pressure was also increased from 1.2 (Mishra and Muthukumar, 2018) to 1.5 bar. The developed cook-stove showed ~22-28 % higher thermal efficiency and maximum reduction of ~84% and 90% in CO and NO_x emission, respectively. Both thermal efficiency and emission performances were found to be decreasing with increasing input power.

Wu et al. (2014) had tested the viability of the LPG operated flat flame burner and found it to be highly efficient and clean for domestic cooking application. The flame stabilized on the top surface of the porous matrix (Fig. 2.16), which allowed higher flame temperatures and therefore, higher heat transfer. Within operating range, the premixed flame layer is flat and closer to the metal porous plug. The metallic porous media comprised of small bronze pellets and formed a plug with a diameter of 50.8 mm and a thickness of 3 mm. The average diameter of the bronze pellet was 0.5 mm and had a porosity of 0.237.

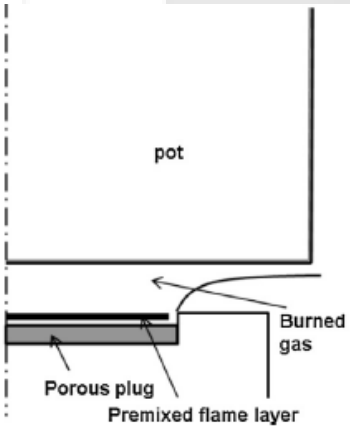

Fig. 2.16: The flat flame burner developed by Wu et al. (2014).

Compared to a CB, the ratio of maximum to minimum output power with a stable flame (turndown ratio) was found to be higher in flat flame burner. For operating range, flat flame burner showed a turndown ratio of 34 to 6.5, whereas same was only 6.2 to 3.17 in case of CB.

With decrease in equivalence ratio, turndown ratio reduced for both the burners. The measured thermal efficiency at input power of 1 kW, was found between 41% to 56% for flat flame burner (equivalence ratio 1 to 0.7), whereas, same was only 38 to 49% in case of CB (equivalence ratio 1 to 0.9). Similarly, emission performance (NO_x and CO) were generally better than those of CB. Another important observation of lower impact of distance between the exit of the burner and the pot/pan surface on efficiency and emission has been made in case of flat flame burner.

In another study, Herrera et al. (2015) had evaluated the combustion stability and thermal efficiency of an LPG operated PRB cook-stove (Fig. 2.17). In this work, thermal efficiency has been measured in two different modes. The second mode is typical in this study and not found in any other work. The first mode was termed as "radiation-convection" mode, where the vessel was placed at 5 cm above the ceramic foam surface and the vessel was heated by radiation from the surface and convection from flue gases leaving the burner. The second mode was termed as "conduction" mode, as it adds the conduction mechanism to the heat transfer since in this case the vessel is directly in contact with the ceramic foam surface. The PRB consists of two layer of different porous media as shown in Fig. 2.17.

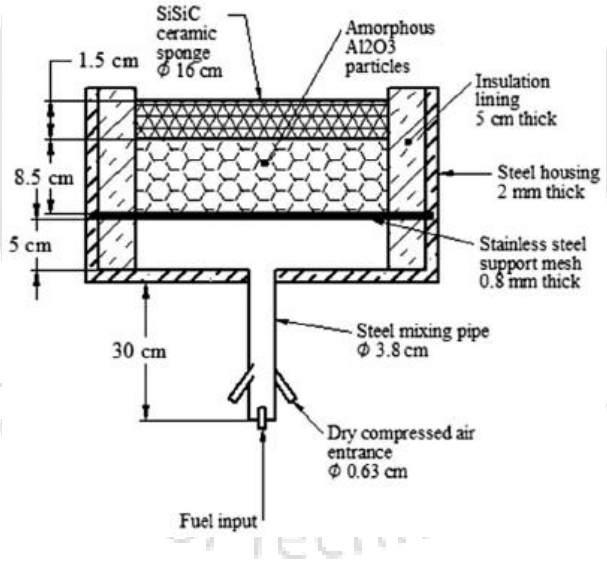

Fig. 2.17: Schematic diagram of the PRB developed by Herrera et al. (2015).

They found that the upper and lower stability limit of equivalence ratio nearly follow a linear trend up to 154 kW/m^2 and then a decrease in the stable range was observed with increase in heat input rate. A similar trend was also reported by Pantangi et al. (2011) and Muthukumar and Shyamkumar (2013). The thermal efficiency found by Herrera et al. (2015) in the "radiation-convection" mode was between 15.7% and 23.6%, which was lesser than the average thermal efficiency of the CB. But with "conduction" mode significant efficiency improvement between 7% to 14% was observed. Up to 154 kW/m^2 heat input rate, CO concentration was

lower than 25 ppm, but for higher heat input rate due to moderate lift-off and quenching on the surface of the burner, sudden increment was observed.

Recently, Pradhan and Mishra (2018) developed an LPG operated self-aspirated PRB for cooking application (Fig. 2.18). They studied the performance variation with shape of the burner viz., circular and square shape. In the power range of 0.5-2 kW, experiments were conducted with five different fuel velocities viz., 0.4 m/s, 1 m/s, 2 m/s, 3 m/s and 3.6 m/s. For experimented velocities, thermal efficiency ranges between ~68-71% for circular PRB, whereas, efficiency for square PRB was found marginally lower than that of circular PRB. Compared to CB, a maximum of 7% improvement in thermal efficiency was observed. The CO and NO_x emissions for both the PRBs were limited to 44-54 ppm and 12-40 ppm, respectively. Corresponding values for CB was found as 125-228 ppm and 73-101 ppm. Emissions for square PRB were slightly more than that of the circular one.

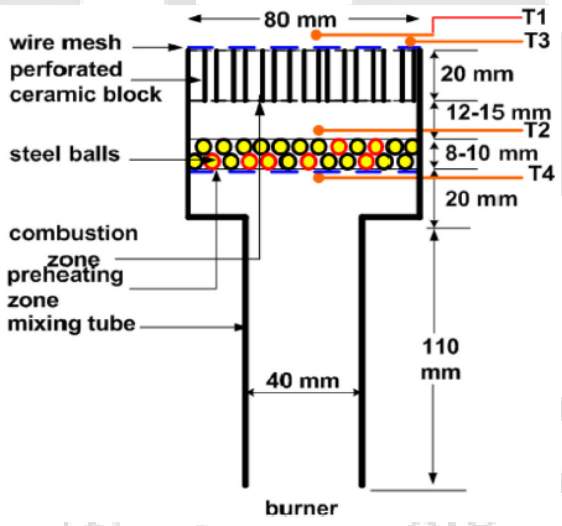

Fig. 2.18: Schematic of self-aspirated PRB tested by Pradhan and Mishra (2018).

2.3 State of art on pressurized kerosene cook-stove with Porous Radiant Burner (PRB)

Liquid fuels used for the cooking application are alcohols (e.g. ethanol, methanol), plant oil, and those generated from fossil fuels (e.g. kerosene, also known as paraffin). Burner based on FFC is widely available for kerosene, so application of PMC has been focused towards kerosene stoves only. Liquid fuel combustion in PRB is little tricky due to the need for complete vaporization of the fuel and then combustion of the vaporized fuel.

Use of right vaporization technique and optimum distance between the vaporizer and the burner are the two essential criteria for stable combustion. Study of PMC technology applied to conventional pressurized kerosene stove are also very limited. The very first investigation was carried out by Kakati et al. (2007), where they examined the thermal efficiency, kerosene consumption rate and emission of domestic burner with porous inserts of pottery clay, sodium silicate, and sawdust and compared the results with the conventional one. Later, Sharma et al. (2009) investigated the performance of same stove (Fig. 2.19) by replacing the inserts with four different porous materials, viz. silicon carbide (SiC), zirconia (ZrO_2), wire mesh roll filled with metal balls and alumina (Al_2O_3). They found an optimum value for mass flow rate (130-140 g/hr) and vessel size (260 mm diameter) which resulted in increased thermal efficiency for all the inserts with a maximum of 7% increase with SiC inert. Further, their observation showed that the insulation of the heat shield ring varies the efficiency by 4 to 5%. Sharma et al. (2011) further modified the stove by incorporating ceramic heat shield of low conducting and radiating alumina (Al_2O_3), which resulted in a 15% increase in thermal efficiency.

Fig. 2.19: Kerosene pressure stove studied by Sharma et al. (2009).

Sharma et al. (2016a) also extended their research by changing the burner geometry. Kerosene stove consisting of two layers of porous matrix of alumina (Al_2O_3) balls and honeycomb structured silicon carbide (SiC) was experimented with three different shapes of burner casing, viz. straight cylindrical, taper and conical. Performance with conical burner casing was found to be the best of all with 10% increase in thermal efficiency at air and fuel flow rate of 120-130 lpm and 220 g/hr, respectively. They also found that for lower emission and higher thermal efficiency thickness of the CZ should be 20 mm. Additionally, they stated that further improvement in the thermal efficiency

could be obtained by changing the vaporization technology and assembly of burner housing. In the same burner, the effect the diameter of the burner on thermal efficiency, emission, and temperature distribution at various air and fuel flow rates was studied by Sharma et al. (2016b). They worked on the optimization of the PM configurations, and a combination of SiC (10 ppi, 20 mm thickness) and Al_2O_3 (2 layers with 7 mm diameter ball) was found to fulfill the requirements with respect to complete retention of the flame within the media. The burner with 70 mm diameter proved to be the best among the three studied burner diameters of 60 mm, 70 mm and 80 mm and resulted in a maximum thermal efficiency of 50%. The burner was also able to produce very low emissions, in the range of 1.2 ppm NO_x and 44 ppm CO. Recently, with new vaporizer design Sinha (2017) developed a self-aspirated PRB for kerosene pressure stove (Fig. 2.20) for the input power range of 1.5-3 kW. With newly developed PRB, they found ~15% improvement in thermal efficiency. The negative impact of input power can be seen as efficiency reduces from 64.3% to 55.5% for input power variation of 1.5 to 3 kW (Sinha and Muthukumar, 2019). They also optimized the vessel diameter and found 270 mm as optimum for developed PRB application. Details of vaporizer design and performance can be found in their recently filed patent (Mishra et al., 2016; Muthukumar et al., 2018).

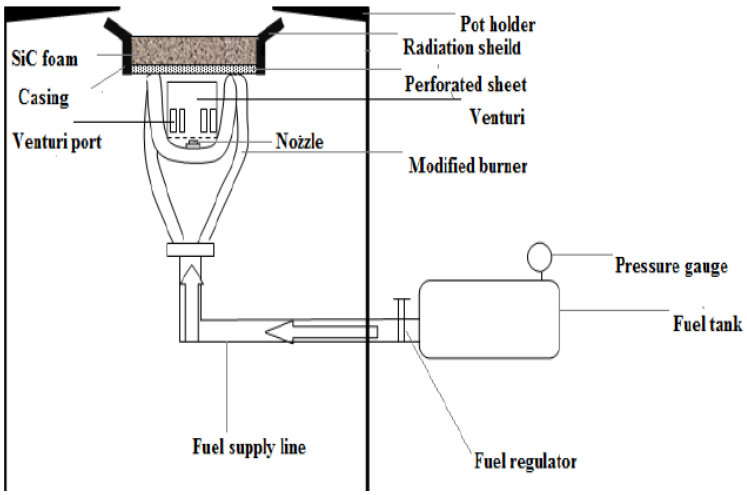

Fig. 2.20: Kerosene pressure stove with PRB developed by Sinha and Muthukumar (2019).

In the following two sections, available literature related to the development and performance assessment of cook-stoves for biogas and plant oils application are presented. As mentioned earlier, cook-stoves with PRB are not yet reported for these

fuels. Whereas, in few works, combustion characteristics of biogas and plant oils in porous media were studied. Literature available for biogas and plant oil cook-stoves were based on FFC. Findings from these works are summarized in the respective sections of biogas and plant oil cook-stove developments.

2.4 State of the art on biogas cook-stove developments

Development of biogas cook-stoves started in the late 1970s, which are categorized by FFC. Chandra et al. (1991a, 1991b) presented detailed hydro-dynamical modeling for a biogas burner and provided explicit expressions for the burner design parameters. They tested different available biogas cook-stoves and found that there was inconstancy in design and performance. They performed parametric investigation and optimized flow pressure, pan-size for its position over the burner head. The result showed optimum performance at 2.2-4.2 cm position over the burner head and 1.016-1.019 bar flow pressure. A similar range of thermal efficiency was also reported by Mahin (1992). Biogas burner design guide with 1.5 kW input power and 55% thermal efficiency was presented by Fulford (1996). Smith et al. (2000) studied the domestic biogas cook-stoves available in India and estimated the Nominal combustion efficiency (NCE), Heat transfer efficiency (HTE) and Total energy efficiency (TTE) as 99.5%, 57.7%, and 57.4%, respectively. Above mentioned efficiencies are elaborated in equations given below, where PIC is products of incomplete combustion.

$$NCE = \frac{1}{k+1} = \text{fraction airborne fuel carbon release as } CO_2 \quad \ldots\ldots. \ (2.1)$$

$$k = \frac{PIC}{PIC + CO_2} \quad \ldots\ldots. \ (2.2)$$

$$HTE = \text{fraction of heat released from fuel going into the pot} \quad \ldots\ldots \ (2.3)$$

$$TTE = \text{fraction of fuel energy going into the pot} \quad \ldots\ldots \ (2.4)$$

Similarly, Center for Energy Studies, Nepal, presented a study report for biogas cook-stove in Nepal and found efficiency of ~49.5%, whereas was ~45% for India (CES/IOE, 2001). Itodo et al. (2007) developed a domestic biogas cook-stove and assessed its performance with boiling water, cooking rice, and beans. For above cases, biogas consumption and thermal efficiency were found as 0.69, 2.81, 4.87 m^3/min and 20, 56, 53%, respectively. The Netherlands Development Organization (SNV) presented a test

report on biogas cook-stove from some Asian and African countries by using three different test standards viz. Chengdu Energy Environment International Cooperation (CEEIC), China, Department of Renewable Energy Sources (DRES), India, and Kiwa Gastec Certification (GASTEC), Apeldoorn (Khandelwal and Gupta, 2009). The reported cook-stove from these countries are shown in Fig. 2.21 and performance (thermal efficiency and CO emission) are given in Table 2.7.

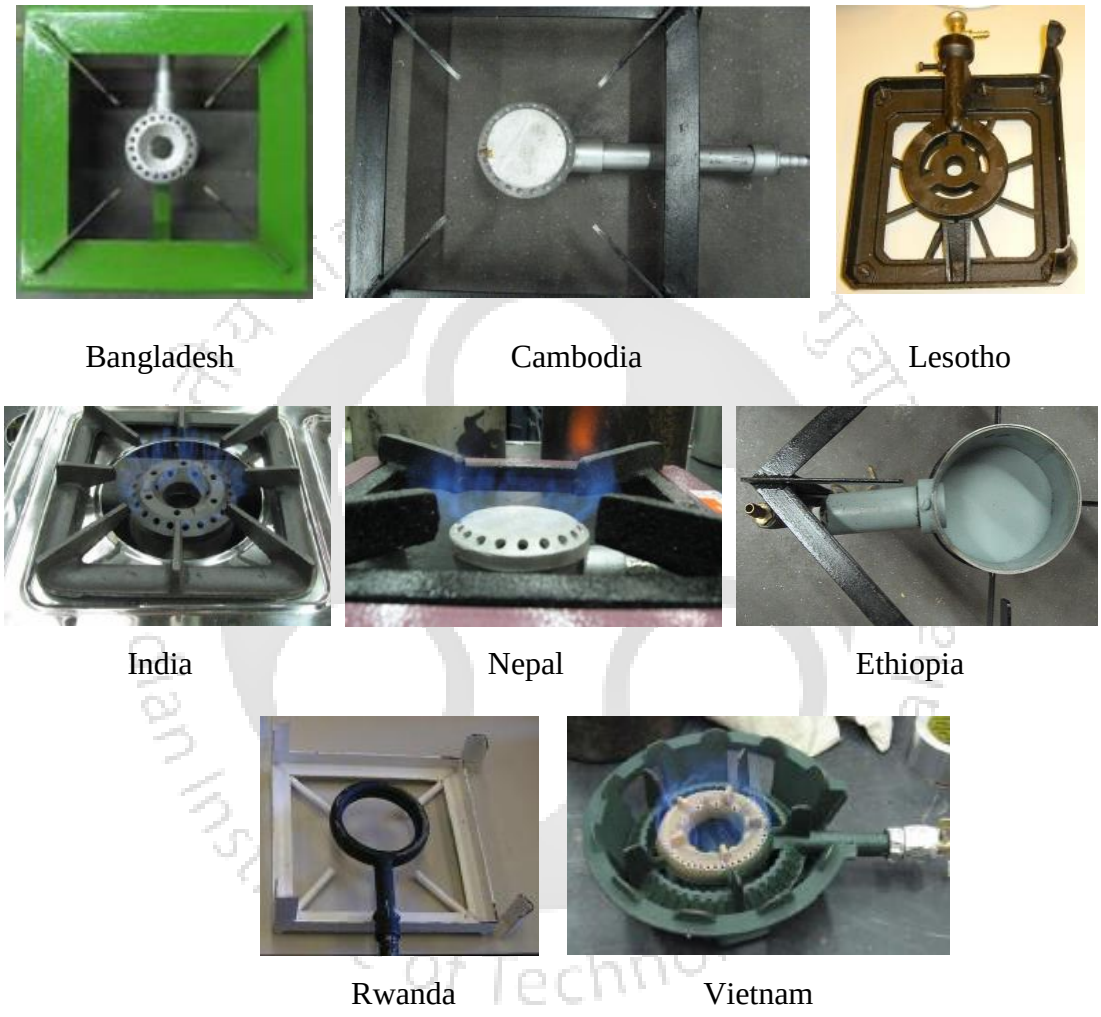

Fig. 2.21: Biogas cook-stoves from Asian and African countries (Khandelwal and Gupta, 2009).

Kurchania et al. (2010, 2011) developed biogas stoves for domestic and community cooking application. For the community cooking stove operating and performance parameters were, Input power = 5.3 kW, inlet pressure = 747 N/m^2 and thermal efficiency = 43.96% (Kurchania et al., 2010). Similarly, for domestic cook-stove, these values were 2.3 kW, 980 N/m^2, 60.1% (Kurchania et al., 2011). Kebede and Kiflu

(2014) developed burner for injera baking application and the reported biogas consumption rating and input power were 0.93 m^3/h and 5.7 kW, respectively. The measured thermal efficiency was only 25%. Obada et al. (2014) developed a biogas burner for domestic cooking application and found thermal efficiency with water boiling test (WBT) and rice cooking. Biogas consumption rate and thermal efficiency for WBT were 21% and 0.47 m^3//hr, respectively. Similarly, for rice cooking same were 60% and 2.87 m^3//hr. Tumwesige et al. (2014) studied eight different biogas stoves available in Sub-Saharan Africa and found that these stoves were poorly designed. Input power and thermal efficiency of these stoves were between 3.9-6.8 kW and 20-28%, respectively. Syamsuri et al. (2015) studied the impact of burner shape viz., regular and cyclone on thermal efficiency. Maximum 58.4% of thermal efficiency at 1.53 kW was achieved with cyclone shaped burner.

Table 2.7: Comparison of thermal efficiency and CO emission of the biogas cook-stove of Asian and African countries (Khandelwal and Gupta, 2009).

Countries	Thermal efficiency (%) and CO emission (ppm)	CEEIC	DRES	GASTEC
Bangladesh	%	57	64.5	52.1
	ppm	>1180	5300	2800
Cambodia	%	55	48.1	45.6
	ppm	>1180	2200	1700
Ethiopia	%	53	40.5	41.2
	ppm	>1180	4350	4463
India	%	53	54.5	53.9
	ppm	>1180	2840	2900
Lesotho	%	41	45.1	45
	ppm	28	4350	8
Nepal	%	55	42.1	42.2
	ppm	>1180	4350	2140
Rwanda	%	60	53.8	54.6
	ppm	>1180	2250	2200
Vietnam	%	39	21.2	31.5
	ppm	>1180	4350	1100

There are very few numerical works reported in which the researchers were tried to optimize biogas cooking burner design. By using CFD and Genetic Algorithm, Jadhav and Sudhakar (2015) targeted to optimize dimensions and fuel flow rate for a 1.55 kW

burner output. With CFD simulation Decker (2017) optimized flame port geometry and found maximum thermal efficiency as 56.8%, compared to 53% of the available one.

In PRBs, biogas combustion was studied by few researchers (Gao et al. 2011, 2013; Keramiotis et al. 2013, 2015) for mainly to understand the impact of CO_2 content on combustion performances. Gao et al. (2011, 2013) with a two-layer spherical alumina bed (Fig. 2.22) found that increment in CO_2 content, moved upper and lower stability limit to higher values. But, this also decreases CO and NO_x emissions. Keramiotis et al. (2013, 2015) with simulated biogas (60% CH_4 and 40% CO_2) found that the combustion inside porous media enables the burner to operate at lean fuel condition ($0.71 \leq \phi \geq 0.9$). The PRB used by Keramiotis et al. (2013, 2015) was made up of two-layers viz., CZ of SiSiC foam and flame trap of Al_2O_3 (Fig. 2.23). For maximum firing rate of 1000 kW/m^2, measured CO and NO_x were 300 ppm and 20 ppm, respectively. They also studied (Keramiotis et al., 2013) the variation of radiation efficiency for firing rate range of 200-800 kW/m^2. For equivalence ratio of 0.8 efficiency varied between 18.5 to 26%. Colorado et al. (2015) with surface stabilized porous burner, observed that increase in CO_2 content increases radiation properties but at the same time reduces the burning velocity.

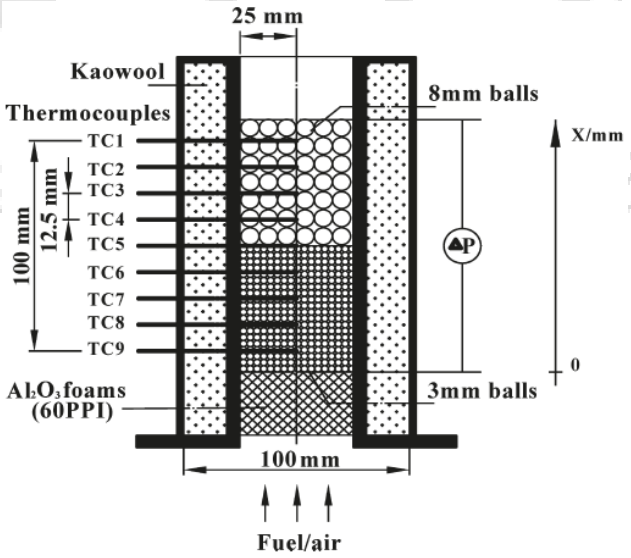

Fig. 2.22: Schematic of the PRB used by Gao et al. (2011, 2013).

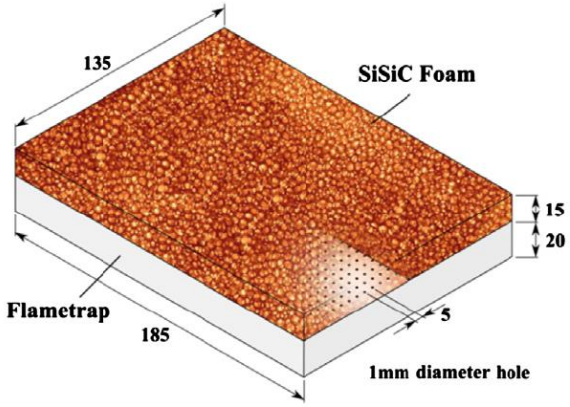

Fig. 2.23: Schematic of the PRB used by Keramiotis et al. (2013, 2015).

2.5 State of the art on plant oil cook-stove developments

The first notable work towards the development of a stove based on plant oil was initiated at Hohenheim University by Stumpf and Mühlbauer (2002). After developing the stove fueled with straight plant oil, the range of input power and thermal efficiency were also optimized (Kratzeisen and Stumpf, 2007). Another Plant oil stove ‘‘Protos’’, was developed (Fig. 2.24) by Bosch and Siemens Home Appliances Group (BSH) with the input power range of 1.6 to 3.8 kW (Shiroff, 2007; Kratzeisen and Muller, 2009). Observation made from the investigation shows that the fatty acid composition present in the cook oil influenced the deposit formation in the vaporizer.

Fig. 2.24: Plant oil stove ‘‘Protos’’, (Shiroff, 2007; Kratzeisen and Muller, 2009).

Fig. 2.25: Oil stove developed by Natarajan et al. (2008).

Natarajan et al. (2008) modified the conventional kerosene pressure stove and with plant oil, the stove yielded 12% higher thermal efficiency than kerosene (Fig. 2.25). Such increase in efficiency may be due to the availability of excess oxygen which

favors the combustion. They also studied the variation in thermal efficiency with four different vessels viz., flat vessel and curved vessel with and without copper bottom, and found that flat vessel with copper bottom was resulted in maximum thermal efficiency.

Others have made attempts to use plant oils as cooking fuel by blending it with kerosene and changing the tank pressure. Maximum percentage of oil blends with kerosene was found to be 50-70% (Murthy et al., 2011; Pande et al., 2017) for cottonseed oil, 20-30% for Jatropha (Singh, 2011; Kakati and Mahanta, 2017) and ~50% for waste cooking oil (Varun et al., 2018; Namoco Jr. et al. 2017). Similarly, different tank pressure such as 1.2 bar (Murthy et al., 2011), 1.4 bar (Singh, 2011), 1.5 bar (Jambhulkar et al., 2015) and 2 bar (Namoco Jr. et al. 2017) have been used for different oil/kerosene blends. By investigating the impact of tank pressure on thermal efficiency, Murthy et al. (2011) found optimum performance at 1.2 bar. The maximum operational blending of cottonseed oil and kerosene was found up to 40% in normal stoves, whereas, with modified stove due to improved preheating, blending moved to 70% (Fig. 2.26a). With cottonseed oil and kerosene blended fuel, the thermal efficiency reported by Murthy et al. (2011) was in a range of 45-47%, whereas the same reported by Pandey et al. (2017) was in the range of 13-15% (Fig. 2.26b). This difference was mainly due the method used for efficiency measurement and difference in tank pressure.

(a) (b)

Fig. 2.26: Modified horizontal pressurized kerosene stove used by (a) Murthy et al., 2011 and (b) Pande et al., 2017.

Using Jatropha oil and kerosene with different blend ratios viz., 10:90, 20:80, 30:70, 40:60, and 50:50, Singh (2011) found that the cooking pump stove yields a satisfactory performance only up to 30:70 blend. Kakati and Mahanta (2017) have also explored the use of Jatropha oil and reported similar observations. Jambhlkar et al. (2015) tested the performance of similar stove used by Murthy et al. (2011) but fueled with spent soya

bean cooking oil and kerosene blend. Experiments were performed with blends of various proportions viz., 25:75, 50:50, and 75:25. The maximum thermal efficiency of ~38.5% was found with 50:50 blend at 1.5 bar tank pressure. The thermal efficiency was found to increase up to 50:50 blend ratio, then started to decrease with increase in spent soya bean cooking oil. Also, at any given blending %, thermal efficiency gradually decreases with an increase in fuel consumption. Varun et al. (2018) have tested the performance of pressure stove fueled with waste cooking oil and kerosene blend and found that for waste cooking oil blending of 20-70%, thermal efficiency varied in the range of 4-20%.

Namoco Jr. et al. (2017) have also tested the performance of pressure stove (Fig. 2.27) fueled with waste cooking oil in terms of water boiling time and found that blending of 50% WCO results in a minimum boiling time of 6:74 min. Whereas, the same was 6:76 min, 7:50 min, and 8:19 min for 0 %, 20 % and 100% WCO blending with kerosene.

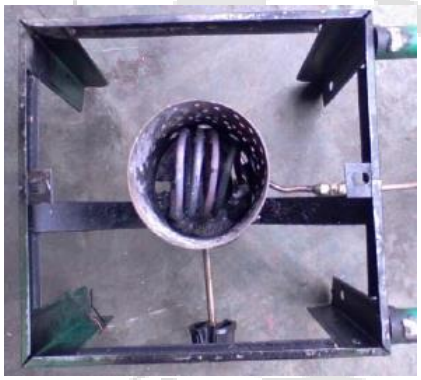

Fig. 2.27: The coiled copper tube with the flame holder used by Namoco Jr. et al. (2017).

Fig. 2.28: Modified pressurized cooking stove, Suhartono et al. (2017a, 2017b).

With Neem and Pongamia oil, Arvind and Bekal (2018) found that the decrement in calorific value and increment in viscosity (reduces fuel mobility and preheating) resulted in low thermal efficiency of the pressure stoves. Suhartono et al. (2017a, 2017b) modified pressurized cooking stove (Fig. 2.28) and experimented with vegetable cooking oils and found that higher calorific value and smaller droplet size increase the flame temperature. Efficiency measurements showed negative impact of flame temperature on thermal efficiency.

The undesirable oil physical properties viz., high auto-ignition temperature, density, flash point, and viscosity have been the main focus of the above research. All the above modified kerosene pressure stove developments have focused on increase in incoming oil temperature, thereby reducing viscosity and ignition time, which ultimately improves their combustion performance.

The second type of stove, i.e., wick stove, was also used by some researchers for demonstrating the applicability of plant oils as cooking fuel. In this type of stove, capillary action raises the fuel to the tip of the wick, which facilitates the combustion. Experiments performed by Wagutu et al. (2010) with fatty acid methyl esters (FAMEs) were not very convincing and showed ~55% higher fuel requirement than with kerosene. Khan et al. (2010) found that in wick stove only 5% of Used Frying Oil (UFO) can blend with kerosene. Further, they extended their study for Karanja oil and found that maximum 10% Karanja oil could be blended with kerosene (Khan et al., 2011). Such a low blending percentage could be due to the high density and gumming and deposit formation tendency of oils. With increase in percentage of oils in blend, they observed decrease in thermal efficiency. Nagaraju and Gopal (2013) reported that it was extremely difficult to ignite a commercial wick stove fueled with blends of kerosene and Pongamia oil. This is mainly due to the high distance of the burning tip from the oil reservoir and high viscosity of oil, which reduces percolation capacity of the oil. A comprehensive study on wick stove fueled with Pongamia oil was also carried out by Shetty et al. (2015). They tested blend of 10 to 90% Pongamia oil and kerosene and found a peak efficiency of only 5.6%. In view of the above, it is observed that high viscosity of plant oil possesses difficulty in proper combustion in these stoves. However, Dinesha et al. (2019) observed stable flame for 50% blend of WCO and Sesame oil with wick stove (Fig. 2.29). With increase in percentage of oils, the transition of flame color from blue to yellow and red showed a negative impact of blending. Increase in blend percentage also reduces the flame intensity, which ultimately increases the time duration for water boiling, i.e., reduces thermal efficiency. Such behavior could be associated with low capillary action due to the high viscosity and fire point of the oils.

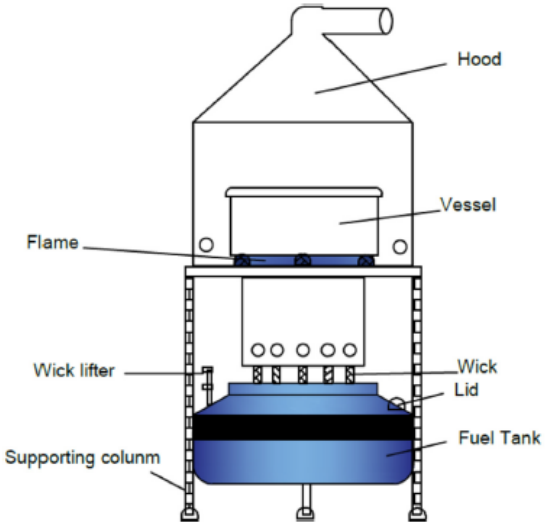

Fig. 2.29: Schematic diagram of wick stove used in experimental work by Dinesha et al. (2019).

Very few works have been carried out using vegetable oils in PRBs. Lapirattanakun and Charoensuk (2017) used spherical ceramic ball inserts for waste cooking oil combustion (Fig. 2.30). Within the firing rate range of 325-548 kW/m^2 with 0.16 kg/min flow rate of water, the maximum thermal and combustion efficiencies were approximately 28% and 99.5%. Similarly, CO and NO_x concentrations were ~171 and ~40 ppm, respectively (at 6% O_2).

Fig. 2.30: Waste vegetable oil burner with porous media, Lapirattanakun and Charoensuk (2017).

Mustafa et al. (2015, 2016) developed a PRB for kerosene-vegetable cooking oil (VCO) blend. They extensively studied the effects of equivalence ratio on the thermal performance and exhaust gas emissions of a PRB (Al_2O_3 porous medium) for thermoelectric power generation. Another carried out on a dual-layer microporous

burner reported that the burner performance was influenced by the size of vegetable oil droplets Janvekar et al. (2019).

2.6 Literature Closure

Porous media combustion technology is a novel dimension to the age-old combustion technology facilitating manifold advantages. In recent times, intense research activities have been carried towards the development of practical burners with low energy consumption and minimal pollutant emissions. Fundamental studies were carried out by several researchers with different porous media. The role of materials in terms of efficiency and emissions have been highlighted. Development of PRBs for domestic as well as commercial cooking application have been found impressive over a decade. Performance of the PRBs and their potentials to replace the available FF based CBs are established. Recent developments on the self-aspirated PRBs for cook stoves are promising but, further investigations in detail, to make it market ready, are still required. Also, no scientific investigations on economic benefit and life cycle performance have been reported for any such cook-stove.

Among the different cooking fuels LPG has received prominence and studies based on kerosene, natural gas and biogas are still limited. The biogas can provide a potential way forward for cooking fuel, but need efficient cook-stoves. Above reviewed works, implies that the design of these available burners are not consistent with the scientific and technical criteria appropriate for such burners. Further, no researchers explored the use of PRB for biogas cook-stove.

Waste cooking oil and other plant oils for rural reach need further detailed assessment in PRBs as kerosene is phasing out from the market. The undesirable oil physical properties viz., high auto-ignition temperature, density, flash point, and viscosity have been the main focus of the research on plant oil stoves. All the modified kerosene pressure stoves developments have focused on increasing incoming oil temperature, thereby reducing viscosity, which ultimately improves their combustion performance. It is observed that there is a lack of consistency and technical uniformity in the reported performances. Further, these stoves are designed on the principle of FFC, which has the inherent unfavorable characteristics of low limits of flammability, low power density, and high toxic emissions. Major concerns of low preheating of the plant oil can be

addressed by using PMC. Above literature review shows that there is no study on waste cooking oil fueled PRB for cooking application.

2.7 Objectives of the Thesis

In view of the above literature closure, the following core objectives are chosen for this thesis work;

- To demonstrate PRB based cook-stove as potential alternative to their conventional counterpart's.
    - To analyze the impact of PRB on daily heat energy requirement per household by performing Control Cooking Test (CCT).
    - To investigate PRBs ability to reduce environmental burden of a typical life cycle of LPG by performing a Life Cycle Assessment (LCA) using "SimaPro v.8.2.0.0" (Pre Consultants 2016) software.
    - To examine PRBs ability to impact the overall cost of cooking.
- To identify the shortcomings in the PRB based LPG cook-stove developed at IIT Guwahati (Mishra, 2015) for its commercialization and propose a new cook-stove design. Also, to perform detailed performance assessment of the newly developed cook-stoves.
- To design and develop a naturally aspirated porous radiant burner for domestic biogas cook-stove and carryout detailed performance assessments.
- To perform experimental investigation to analyze waste cooking oil (WCO) as an alternative cooking source, and design and test a domestic cook-stove for its application.

Chapter 3

Performance Assessment of Self-aspirated LPG Cook- stoves with Porous Radiant Burner

The self-aspirated PRBs, developed by Mishra (2017) for domestic as well as medium scale cooking application using LPG as fuel is shown in Fig 3.1. The reported thermal efficiency and emission performance are given in Table 3.1.

(a) (b)

Fig. 3.1: Cook-stove with PRB (a) 1-3 kW domestic and (b) 5-10 kW medium scale.

Table 3.1: Thermal efficiency and emissions (CO and NO_x) of self-aspirated PRB reported by Mishra (2017).

Parameters	1-3 kW domestic PRB		5-10 kW medium scale PRB	
	CB Stove	PRB Stove	CB Stove	PRB Stove
Thermal efficiency (%)	60-65%	71-73%	30-45%	44-55%
CO emission (ppm)	220-250	30-140	335-1165	60-190
NOx emission (ppm)	5-25	0.2-3.5	28-110	2-10

The main objective of study is to demonstrate PRB based cook-stove as potential alternative to their conventional counterpart's. To test the feasibility of the PRB for

commercial application, thermal efficiency and emission tests alone will not provide the substantial information. Therefore, three performance tests viz., Control Cooking Test (CCT), life Cycle Assessment (LCA) and Techno-economic Assessment (TEA) have been proposed in this investigation. As discussed in chapter 1, the problems associated with conventional cook-stoves can be classified into three categories and each of the above proposed tests deal a specific problem as shown in Fig. 3.2. In next paragraph each of these tests are discussed in details.

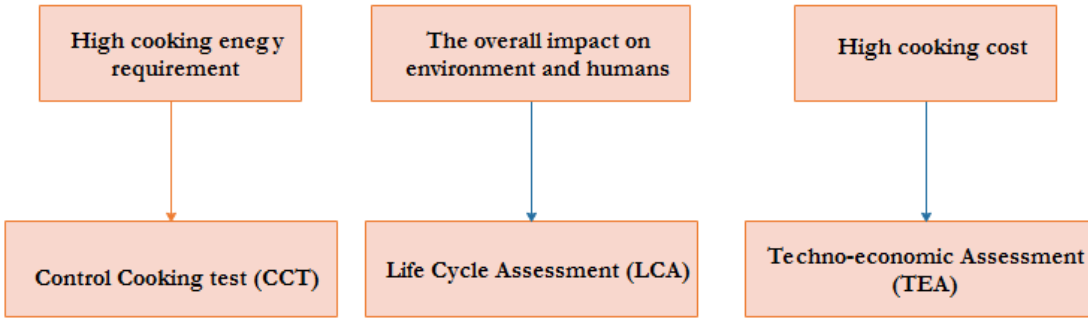

Fig. 3.2: Problems associated with conventional cook-stoves and selected test method for assessment.

For the estimation of thermal performance of PRB, Mishra (2017) employed only standard Water Boiling Test (WBT), but, the cooking process is not only the boiling of water but depends on various factors viz. stove efficiency, fuel used, dish ingredients, cooking methods and condition. To obtain a true picture of the PRB based cook-stove performance during cooking, it is necessary to conduct Control Cooking Test (CCT). Therefore, in the present investigation CCT was performed for domestic scale cook-stove (Fig. 3.1a), and details are discussed in this chapter. Also, Chapter 1 highlights the need of cleaner cook-stoves due to large emission generated form cooking appliances. The PRB based cook-stoves developed by Mishra (2017) showed reduced emission compared to a conventional cook-stoves. To further investigate their ability to reduce environmental burden of a typical life cycle of LPG, a Life Cycle Assessment (LCA) has been performed by using "SimaPro v.8.2.0.0" (Pre-Consultants 2016) software and the result are presented in this chapter. This analysis provides a holistic view of PRB's ability to influence climate change and human health compared to that of a conventional stove. Further, as discussed in chapter 1, economic constraint is one

of the drawbacks of clean cooking initiatives and to highlight the economic impact of PRB based cook-stove, a Techno-economic Assessment (TEA) has been performed. TEA includes both direct cost related to fuel and indirect cost (emission cost) throughout the life of the stove.

3.1 Control Cooking Test of LPG operated domestic cook-stove with PRB

A 14.2 kg LPG domestic cylinder is connected to a pressure regulator, and then with a Coriolis flow meter, the fuel flow rate is monitored using a suitable flow control valve. Using an igniter, the combustion is initiated, and appropriate cooking vessel is placed over it for conducting the cooking experiments. Ingredients are measured using a weighing balance (WB) and beaker. The time required for cooking each item is recorded by using a stopwatch and at the same time, the LPG consumption for the preparation of each item is noted. Important factors such as stove efficiency, fuel used, dish ingredients, cooking methods, etc. have to be considered to know the actual energy requirement for cooking. Households use various types of fuels, starting from traditional biomass fuels, bricks or clay to fossil fuels. The type of meals cooked in households also varies to a great extent depending on income levels, regional taste and flavor and different type of cooking methods used in rural and urban areas. Because of such diversity in the type of food consumed by the citizens, the task of determining the average cooking energy demand for an average household becomes extremely complex. The present study involves the preparation of typical meals based on daily average food intake, as suggested in NSS (2011-12). Following deductions have been made after rigorous survey of literature:

(i) The cooking energy demand in both rural and urban areas remain the same if the type of food, quantity and cooking method remain similar.

(ii) The type of food consumed in rural and urban areas remain the same to a large extent.

(iii) The fuel quantity required is determined by the net calorific value of the fuel used and stove efficiency.

Based on the average daily intake of food type and quantity reported by NSS (2011-12) as given in Table 3.2, different dishes were cooked in both LPG stove with PRB and LPG conventional cook-stove.

Table 3.2: Estimation of daily food intake by households (NSS, 2011-12).

India: Daily average food consumption/ HH = $\left\{\left(r_i \times 4.9\right)\times .69+\left(u_i \times 4.6\right)\times .31\right\}\times \frac{12}{365}$

Main Ingredients	Per capita per month consumption		Daily food consumption/HH
	Rural (r_i)	Urban (u_i)	
Rice (g)	5976	4487	875
Cereal (g)	4288	4011	665
Pulses (g)	783	901	130
Milk (ml)	4333	5422	736
Edible oil (g)	674	853	115
fish & meat (g)	597	642	965
Vegetables (g)	6760	6842	1073
Tea (g)	79.925	95.32	14

[1](4.9, 4.6), and (.69, .31) are Urban and rural household size and % population in India, respectively (NSS, 2011-12).

Three menus (A, B and C, Table 3.3) were prepared after conducting a small query in the families of a rural and urban household. While conducting the experiments, the cooking time and amount of LPG consumed for preparation of the dishes were recorded (Table 3.4-3.6). The average value of fuel consumed by menu A, B and C give the daily heat energy requirement per household.

Table 3.3: Menus for estimating the average heat energy requirement.

Dish	Menu A	Menu B	Menu C
Dish 1	Rice (875 g + 3 kg water), boiled, open vessel	Rice (875 g + 3 kg water), boiled, cooker	'Khichdi' (rice 500 g + pulse 130 g + 3 kg water), boiled, cooker
Dish 2	Pulse 'dal' (130 g + 676 g water), boiled, cooker	Pulse 'dal' (130 g + 676 g water), boiled, Cooker	Vegetables 'Mix veg' (1073 g + 40 g oil), fried, open vessel
Dish 3	Vegetables 'Cabbage' (1073 g + 30 g oil), fried, open vessel	Vegetables 'Cauliflower' (1073 g + 40 g oil), fried, open vessel	'Kheer' (milk 636 ml + 375 g rice), boiled, open vessel

Dish 4	Chicken (965 g + 85 g oil), fried, open vessel	Fish curry (965 g + 75 g oil), open vessel	Fish (965 g + 75 g oil), fried, open vessel
Dish 5	Leaf bread ‘chapatis’ (665 g wheat), hot plate cooking	Fried Leaf bread ‘parathas’ (665 g wheat), hot plate cooking	Fried Leaf bread ‘Chapatis’ (665 g wheat), hot plate cooking
Dish 6	Milk 636 ml, boiled, open vessel	Milk 736 ml, boiled, open vessel	Tea-5 cups (14 g + 75 g sugar + 100 ml milk), boiled, open vessel
Dish 7	Tea-5 cups (14 g + 75 g sugar + 100 ml milk), boiled, open vessel	Tea-5 cups (14 g + 75 g sugar), boiled, open vessel	-

Table 3.4: Cooking time and LPG requirement for preparation of Menu-A.

	Menu A	**PRB**		**CB**	
		Time (min)	LPG (g)	Time (min)	LPG (g)
Dish 1	Rice (875 g + 3 kg water), boiled, open vessel	22	42.29	29	55.78
Dish 2	Pulse ‘dal’ (130 g + 676 g water), boiled, cooker	8	16.37	13	26.58
Dish 3	Vegetables ‘Cabbage’ (1073 g + 30 g oil), fried, open vessel	14	25.23	25	44.78
Dish 4	Chicken (965 g + 85 g oil), fried, open vessel	26	43.46	34	59.61
Dish 5	Leaf bread ‘chapatis’ (665 g wheat), hot plate cooking	33	54.98	44	72.98
Dish 6	Milk 636 ml, boiled, open vessel	7	11.86	12	20.34
Dish 7	Tea-5 cups (14 g + 75 g sugar + 100 ml milk), boiled, open vessel	5	9.3	9	16.69
	Total	**115**	**203.49**	**166**	**296.76**

Table 3.5: Cooking time and LPG requirement for preparation of Menu-B.

	Menu B	PRB		CB	
		Time (min)	LPG (g)	Time (min)	LPG (g)
Dish 1	Rice (875 g + 3 kg water), boiled, cooker	12	20.98	19	33.21
Dish 2	Pulse 'dal' (130 g + 676 g water), boiled, Cooker	9	18.32	14	28.49
Dish 3	Vegetables 'Cauliflower' (1073 g + 40 g oil), fried, open vessel	20	34.98	31	53.87
Dish 4	Fish curry (965 g + 75 g oil), open vessel	29	48.98	38	63.98
Dish 5	Fried Leaf bread 'parathas' (665 g wheat), hot plate cooking	35	58.13	47	77.95
Dish 6	Milk 736 ml, boiled, open vessel	9	15.23	16	26.87
Dish 7	Tea-5 cups (14 g + 75 g sugar), boiled, open vessel	4	7.8	6	11.65
	Total	**118**	**204.42**	**171**	**296.02**

For preparing menu-A, given in Table 3.3, the conventional stove consumed 296.76 g of LPG whereas stove with PRB utilized only 203.49 g. Further, it is also to be noted that the rate of fuel savings is different for different food items. Fuel savings is approximately 93.27 g per day per household. For Menu-B, fuel consumed by conventional stove and stove with PRB are 296.02 g and 204.42 g respectively, with a fuel-saving of 91.6 g by the stove with PRB. Similarly, for Menu-C, these values are 311.11 g, 222.71 g, and 88.4 g respectively. The average heat energy requirement per household for daily cooking activities is estimated as 9283 kJ and 13306 kJ for stoves with Conventional Burner (CB) and PRB, respectively. It can be seen that stove with PRB complies with the heat energy requirement values (6339~9502 kJ) as suggested by Planning Commission of India, but the stove incorporated with CB requires 13306 kJ, which is higher than the recommended limit. In present study, the time taken by two different stoves to cook the listed meals given in Table 3.3, has been measured. The result shows that time required to cook in stove with PRB is lesser than conventional

stove. Time taken for complete cooking by stove with the conventional stove is 166 min, 171 and 170 min for Menu-A, Menu-B and Menu-C respectively. On the other hand, PRB incorporated stove required only 115 min, 118 min and 122 min, respectively for the same food items. Average time saving is approximately 51 min, and this explains the extent to which time budgets can be affected by cook-stove with PRB.

Table 3.6: Cooking time and LPG requirement for preparation of Menu-C.

	Menu C	**PRB**		**CB**	
		Time (min)	LPG (g)	Time (min)	LPG (g)
Dish 1	'Khichdi' (rice 500 g + pulse 130 g + 3 kg water), boiled, cooker	17	33.78	22	43.69
Dish 2	Vegetables 'Mix veg' (1073 g + 40 g oil), fried, open vessel	21	34.95	28	46.63
Dish 3	'Kheer' (milk 636 ml + 375 g rice), boiled, open vessel	29	56.98	40	78.56
Dish 4	Fish (965 g + 75 g oil), fried, open vessel	18	34.25	27	51.35
Dish 5	Fried Leaf bread 'Chapatis' (665 g wheat), hot plate cooking	31	51.4	42	70.12
Dish 6	Tea-5 cups (14 g + 75 g sugar + 100 ml milk), boiled, open vessel	6	11.35	11	20.76
	Total	**122**	**222.71**	**170**	**311.11**

3.2 Life Cycle Assessment (LCA) of LPG Operated Cook-stoves with PRB

Life cycle assessment (LCA) is a tool to evaluate the environmental effects of a product or process throughout its entire life cycle. An LCA entails examining the product from the extraction of raw materials for the manufacturing process, through the production and use of the item, to its final disposal, and thus encompassing the entire product system. A schematic representation of a product life cycle is given in Fig. 3.3.

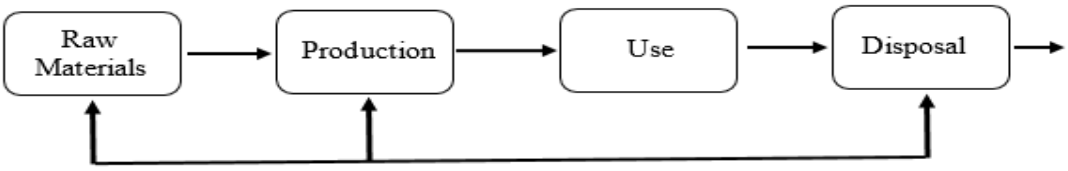

Fig. 3.3: Schematic representation of a product life cycle.

The assessment process includes identifying and quantifying energy and materials used and wastes released to the environment, assessing their environmental impact and evaluating opportunities for improvement as illustrated in Fig. 3.4. The unique feature of this type of assessment is its focus on the entire life cycle, rather than a single manufacturing step or environmental emission. The theory behind this approach is that operations occurring within a facility can also cause impacts outside the facility's gates that need to be considered when evaluating project alternatives.

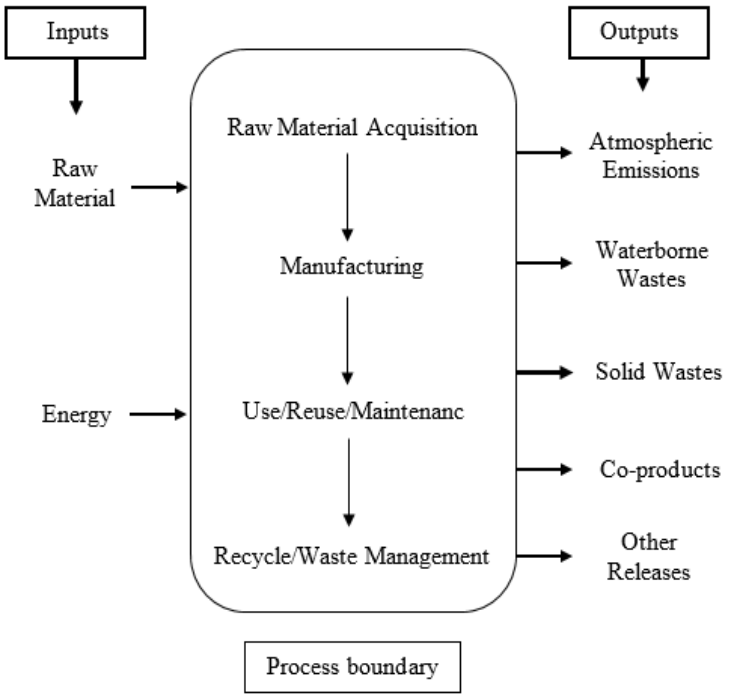

Fig. 3.4: System boundary for LCA.

According to the ISO 14040 and 14044 standards, LCA is carried out in four distinct phases as illustrated in Fig. 3.5. The phases are often interdependent.

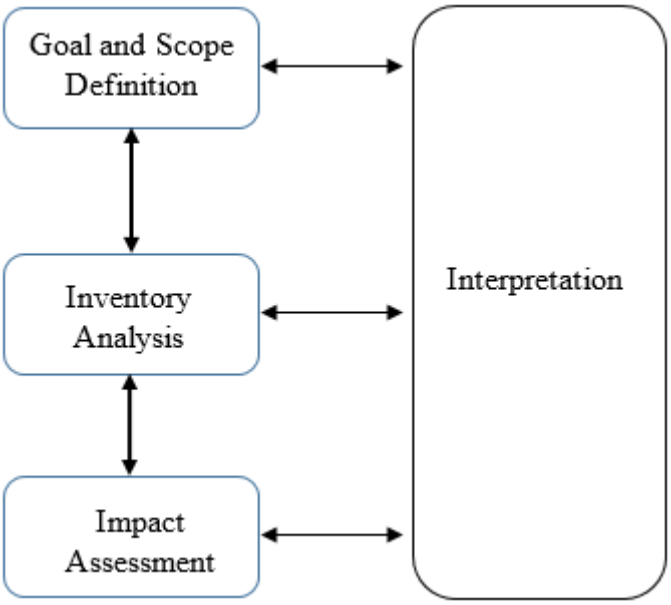

Fig. 3.5: Illustration of LCA phases.

Phase 1: Goals and Scope: The scoping step determines which processes will be included, which environmental concerns will be included, what economic or social good is provided by the goods or services in question, resolves any technical issues and defines the audience for the LCA.

Phase 2: Life Cycle Inventory (LCI): The inventory provides information about all environmental inputs and outputs from all parts of the product system involved in the life cycle assessment. This involves modelling of the product system, data collection, and verification of data for inputs and outputs for all parts of the product system. Inputs include inputs of materials, energy, chemicals and 'other.' Outputs include emissions through water and air, solid waste.

Phase 3: Life Cycle Impact Assessment: The assessment takes inventory data and converts it to indicators for each impact category. A typical list of impact indicators includes Global Climate Change, Stratospheric Ozone Depletion, Global Climate Change, Smog, Ecotoxicity, Human toxicity, Eutrophication and Natural resources (habitat, water, fossil fuels, minerals, and biological resources).

Phase 4: Interpretation: The last step is an analysis of the impact data, which leads to the conclusion of whether the ambitions from the goal and scope can be met.

3.2.1 System boundary and life cycle inventory for LPG

The system boundary defines the processes which are included in LCEA of LPG. Different stages in the life cycle of LPG in India are shown in Fig. 3.6, whereas for one specific complete LPG life cycle which has been used in the current study is shown in Fig. 3.7. The raw material for the production of LPG is crude oil and natural gas, which are extracted (in India) from onshore and offshore sources and also imported. Extracted resources are transported by pipeline or tanker to the processing facilities. LPG from crude oil is processed in refineries and from natural gas in gas processing plants. LPG is then transported to the bottling plants by means of rail or road. Through road trucks, LPG-bottles are delivered to the retailers and then distributed to the customers for household/commercial cooking application, and this completes the life cycle of LPG. Due to large variation in LPG production and unavailability of relevant data, a specific LPG life cycle is chosen and restricted life cycle assessment has been done in present study. Some of the required data have been taken from the Ecoinvent database.

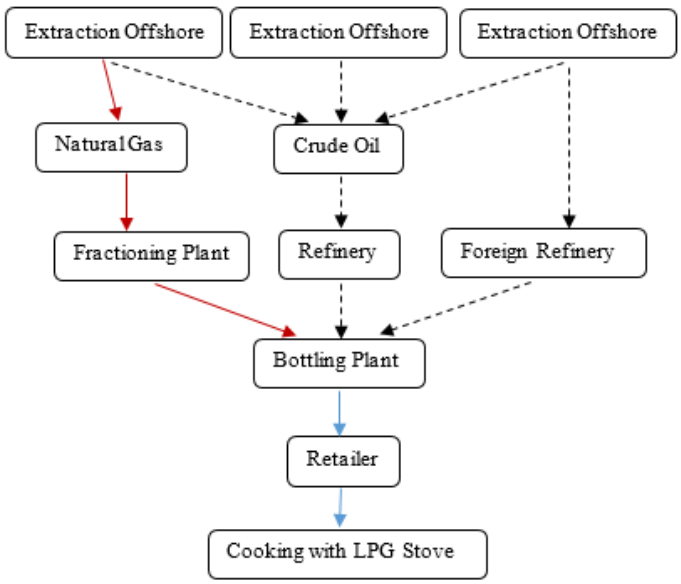

Fig. 3.6: Stages in the life cycle for liquefied petroleum gas in India.

Simapro LCA software has been used for LCA, and the data required have been collected from the relevant industries. During extraction, the principle materials used per kg of extracted crude oil are cement (121 mg), steel (11.18 g), chemicals (1.35 g) and lubricants (92.37 g). In Assam, the extraction of crude oil is mainly done by Oil and Natural Gas Corporation (ONGC) and Oil India Ltd. (OIL) and the extracted crude

oil is transported to different refineries viz., Indian Oil Corporation Ltd. (IOCL), Numaligarh Refinery Ltd. (NRL). A survey has been carried out in IOCL Guwahati refinery, which receives crude oil through pipelines from Narangi branch. The expenditure of crude oil for this transportation is 0.99 g/kg of crude oil transported. Transportation loss is around .0013% of crude oil transported. Internal fuel oil (0.052 kg/kg crude processed) and fuel gas (0.0479 kg/kg crude processed) are the main fuels used in the refining process. The refinery losses are taken as 0.3%. The calorific content of the produced LPG is 44160 kJ/kg. Bullet tankers of size 18 MT are used for transportation of LPG from refinery (IOCL) to Guwahati bottling plant where it is filled in steel cylinders of capacity 14.2 kg and 19 kg for domestic and commercial applications, respectively. The electricity required during bottling is purchased from Assam State Electricity Board (ASEB) and also produced in the plant using diesel generator. The electricity required for bottling per kg of LPG is 0.0117 kWh, and the bottling losses are taken as 3.4% (IOCL, 2014-15). The overall efficiency of coal-based thermal power plant is taken as 32.8% and electricity distribution and transportation losses as 21.46% (GOI, 2015). LPG cylinders are transported to retailers by means of trucks, and each truck carries 306 cylinders at one go and due to large variation in distribution point an average transportation distance of 250 km has been considered in this study. The life cycle inventory of LPG is presented in Table 3.7.

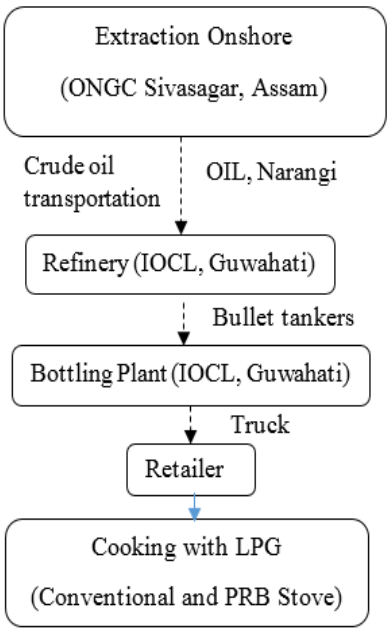

Fig. 3.7: Stages in the life cycle for liquefied petroleum gas for the current study.

Table 3.7: Life cycle inventory (energy and emission) of LPG.

Life cycle stages ⟶	Extraction	Refinery	Bottling	Transport (Road)
Energy (kJ per kg fuel) ↓				
Liquid fuels	4602.3	2246.75	-	682
Gaseous fuel	318	2221.65	-	-
Solid fuels	-	431	-	-
Grid electricity use	104.6	-	42.17	-
Manual Labor use	12.55	46.03	33.89	15.4
Total Energy Input (E_t)	5037.45	4945.43	76.06	697.4
Air pollution				
CO_2 (kg/kg)	0.00962	0.02939	0.03977	0.04308
CO (kg/kg)	2.39×10^{-4}	0.0778×10^{-2}	6.63×10^{-6}	4.2864×10^{-3}
NO_x (kg/kg)	5.96×10^{-4}	1.073×10^{-3}	1.33×10^{-4}	5.3028×10^{-4}
SO_2 (kg/kg)	1.19×10^{-4}	3.18×10^{-4}	3.093×10^{-4}	2.6514×10^{-4}
NMVOC (kg/kg)	3.97×10^{-5}	3.97×10^{-5}	4.4189×10^{-5}	2.0327×10^{-3}
CH_4 (kg/kg)	1.787×10^{-3}	1.35×10^{-3}	2.2095×10^{-4}	4.4189×10^{-4}
PM_{10} (kg/kg)	7.95×10^{-5}	1.51×10^{-4}	4.4189×10^{-5}	-
Water pollution				
BOD (mg/kg)	5.5068	1.85	-	-
COD (mg/kg)	12.8492	13.51	-	-
Phenol (mg/kg)	5.163×10^{-4}	7.546×10^{-5}	-	-
TDS (mg/kg)	220.272	3.304	-	-
TSS (mg/kg)	0.0764	2.5	.006	-
Oil & Grease (mg/kg)	.0139	.0011	-	-

There are three direct methods of estimating energy use per worker-hour (EPWH), i.e., human metabolic activity, total primary energy supply, and non-industrial energy supply (Zhang and Dornfeld (2007). EPWH calculated from human metabolic activity produces lower bound of energy and total primary energy produces upper bound of

energy, respectively per worker-hour. Non-industrial energy supply method proposed by Zhang and Dornfeld (2007) is recommended for LCA, which has been adopted in this study. They used non-industrial energy supply, which includes all primary energy except that supplied to industry and transport sectors to estimate EPWH for the industrial sector (given in Eq. 3.1).

$$IPES = TPES \times \frac{IFC}{TFC} \quad \text{..... (3.1)}$$

$$EPWH = 3942 \text{ kJ}$$

Where, TPES denotes Total Primary Energy Supply of a country or region, which indicates the sum of production and imports subtracting exports and storage changes. IPES stands for Industrial Primary Energy Supply, and IFC is Industrial Final Consumption. TFC is the Total Final Consumption of Energy, which is the aggregate of all the energy used for providing various energy services. For India, TPES =775.445 Mtoe, IFC =253.885 Mtoe, and TFC = 528.337 Mtoe (IEA, 2014), and estimated worker population = 488 million (GOI, 2013-2014).

3.2.2 LCA of medium scale cook-stove with PRB

The goal of the present work is to determine the LCA of both the LPG stoves with PRB and CB. Environmental impacts of pollutants emitted during fuel (LPG) production and application are considered in this analysis. The functional unit for current study is defined based on the data collected from IIT Guwahati canteen. Per day eight cylinders of LPG, each weighing 14.2 kg are used in 12 conventional burners of 5-10 kW capacity for meeting the food requirements of 850 students. So one burner consumes around 9.5 kg of LPG in one day and hence, the functional unit for this study is defined as '419512 kJ heat energy transferred to single conventional burner'.

Estimation of total energy consumption is an important component of any LCA study. LCEA is a technique for analyzing the way energy is used in the development of a product and during its useful lifetime. It is a cradle to grave analysis of the product, which starts from the energy required to extract raw materials from the ground, followed by transportation of raw materials to processing plant, processing the raw materials into usable materials, manufacturing a product, the energy consumption

during the product's useful life and energy consumed during recycling and disposal of the product.

Based on the types of energy sources acknowledged to quantify the life cycle based energy efficiency, there exists different concepts, viz., are source conservation concept where only non-renewable energy sources are considered, in climate change oriented concept only fossil energy is considered and total energy demand concept, where all energy sources are accounted (Rolf et al., 2015). The standardized LCA methodology (ISO 14040-14043) has been adopted in the current work for LCEA and was restricted only to energy aspects (material consumption is excluded). To compute the energy efficiency of medium scale LPG, cook stoves with both CB and PRB 'total energy demand' concept has been used and the calculated values were based on the 'net calorific value (NCV)' of energy sources considered. During LCEA, LCEE has been determined by using relations 3.2-3.5.

$$LCEE = \frac{FEC}{E_p + E_t} \quad \ldots\ldots (3.2)$$

$$FEC = m_f \times NCV \times \eta_{th} \quad \ldots\ldots (3.3)$$

$$E_p = m_f \times NCV \quad \ldots\ldots (3.4)$$

$$E_t = m_f (e_E + e_R + e_B + e_T) \quad \ldots\ldots (3.5)$$

Where, FEC =final energy consumption (kJ), m_f = mass of LPG (kg), E_p = primary energy (kJ), E_t = Secondary total energy (kJ), e =specific energy required for LPG (kJ/kg), subscript E = Extraction, R =Refinery, B =Bottling, T =Transportation

From the energy inventory presented in Table 3.7, energy flow diagrams have been prepared for LPG cooking stove with CB and PRB of 5-10 kW input power and for 5 kW presented in Fig. 3.8 (others are given in Appendix II) which portrays the impact of burner efficiency on the life cycle energy flow stream of cooking fuels.

Figure 3.9 shows that the LCEE variation for PRB is 38.2% to 36.7%, whereas for CB, it is varied from 31.4% to 25.1% for the same input power range of 5-10 kW. PRB has

a minimum of 7% (5 kW) to maximum 11.6% (10 kW) higher LCEE than CB. This is mainly due to the difference in thermal efficiency of the burners with input power, for PRB it is varied from 55% to 52.6% whereas for CB, it is varied from 45% to 36% for the input range of 5-10 kW. Higher thermal efficiency of PRB results in reduced fuel requirement, which finally leads to higher LCEE.

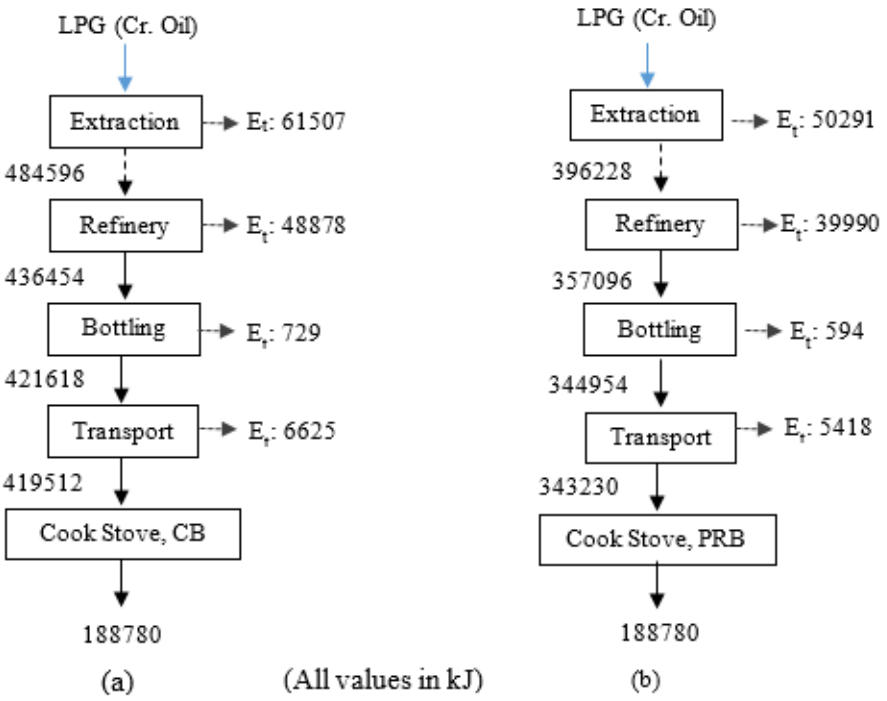

Fig. 3.8: Energy flow diagram for LPG at 5 kW input power of stove.

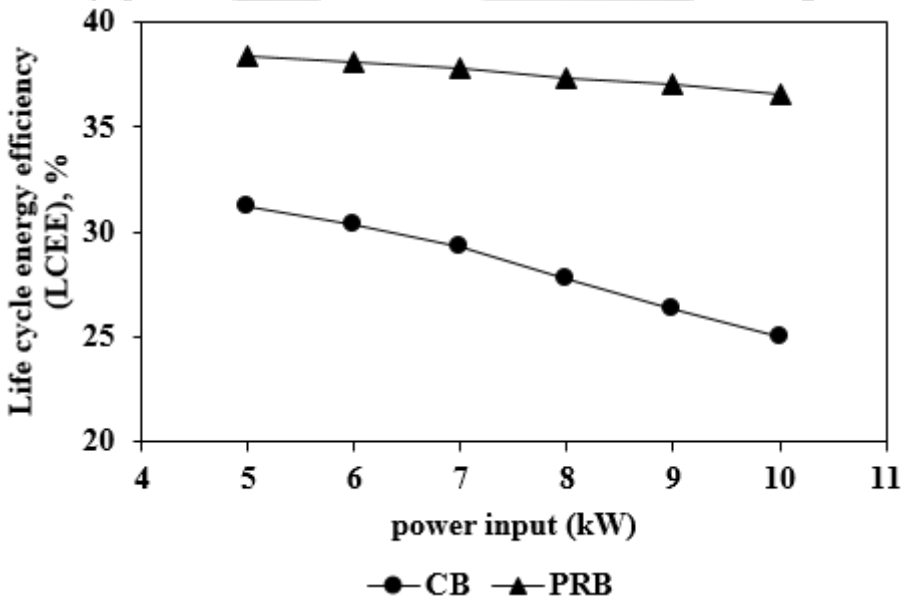

Fig. 3.9: Variation of LCEE of LPG stove with CB and PRB with input power.

In this analysis, “SimaPro v.8.2.0.0” (Pre-Consultants 2016) LCA software with embedded background “ecoinventv3 database has been used”. In order to compare the environmental impact of the newly developed LPG cooking stove with PRB, emission related to LPG production from crude oil and emissions during the operation of burners were considered. While evaluating the performance, ReCiPe environmental impact categories, namely: (1) climate change human health, (2) photochemical oxidant formation, (3) particulate matter formation, (4) climate change Ecosystem and (5) terrestrial acidification were considered. Impact assessment for 5-10 kW was performed and for 5 kW input power is presented in Fig. 3.10 (others are given in Appendix II) compares the relative contributions of various processes such as extraction, refinery, bottling, transportation and burner (stove) during the life cycle of LPG with respect to different impact categories (climate change human health, photochemical oxidant formation, particulate matter formation, climate change Ecosystem and terrestrial acidification) for both conventional and PRB stoves having 5-10 kW. PRB reduces the impact in all categories and the largest reduction of 87% is found for photochemical oxidant formation at 5 kW power input but the same reduces to 81% for power input of 10 kW. This declination can be attributed to decrease in thermal efficiency from 55% to 52.6% which in turn increases the fuel requirement. Emission of CO and NO_x that vary from 60 ppm to 190 ppm and 2 ppm to 10 ppm at 5 and 10 kW, respectively.

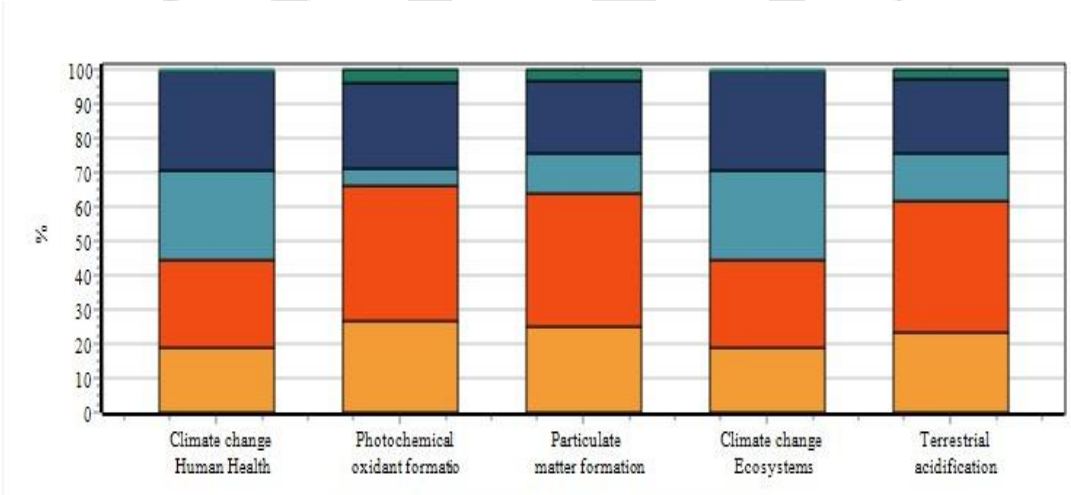

Fig. 3.10a: Distribution of environmental impacts from LPG life cycle with CB at 5 kW input operating power.

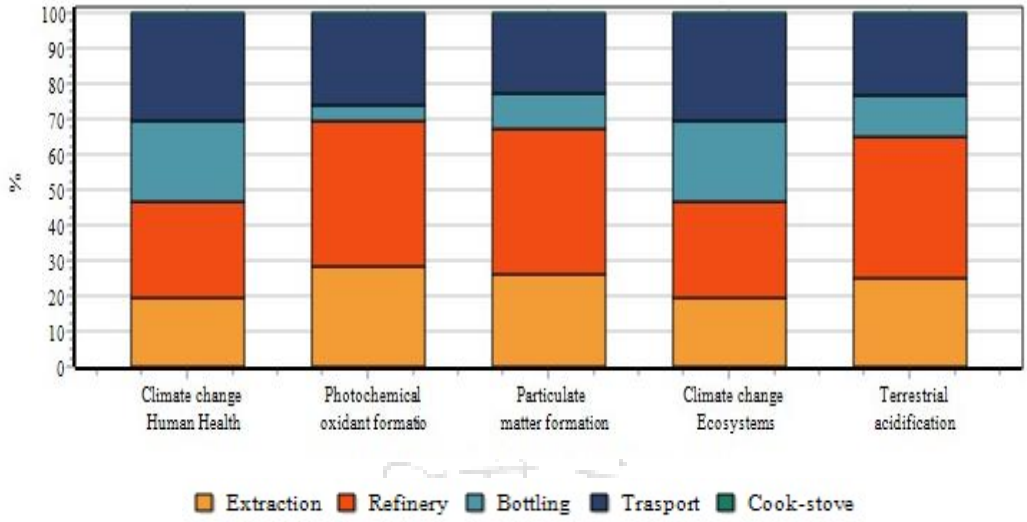

Fig. 3.10b: Distribution of environmental impacts from LPG life cycle with CB at 5 kW input operating power.

3.2.3 LCA of domestic scale cook-stove with PRB

For LCA of domestic scale procedure explained in section 3.2.1 was followed. In this case, average heat energy requirement per household for daily cooking activities estimated by CCT (section 3.1) was used as function unit. Energy flow diagrams have been prepared for 1-3 kW, domestic LPG cooking stove with CB and PRB and presented in Fig. 3.11.

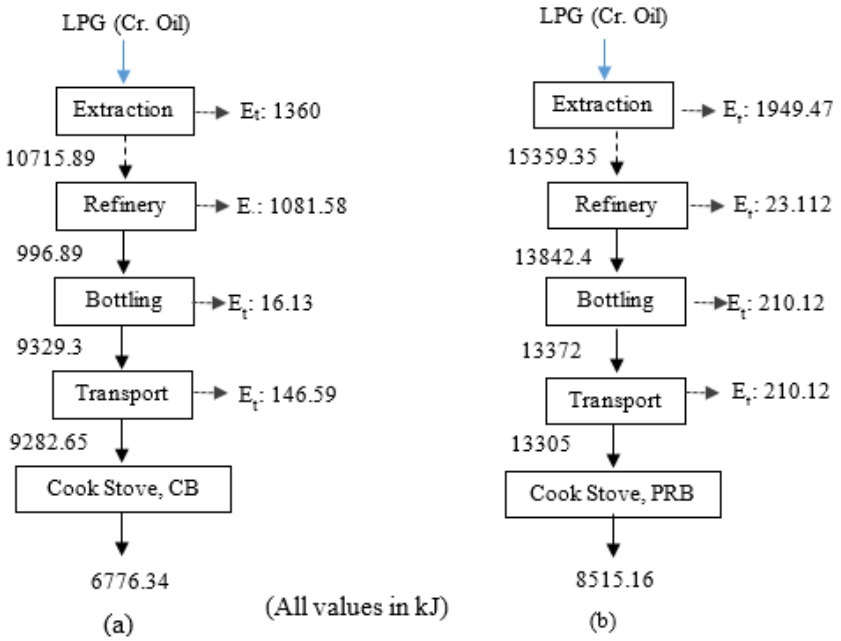

Fig. 3.11: Energy flow diagram of LPG used in cook-stove with PRB and CB.

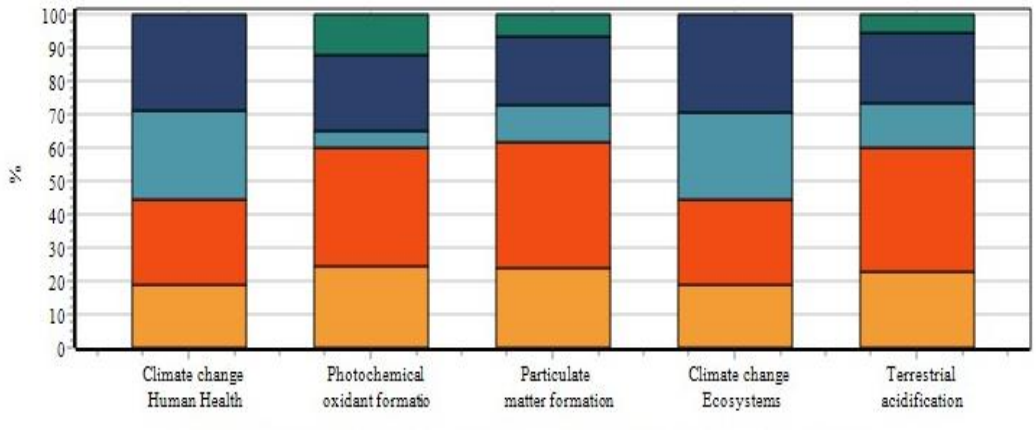

Fig. 3.12a: Distribution of environmental impacts from LPG life cycle with conventional domestic cook-stove.

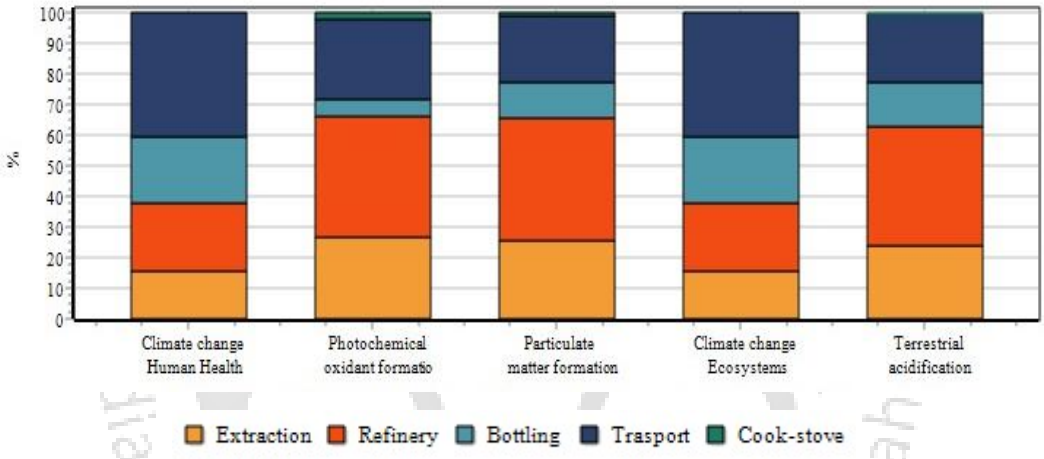

Fig. 3.12b: Distribution of environmental impacts from LPG life cycle with PRB incorporated cook-stove.

LCEE was found as 50.87% and 26.28% for stove with PRB and CB, respectively. Similarly, distribution diagram of environmental impacts for 1-3 kW, domestic LPG cooking stove with CB and PRB are presented in Fig. 3.12a and 3.12b. Figure 3.12b shows negligible impact due to PRB stove, whereas a considerable impact can be seen due to conventional one (lower thermal efficiency and higher emissions).

3.3 Techno-economic Assessment (TEA) of LPG Operated Cook-stoves with PRB

Techno-economic assessment TEA in principle is a cost-benefit comparison using different methods. These assessments are used for tasks such as:

- Evaluate the economic feasibility of a specific project

- Investigate cash flows (e.g. financing problems) over the lifetime
- Evaluate the likelihood of different technology scales and applications.
- Compare the economic quality of different technology applications providing the same service.

From this list it can be seen, that TEA is used for very different objectives. There is no specific format proposed for doing the assessment, because practical calculation uses different methods. In present study, total cost associated with cook-stove is considered in two aspects. First is the direct monetary cost associated with the cook-stove themselves, which includes cook-stove purchase cost and operation related costs (fuel cost and maintenance cost). Second is the indirect cost, which incorporates the cost associated with pollutant emitted during the cooking. The approach used for direct monetary cost comparison is based on the methods described by Keown et al. (2015) and Thumann and Mehta (1991), whereas to monetize the emissions (indirect cost), Environmental Product Strategies approach (EPS) proposed by Steen and co-workers (Steen, 1999a; 199b) is used. Economic analysis includes capital cost, life cycle cost, cash flow diagram, accounting rate of return, payback period and graph of annual saving as a function of time. The parameters and equations used for monetary cost comparison are summarized as follows:

(A) Capital Cost (C); which consist capital needed to purchase a stove.
(B) Annual operating cost (C_{OP}); this includes cost associated with the fuel consumption and maintenance of the stove. Where C_M is maintenance cost and C_F is Fuel cost.

$$C_{OP} = C_F + C_M \quad \text{……. (3.6)}$$

$$C_F = m_F \times C_f \times Yearly\ operating\ day \quad \text{……. (3.7)}$$

C) Indirect monetary cost or cook-stove emission cost ($C_{emission}$): for its calculation, unit Environmental Loading Unit (ELU) for emissions are given in Table 3.8. Emissions from cooking stoves on yearly basis are calculated based on Eq. (3.8).

$$E_i = P \times C_i \times Yearly\ operating\ day \quad \text{…… (3.8)}$$

Where, E_i= Emission of pollutant *i* (Kg/Year), C_i = Pollutant concentration (mg/kWh), P = Input power (kW).

D) Life cycle cost (C_{LS}); which is the sum of the actual capital cost ($\frac{C}{L_s}$), the operating cost (C_{OP}), and $C_{emission}$ cook-stove emission cost, where L_s is life (year) of the stove.

$$C_{LS} = \frac{C}{L_s} + C_{OP} + C_{emission} \quad \ldots\ldots. (3.9)$$

The above equations are used to calculate the cost of individual stove and later the cost parameters of the PRB and CB stoves are compared with the help of the following equations.

E) Annual saving (S): which is the life cycle cost difference between PB and CB.

$$S = (C_{LS})_{PB} - (C_{LS})_{CB} \quad \ldots\ldots. (3.10)$$

Where $(C_{LS})_{PB}$ is the annual life cycle cost of the PRB, $(C_{LS})_{CB}$ is the annual life cycle cost of the conventional stove.

(F) Net Present Value (NPV): It is used for analyzing an investment decision and positive NPV is used as the base to accept a proposed investment. NPV with consideration of interest and inflation rate are calculated by using the following equations:

$$P_a = \frac{F_a}{(1+f)^n} \times \frac{1}{(1+I)^n} \quad and \quad NPV = \sum_{n=0}^{n=L_s} P_a \quad \ldots\ldots. (3.11)$$

Where, i = interest rate, P_a= Present worth, F_a = future worth, f = inflation rate, L_s life of cook-stove and n is a positive integer.

(G) Payback method: Payback period (N_{PB}) is the ratio of the amount of initial investment and estimated annual net cash flow. While operating the stove, when Running Total (RT) is zero, it gives the number of years required to recover all the invested money.

$$RT = C - S \times N_{PB} \quad \ldots\ldots. (3.12)$$

(H) Internal Rate of Return (IRR) is used for measuring the profitability of potential investment. IRR is a discount rate that makes the net present value (NPV) of all cash flows from a particular project equal to zero.

Table 3.8: Unit Environmental load unit (ELU/kg), ₹/kg for emission (1 Euro = ₹75) (Steen, 2000a).

Emission	CO_2	CO	NO_x	SO_2	NMVOC	CH_4	PM_{10}
ELU (₹/kg)	8.1	24.825	173.25	245.25	180.75	204	2,700

3.3.1 Techno-economic Assessment (TEA) of medium scale PRB

The purchase price of various components has been obtained from the field/market survey. The assumptions made during the study are listed below:

1. The capital cost includes the transportation fee.

2. Maintenance cost include both burner head cost and maintenance fee.

3. The cost of LPG is based on the price provided by Indane Gas (Indian Oil).

From the capital cost of stoves, it is seen that PRB stove is cheaper with a unit capital cost of ₹700, than the conventional stove which costs around ₹1,150. This is due to lower manufacturing and burner cost of the PRB stove. The annual operating cost diagram (illustrated in Fig. 3.13) shows that the conventional stove demand higher annual operating cost of ₹2,15,498 than the PRB stove, which is just ₹1,76,014 for the same power input of 5 kW. It should be noted that the same functional unit has been considered for all power inputs and therefore, the annual operating cost of the conventional burner is the same for all power inputs. With increase in power input, annual operating cost difference between CB and PRB stoves increases. Since, at higher input power of 10 kW, thermal efficiency of conventional stove is very low (36%) as compared to PRB stove (52.6%). This results in increase in the annual operating cost saving of PRB stove from ₹39,484 to ₹68,240. Considering 10 year of service, the cost for owning and operating the stoves for medium scale cooking purpose has been estimated from the life cycle cost analysis.

It is clearly seen from Fig. 3.14 that share of capital cost in case of conventional stove is around 5%, whereas in case of PRB stove these are less than 0.5%, which means that around 99.5% of expense is in fuel consumption, due to which the energy efficient PRB stove is very cost effective.

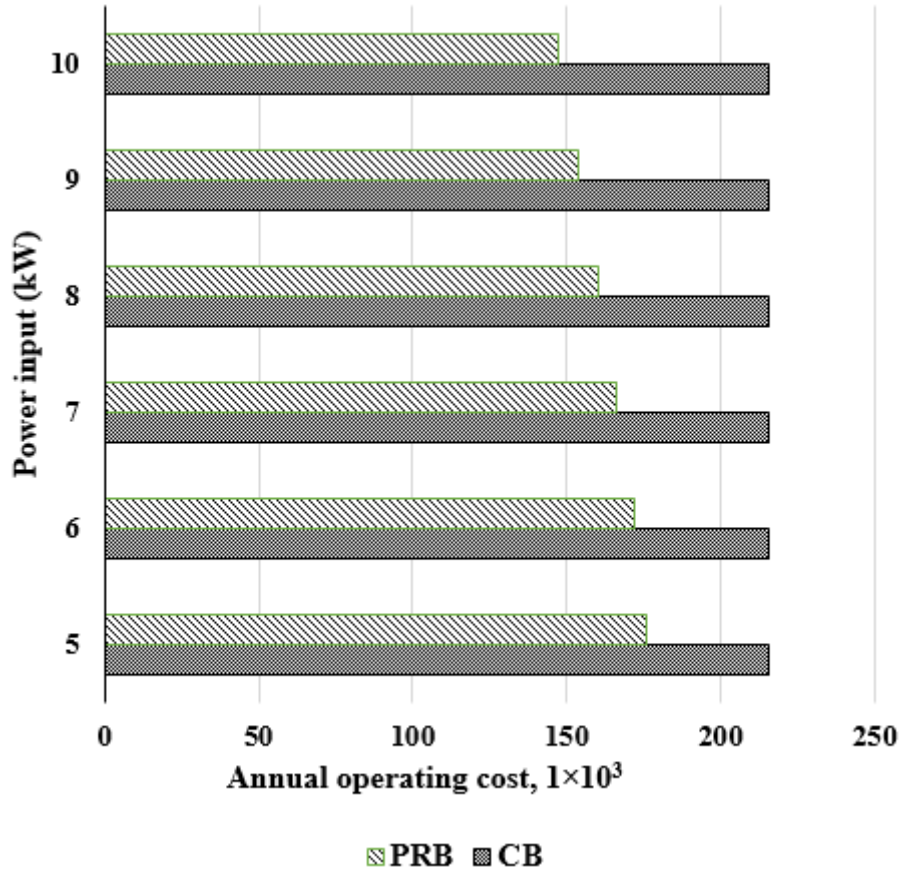

Fig. 3.13: Annual operating cost diagram.

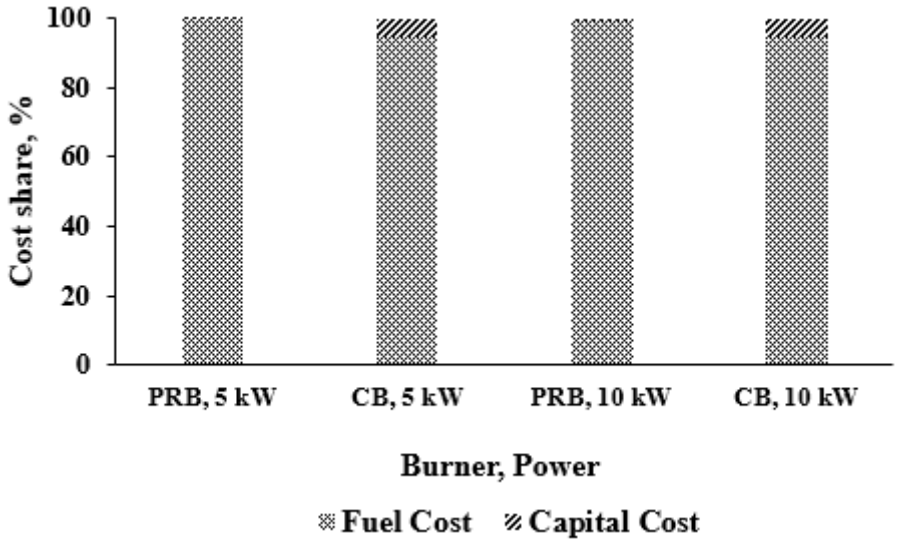

Fig. 3.14: Percentage cost share for cook-stoves.

To find the operating cost saving from the replacement of conventional stove by PRB stove in its life time, a graph illustrating the Annual operating cost saving over a period of 10 years for 5-10 kW input power is presented in Fig. 3.15. From Fig. 3.15, it is observed that the replacement of single PRB may save the operating cost of ₹3,94,136

to ₹6,81,695 for 5 to 10 kW input powers, respectively in the life span of 10 yr. The total annual expenditures of LPG stove with PRB, which includes capital cost, operating cost and emissions cost, are ₹1,87,333 for 5 kW input power and ₹1,56,612 for 10 kW input power and the yearly saving may rise from ₹42,157 to ₹72,915 for same power inputs.

Methods of financial appraisal explained in Section 3.3 have now been used to compare the cost parameters in relation to two different types of medium scale LPG cook-stove, i.e. optional case (PRB stove) with the original case (conventional stove).

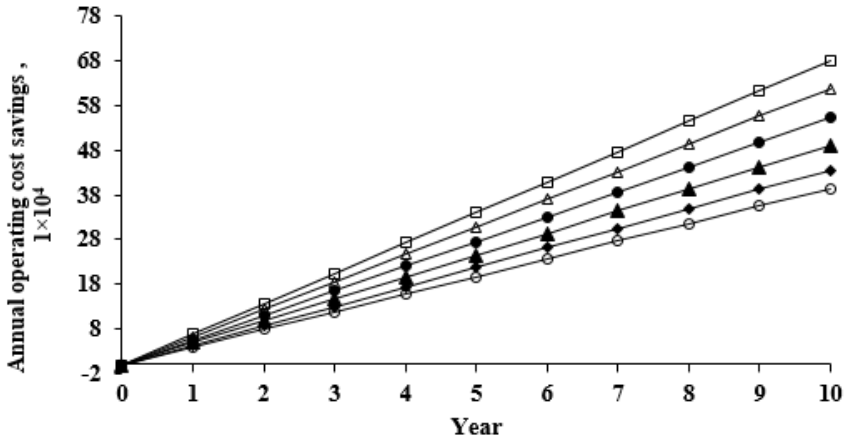

Power input	Equation for Net Annual Saving	Power input	Equation for Net Annual Saving
5 kW	$y = 3.9484x - 0.07$	6 kW	$y = 4.3625x - 0.07$
7 kW	$y = 4.9091x - 0.07$	8 kW	$y = 5.5239x - 0.07$
9 kW	$y = 6.1817x - 0.07$	10 kW	$y = 6.8239x - 0.07$

Fig. 3.15: Cumulative annual saving of the PRB stove.

Table 3.9 shows the calculated value of the annual saving, the present worth of the annual saving and the cumulative present worth of the annual saving for each year of life of the PRB cook-stove at 5 kW input power. With 5% inflation rate and 8% interest rate, the cumulative present worth of the annual savings for PRB stove over the life has been found as ₹3,44,991. The investment for the PRB stove is ₹700. It means that by investing ₹700 to procure a cook-stove today, one can save ₹3,44,991 over the life of the stove. Fig. 3.16 shows PRB cook-stove's NPV for 5-10 kW input power range. It is clear from Fig. 3.16 that with increasing input power NPV increases and largest NPV of ₹5,96,708 has been found at 10 kW input power.

Table 3.9: Economics of the medium scale cook-stove with PRB at 5 kW input power.

Year	Annual savings (₹)	Present worth of annual saving (₹)	Present worth of cumulative saving (₹)
1	42156.56	39033.85	39033.85
2	44264.39	37949.58	76983.43
3	46477.61	36895.43	113878.86
4	48801.49	35870.55	149749.41
5	51241.56	34874.15	184623.55
6	53803.64	33905.42	218528.98
7	56493.83	32963.61	251492.58
8	59318.52	32047.95	283540.53
9	62284.44	31157.73	314698.26
10	65398.66	30292.24	344990.49

Internal Rate of Return (*IRR*) is a financial ratio, used to calculate the yearly return generated from the proposed investment. According to this method, the rate of return is worked out by arriving at the percentage ratio of the net gain over the initial anticipated investment of the project. The *IRR* of PRB stove has a high value of 5573.5% and 9642.2% for 5 and 10 kW respectively, as the initial investment for one PRB stove was only ₹700 and the calculated average total annual cost saving are ₹42,157 and ₹72,915 for 5 and 10 kW, respectively. At 5 kW with an *IRR* of 5573.5%, the PRB technology is expected to earn ₹56 out of each ₹1 invested (yearly) and maximum of ₹96 at 10 kW with an *IRR* of 9642.2%. The payback period of less than a week for all input power shows recoupment of the original capital invested. Based on the functional unit selected for this study, the maximum and minimum time duration for PRB stove to overcome initial investment are estimated to be only 6 and 4 days at 5 kW and 10 kW power inputs, respectively. This short duration of payback period is possible as the daily savings are ₹115 and ₹200 for mentioned input power and cost of PRB stove is only ₹700.

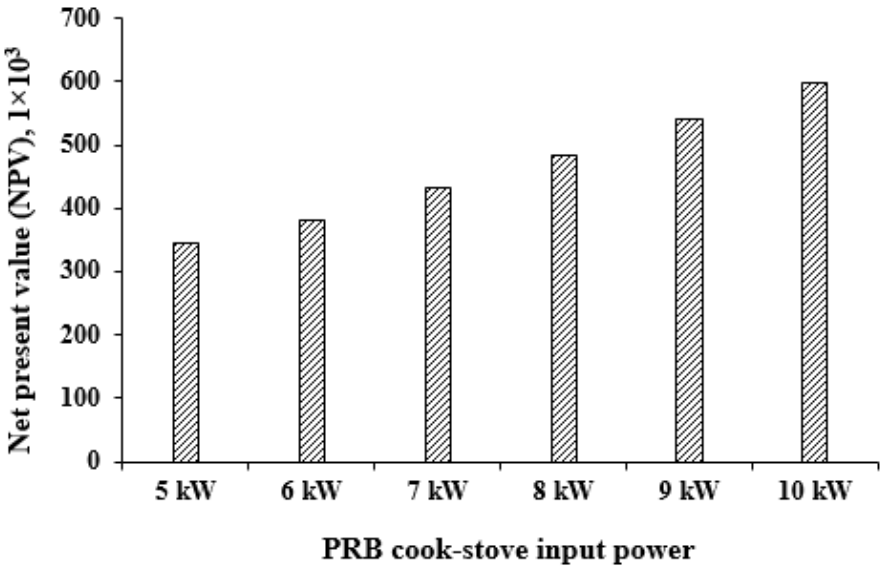

Fig. 3.16: Net present value (NPV) for 5-10 kW medium scale PRB cook-stove.

3.3.2 Techno-economic Assessment (TEA) of domestic scale PRB

Similar procedure as defined in Section 3.3 is also followed for domestic scale burner. For functional unit, as found from CCT (average heat energy requirement per household for daily cooking activities) was used for estimation. Result from economic analysis are tabulated below (Tables 3.10 and 3.11)

Table 3.10: Capital cost, operating cost, cook-stove mission cost, life cycle cost and annual saving for 1-3 kW PRB and conventional stove.

Parameters	Conventional stove	Stove with PRB
C	₹1200 /-	990 /-
L_s	10 Years	10 Years
Annual financial appraisal		
C_F	₹6818.34 /-	₹4758/-
C_M	₹60 /-	₹20 /-
C_{Op}	₹6878 /-	₹4778 /-
$C_{emission}$	₹450.4 /-	₹367.85 /-
C_{LS}	₹7449 /-	₹5245 /-
S	-	₹2204 /-

Table 3.11: Present worth of the annual saving and the cumulative present worth of the annual saving by 1-3 kW stove with PRB (5% inflation and 8% interest rate).

Year	Annual savings (₹)	Present worth of annual saving (₹)	Present worth of cumulative saving (₹)
1	2204	2040.74	2040.74
2	2314.2	1984.05	4024.79
3	2429.91	1928.94	5953.73
4	2551.41	1875.36	7829.09
5	2678.97	1823.26	9652.35
6	2812.92	1772.62	11424.97
7	2953.57	1723.38	13148.35
8	3101.25	1675.51	14823.86
9	3256.32	1628.97	16452.83
10	3419.13	1583.72	18036.55

3.4 Summary

Cooking process is one of the major consumers of non-renewable energy and also a potential contributor to air pollution. It is a daily process, thus it has great impact on the health and economy of every household. Extensive scientific investigations have been carried out to compare the energy saving and the environmental impact of the developed LPG cook-stove with PRB with its counterpart CB. Study concludes that PRB shows better performance as compared to CB at all three fronts of energy saving, emissions and overall cost. LCEE of LPG operated stove with PRB shows better result in comparison to its counterpart, CB, and has a surplus of 7% LCEE for input power of 5 kW which further rises to 11.6% for 10 kW. LCEE of PRB displays an escalating trend with increase in power due to larger difference in thermal efficiency between PRB and CB stoves at higher input power. Due to the higher thermal efficiency, the daily fuel saving from PRB based stove (based on the functional unit) was found to be 1.73 kg at 5 kW and the same has been increased to 3 kg when the stove was operated at 10 kW, input power. Usage of PRB in cook-stoves also reduces the total emissions during the life cycle of LPG. Similarly, lower direct emission (CO and NOx) from the combustion of LPG in PRB also reduces the negative impact of pollutants. With reference to the

functional unit tested at IIT Guwahati, the life cycle cost of the LPG cook-stove with PRB can be reduced to a great extent with an annual saving of ₹42,157 and ₹72,915 as compared to conventional stove CB at 5 and 10 kW, respectively.

Similarly, for domestic cook-stove comparative study of conventional and PRB based cook stoves has been conducted by following CCT method. The CCT method gives a closer estimation of the performance of a cook stove as it is based on the realistic consideration of cooking environment. The experiments conducted exhibits the energy, time and emission assessment of both the stoves. The newly developed stove with PRB has clearly proved to be a better burner than its counterpart. It results in 30.23 % saving of fuel, 29.98% saving in time and 84.53% and 91.37% reduction in CO and NO_x emission, respectively, on a daily basis. PRB operated domestic cook stoves can be a favorable alternate for the currently used conventional one. Life cycle economic assessment shows yearly saving of ₹2204 and estimated cumulative present worth of the annual saving for 10 years' life of the cook-stove is ₹18036. This is much higher than the capital cost of stove with PRB.

Both the PRB based cook-stove reduces the adverse impact on both human health and ecosystem significantly. This reduction is because of curtailment of both pollutant emission and fuel requirement.

Chapter 4

Development and Testing of Commercially Viable LPG Cook-stove with Porous Radiant Burner

The comprehensive performance assessment of PRB based cook-stove in the previous chapter showed its feasibility as an alternative to the available conventional cook-stoves. Pressure regulators, used in the designed PRB, of 1.5 bar for medium scale application and 1.2 bar for domestic scale application, was found unsuited for the Indian market. Any change in LPG pressure regulator for cooking application (for domestic 2.942 kN/m^2 and unreduced pressure regulator for medium scale, shown in Fig. 4.1) is strictly prohibited.

When the medium scale cook-stove was operated with unreduced pressure regulator, unstable burner operation was observed. As the self –aspirated PRB is designed for 1.5 bar LPG supply, fuel air distribution system, which is the most critical part for self-aspiration of air, is unable to deliver proper fuel air mixture to sustain combustion inside porous media. To overcome this deadlock, design modification has been carried out to develop commercially viable self-aspirated PRB for medium scale cooking application. Details of the development and performance of the newly designed self-aspirated PRB are presented in this chapter.

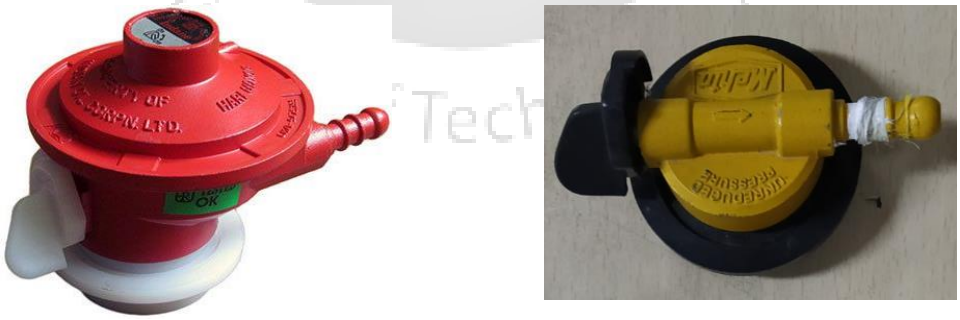

(a) (b)

Fig. 4.1: LPG regulators for (a) domestic and (b) medium-scale cooking application.

4.1 Scope of Modification in Self-aspirated PRB for Medium Scale Cooking Application

Various parts of the self-aspirated PRB for medium-scale cooking application developed by Mishra (2017) are shown in Fig. 4.2. Detailed specification of each parts are given in Table 4.1. The developed PRB is a two-layer burner consisting of SiC foam as Combustion Zone (CZ) and Al_2O_3 matrix as Preheat Zone (PZ). The combination of these layers is kept same during current investigation. Thickness of PZ was increased to 15 mm as previously used 10 mm thickness showed thermal cracking. Burner casing was also kept similar, only instead of Teflon (mixing chamber) same size galvanized iron (GI) socket is used. This can be easily incorporated in the burner casing during casting. Burner casing is made up off castable cement, for which casting is done locally. Two cook stove parts viz., orifice and burner port is considered for the current investigation. Selection of these two parts is based on correlation provided by Pichard et al (1977) for rate of primary air entrainment from an orifice to the mixing tube (Eq. 4.1). In which other than orifice diameter and burner port most of the parameters are almost fixed.

$$R = -\frac{(1+\sigma)}{2} + \sqrt{\frac{\sigma D_P^2}{D_I^2\sqrt{1+C_L}}} \qquad \ldots\ldots\ldots (4.1)$$

where, R is ratio of air and gas entrainment; σ is relative density of gas (ratio of density of LPG and air); D_P is burner port diameter; C_L is loss coefficient, and D_I is orifice diameter.

Pressure regulator

Alumina matrix (PZ)

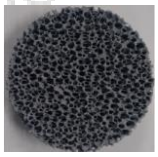

SiC matrix (CZ)

Casing

Teflon

Burner ports with connector

Orifice

Base plate with four orifice

Fig. 4.2: Different parts of self-aspirated PRB developed by Mishra (2017).

Table 4.1: Detailed specification of different parts of self-aspirated PRB (Mishra, (2017)).

PRB parts	specification
Burner ports	ID = 21 mm, OD = 23 mm, vertical length = 90 mm, slots of 10 ×30 mm
Orifice	0.25 mm diameter
Pressure regulator	LPG at 1.5 bar gauge pressure
Alumina matrix (PZ)	Pore diameter: 1.5 mm, number of pores: 463; diameter: 120 mm, thickness: 10 mm
SiC matrix (CZ)	Porosity: 90%, diameter: 120 mm, thickness: 25 mm

4.2 Working Principle of Self-aspirated LPG Cook-stove with PRB

A LPG cylinder was connected to an unreduced pressure regulator and then to a Coriolis flow meter for fuel flow rate measurement. The fuel flow rate was monitored using a suitable flow control valve. LPG passes through an orifice in the burner port. Due to the venturi effect, the high velocity LPG jet creates a low static pressure near the burner port and this causes suction of primary air through the two primary air slots. Air and gas move via burner port through a mixing chamber and reaches to the burner casing. Using an igniter, the combustion is ignited. The combustion takes place inside the PRB. After some time, the PRB becomes the fully red hot. The temperature fluctuation over the burner surface was observed for stable burner operation. Burner is considered as stable when temperature fluctuation remained within 10°C for at least 30 minutes. The flame stabilization signifies the absence of blow off and flashback. Flashback occurs when flame travels upstream into the mixing chamber, whereas, detachment of flame from the burner surface implies blow off. Once the burner reached stable condition, performance viz., thermal efficiency and emissions have been estimated. Detailed procedure of performance measurement is explained in following sections.

4.3 Procedures of Thermal Efficiency and Emission Measurement

In this section, the procedures adopted for thermal efficiency estimation and emission measurement are presented. Thermal efficiency is estimated by conducting the standard water boiling test as per the guidelines prescribed in the Indian Standard (IS): 4246:2002. This IS standard is only applicable for domestic LPG cook stove. However,

the procedure for other range of stoves remains same, only the size of Aluminum vessel and mass of water used during experiment varies as per the fuel flow rates. Due to different calorific value of fuel, the prescribed vessel size and mass of water used in the test differ for same power rating for fuel to fuel. Aluminum vessel along with lid and stirrer for the experiment are selected as per IS standards and filled with known amount of water at room temperature (~30°C). Weight of the vessel with water is noted with the help of a weighing balance. Initial temperature (T_1) of water is measured using glass-in-mercury thermometer. Sample 5 kg LPG cylinder is connected to the stove. The burner is ignited and after the burner reaches its stable condition, the vessel is kept above the burner. Now, the initial weight of LPG cylinder is noted with help of a precision balance (accuracy: ± 0.1 g). Water is heated up to 80 °C, and for uniformity in temperature, stirring is started and continued until the end of the test when the temperature of water has reached temperature of 90 ± 0.5°C. At this stage, the burner is switched off. The time taken to raise the temperature of the water from initial temperature to 90°C is noted, if fuel flow rate is measured. Otherwise weight difference of LPG cylinder before and after the tests give fuel consumption. In every case, experiments are repeated at least three times, and the average of three was taken for the analysis. For thermal efficiency prescribed formula in (BIS): 4246:2002 is given in Eq. 4.1

$$\eta_{th} = \frac{(M \times C_p + m \times C_w) \times (T_2 - T_1)}{m_{fuel} \times LCV_{fuel}} \quad \text{…….. (4.1)}$$

where, *M* is mass of the pan along with stirrer and lid (kg), *m* is mass of water in the pan (kg), *C* is the specific heat (kJ/kg-k, p: pan and w: water), T_2 and T_1 are the final and initial temperatures of water (°C), m_{fuel} is fuel consumed during experiment and LCV_{fuel} is low calorific value of fuel (kJ/kg).

For present medium scale cook-stove's power rating, no BIS standard is available. In case of LPG, IS 4246:2002 and IS 14612:1999 are available for 0-2.5 kW and 12.67-44.35 kW, respectively. Details of pan size and mass of water are presented in Appendix–IV. Therefore, in present investigation, the effect of thermal efficiency on vessel size and mass of water is presented. The Coriolis mass flow meter is connected to the supply line for the measurement of LPG consumption. Properties of the LPG is presented in Appendix–I. The detailed specifications of the instruments/equipment used

in the experiment and uncertainty in the efficiency measurements are presented in Appendix III, respectively.

For the emission measurements, the flue gas sampling is done according to the IS: 4246:2002. A hood shown in Fig. 4.3, was fabricated according to the dimensions mentioned in IS: 4246. The hood was placed above the burner along with the vessel and the portable flue gas analyzer probe was placed in the first sampling hole. The hood was used to isolate the flue gases from the atmosphere and then emission concentrations were recorded in the portable flue gas analyser (Testo 340). In present study, CO and NO_x concentrations referred to dry-basis measurement, with correction to a 3% fixed O_2 level is considered.

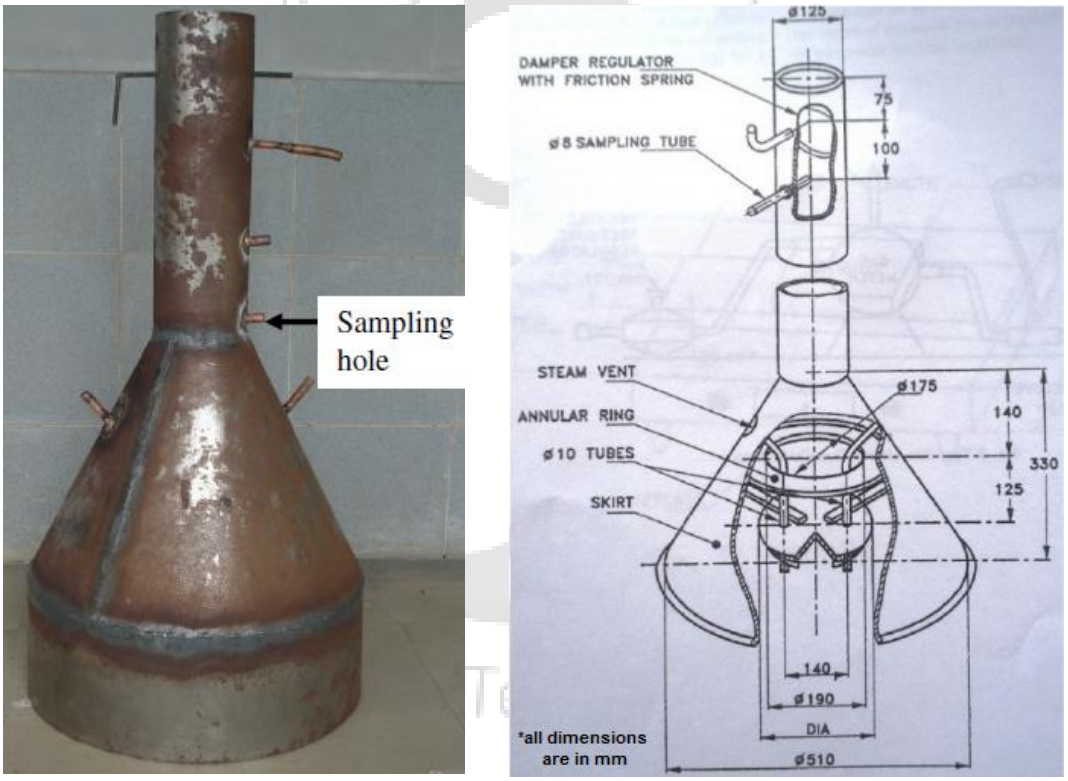

Hood for flue gas sampling

Schematic of the hood for flues gas sampling (imported from IS: 4246)

Fig. 4.3: Pictorial view and schematic of the hood for flues gas sampling.

4.4 Development of Self–aspirated LPG Cook-stove with PRB for Medium-scale Cooking Application

In the previous design of self–aspirated PRB (Mishra, 2017) with combination of 0.25 mm diameter orifice and port diameter of 21 mm, the best thermal performance was

achieved. So, for the new design of PRB with unreduced pressure regulator, orifice and port dimensions around the same values have been explored. Three different types of orifices, i.e., 0.25 mm, 0.35 mm, and 0.5 mm diameters are investigated. Similarly, three types of burner port of internal diameters of 15.8 mm, 19 mm and 21 mm and length of 90 mm with slot length of 20 mm and slot width of 10 mm for the air-entrainment were fabricated. Different orifice and burner ports with connector used in the present work is shown in Figs. 4.4 and 4.5.

Fig 4.4: Different burner ports (Dia. 15.8 mm, 19 mm and 21 mm) with connector used in the present work.

Fig. 4.5: Orifices of 0.25 mm,0.35 mm,0.5 mm and 0.8 mm diameters.

From the above tested combinations, 15.8 mm diameter port and 0.35 mm orifice diameter resulted in most stable burner operation. Pictorial view of cook-stove in running condition is shown in Fig. (4.6). With the above burner design, the operating power was found in the range of 5-7 kW, whereas, same was 5-10 kW in previous designed PRB with 1.5 bar pressure regulator. Further, when previously designed burner was tested for long hour of continuous operation (more than 4 hours) due to overheating of burner casing, flash back was observed. PRB shown in Fig. 4.6 works on the submerged combustion mode in which flame is trapped inside in porous matrix (CZ: SiC) and resulted in large preheating. Longer operating hours also heats the burner casing and add in to preheating of fuel air mixture in mixing chamber. To lower overheating, PRB needs further modification.

Fig. 4.6: Pictorial view of the LPG operated PRB cook stove (5-7 kW) in running condition.

The main cause of overheating is the large contact area between the CZ and burner casing, as it is the only way for combustion heat to transfer outside the burner, because the burner size is not changed. To overcome this problem, the burner is designed for partially submerged mode of operation. This lowered the entrapped heat and thereby prevented the auto ignition of fuel air mixture (flashback). This mode of operation was achieved by changing the port diameter (single port instead of two in previous design) and also reducing the contact area between combustion zone matrix (SiC) and burner casing. Schematics of final design is shown in Fig 4.7. Pictorial view of cook stove is shown in Fig. 4.8.

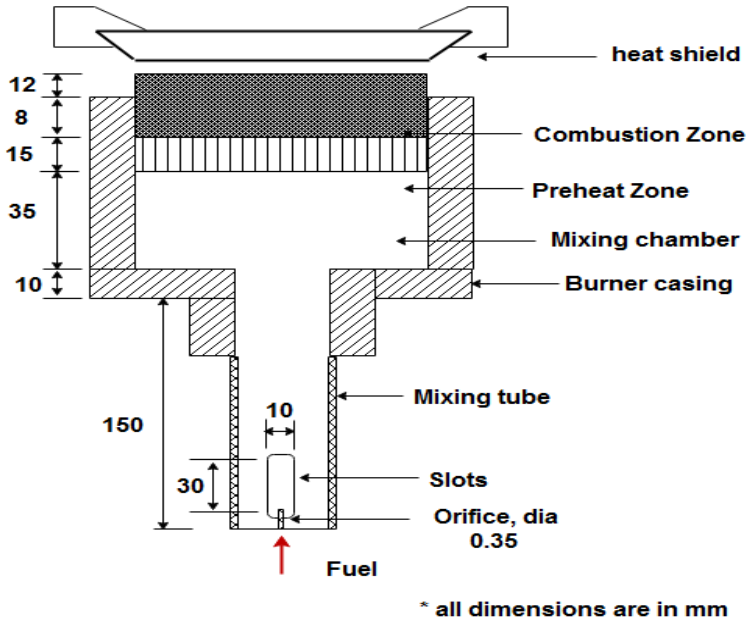

Fig. 4.7: Schematic of self-aspirated medium-scale LPG cooking stove with PRB (partially stabilized mode).

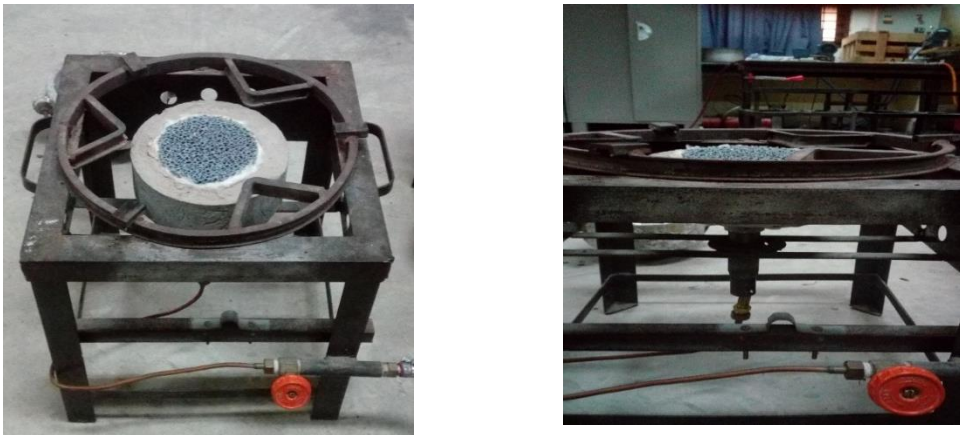

Fig. 4.8: Pictorial view of the cook stove cooking stove with PRB (partially submerged mode).

4.4.1 Result and Discussion

The designed cook-stove was found to be operational for the input power range of 5-7 kW. Thermal efficiency and emission measurements were carried out and compared with a conventional counterpart. To check the burner start-up time, surface temperature variation was also measured. As discussed previously that for this power rating, BIS standard is not available. In order to find the effects of pan diameter and mass of water on thermal efficiency, different experiments were performed at 5 kW input power. After that combination resulting in highest efficiency was further used for other power input and also compared with conventional cook-stove. Table 4.2 shows the pan diameter and mass of water used for thermal efficiency measurement. Efficiency variation is given in Table 4.3. Among the tested combinations pan size of 350 mm diameter with 11 kg of water showed the highest efficiency.

Table 4.2: Pan and mass of water used for efficiency measurement (5-7 kW, LPG).

Pan ID	Diameter (mm)	Height (mm)	Mass of pan and lid (g)	Mass of water (kg)
A	300	150	1058.8	9
B	320	160	1223.8	9, 10
C	350	180	2779.3	9, 10, 11, 12
D	375	200	3484.2	11, 12, 13, 14

Table 4.3: Thermal efficiency variation with pan diameter and mass of water.

Pan ID	Mass of water (kg)	Thermal efficiency (%)
A	9	60.65
B	9	61.30
	10	63.50
C	9	55.54
	10	62.50
	11	65.24
	12	64.68
D	11	61.92
	12	63.02
	13	64.49
	14	64.58
	15	64.85

For Temperature measurement thermocouple locations are shown in Fig. 4.9 and results of temperature measurement during start-up of the burner for input power of 5 kW, 6 kW and 7 kW are shown in Fig 4.10, respectively. For stabilizing temperature over the surface, 5 to 6 minutes of start-up time was observed.

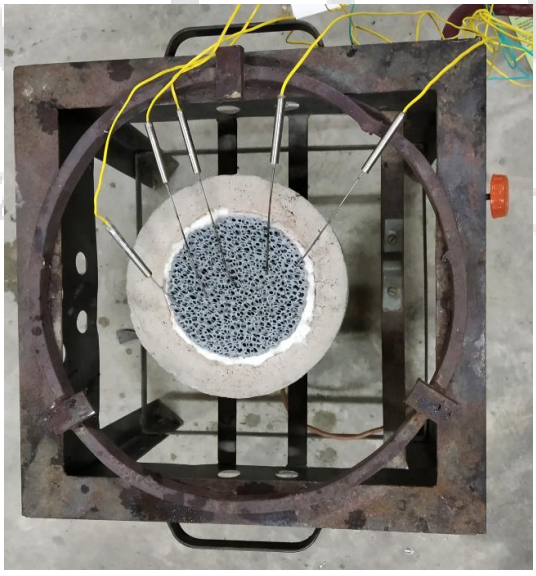

Fig. 4.9: Photographic view of thermocouple over self-aspirated PRB surface (5-7 kW).

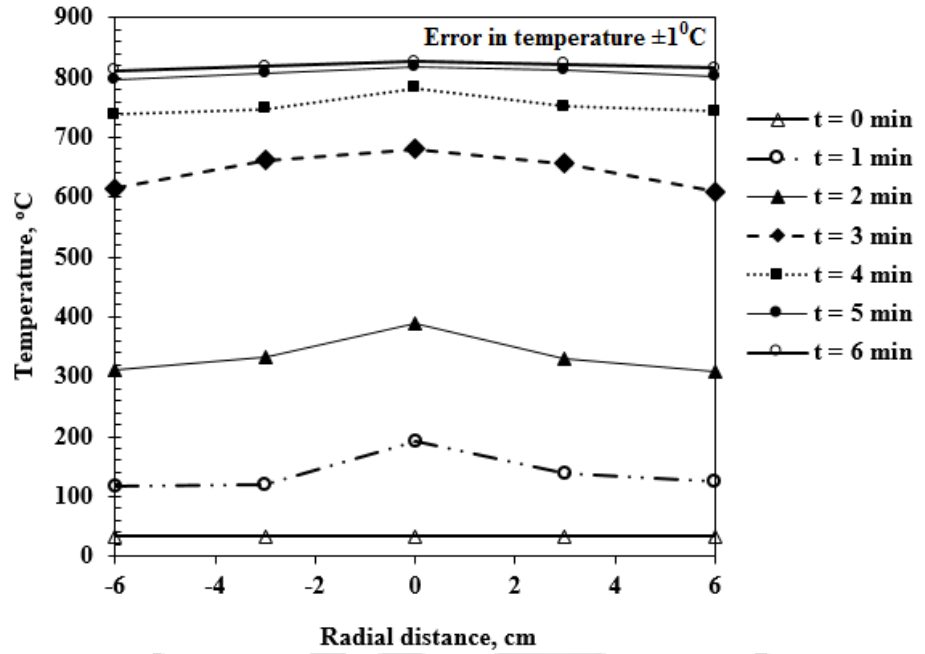

(a)

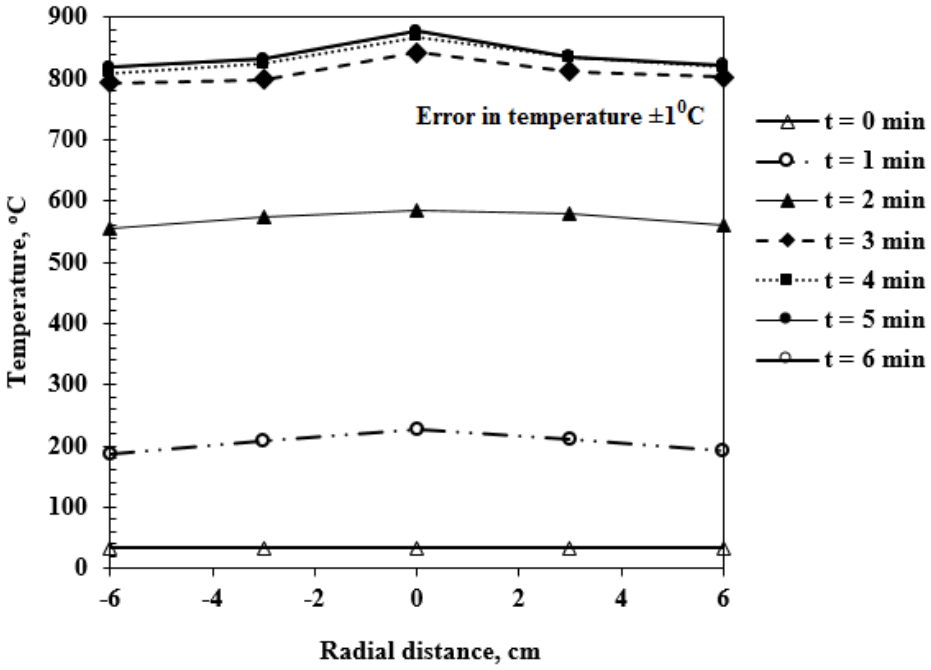

(b)

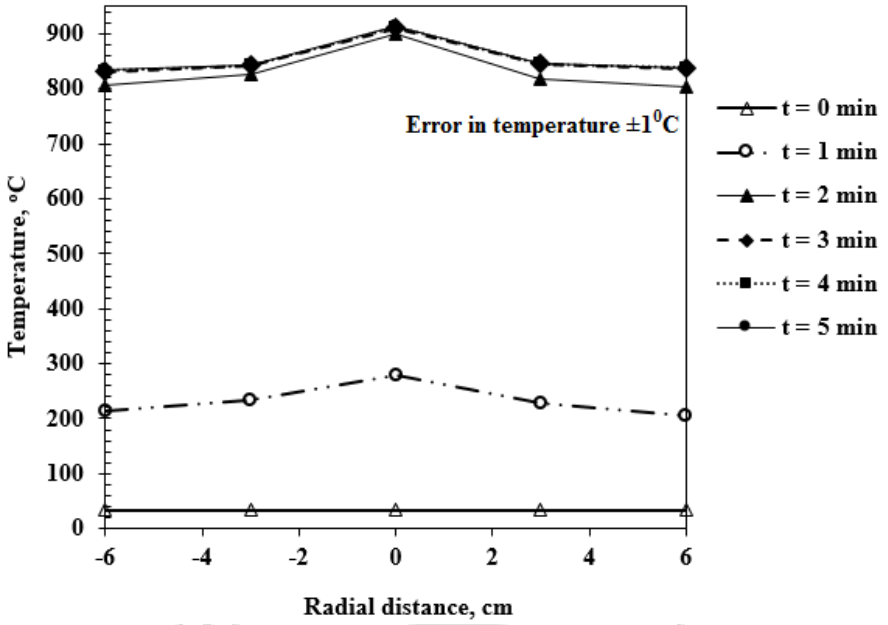

(c)

Fig. 4.10: Temperature variation over self-aspirated PRB with time for input power of (a) 5 kW, (b) 6 kW and (c) 7 kW.

Performance of the newly developed PRB for commercial power rating has been compared with a PRB developed by Mishra (2017) and a CB. As discussed before, mode of operation in case of Mishra (2017) was submerged, whereas, the newly designed PRB is operational in partially submerged mode. Within the input power range of 5-7 kW, thermal efficiency and emission variation are shown in Fig. 4.11 and Fig 4.12, respectively. With newly designed PRB, the maximum thermal efficiency was found as 64%, whereas, same is only 55% for Mishra (2017). Higher efficiency of newly designed PRB shows that for cooking application, partially submerged mode is more favourable than submerged mode operation. Reduction in efficiency with increasing input power was found more in the new design, but, efficiency was always higher than that of Mishra (2017). Emission characteristics of both the PRBs was far better than CB. The maximum CO and NO_x reductions compare to the CBs were more than 85% for both the PRBs. Comparison of temperature over PRB surface shows higher values in case of Mishra (2017), which was because of trapped flame inside the porous matrix (Fig. 13). The maximum temperature fluctuation between centre to periphery was found as 134°C in case of Mishra (2017), whereas it was only 74°C for newly designed PRB.

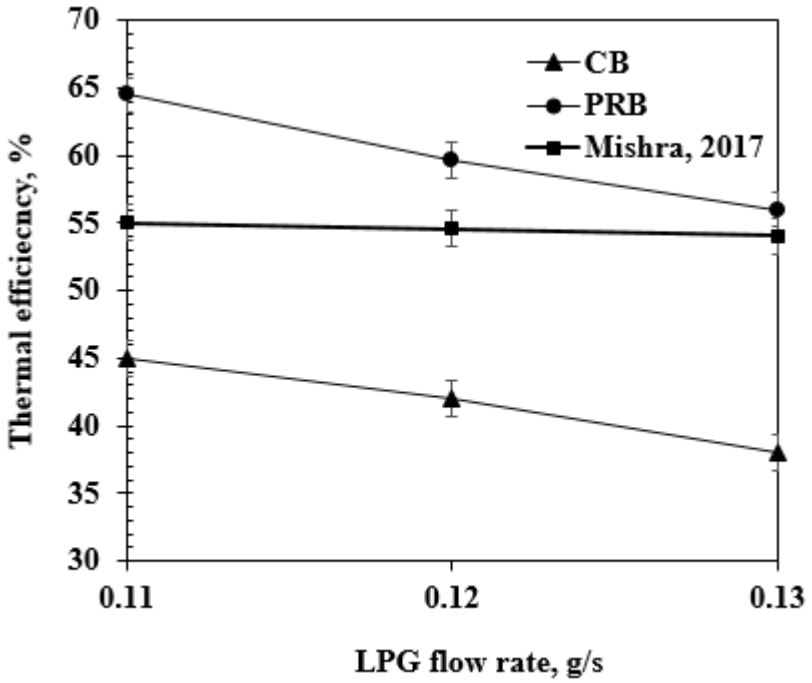

Fig. 4.11: Comparative thermal efficiency for input power range of 5-7 kW.

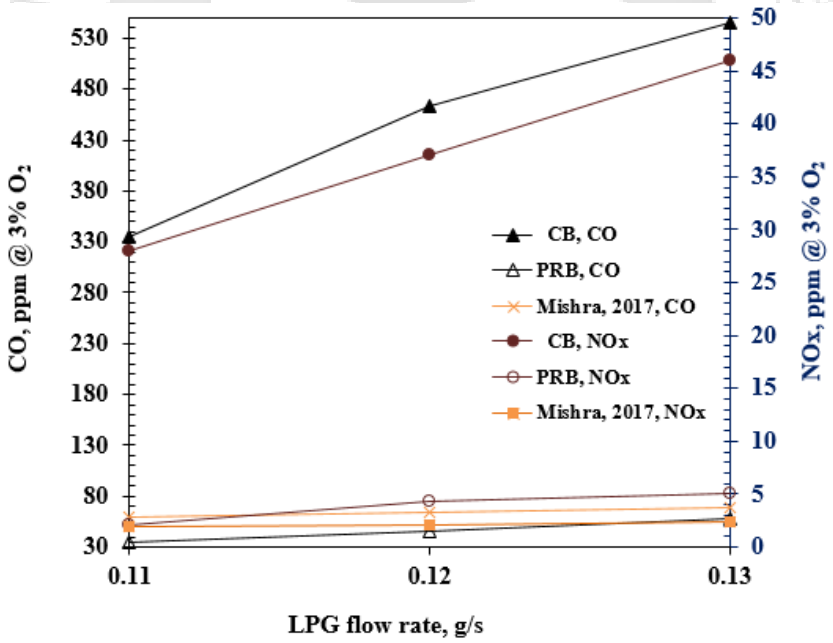

Fig. 4.12: Comparative CO and NOx emission for input power range of 5-7 kW.

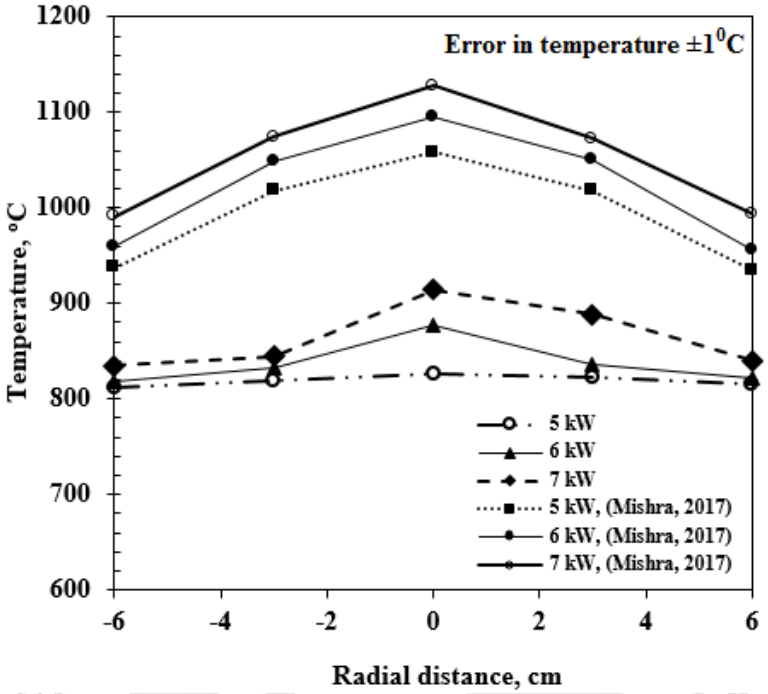

Fig. 4.13: Surface temperature variation with input power.

4.4.2 Summary

A commercially viable self-aspirated medium scale (5-7 kW) LPG cooking stove with a two-layer PRB has been designed and developed. The performances in terms of temperature distributions, thermal efficiency and CO and NO_x emissions of the stove were experimentally investigated. Partially submerged mode of operation was found favourable, for cooking application, as compared to submerged mode operation. This mode of operation results in higher thermal efficiency and also showed more uniform temperature over the burner surface. The thermal efficiency in the operational range of 5-7 kW was found as 64-56%, whereas, the same of only 38-45% in case of CB. From newly designed PRB, the highest values of CO and NO_x emissions were 58 ppm and 5 ppm, respectively. These values evidently signify cleaner combustion in newly developed PRB as its counterpart delivered much higher values of 545 and 46 ppm, respectively. Both CO and NO_x emissions revealed increasing trend with increase in LPG flow rate for both the cook-stoves. As the PRB has been designed with unreduced pressure valve (applicable for Indian market), this new PRB has the potential to replace its counterpart.

Chapter 5

Bio-gas Operated Domestic Cook-stove with PRB

In this chapter, the design of PRB and fabrication of experimental set-up for the biogas operated domestic cook-stove are presented. A brief discussion about the experimental procedure is also presented. This chapter broadly is divided in to three subsections. In the first section, performance assessment of domestic scale conventional cook-stove available in Indian market is presented. The second section focuses on the investigation of the Bio-gas operated PRB performance with forced air supply designed for domestic cook-stove power range. Third section covers the design of self-aspirated bio-gas operated PRB applicable for domestic cooking appliances. The performance assessment includes temperature, thermal efficiency and emission measurement at different input powers of bio-gas operated PRB is also presented.

5.1 Performance Assessment of Domestic Scale Conventional Biogas Cook-stove

Different types of domestic biogas cook-stove available in the Indian market are shown in Fig. 5.1, and the total gas input (burner rating) ranges from 225 l/h to 850 l/h. Here combustion takes place over the surface of the burner which is exactly above the head of the burner. The biogas cooking stove works on the same principle of FFC which is explained in chapter 1. The primary air entrainment in biogas cook-stove takes place through the opening around orifice and mixing pipe and then, the mixture reaches the burner via a mixing chamber, and then combustion takes place on the burner head.

(a) (b) (c)

Fig. 5.1: Burner rating of domestic biogas cook-stove (a) 225 l/h, (b) 450 l/h and (c) 850 l/h.

Estimation of thermal efficiency and emission of domestic scale biogas cook-stove are prescribed in the Indian Standard, (IS) 8749:2002. The procedure followed is briefly

described in the following.

The biogas used in the present study was produced locally from anaerobic digestion of cow dung. It was majorly comprised of CH_4 and CO_2 and has a LCV of ~17 MJ/kg. The composition and thermo-physical properties of the biogas used in the current work are given in the Appendix – I. The compressed biogas from biogas balloon was supplied to the cook-stove and the flow rate was measured with a Coriolis Mass Flow Meters (MFMs). Required flow rate was regulated through a control valve. The schematic of biogas supply line is shown in Fig. 5.2. For thermal efficiency measurement, Water Boiling Test (WBT) was used. An aluminum pan along with stirrer and lid for WBT was selected as per (IS) 8749:2002. Details of pan size and mass of water are presented in Appendix–IV. The pan was filled with a fixed quantity of water at room temperature and the initial temperature of water (T_1) was measured using a mercury-in-glass thermometer (accuracy ± 0.5ºC). Then, the pan was then kept above the pan support of cook-stove and water in it was heated up to 80°C, and for uniformity in temperature, stirring was started and continued until the end of the test i.e., when the temperature of water (T_2) reached 90 ± 0.5°C. At this stage, the cook-stove was switched off. The time required to raise the temperature was noted. In every case, experiments were repeated at least three times, and the average of three was considered for the analysis. Eq. 5.1 is used for calculating the thermal efficiency.

$$\eta_{th} = \frac{(M \times C_p + m \times C_w) \times (T_2 - T_1)}{\dot{m}_{biogas} \times \Delta t \times LCV_{fuel}} \quad \ldots\ldots\ (5.1)$$

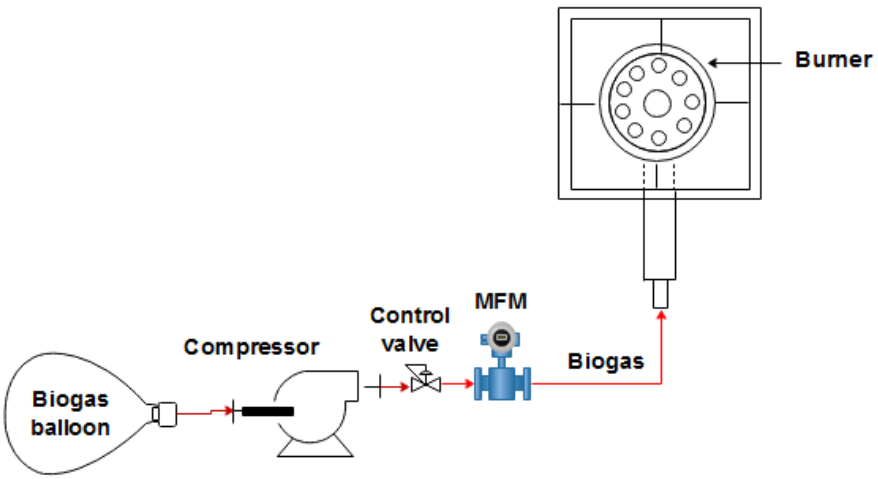

Fig. 5.2: The schematics of biogas supply line.

where, M is mass of the pan along with stirrer and lid (kg), m is mass of water in the pan (kg), C is the specific heat (kJ/kg-k, p: pan and w: water), T_2 and T_1 are the final and initial temperatures of water (°C), $\dot{m}_{biogas}$ and LCV_{fuel} are mass flow rate (kg/s) and low calorific value of fuel (kJ/kg), and Δt is the time required to raise the temperature of water from T_1 to T_2. The uncertainty in the efficiency was found to be ± 1.4% (detailed uncertainty analysis is presented in Appendix – III). The thermal efficiencies of conventional biogas cook-stove was estimated for the flow rate range of 177 to 530 l/h (1-3 kW), and were found in the range of 43 to 52%. The measured efficiencies are shown in Fig. 5.3. Increase in flow rate causes enhanced heat loss by convection, and hence, decreasing trend was observed.

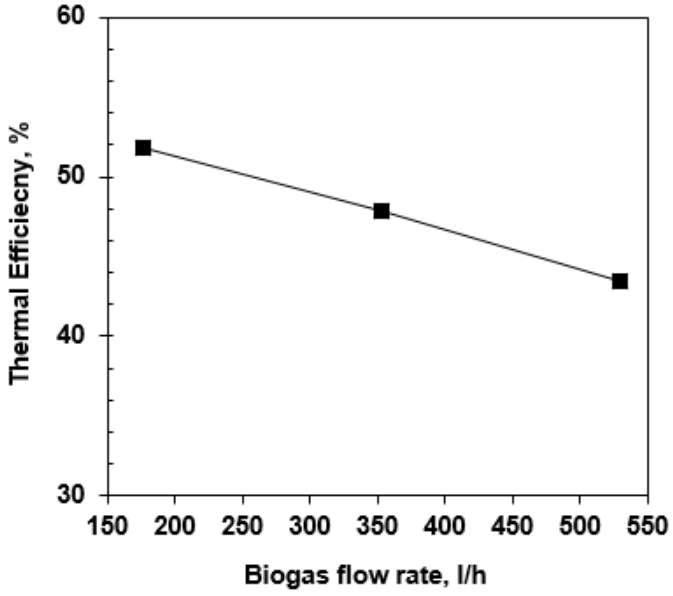

Fig. 5.3: Thermal efficiency of the conventional biogas cook-stove.

For the emission measurement, the flue gas sampling was done as explained in Chapter 4. In the IS standard for biogas (8749:2002), the hood dimensions are not specified. In the standard, it is mentioned that hood should not interfere in any way with the normal combustion of the burner and collects a fairly high proportion of the flue gases. Previously designed hood (chapter 4) fairly matches this requirement and therefore, same hood was also used for biogas emission measurement. The permissible CO emission level is prescribed as 500 ppm. The measured emission (CO and NO_x) levels for flow rate range of 177 to 530 l/h are shown in Fig. 5.4. The measured CO and NO_x emissions were found in the range of 211-276 ppm and 9-15 ppm, respectively. It was observed that for higher biogas flow rate, both CO and NO_x emissions were found to

increase. As the conventional biogas burners are designed for fuel reach combustion, incomplete combustion in the conventional cook-stove results in high CO emission. A similar increasing trend of NO_x emission was also observed.

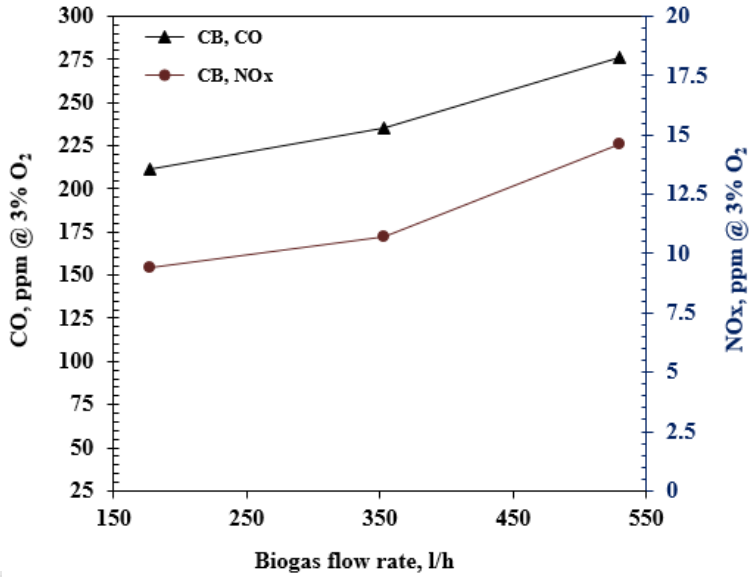

Fig. 5.4: CO and NO_x emission of the conventional biogas cook-stove.

5.2 Investigation of PRB Performance with Forced Air Supply

The performance investigation of the newly designed PRB applicable for domestic cooking appliances is presented in this section. The schematic of the in house developed PRB is shown in Fig. 5.5. The PRB consists of 90 mm disk of SiC and Al_2O_3 ceramic. The SiC foam and Al_2O_3 ceramic act as Combustion zone (CZ) and Preheat Zone (PZ), respectively. The high-temperature resistant castable cement is used for the fabrication of burner casing. Biogas is filled in a balloon and supplied by a compressor through a pressure regulator and a control valve. Specifications of the porous insert used in the PRB and fuel and air supply line details are provided in Table 5.1.

Table 5.1: Details of fuel and air supply line and porous inserts in biogas operated PRB.

Components		Specification
Fuel and Air supply		Fuel: Orifice diameter 4 mm, Port diameter for air supply: 10 and 18 mm Mixing pipe diameter: 20 mm
Porous inserts	SiC	Diameter 90 mm, thickness 20 mm, porosity 90%
	Al_2O_3	Diameter 90 mm, thickness 20 mm, porosity 31%

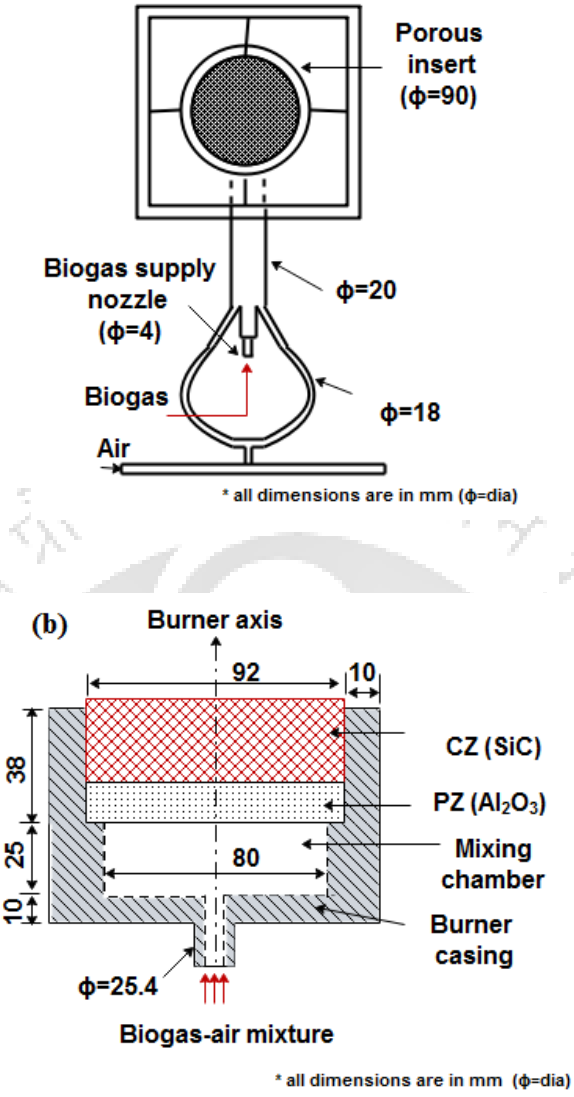

Fig. 5.5: Schematic of (a) cook-stove assembly and (b) details of PRB (Forced Air Supply).

Carbon dioxide in biogas acts more like a diluent and it does not actively contribute to the energy content of the nominal thermal load. This study, therefore, does not consider CO_2 as a part of the fuel for calculation of the equivalence ratio. The global combustion equation of biogas along with the definition of equivalence ratio (ϕ) for the study of burner performance are given in Eqs. 5. 1 and 5.2, respectively (Gao et al., 2013).

$$(1-\alpha)CH_4 + \frac{1+\phi}{\phi}(1-\alpha)(O_2 + 3.76N_2) + \alpha CO_2 \rightarrow CO_2 + 2(1-\alpha)H_2O + 7.52(1-\alpha)N_2 + \frac{1-\phi}{\phi}(1-\alpha)(O_2 + 3.76N_2) \quad \ldots\ldots (5.1)$$

$$\phi = \frac{\left(\frac{\dot{m}_{fuel}}{\dot{m}_{air}}\right)_{actual}}{\left(\frac{\dot{m}_{fuel}}{\dot{m}_{air}}\right)_{stoichiometry}} = 9.52 \times \frac{\dot{V}_{Biogas}}{\dot{V}_{air}} \quad \text{..... (5.2)}$$

where, α is CO_2 mole fraction, $\dot{m}$ (kg/hr) is the mass flow rate and $\dot{V}$ (m^3/hr) is the volumetric flow rate. The detailed procedure followed for various parametric investigations are presented below.

5.2.1 Experimental procedure and performance indicators

The flow rate of biogas is monitored through a Mass Flow Meter (MFM). The air supply system consists of compressor, pressure regulator, control valve and rotameter. At a pressure of 1.2 bar, both biogas and air reach the burner through their respective MFM. For proper mixing of biogas and air, a mixing pipe along with the mixing chamber is provided at the bottom of the PRB. The schematic of the experimental setup used for characterizing biogas combustion is shown in the Fig. 5.6.

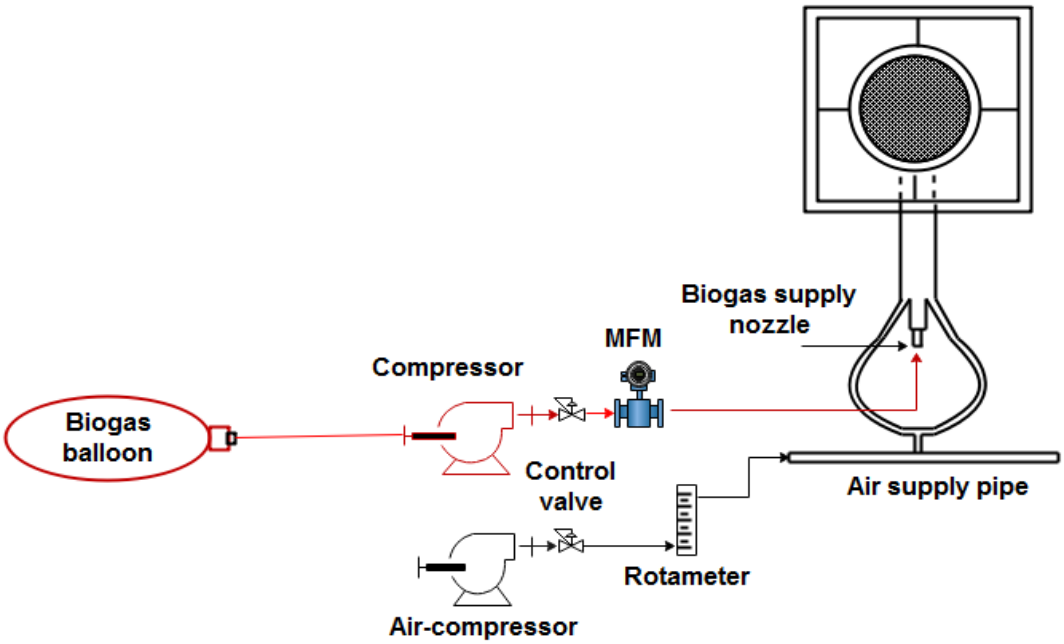

Fig. 5.6: Schematic of biogas cook-stove experimental set up (Forced air supply).

Initiation of the combustion process in both conventional cook-stove and PRB are quite similar, but the principal of sustained operation is totally different. In conventional cook-stove, when a heat (lighter or candle) source is applied on the biogas-air mixture,

it readily reacts with oxygen in the air, which gives off enough heat in the subsequent exothermic reaction, thus sustaining a consistent flame. However, in PRB, the flame is trapped by ceramic materials and highly emissive nature of porous insert (SiC) promotes radiative heat transfer in all possible directions. Further, the ceramics becomes red hot and sustains the combustion. In present investigation three main performance indicators viz., stability, thermal efficiency, and emissions, are used to characterize the PRB performance. Further, thermal efficiency and emissions are also compared with conventional cook-stove.

In PRB, the biogas-air mixture enters through Al_2O_3 porous matrix and is fired upon the top surface of SiC. Initially, the PRB was ignited at a high ϕ at a particular biogas flow rate and then, the air flow rate was gradually increased to achieve a specified ϕ. During stabilization, three conditions can take place as explained in Chapter 4. Flame stabilization signifies the absence of blow off and flashback. The ranges of ϕ in between these two instabilities are termed as stability limit of burner operation. The radial positions of the thermocouples placed on PRB top surface are shown in Fig. 5.7. The surface and axial temperature of the PRB was measured using K type thermocouples and the output was acquired with the help of a Data acquisition unit (DAQ). Once the stable range was specified, measurements of thermal efficiency and pollutant emissions were taken within this range for different biogas flow rates of 177, 353 and 530 l/h. Similarly, the locations of thermocouples for axial temperature measurements are shown in Fig. 5.8.

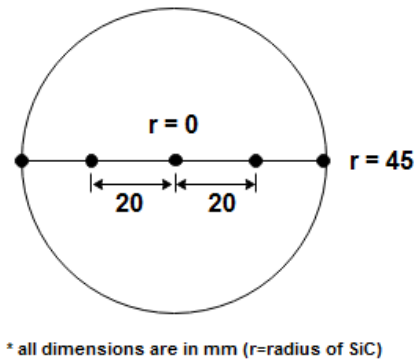

Fig. 5.7: Radial position of thermocouples on top surface of the biogas operated PRB.

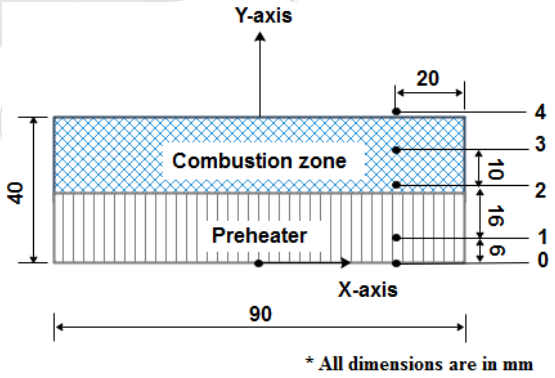

Fig. 5.8: Position of thermocouples in axial direction of biogas operated PRB.

As shown in Fig. 5.8, the locations 0, 1, 2, 3 and 4 indicate the temperatures in the base of the preheater, inside preheater, the reaction zone, the combustion zone and burner surface, respectively. All the measurements were taken at a radial distance of 20 mm from the periphery of the burner. The schematic of the experimental setup used for thermal efficiency and emission measurements are shown in Fig. 5.9. The procedure explained above for efficiency and emission measurement of conventional biogas stove was also followed for PRB. For experimental investigation, determination of uncertainty in the estimation of dependent parameters is very important. Instrumental uncertainties are given in Appendix-V.

5.2.2 Result and discussion

According to the procedure discussed in section 5.2.1, PRB stable operating range was found in the ϕ range of 0.75-0.95. The measurements of burner surface temperature, efficiency, and pollutant emissions were done within this range of ϕ for biogas flow rates of 177, 353 and 530 l/h. Obtained results are presented below.

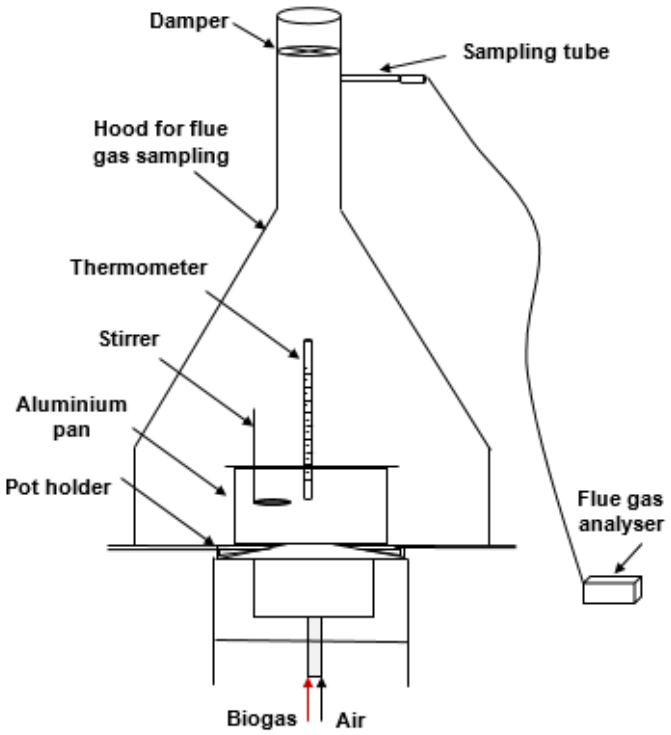

Fig. 5.9: Experimental setup used for thermal efficiency and emission measurements of Biogas cook-stove with PRB (Forced air supply).

The burner surface temperature distributions for different ϕ and biogas flow rates are shown in Fig. 5.10a-c. Biogas flow rate and ϕ increment show a similar impact on the trend of the maximum surface temperature of the PRB. Increment on both these parameters, ultimately increases the burner surface temperature. For all the cases, the maximum temperature was always occurred at the center of the burner and gradually decreases towards the periphery. The loss of heat by conduction and radiation from the burner casing to the environment are the main reason causing such heat distribution. Due to the burner casing shape, in the central region, the air-fuel mixture encounters less flow resistance than the region closes to the periphery of the burner. The maximum temperature difference between center to the periphery was 83°C for ϕ of 0.95 and biogas flow rate of 530 l/h. Due to the increased amount of air, lower ϕ escalates proper mixing of fuel and air and resulting in lesser temperature difference between center and periphery. Higher biogas flow rate also displays a similar trend. Lower flow rate hinders the uniform distribution of heat causing a higher temperature difference between maximum and minimum values. Previous works by Devi et al. (2019) and Gao et al. (2011, 2013) also showed the similar trends in surface temperature.

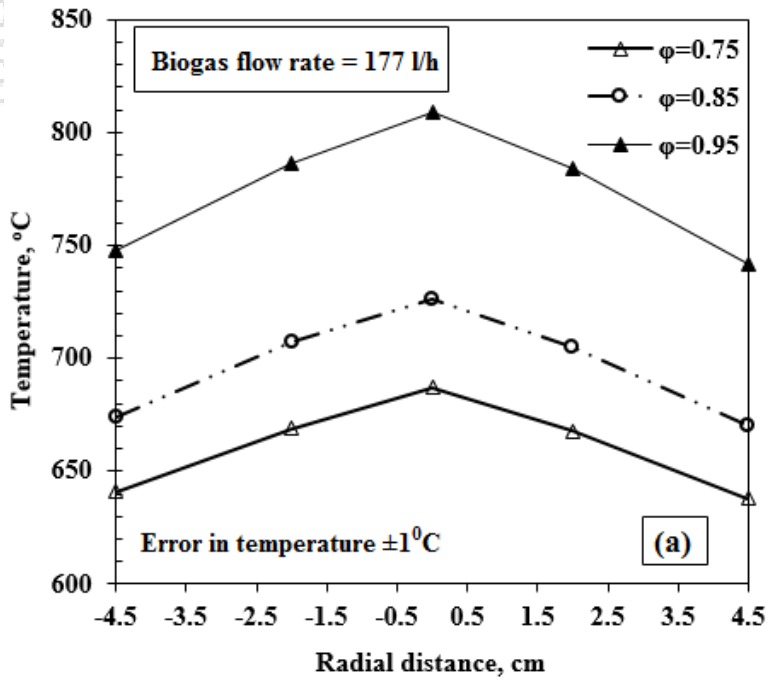

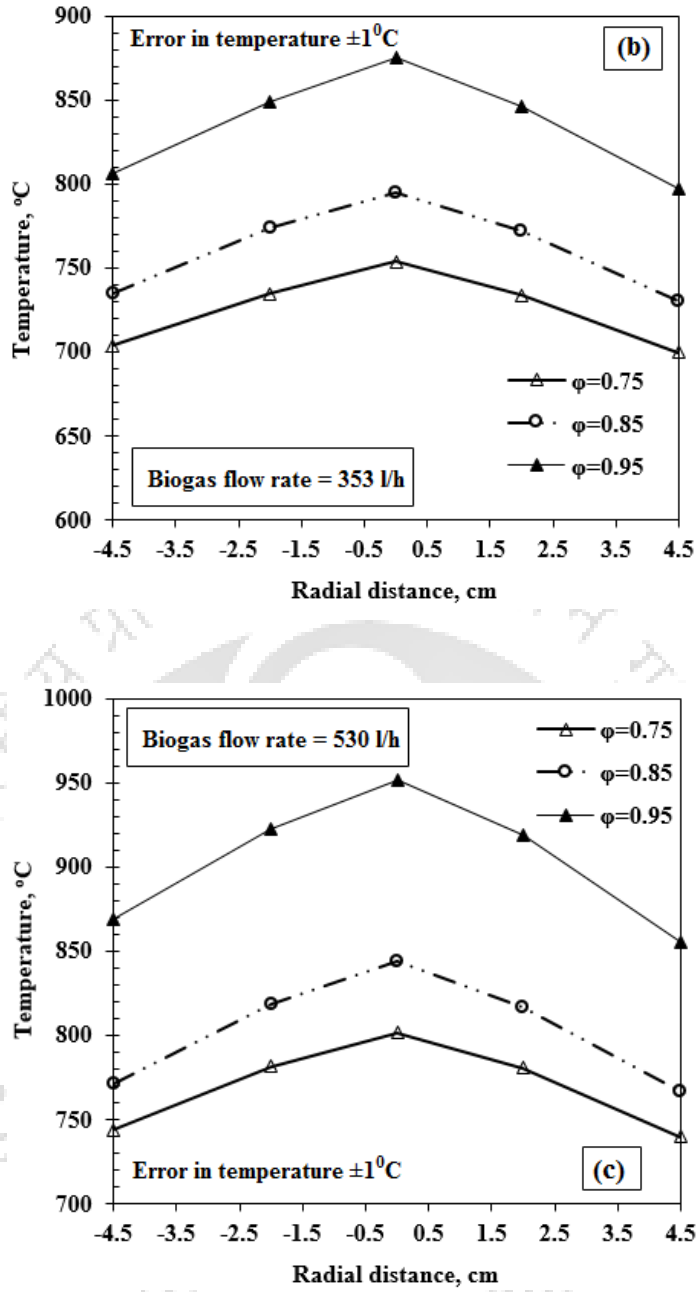

Fig. 5.10: Radial temperature distribution on top surface of the PRB (Forced air supply) with biogas flow rate of (a) 177 l/h, (b) 353 l/h and (c) 530 l/h.

The temperature variation of PRB in axial direction was measured for the combination of biogas flow rates of 177, 353 and 530 l/h and ϕ ratio of 0.75, 0.85 and 0.95. The behavior of temperature variation for all biogas flow rates shows a similar trend (Fig. 5.11). The temperature variation at all locations is always increasing with increase in biogas flow rate and ϕ. In PRB, continuous increase in temperature is seen up to position 2 and after that it gradually decreases. This region of maximum temperature (position 2 in Fig. 5.8) is the reaction zone where the combustion stabilizes. The

recorded maximum temperature for the biogas flow rate of 530 l/h and ϕ of 0.95 varied between 1001-1123°C, while the minimum temperature in the range of 63-73°C occurred in the position 0, which gave the thermal condition of the mixing chamber (Fig. 5.8).

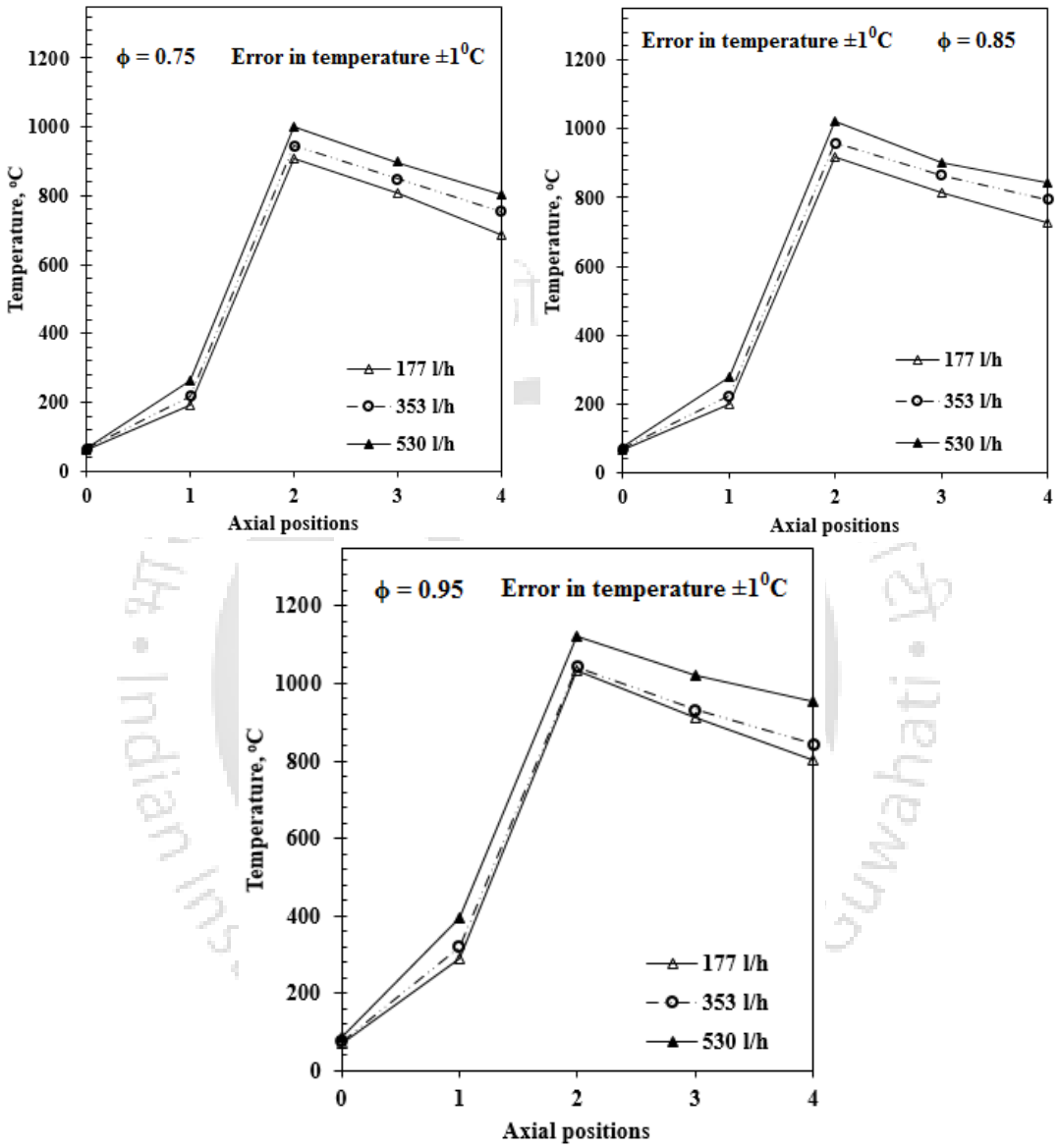

Fig. 5.11: Axial temperature distribution of biogas operated PRB (Forced air supply) (a) ϕ =0.75, (b) ϕ =0.85, and (c) ϕ = 0.95.

At all situations, the temperature of the mixing chamber was far less than the ignition temperature of biogas (~650°C), which eliminated the possibility of occurrence of flame flashback. A considerable preheating of air-fuel mixture was observed because of solid to solid conduction and radiation. The temperature of the preheater was found in the range of 278-395°C. Because of enhanced heat transfer in PM, the temperature measured at downstream was lesser than the reaction zone, which also contributed in

reduced production of harmful NO_x emission. Other combination of biogas flow rate and ϕ also shows a similar trend but temperature values was lower with decrease in biogas flow rate, which is obvious because of reduction in heat input. Thermal efficiency variation of PRB with fuel flow rate and ϕ is shown in Fig 5.12a. For a given flow rate of biogas, thermal efficiency shows a decreasing trend with an increase in ϕ. Such behavior is because of leaner condition, which moves the flame front downstream due to higher air flow rates, resulting in maximum volumetric heat release. Within the biogas flow rate investigated, lowest flow rate yields the maximum efficiency. The maximum efficiency of 62% was obtained for the biogas flow rate and ϕ of 177 l/h and 0.75, respectively. Similarly, the minimum value (51%) was achieved for 530 l/h and 0.95, respectively. A comparison between the thermal efficiency of conventional cook-stove and PRB is shown in Fig. 5.12b. As the conventional cook-stove is designed for fuel rich condition, PRB operating at ϕ of 0.95 has been chosen for comparison. Within the biogas flow rate of 177-530 l/h, thermal efficiency for conventional cook-stove ranged between 52 to 43% (Section 5.1), whereas the same was 58-51% in case of PRB. From efficiency data, it is clear that the percentage improvement in thermal efficiency of PRB is in the range of 11-16%.

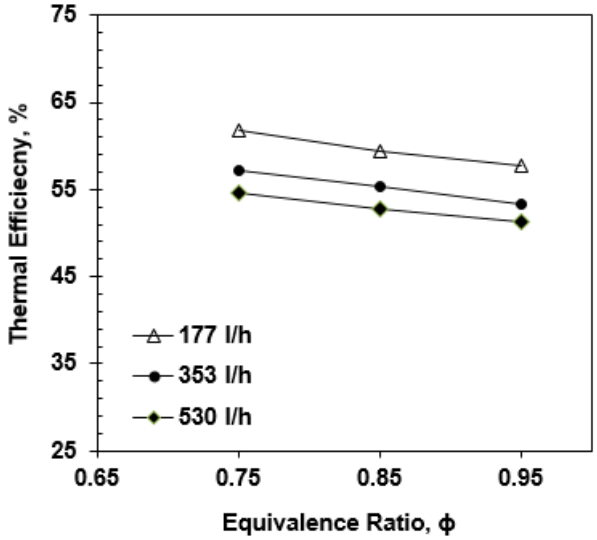

Fig. 5.12a: Variation of thermal efficiency with respect to equivalence ratio in biogas operated PRB (Forced air supply).

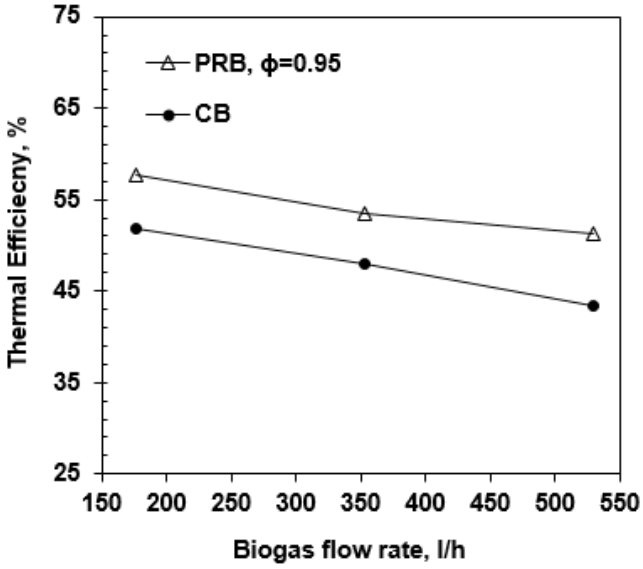

Fig. 5.12b: Thermal efficiency of biogas operated PRB (forced air supply) and CB.

With an increase in biogas flow rate, conventional cook-stove efficiency decreases and decrement is higher than that of PRB. The reason behind such behavior is associated with the fact that, with an increase in flow rate, the height of the flame increases which results in more convective heat loss. Due to the combined effects of radiative and convective heat transfer of the highly emissive porous material, for all the cases, PRB shows higher thermal efficiency than conventional cook-stove. Since PRB has been explored for domestic cooking application, the measurement of CO and NO_x emissions are very important due to direct contact of the burner flue gases with the user. In the present investigation, all the emission values are taken on dry-basis, with a correction to 3% oxygen level. The effects of ϕ and biogas flow rate on emissions of CO and NO_x are given in Fig. 5.13a. Similar to thermal efficiency, for comparison of emission values, ϕ of 0.95 in case of PRB was used. Comparison of CO and NO_x values between conventional cook-stove and PRB is shown in Fig. 5.13b. In PRB, measured values of CO and NO_x were found in the range of 29-80 ppm and 1-4 ppm, respectively, in the whole range of fuel flow rate. Whereas, in case CB same were 211-276 ppm and 9-15 ppm, respectively (Section 5.1). In PRB, increment in both ϕ and flow rate, increase CO and NO_x emissions. In the case of higher ϕ, due to lower % of air, fuel mobility decreases, which in turn reduces the mixing rate of air and fuel and causes higher emissions. Another reason for high CO is associated with reduced residence time in the porous matrix, which leads to higher unconverted CO. In PRB, thermal NO_x is predominant which is increased by an increase in temperature as the ϕ increases. Figure

5.13a, shows the impact of fuel flow rate on NO_x emission, since NO_x concentration reaches a threshold depending only on the ϕ. Similar, NO_x emission pattern was also presented in previous work by Keramiotis (2013). From Fig. 5.13b, it is observed that with increase in biogas flow rate, both the CO and NO_x emissions increase for both conventional cook-stove and PRB. Measured CO emissions of PRB are lower than that of conventional cook-stove, because of better combustion and more residence time. Similarly, the NO_x emission of PRB is also found much lower than that of the CB. In the PRB, lower global temperature (surface temperature of the burner) causes lower NO_x emission. Whereas, higher NO_x from CB is because of the fuel-rich combustion, which in turn results in high temperature in the reaction zone. From above investigation of biogas combustion in PRB, in the flow range of 177-530 l/h, the stable operation occurs within the equivalence ratio of 0.75 to 0.95. Within the operational range, leaner biogas combustion is possible. Compared to its conventional counterpart, a maximum of ~18% improvement in thermal efficiency and ~73% and ~80% reduction in CO and NO_x, can be achieved in PRB. Overall performances of the PRB suggest that it can replace the conventional cook-stove provided if it is designed for self-aspirated operation. Therefore, in order to make the PRB work on self-aspiration mode, further modifications are required. Details of modifications and its impact on burner performance are discussed in the following section.

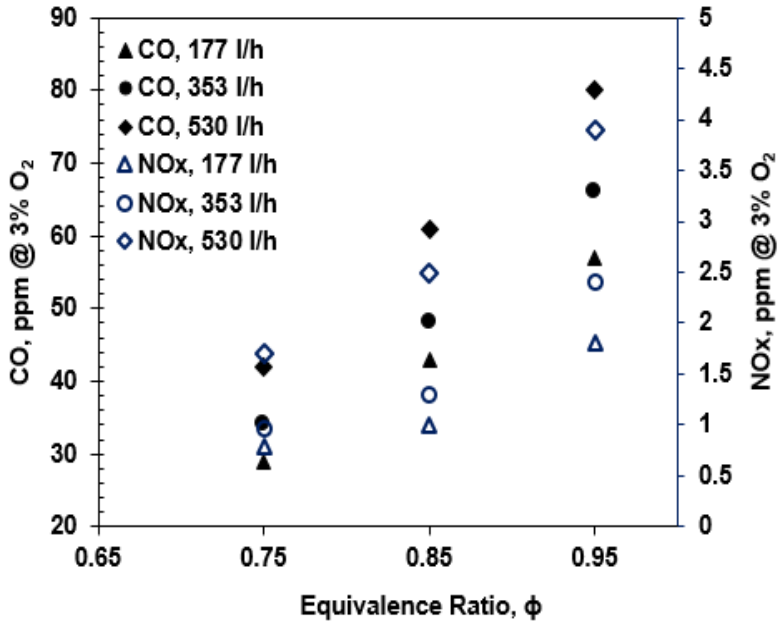

Fig. 5.13a: Variation of CO and NO_x emissions with respect to equivalence ratio in biogas operated PRB (Forced air supply).

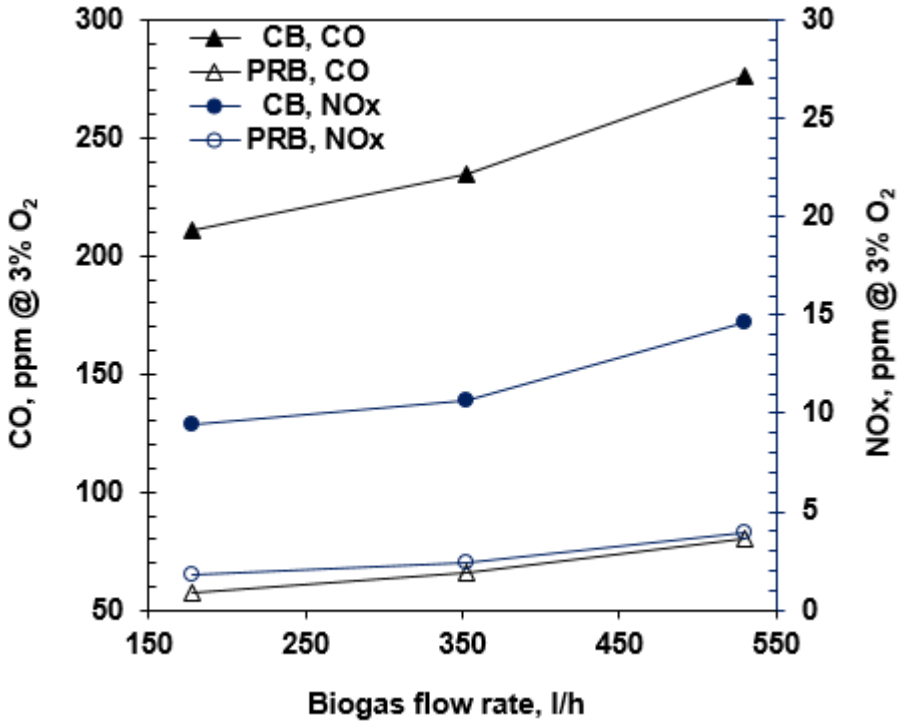

Fig. 5.13b: Comparison of CO and NO_x emissions of biogas operated PRB (Forced air supply) and conventional cook-stove (CB).

5.3 Development of Self–aspirated Biogas Cook-stove with PRB

As discussed in chapter 4, finding a proper combination of orifice and port diameter is most important factor to develop a self–aspirated cook-stove. Here, nine combinations of orifice and port have been explored, keeping other dimensions same (Fig. 5.5b), for providing sufficient air entertainment. All the ports are provided with equal opening slot for primary air-entrainment (slot length of 15 mm and slot width of 10 mm). Orifice and the fabricated ports are shown in Fig. 5.14.

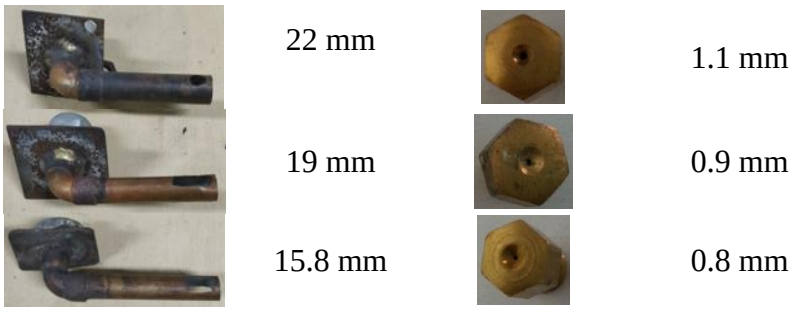

Fig. 5.14: Port and Orifice for biogas operated Self–aspirated PRB.

Table: 5.2: Result of stability analysis for biogas operated self–aspirated PRB.

S. No.	Port diameter (mm)	Orifice diameter (mm), Flash back (FB)		
		0.8 mm	0.9 mm	1.1 mm
1	15.8	FB	Stable	FB
2	19	FB	Stable	360-390 l/h: Stable
3	22	FB	360-390 l/h: FB 420-530 l/h: Stable	FB

For each burner port and orifice diameters, the stability analyses (details are given in chapter 4) have been performed and the same has been presented in Table 5.2. The observation from stability analysis showed that within the tested flow range of 177-530 l/h, 0.9 mm orifice diameter resulted in most stable operation. For an orifice diameter of 0.8 mm, flash back was observed and it was found unsuitable with any of the port diameter. In case of 1.1 mm diameter orifice, stable operation was observed with 19 mm port diameter only, and stable flame was limited between 360 l/h to 390 l/h flow rate of biogas. Further to finalize the port diameter, thermal efficiency test was performed with all three port diameters and 0.9 mm diameter orifice.

The thermal efficiency test procedure adopted has been explained in section 5.2.1. For all the stable conditions, efficiency test results are shown in Table 5.3. With increase in flow rates of biogas, the thermal efficiency is found to be decrease for port diameters of 15.8 mm and 19 mm, whereas for 22 mm port diameter, the efficiency increases. Within the tested biogas flow rate range of 360 to 480 l/h, the efficiency for 15.8 mm port diameter varied between 54.4 to 47.2%, whereas same was 58.48 to 53.76% in case of 19 mm port diameter. Further, from the estimated values of thermal efficiency, it was observed that 22 mm port diameter may be suited for larger biogas flow rate application. As the focus of current investigation is the development of a domestic cook-stove (the power rating for 22 mm diameter is above ~2.4 kW), this combination was not further explored. Among the tested combinations, 19 mm port diameter and 0.9 mm orifice diameter showed better efficiency. So, a detailed comparative performance assessment of this combination with conventional cook-stove, in the biogas flow rate range of 360 to 480 l/h have been performed. Result of comparative assessment are discussed in the next section.

Table 5.3: Thermal efficiency test results for orifice diameter 0.9 mm (biogas operated self–aspirated PRB).

Biogas flow rate (l/h)	Port diameter (mm)		
	15.8	19	22
360	54.4	58.48	-
390	52.7	57	-
420	51.6	55.77	47.8
450	49.8	54.8	50.3
480	47.2	53.76	55.2

5.3.1 Results and discussion

Specification of self-aspirated domestic biogas cook-stove with PRB is shown in the Fig. 5.15. Developed self-aspirated biogas cook-stove with PRB (1), consist of (2) a pressure regulator that supply biogas at 1.2 bar gauge pressure. Biogas flow through (3) 0.9 mm diameter orifice in to the (4) burner port of 19 mm diameter. Burner port is provided with (5,6) slots of length 15 mm and width of 10 mm for primary air suction. The mixing chamber (7) is provided for biogas air mixing. Burner casing (8) of total length 73 mm is made of castable cement. Casing is made in two sections, the bottom section of length 25 mm has inner diameter of 80 mm and outer diameter of 112 mm. The top section of length 38 mm is of inner diameter 92 mm and outer diameter 112 mm.

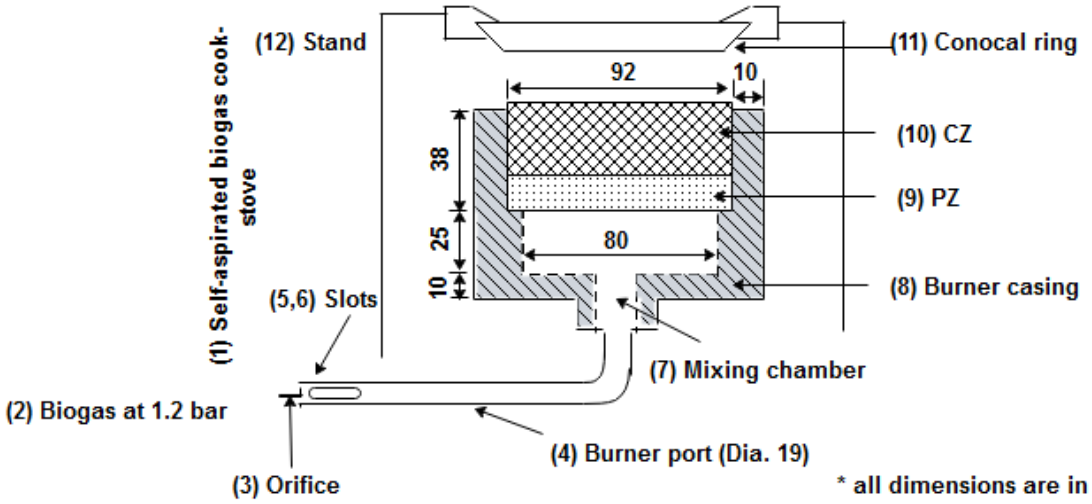

Fig. 5.15: Schematic of self-aspirated domestic biogas cooking stove with PRB.

The preheating zone (9) is made of alumina porous matrix of diameter 90 mm and thickness 20 mm with through holes (2 mm diameter, porosity 31%). The combustion zone (10) made of SiC with diameter 90 mm, thickness 20 mm and porosity 90%, is placed over the preheating zone. A detailed temperature measurement along axial and radial direction of self-aspirated PRB and emission measurement have been carried out. For radial and axial temperature measurement, position of thermocouples is similar to that shown in Figs. 5.7 and 5.8, respectively. Similarly, for emission measurements (CO and NO_x), procedure given in Section 5.1 was followed.

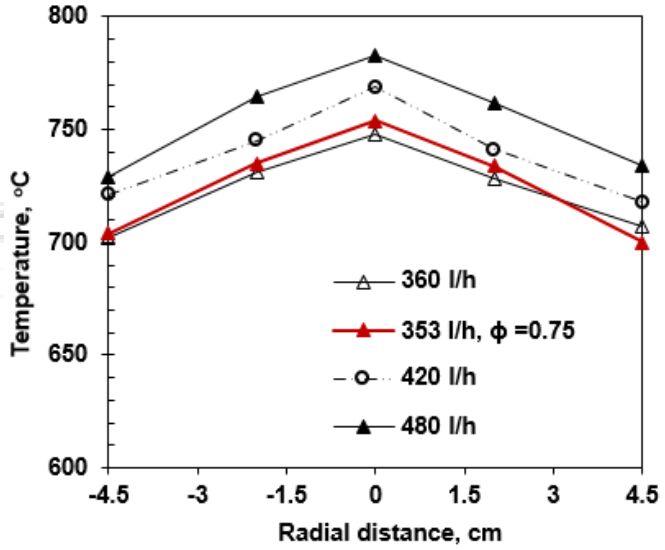

Fig. 5.16: Radial temperature distribution of self-aspirated PRB.

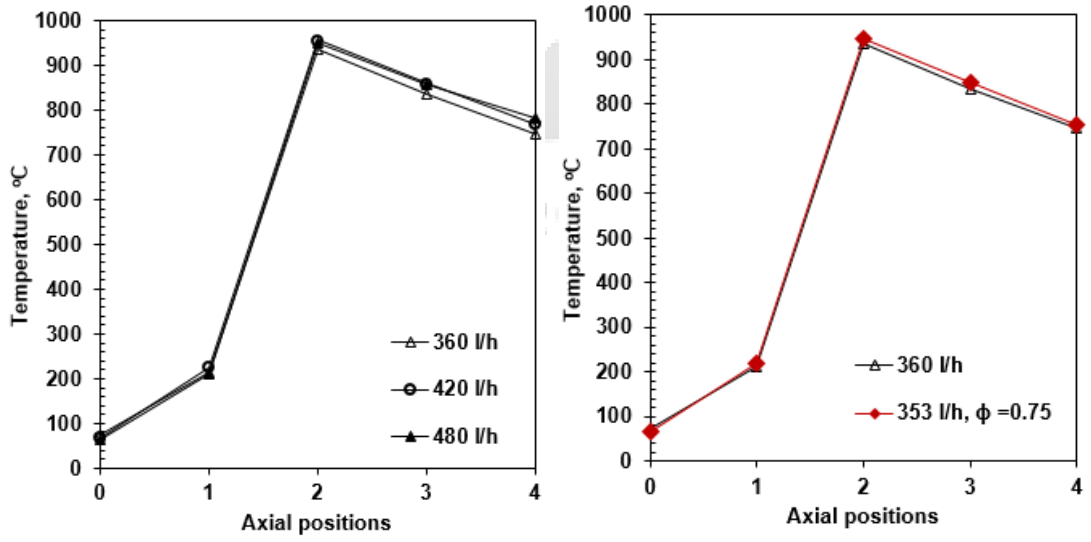

(a) (b)

Fig. 5.17: Axial temperature distribution of self-aspirated PRB.

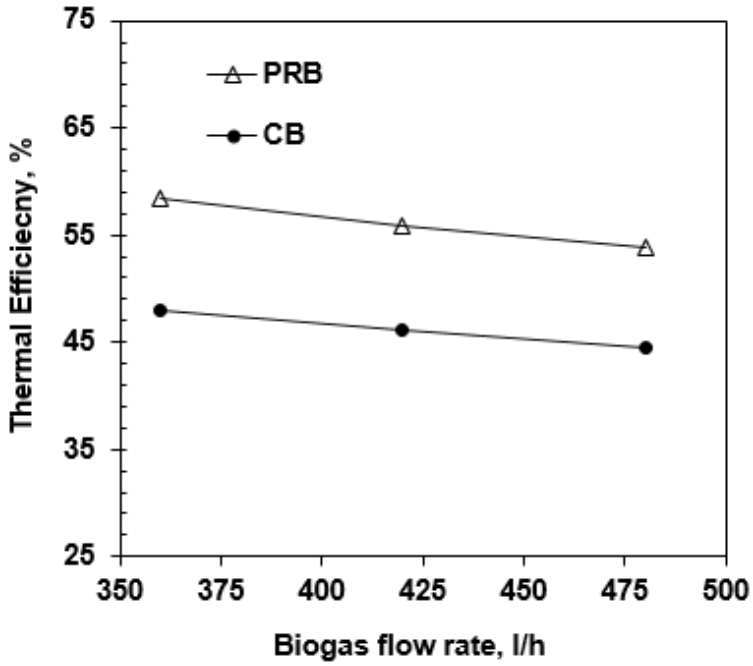

Fig. 5.18: Comparative thermal efficiency of self-aspirated PRB and conventional biogas cook-stove.

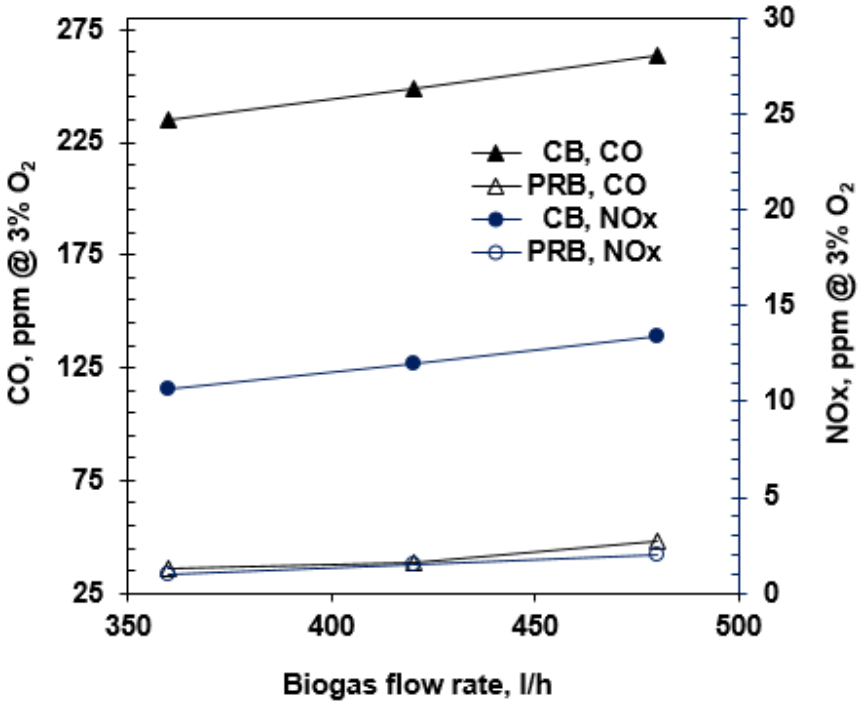

Fig. 5.19: Comparative CO and NO_x of self-aspirated PRB and conventional biogas cook-stove.

For the operational biogas flow rate range of 360 l/h to 480 l/h, radial and axial temperature distribution are shown in Figs. 5.16 and 5.17, respectively. Both radial and axial temperature distribution found for self-aspirated PRB is also follow similar trends as that of the forced air supplied PRB. The radial and axial temperature values for self-aspirated (360 l/h) PRB and that of forced air supply PRB (at 353 l/h), are found to be closer at equivalence ratio of 0.75 (Fig. 5.16 and 5.17b).

Comparative thermal efficiency of self-aspirated PRB and conventional biogas cook-stove within the operating biogas flow rate range of 360 l/h to 480 l/h is shown in Fig. 5.18. Within the tested flow rates of biogas, a maximum ~23% improvement in thermal efficiency was observed. Similarly, maximum ~85% reduction in CO emission and ~90% reduction in NOx emission show improved combustion (Fig. 5.19). Overall performance of self-aspirated PRB shows that it is perfectly suitable for domestic cooking applications.

5.4 Summary

The main focus during the present investigation was to understand the combustion characteristics of biogas in a PRB, applicable for domestic cooking appliances. Developed PRB consists of two-layer of porous matrices viz., Silicon carbide (SiC) and Alumina (Al_2O_3). First, with the help of forced air supply, stability and performance analysis were performed and later, a self-aspirated one was developed. The effects of biogas flow rate and equivalence ratio on thermal efficiency and emission characteristics of the burner were investigated and also compared with its conventional counterpart. Overall performance assessment showed that PRB operating at lower equivalence ratio and input power resulted in better thermal efficiency with lower CO and NO_x emissions. The thermal efficiency of self-aspirated PRB varied between 53-58%, and the maximum is found at biogas flow rate of 360 l/h. Within the studied biogas flow rate range (360-480 l/h), CO emission values were found to be in the range of 36-48 ppm and NO_x concentration is always lower than 2 ppm. Whereas, for conventional burner (CB), thermal efficiency, CO and NO_x emission were 44-47%, 235-263 ppm and 10-13 ppm, respectively. The overall performance showed that PRB is capable of burning a lean biogas-air mixture with better efficiency and lower emissions.

Chapter 6

Waste cooking oil (WCO) Operated Domestic Cook-stove with PRB

In this chapter, the preparation of blend samples of waste cooking oil (WCO) and kerosene is discussed. Construction details of conventional kerosene pressure stove (CKPs) and a newly developed Porous Radiant Burner (PRB) based kerosene pressure stove (PKPs) are also presented. Performances of the burners with blend samples and its comparison with pure kerosene are discussed.

6.1 Thermo-physical properties of blend samples of waste cooking oil (WCO) and kerosene

For the present work, WCO was collected from IIT Guwahati campus canteens and before blending, contaminants and residues were filtered by using wire mesh. For the blending of WCO with kerosene, a magnetic stirrer used is shown in Fig. 6.1.

Fig 6.1: Magnetic stirrer (IKAC – Mag, Model: HS7).

The mixture was stirred for 2 hours and sample was maintained at room temperature for the same period. The polarity of the developed magnetic field on the magnetic stirrer plate was altered by the AC supply. The magnetic bead (shown in Figure 6.1) was kept inside the sample container to respond to the altered magnetic field due to which rotation of magnetic bead took place inside the sample. This leads to the dispersion of WCO in kerosene. After that, blend samples were observed for 72 hours to check for any physical separation for ensuring uniform fuel properties throughout the sample.

Blend samples of WCO and kerosene were prepared on a volume basis. One of the blend sample, pure WCO and kerosene are shown in Figure 6.2.

(a) (b) (c)

Fig. 6.2: Fuel samples (a) WCO and kerosene blend prepared using magnetic stirrer, (b) Pure WCO and (c) Pure kerosene.

The calorific value and viscosity were estimated according to the standards of ASTM-D4809 and ASTM-D2983, respectively. Three blend samples (volume % of kerosene and WCO) viz., BS_1 (90/10), BS_2 (75/25) and BS_3 (50/50) have been prepared for investigation. The thermo-physical properties of the blend samples are given in Table 6.1.

Table 6.1: Thermo-physical properties of WCO and kerosene Blend Sample (BS).

Fuel properties	Fuel samples				
	100% kerosene	(BS_1) 90/10	(BS_2) 75/25	(BS_3) 50/50	100% WCO
Calorific value (MJ/kg)	43.89	43.47	42.81	41.72	39.53
Viscosity (mm^2/s)	1.3	5.79	9.94	14.48	40.42
Flash point (°C)	55	63	78	92	196
Fire point (°C)	61	76	94	119	218

6.2 Design and fabrication of WCO/kerosene blend operated PRB

Proper selection of porous matrix is the key factor for achieving better thermal efficiency and lower emissions. In order to study the effect of porous matrix diameter on the thermal efficiency of the burner, series of experiments have been performed (Sharma et al., 2011, 2016a, 2016b). It was found that the burner with 70 mm diameter

yielded the maximum thermal efficiency. Therefore, SiC matrix of 70 mm has been chosen for the present investigations. This work is an extension of the earlier PhD work on the development of pressurize kerosene burner for kerosene stove (Sinha, 2017). Figure 6.3 shows the schematic of the earlier developed PRB for kerosene application. Retrofitting the PRB in the commercial pressure kerosene stove leads to the significant improvement in thermal efficiency and reduction in emissions (Sinha, 2017). However, this burner was designed for pure kerosene application. Therefore, for WCO application vaporizer has been modified.

Fig. 6.3: Kerosene operated PRB developed by Sinha, 2017.

With the vaporizer developed by Sinha (2017) only partial red hot surface was noticed in SiC for WCO blend samples. It was because of increase in viscosity of fuel which degraded the spray characteristics. As heating of incoming WCO and kerosene blend before spray nozzle is the only option to improve the combustion characteristics. Vaporizer developed by Sinha (2017) was unable to recirculate heat to incoming fuel (Fig. 6.4). Reason behind this is the less contact area available between the porous media and burner (vaporizer). Therefore, a new vaporizer was developed with modified design. The modified vaporizer is shown in Figure 6.5.

Fig. 6.4: PRB assisted kerosene vaporizer developed by Sinha, 2017.

Fig. 6.5: Newly developed PRB for WCO and kerosene blend application.

In PRB, four 8 mm diameter copper tubes, two each ascending and descending, connected with a circular tube of 9 mm diameter copper tube (vaporizer) on top and SiC as CZ in mild steel burner casing, act as the burner (Fig. 6.5). Schematic of newly developed PRB is shown in Fig. 6.6. Stoves with PRB consists of a hand pump, fuel tank with integrated pressure gauge and one rising tube. Pressurizing the fuel in tank forces it to move through the rising tube and then to the vaporizer. A regulator is provided to maintain the intended amount of fuel flow rates. Apart from these components, the PRB is provided with a heat shield ring which reduces the heat loss to the surrounding. For comparative performance assessment with CB, BIS specified Roarer stove was used (Fig. 6.7). As shown in Fig. 6.8, the CB consists of two ascending and two descending tubes. These tubes touch the vaporizer (which is a flat circular chamber) and the ascending tubes remain connected with the riser. Middle section of the descending tubes contains the spray nozzle, through which kerosene vapor is sprayed in air. Apart from these components, the CB is provided with a flame holder, which helps in stabilizing the flame.

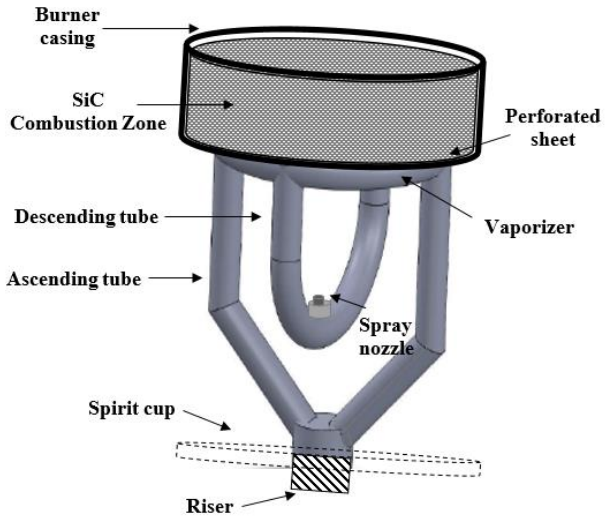

Fig. 6.6: Schematic of newly developed PRB for WCO and kerosene blend application.

Fig. 6.7: BIS specified Roarer stove.

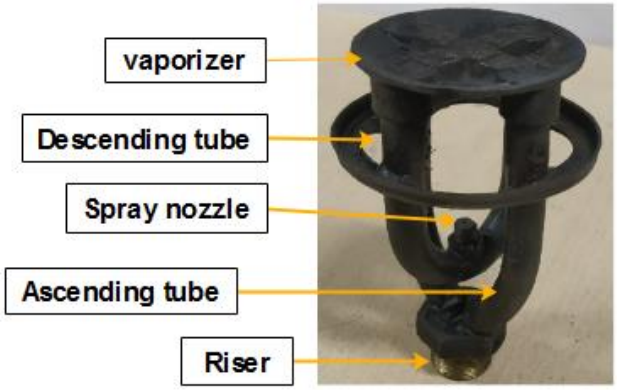

Fig. 6.8: Details of CB in Roarer stove.

Detailed specifications of the stove, nozzle, CB, and porous insert used in the investigation are provided in Table 6.2.

Table 6.2: Specifications of CB and PRB for WCO and kerosene blend application.

S. No.	Components		Specification
1.	Fuel tank capacity		3 liter
2.	Fuel tank pressure		1.5 bar
3.	Fuel used		kerosene and WCO blends
4.	CB		Commercially available burner
5.	Nozzle		Spray nozzle with 0.454 mm diameter
6.	PRB	SiC	70 mm dia., 20 mm thickness, 90% porosity
		Perforated sheet	70 mm dia., 2 mm thickness, 17% porosity, 1.5 mm hole dia.

Initiation of the combustion process in both burners is quite similar, but the principle of combustion is different. The vaporization process in both burners is initiated when a little quantity of kerosene is burnt in the spirit cup (provided just below the burner). The liberated heat is transferred to the vaporizer, and vaporized fuel moves down through descending fuel tubes and is ejected from a central nozzle. In CB, fuel vapor from the nozzle burns near the vaporizer and downward heat transfer from the flame sustains further combustion. However, in PRB, the flame is trapped by ceramic material (SiC), and the highly emissive nature of the porous insert promotes the radiative heat transfer in all possible directions, which is insignificant in CB. A clear visible flame near the vaporizer is not seen, rather the ceramic becomes red hot. The PRB is then said to operate in radiative mode. Temperature fluctuations on the burner surface have been observed. Burner operation is considered stable when the fluctuations remain within 10°C for at least 30 min. Schematic of the experimental setup used for thermal efficiency and emission measurements is shown in Figure 6.9. Technical specifications of different instruments used during experiments are given in Table 6.3.

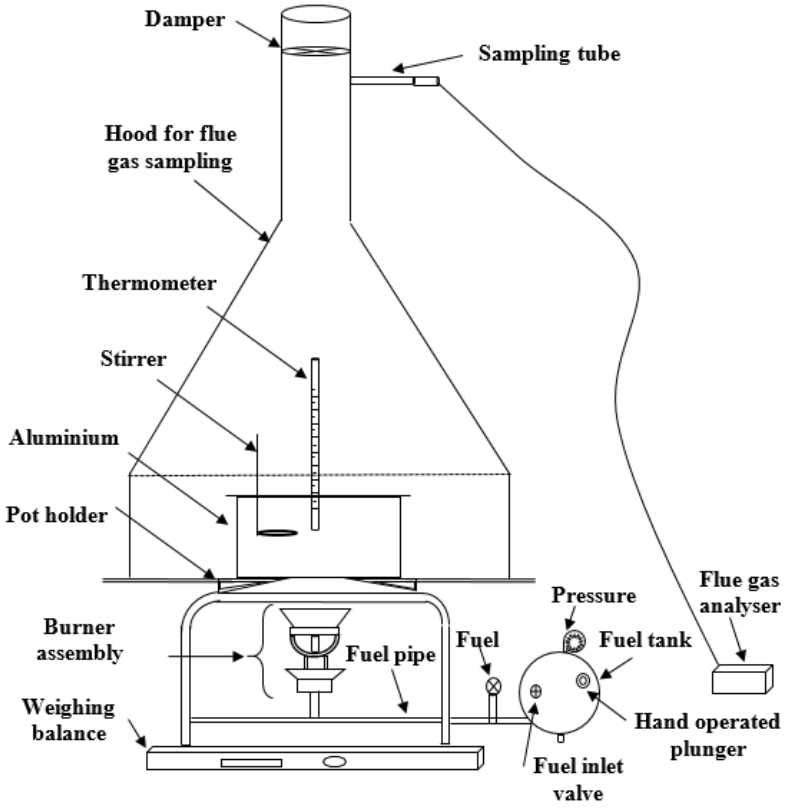

Fig. 6.9: Schematic of the experimental setup for WCO and kerosene blend operated cook-stove.

Table 6.3: Technical specifications of the instruments used in experimental studies.

Instruments	Functions	Uncertainty
Weighing balance (SES15TH)	Measurement of the weight of the stove, water, Aluminium vessel, and food items	±1 g
Portable flue gas analyzer (Testo 340)	CO	±2 ppm
	NO_x	±2 ppm
Thermometer	Temperature of water	±1°C
Thermocouples & Data acquisition unit (DAQ)	Temperature of burner	±1°C
Pressure gauge	Pressure in fuel tank	±1 mbar

6.3 Experimental procedure and performance indicators

At stabilized condition, experimental measurements were taken (as discussed in section 6.2) for the input power range of 1.5-3 kW. The following paragraph describes the performance of the cook-stove with the evaluation procedure. Cook-stove with conventional burner and porous radiant burner are designated as CKPs and PKPs, respectively.

6.3.1 Temperature mapping

For assessing the thermal performance, temperature mapping of the burner is very essential. Temperature distribution can explain the variation in efficiency and emissions with different geometrical and operational parameters. In PRB, surface temperature illustrates the radiative heat transfer from the burner to the load and in turn the radiation efficiency. Uniform surface temperature shows the proper distribution of fuel-air mixture, whereas non-uniformity results in a local hot spot, which in turn increases NO_x emission. Figure 6.10 shows the thermocouple locations for radial temperature measurement in the PRB. In PRB, the maximum temperature along the burner axis shows stable flame position. Displacement of stable flame location in PRB directly impacts the combustion characteristics. For comparison, the temperature measurement has also been carried out in the axial direction of CB. Figure 6.11 shows the position of thermocouples in the axial direction of both CB and PRB. The temperature along the axial direction of conventional kerosene pressure stove (CKPs) measured from the

burner head and, in case of porous kerosene pressure stove (PKPs), they measured within the porous matrix except for the zero position.

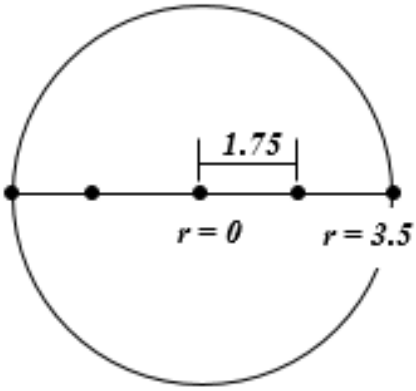

Fig. 6.10: Radial thermocouples position in PKPs (in cm).

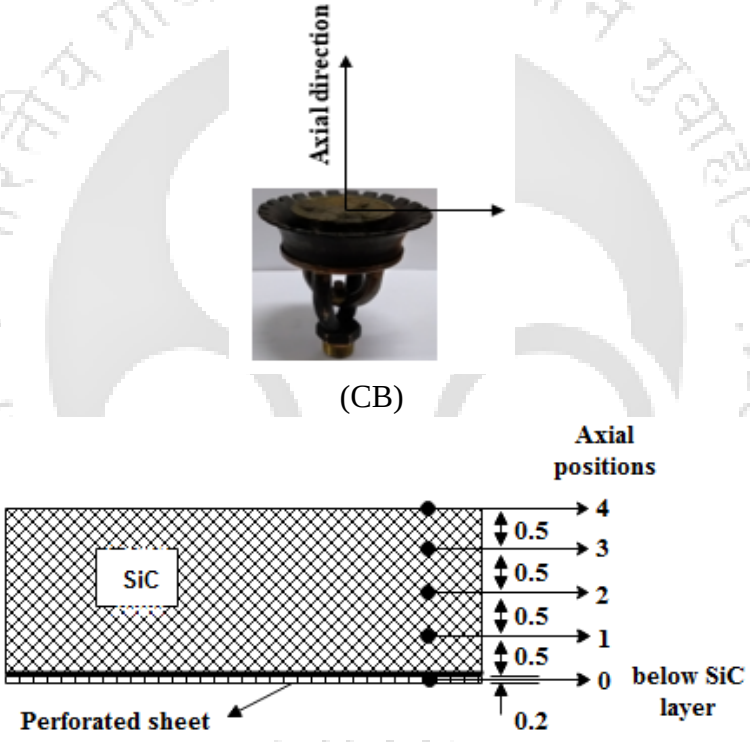

Fig. 6.11: Axial positions of thermocouples WCO/kerosene blend operated CB and PRB (in cm).

6.3.2 Radiation efficiency

Thermal radiation efficiency, which is the ratio of radiative heat transfer and input power to the burner, is calculated by using Eq. 6.1. Due to its dependency on the fourth power of temperature, radiant burner with high surface temperature is desirable. Also, high temperature leads to the mild and negligible influence of surrounding temperature

variation. During temperature measurements ambient temperature have been varied between 25 to 29°C. Therefore, for the calculation of the radiation efficiency, a suitable consistent value of surrounding temperature (27°C) has been considered.

$$\eta_{rad} = \frac{\varepsilon\sigma(T_{surf}^4 - T_{surr}^4) \times A_{BS}}{P_i} \quad \ldots\ldots\ldots \quad (6.1)$$

where, ε is surface emissivity (~0.9) of the SiC, σ is the Stefan-Boltzmann constant (5.67×10^{-8} W/m^{2}K^4) and T_{surf} and T_{surr} are the temperature of burner surface and surrounding, respectively. The A_{BS} is surface area of the burner (m^2) and P_i is input power to the burner.

6.3.3 Thermal efficiency

The method described in BIS (IS 10109:2002) has been used for the estimation of thermal efficiency. As per the standard Water Boiling Test (WBT), water mass and pan size have been chosen for the different fuel consumption rates. Details of pan size and mass of water are presented in Appendix–IV. The initial weight of the stove is measured after reaching steady-state (section 6.2). Then, the recommended quantity of water is poured and the pan is placed above the stove. Water is heated up to 90±1°C and the respective time and fuel consumption rate are noted for calculating the thermal efficiencies (Eqs. 6.2, 6.3).

$$\text{Thermal efficiecncy} = \frac{Heat\ utilized}{Heat\ produced} \quad \ldots\ldots\ldots \quad (6.2)$$

$$\eta_{th} = \frac{(m_p \times C_p + m_w \times C_w) \times (T_2 - T_1)}{m \times LCV_{BS}} \quad \ldots\ldots\ldots \quad (6.3)$$

Where, m_p is mass of the vessel with lid and stirrer (kg), m_w represents mass of water in the pan (kg), C is the specific heat (p: pan and w: water), T_2 and T_1 are the final and initial temperature of water. The m and LCV_{BS} are mass of blend sample fuel (kg) consumed during experiment, i.e. to raise the water temperature from T_1 to T_2 and lower calorific value of the fuel, respectively. The efficiencies have estimated for various combination of parameters. Maximum uncertainties were ±2.9% and ±1.26% for

radiation and thermal efficiency measurement. Details of the uncertainty analysis is presented in Appendix – III.

6.3.4 Emissions

Exhaust gas emissions estimate the nature of the combustion. Flue gas measurement is done by sampling of flue gas, according to BIS (IS 10109:2002). By using hood as per BIS standard, the exhaust gas is secluded from the atmosphere, and then the emission concentrations are recorded using a portable flue gas analyzer (Testo 340). CO and NO_x emission values in current study refer to dry-basis measurements, with a correction of 3% in oxygen level.

6.3.5 Control Cooking Test (CCT) and Techno-economic Assessment (TEA)

As discussed earlier (Chapter 3), **t**he feasibility testing of developed cook-stove needs more verification than just a WBT. The principal objective of Control Cooking Test (CCT) is to examine fuel and time consumptions of stoves during the cooking operation. In the present study, to find the daily food consumption per household "menu A" has been selected. The average value of the fuel consumed indicates the per day requirement of heat energy per household, which has been further used for Techno-economic Assessment (TEA). Various parameters and equations used for estimating the cost are discussed in detail in chapter 3.

6.4 Results and discussion

The prime purpose of the present analysis is to explore the use of WCO as an alternative option for kerosene fuel. Observation made during the operation of cook-stoves (PKP_S and CKP_S) with 100% WCO showed that the stoves were not capable of burning highly viscous WCO. The experiments were initiated with blend samples of WCO and kerosene, and then the burner performance was evaluated with increases in WCO blending. Results showed the continuous burner operation for maximum up to 50% WCO blending. Both the stoves exhibited incomplete vaporization for more than 50% blending which lead to unstable flame and finally the burner shutdown. But at the same time, because of the better preheating effect in the porous matrix, PKP_S showed comparatively better combustion characteristics. With increase in percentage of WCO (10%, 25% and 50%, fuel samples BS_1, BS_2, and BS_3, respectively), comparative

assessments of temperature distribution, thermal and radiation efficiencies, and emissions were performed for P_i range of 1.5-3 kW (range for domestic cook-stove). Also, with maximum operable blend ratio (BS_3), CCT and TEA were performed, and results are presented in the following sections.

6.4.1 Axial and radial temperature distribution

Understanding the combustion behavior needs detailed temperature mapping of the burner. In PKPS, burners axial as well as radial temperature distributions suggest the stable flame position, which consequently explains the variation in the thermal performance. Whereas, in CKPS, movement of CZ over the burner head can be visualized through axial temperature distribution only. In P_i range, the variations of axial temperature in CB and PRB for samples $BS_{1\text{-}3}$ are provided in Fig. 6.12(a)-(c) and Fig. 6.13(a)-(c), respectively. For all the experiments in CB, the maximum temperature of flame was noticed near the evaporative head. A very sharp temperature rise above the burner head was recorded, which is typical of the FFC (Kakati et al., 2007; Sharma et al., 2009). With increase in WCO percentage, the maximum flame temperature or reaction zone moved towards the vaporizer. It was seen that at 2.5 cm, the temperature varied between 1108-1184°C for sample BS_1, and similarly, 1051-1123°C and 1019-1093°C for sample BS2 and BS3, respectively. The downward flame shift raises the evaporative head temperature, which helps in vaporization of blend samples.

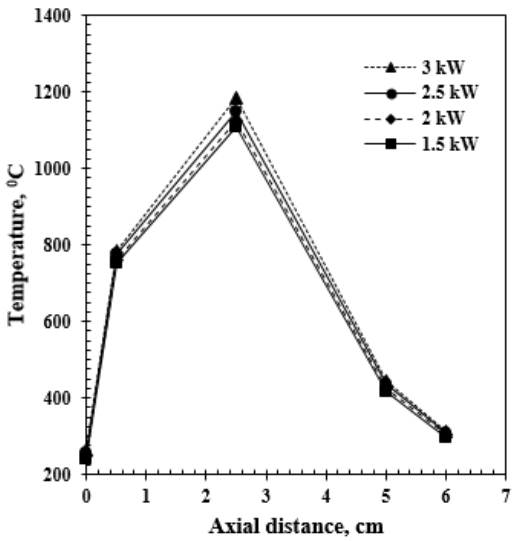

(a): BS_1

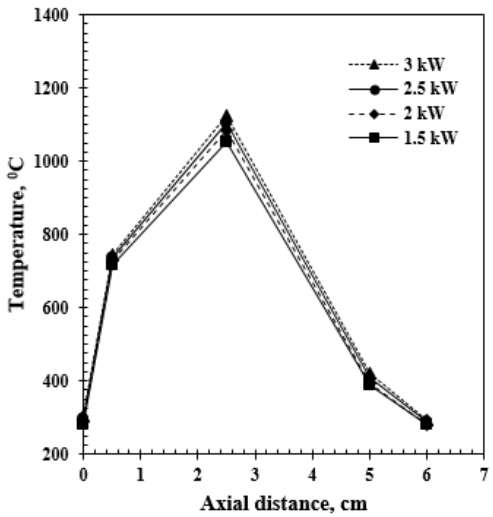

(b): BS_2

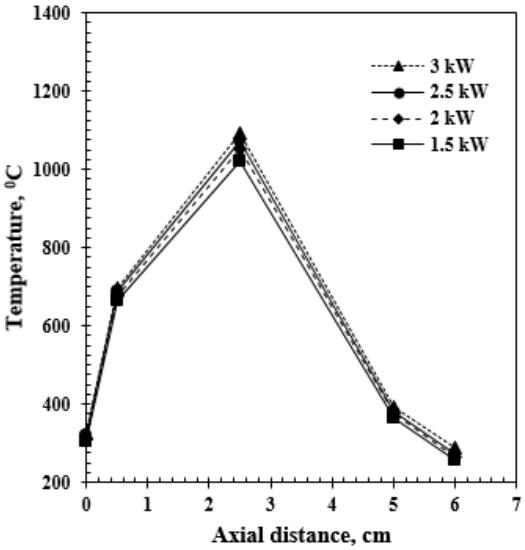

(c): BS_3

Fig. 6.12: Axial temperatures of CB with P_i of 1.5-3 kW for blend samples.

Recorded maximum vaporizer plate temperature was found at 3 kW for all the blend samples and the respective value were 264°C, 326°C and 356°C for sample BS_1, BS_2, and BS_3, respectively. The trend of increase in temperature with the P_i for all the cases is due to the increment in flow rate of fuel, which in turn surges the heat generation. The temperature of the flame after a height of 2.5 cm decreases with an increase in the percentage of WCO, because of the combined influence of improper combustion and lower heating value. In the axial direction of PRB, maximum temperature (Fig. 6.13) was observed near position 1 (stable flame region).

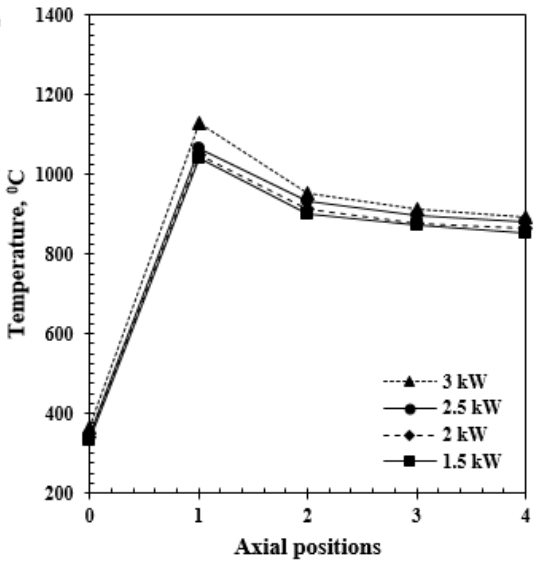

(a): BS_1

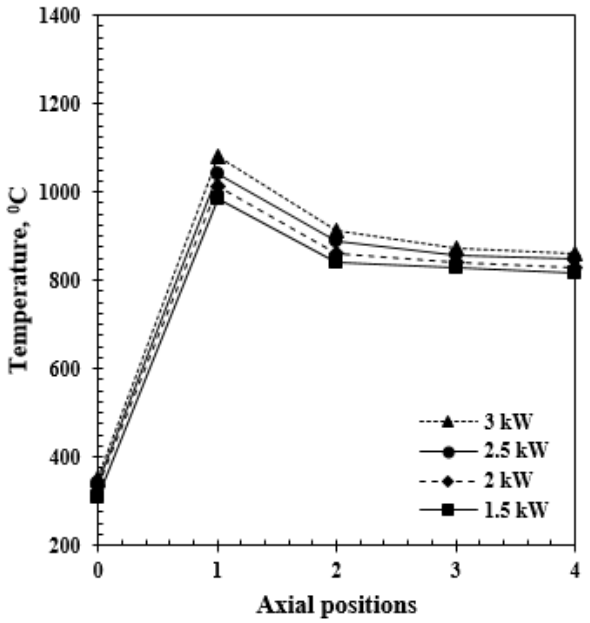

(b): BS_2

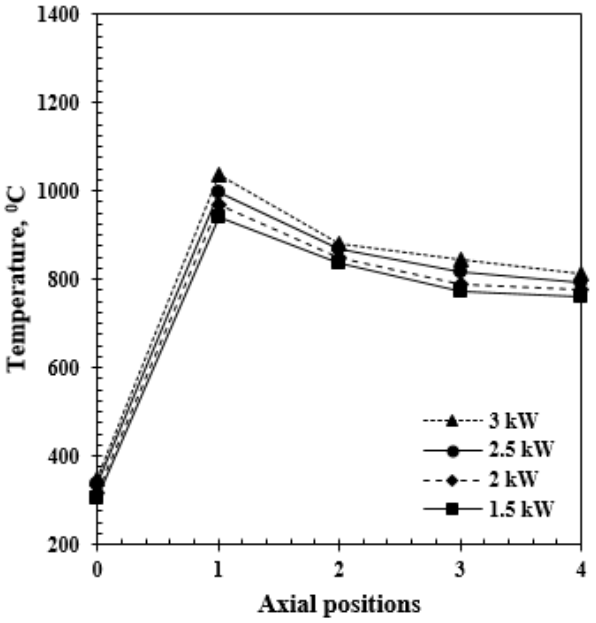

(c): BS_3

Fig. 6.13: Axial temperatures of PRB with P_i of 1.5-3 kW for blend samples.

From radial temperature measurement over burner surface (Fig. 6.14), it was found that increasing WCO percentage and P_i have opposite influence on the radial temperature distribution. With increase in P_i, both maximum temperature and temperature difference (between center and periphery, $\Delta T_{surface}$) increases. For 3 kW, maximum $\Delta T_{surface}$ of ~160°C and for 1.5 kW, $\Delta T_{surface}$ of ~141°C was obtained for BS_3. Highest value of surface temperature occurred at the center of the burner while lowest value was obtained

at its periphery. The higher $\Delta T_{surface}$ is because of the loss of heat by conduction through the casing and subsequently by radiation from the periphery to surrounding. Previous works (Mishra et al. 2015a, Sharma et al., 2016a) also showed similar observations, and these also indicates non-uniform heat flux.

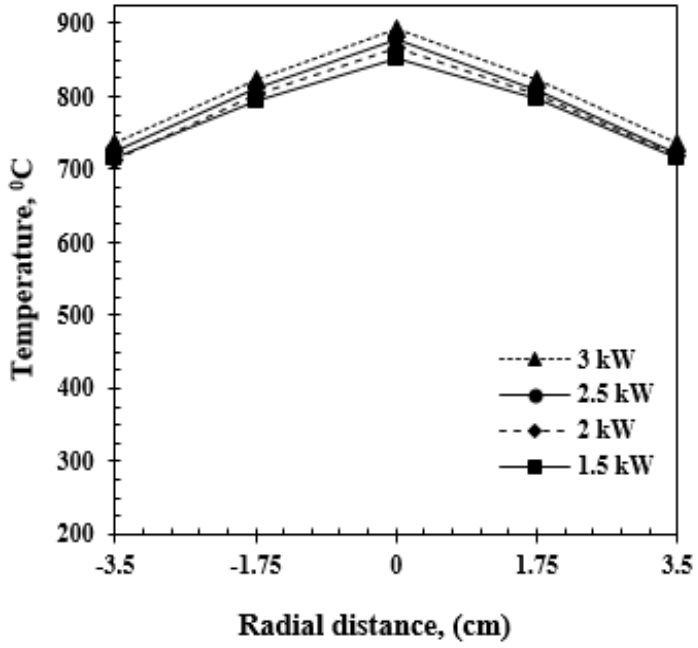

(a): BS_1

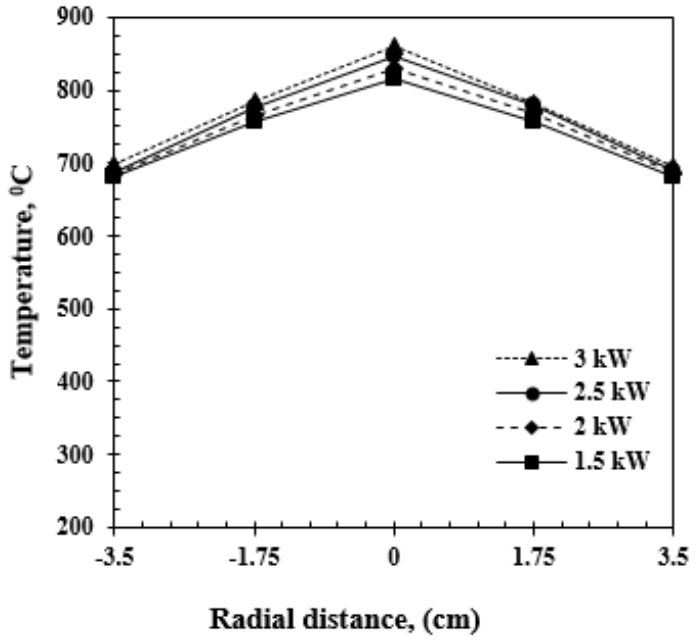

(b): BS_2

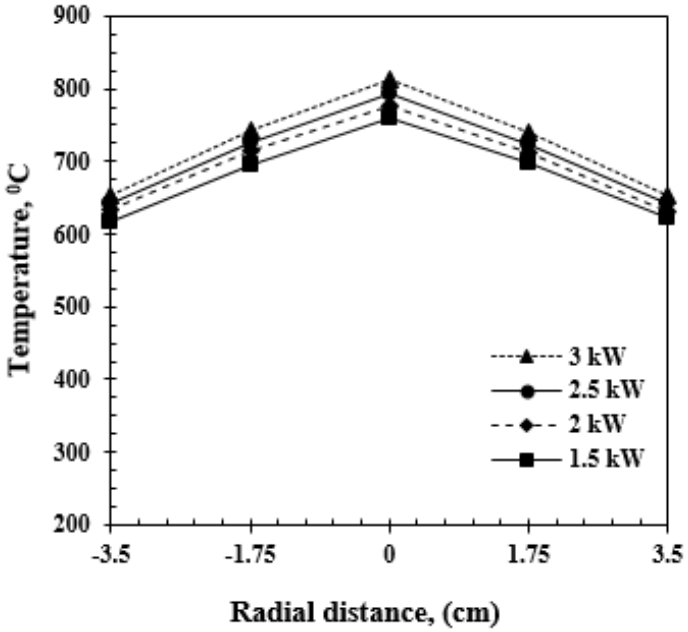

(c): BS_3

Fig. 6.14: Radial temperatures of PRB with P_i of 1.5-3 kW for blend samples.

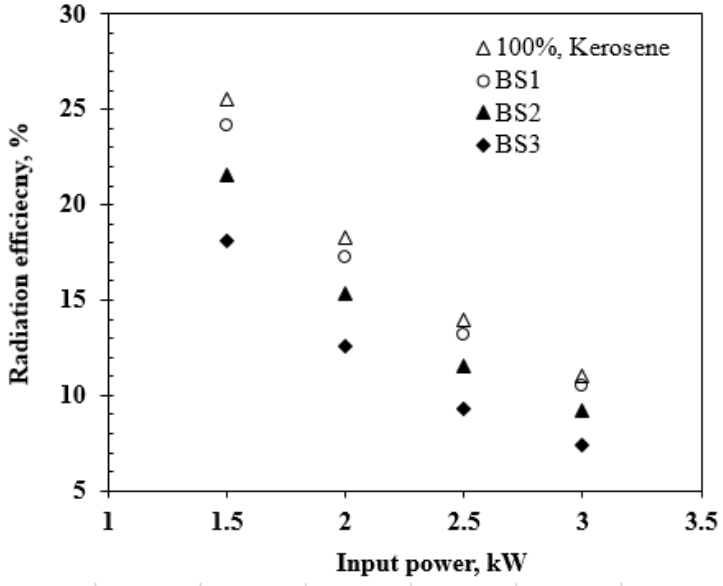

Fig. 6.15: Radiation efficiency variation with P_i of 1.5-3 kW.

For samples $BS_{1\text{-}3}$, radiation efficiency variation with P_i is presented in Fig. 6.15. Experiments were performed at surrounding temperature of ~25°C. Within the P_i range, maximum radiation efficiency for BS_1 was found as 24.2%. Whereas the same was 21.6% and 18.2% for BS_2 and BS_3, respectively. Both the amount of WCO and P_i have negative effect on radiation efficiency. Increasing P_i results in higher burner

surface temperature, but this cannot overcome the negative impact of increased input heat (Eq. 6.1) and therefore, decrease in radiation efficiency is observed.

6.4.2 Thermal efficiency

Results obtained from the thermal efficiency tests are shown in Figs. 6.16 and 6.17. For sample BS_1, in the P_i range, the maximum efficiency was found as 51.3% and 43% in PKP_S and CKP_S, respectively. Similarly, for BS_2 and BS_3, these values were 48.6% and 41.4%, and 45.3% and 36.2%, respectively. Because of the collective effects of conductive and radiative heat transfer in the highly emissive porous material, for all the tests, PKP_S showed higher thermal efficiency than CKP_S. Within the operating P_i range, the lowest P_i offered the maximum efficiency, and the decrease in efficiency is higher in the case of CKP_S. Such behavior of CKP_S is because of increased convective heat loss with increase in flame height, which occurs due to increment in P_i (Murthy et al., 2011; Singh, 2011).

Increment in percentage of WCO, resulted in lower efficiency for both the stoves. Such behavior is due to the increase in viscosity and decrease in calorific value. High viscosity of oil causes poor atomization of fuel which results in incomplete combustion (Pande et al., 2017; Mamoco Jr. et al., 2017), which consequently adversely affects the burner performance. Reduction in efficiency is lower in case of PKP_S because of more preheating of unburnt fuel than in CKP_S. From literature (Varun et al., 2018; Suhartono et al., 2017a, 2017b), it has been already confirmed that heating of WCO reduces the viscosity and improves the spray characteristics.

6.4.3 Emissions

The concentrations of CO and NO_x emissions for the test samples are shown in Fig. 6.18. Within the P_i range, measured values of CO in PKP_S varied between 268-484 ppm, 303-557 ppm, and 361-664 ppm for sample BS_1, BS_2, and BS_3, respectively. Whereas, the CO emission is as high as 682-997 ppm, 776-1129, and 905-1300 ppm, respectively in case of CKP_S. For all the tested samples, a large reduction in CO emissions was observed with PKP_S. Such reduction is because the flame front is stabilized at the lower part of the SiC of the burner, providing more residence time for the combusted gases to oxidize in the burner section. Similarly, maximum NO_x

value for CKP_S was found as 59 ppm, 119 ppm, and 180 ppm for sample BS_1, BS_2, and BS_3, respectively.

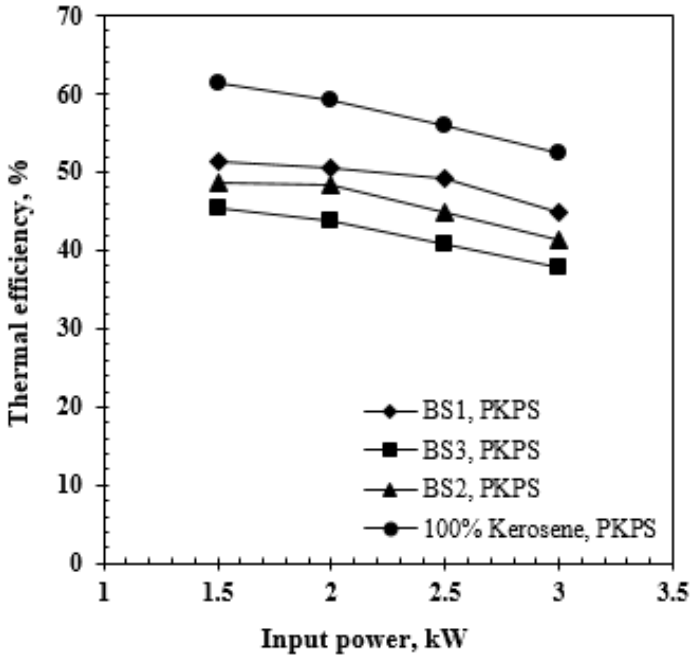

Fig. 6.16: Test results of thermal efficiency for PKP_S.

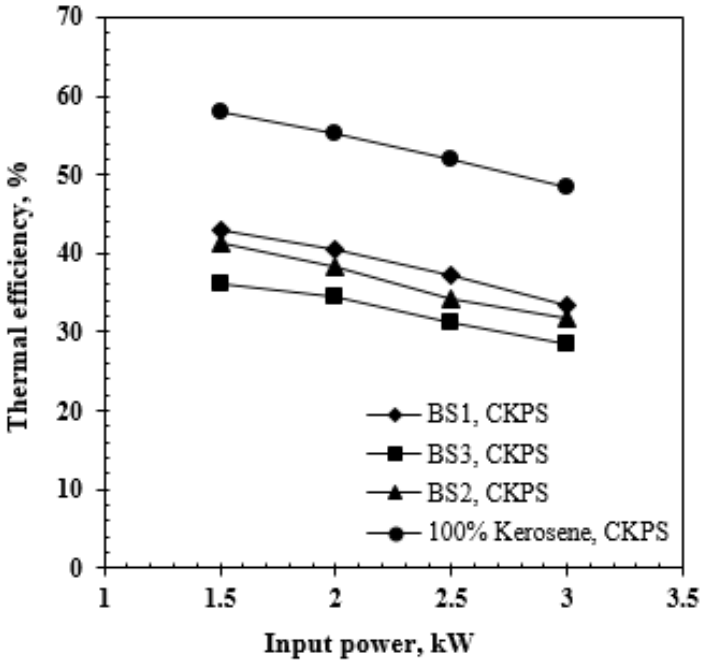

Fig. 6.17: Test results of thermal efficiency for CKP_S.

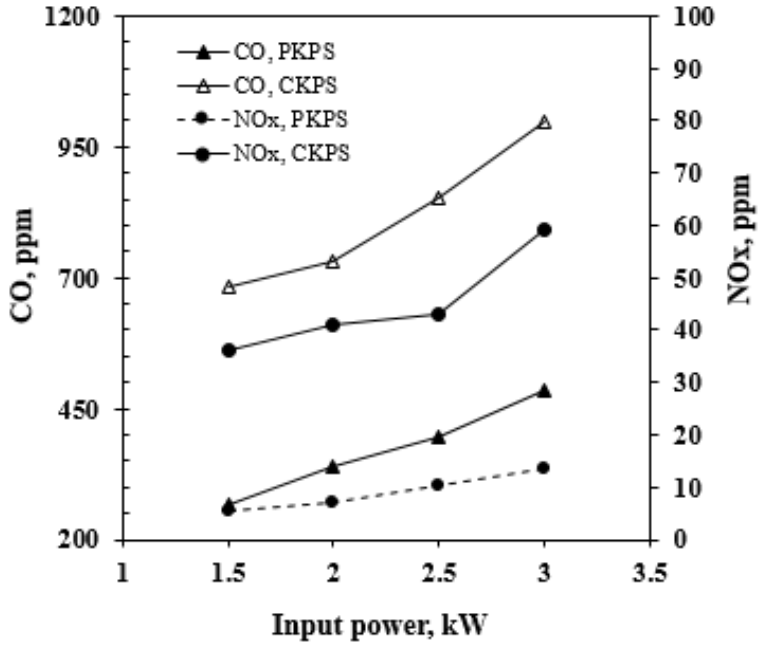

(a): BS_1

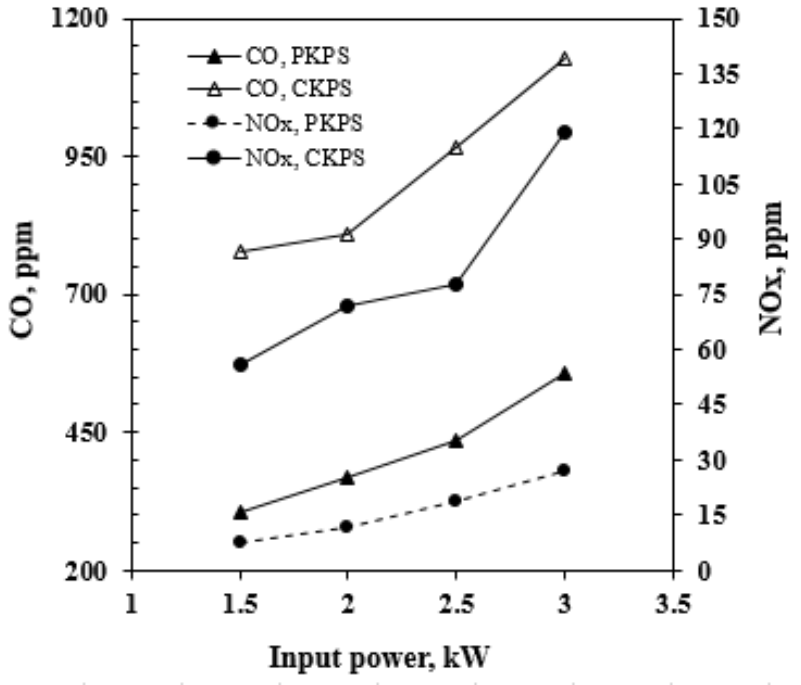

(b): BS_2

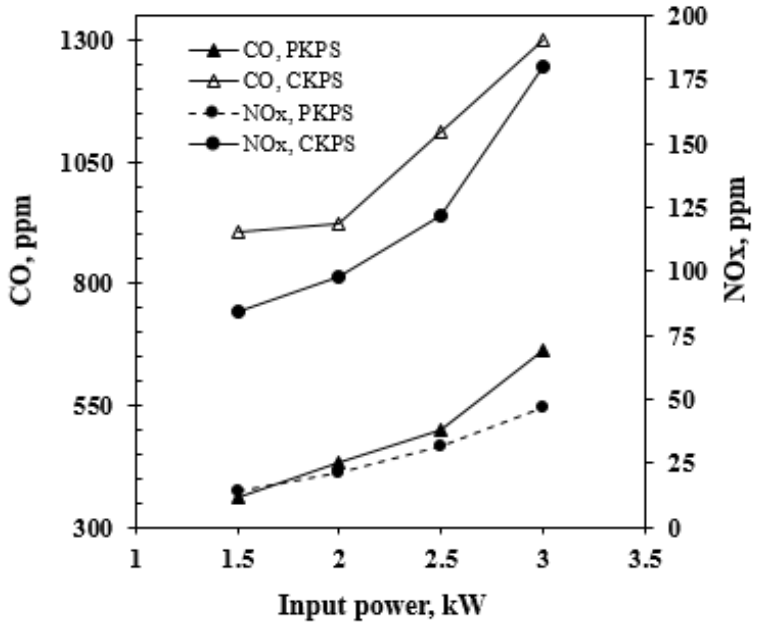

(c): BS_3

Fig. 6.18: CO and NO_x emissions for blend samples with P_i of 1.5-3 kW.

For all the test cases in PKPs, NO_x emissions were within 47 ppm. In the PKP_S, NO_x emission is lesser due to lower burner surface temperature. High NO_x from CKPS is also because of fuel-rich combustion, which gives high temperature in the CZ. The increase in emissions from BS_1 to BS_3 is because the higher percentage of WCO which reduces mobility of fuel and this consequently results in reduction of mixing rate of air and fuel, ultimately resulting in higher emissions. It was also found that with increase in P_i, both the CO and NO_x concentrations increase for all the test cases, which agree with the reported studies (Sharma et al. 2011, 2016a; Sinha and Muthukumar, 2019).

6.4.4 Empirical correlation for PKPs thermal efficiency (η_{th})

To predict the thermal efficiency (η_{th}) of PKPs in terms of input power (P_i) and kerosene % in blend (K i.e., WCO blend % = 100-K), an empirical relation has been developed based on data from experimental analysis. This relation is valid only within the studied operating range of the parameters (Table 6.4).

Table 6.4: Reference values and operating parameters chosen for experimental analysis.

Inlet parameters	Range/Values
Inlet power (P_i)	1.5-3 kW
WCO blending %	10- 50%
ε	0.9
σ	5.67×10^{-8} W/m^{2}K^4
A_{BS}	3.85×10^{-3} m^2
C_p	0.8959 kJ/kg-k
C_w	4.18 kJ/kg-k
T_{surr}	300 K

The empirical relation (Abnisa et al., 2015) has been developed by means of regression analysis, and the equations are formulated as given below:

$$\eta_{th} = \lambda_1 P_i + \lambda_2 K + \tau \quad \ldots\ldots\ldots \quad (6.4)$$

where, λ and τ are coefficients and constants of individual model terms, respectively. To identify the significance of direct and interactive effects of P_i and K on PKPs thermal efficiency (η_{th}), analysis of variance (ANOVA) was implemented (P-value less than 0.05 is considered). During this analysis, it is observed that the relationship between the thermal efficiency and the input power and kerosene % in blend is best fitted to a first-order polynomial equation. The best–fit equation and the statistical parameters obtained from the ANOVA are given in Table 6.5. It can be seen from Table 6.5 that the maximum R^2 value is 97%, whereas the respective adjusted R^2 value is 95%. The adjusted R^2 value describes the perfectness of the developed correlation, and higher the value of adjusted R^2 signifies higher reliability of the developed correlation (Abnisa et al., 2015; Naik and Muthukumar, 2019). From Table 6.5, it is observed that the both independent parameters have a significant effect on thermal efficiency (P-value < 0.05). Thermal efficiency predicted from correlation (Table 6.5) and those observed from experiments were compared in Fig. 6.19. It was found that the developed correlation has a good agreement with the experimental findings and match within 5%.

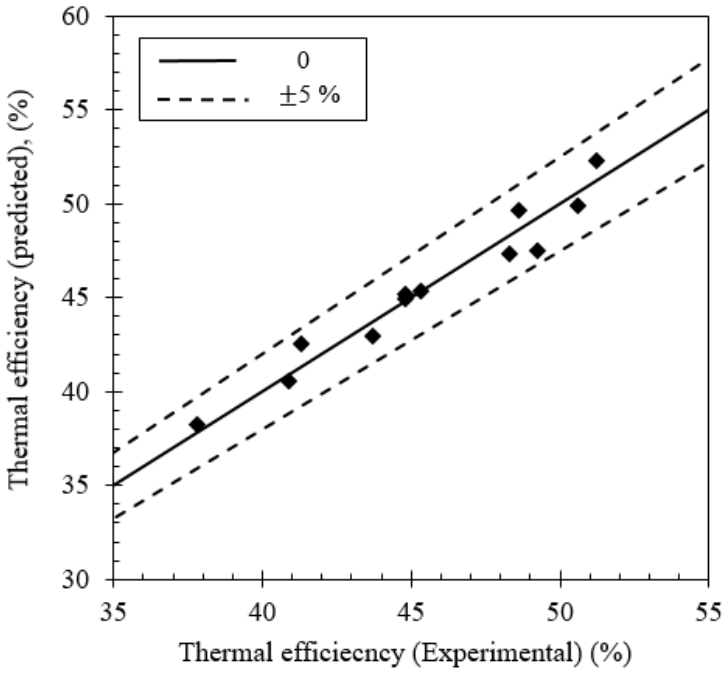

Fig. 6.19: Comparison of thermal efficiency predicted from correlation and obtained from experiments.

Table 6.5: Analysis of variance (ANOVA) of the PKPs thermal efficiency.

Correlation for thermal efficiency, $\eta_{th} = \lambda_1 P_i + \lambda_2 K + \tau$			
Coefficients	λ_1	λ_2	T
	- 4.76	0.174	43.8
Statistical information			
Regression Statistics			
R^2	0.97		
Adjusted R^2	0.95		
F significance	1.6×10^{-6}		
P-value	λ_1	λ_2	T
	7.4×10^{-6}	0.00	1.2×10^{-9}

6.4.5 Daily heat energy requirement per household by CCT

Dishes and details of the time and amount of fuel required for cooking are given in Table 6.6 and Table 6.7, respectively. The total amount of fuel for preparing the seven dishes (selected as typical for an Indian household) is found as 491.6 g for CKPs. Whereas, only 308.9 g is required for the PKPs which shows that as compared to CKPs,

use of PKP_S results in daily fuel savings of around 182.7 g per household. It can be seen that in spite of large fuel savings, the heat energy requirement is still higher than the recommended value (6339~9502 kJ/day/HH) by the Planning Commission of India. It has also been found that the rate of fuel savings is different for various food items. Cooking time in PKP_S is less than that in CKP_S, as time-saving is approximately 49 min. This shows the extent to which the time budgets can be affected by the newly developed PKP_S.

Table 6.6: Menu-A for estimating the average heat energy requirement.

Dish	Menu A
Dish 1	Rice (875 g + 3 kg water), boiled, open vessel
Dish 2	Pulse 'dal' (130 g + 676 g water), boiled, cooker
Dish 3	Vegetables 'Cabbage' (1073 g + 30 g oil), fried, open vessel
Dish 4	Chicken (965 g + 85 g oil), fried, open vessel
Dish 5	Leaf bread 'chapatis' (665 g wheat), hot plate cooking
Dish 6	Milk 636 ml, boiled, open vessel
Dish 7	Tea-5 cups (14 g + 75 g sugar + 100 ml milk), boiled, open vessel

Table 6.7: Cooking time and fuel (BS_3) requirement for preparation of food menu A.

Dishes	PKP_S		CKP_S	
	Time (min)	Fuel (g)	Time (min)	Fuel (g)
Dish 1	25	62.8	36	91.3
Dish 2	11	24	18	42.2
Dish 3	17	41.8	29	80.9
Dish 4	28	65.7	37	98.2
Dish 5	38	84.8	42	124.2
Dish 6	8	16.6	11	32.3
Dish 7	6	13.2	9	22.5
Total	**133**	**308.9**	**182**	**491.6**

6.4.6 Techno-economic Assessment (TEA)

The economic benefit of using WCO in PKPS is presented in this section. For this analysis, fuel requirement per household was found from CCT and has been used as a functional unit for TEA. Various prices have been obtained from the market survey and some assumptions are considered during assessment viz., both the replacement cost of burner parts and labor cost is considered in maintenance cost, and for emission cost estimation, average emission values are considered, as burner power fluctuates during cooking. Annual saving of ₹2055 is achieved due to efficient cooking in PKP_S. In comparison with the CKP_S, it can be observed that PKP_S offers an indirect cost savings (by minimizing the emissions). With 10 years as the life of the stove, PKP_S resulted in ₹16,817 as cumulative present worth of annual savings (Table 6.8). Similarly, the calculated Internal Rate of Return (IRR) and payback period are estimated as 268.5% and less than 5 months, respectively. With an IRR of 268.5%, the PKPS is expected to earn ₹2.7/- out of each ₹1/- invested (yearly), and IRR is much higher than the rate of return (8%). Compared with the life of the cook-stove (10 years), the payback period is also very small.

Table 6.8: Present worth of the annual saving and the cumulative present worth of the annual savings by PKP_S (5% inflation and 8% interest rate).

Year	Annual savings (₹)	Present worth of annual saving (₹)	Present worth of cumulative saving (₹)
1	2055	1903	1903
2	2158	1850	3753
3	2266	1799	5551
4	2379	1749	7300
5	2498	1700	9000
6	2623	1653	10652
7	2754	1607	12259
8	2892	1562	13821
9	3036	1519	15340
10	3188	1477	16817

Figures 6.20, 6.21, 6.22, 6.23 and 6.24 show the pictorial views of pressure kerosene stove with PRB and CB taken during different stages of the investigations.

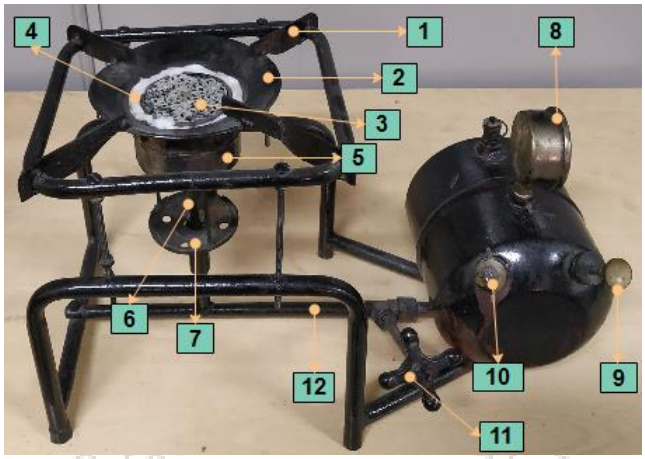

Fig. 6.20: Pressure kerosene stove with PRB (1: Pot-holder; 2: Radiation shield; 3: Porous burner; 4: Ceramic wool; 5: Aluminium sheet; 6: Vaporiser tube; 7: Vaporiser cup; 8: Pressure gauge; 9: Hand plunger; 10: Stove key; 11: Fuel regulator; 12: Fuel supply line).

Fig. 6.21: Photographic view of experimental setup for measuring thermal efficiency.

Fig. 6.22: Photographic view of experimental setup for measuring emissions.

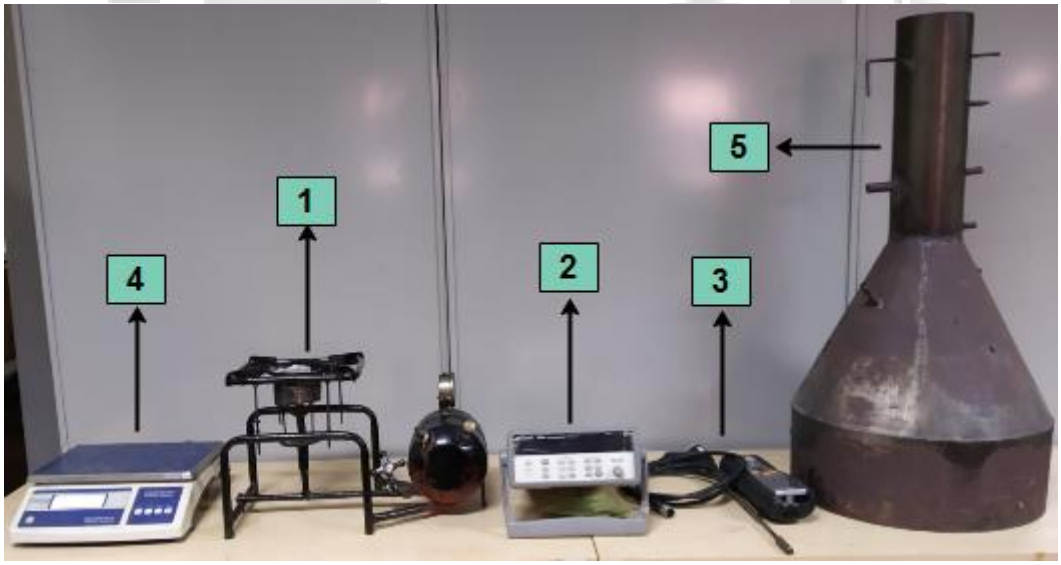

Fig. 6.23: Experimental tool (1: PRB kerosene stove; 2: data acquisition system; 3: Flue gas analyzer; 4: weighing balance machine; 5 Emissions hood).

(a) (b)

Fig. 6.24: Burning of WCO/kerosene blend operated (a) PRB stoves and (b) CB stove.

6.5 Summary

Two basic requirements for clean cooking option are efficient cook-stove and local and economical fuel supply. In a developing country like India, specifically in rural areas, people use kerosene as a clean cooking fuel. Use of kerosene for cooking is phasing out due to economic and environmental concern. The use of waste cooking oil (WCO) as a substitute for kerosene in a cook-stove is explored in present research, which also provide an alternate option for solving WCO disposal problem. The present assessment provides very interesting insights on Porous Radiant Burner's (PRBs) ability to combust WCO. Investigation shows that the undesirable properties of WCO as a cooking fuel can be overcome by enhanced upstream heat transfer in PRB. Compared to its conventional counterpart, a maximum improvement of ~9% in thermal efficiency and reduction of 50-60% and 74-83% of CO and NO_x emission, respectively, showed enhanced combustion of WCO in PRB. From the control cooking test, it has been found that, on per day basis, cook-stove with PRB results in 49 minutes and ~59% saving in cooking time and fuel consumption, respectively. The economic assessment indicates that, in 10 years, newly developed cook-stove can offer a sum of ₹16,817 as the net present worth of savings. Comparative assessment of cooking energy and its respective economic impact highlights the extent to which PRB can impact cooking time and daily economics of any rural household. In present PRB, performance reduction with increase in WCO blending indicates lack of preheating and suggests further investigation in the matter. Above results of the experimental study are encouraging and can help in developing an improved version of PRB for 100% WCO utilization.

Chapter 7

Conclusions and Future Work

7.1 Conclusions

This chapter presents the important conclusions obtained from the various stages PRB developments. Investigations have been done for different PRBs, which work on LPG, biogas and waste cooking oil (WCO).

While investigating the LPG based self-aspirated PRBs, developed by Mishra (2015) for domestic as well as medium-scale cooking application, the main objective was to demonstrate the PRB based cook-stove as a potential alternative to their conventional counterpart's. The three main problems associated with conventional cook-stoves viz., high cooking energy requirement, the overall impact on environment and humans, and high cooking cost have been assessed by performing Control Cooking Test (CCT), Life Cycle Assessment (LCA) and Techno-economic Assessment (TEA), respectively. The cooking assessment (CCT) of self-aspirated PRB for domestic scale has clearly proved it to be a better choice than its conventional counterpart. It results in 30.23% saving of fuel and 29.98% saving in cooking time, on a daily basis. Life cycle economic assessment on domestic as well as medium scale cook-stove shows a yearly saving of ₹2204 (1-3 kW) for domestic and ₹73,219/- (10 kW) for commercial cooking applications, respectively. The calculated payback period over operating range are very less (maximum around 6 month) considering the life of the cook-stove (10 years). The PRB stove reduces the adverse impact on both human health and ecosystem significantly. This reduction is because of curtailment of both pollutant emission and fuel requirement.

In the next phase, focus has been paid on improving the existing design of self-aspirated PRB developed by Mishra (2017) for medium scale application. During testing, it was found that submerged mode of combustion was not very promising for cooking application as it was resulted in flashback due to overheating of burner casing. Necessary design modifications have been made to work the PRB on partially submerged mode. With partially submerged mode of combustion, the operation was found stable and yield a maximum efficiency was found as 64%, against 55% reported

by Mishra's (2017). The maximum temperature fluctuation between the center and periphery was found as 134°C in case of Mishra (2017), whereas it was only 74°C in the newly designed PRB. Compared to its conventional counterpart maximum of ~47% thermal efficiency improvement was observed. CO and NO_x reductions as compared to a CB were found to be ~90% for both. As the newly designed PRB works with unreduced pressure valve (applicable for Indian market), it can replace the existing stoves without any practical difficulties.

Third phase of work is devoted to the development for biogas cook-stove, and it has been carried out in two parts. In the first part, with external air supply, stability range of the burner was identified and then burner dimensions have been fixed for domestic power range application. With forced air supply, the range of biogas flame stability limit (equivalence ratio) in two-layer PRB was found as 0.75-0.95 for domestic power range. With selected parameters (diameter of burner, porous matrix porosity, thickness and burner casing dimensions), further experiments have been performed to convert it for naturally aspirated operation. Various combination of orifice diameters and port diameters have been tested. For stable combination, detailed performance investigations have been carried out and also compared with that of forced air supply to see its working equivalence ratio (ability of self-aspiration). Further, with self-aspirated mode, the newly designed PRB showed about 22% improvement in thermal efficiency compared to CB. CO emission is found as 36-48 ppm with self-aspirated PRB, whereas same is 235-276 ppm in case of CB. Similarly, NO_x emissions are always found lower than 2 ppm in PRB. whereas the same is 15 ppm in case of CB.

In the last phase of work, investigations have been made to demonstrate WCO as an alternate option of cooking fuel. Comparative study of combustion characteristics of WCO in a pressurized kerosene stove with CB and PRB (with new vaporizer design) has been performed, with the following specific objectives. The first objective is to investigate the maximum % of the WCO, which can be blended with kerosene for domestic scale cooking application. The second objective is to measure the temperature distribution, thermal efficiency and emission with the obtained blending %. Third is to carry out CCT and TEA to get a proper understanding of cooking energy requirement and economic benefit of PRB. Maximum of 50% WCO and kerosene blend combustion can be sustained in both the test stoves. At condition of maximum blending (50%

WCO), maximum ~9% improvement of thermal efficiency has been found in case of PRB. The PRB reduces CO and NO_x emission by 50-60% and 74-83%, respectively. From CCT, it has been found that, on per day basis, PRB results in 49 minutes and ~59% saving in cooking time and fuel consumption, respectively, as compared to CB. Techno-economic Assessment (TEA) indicates that, in a span of 10 years, PRB can offer a sum of ₹16,817 as net present worth of savings.

7.2 Scopes for future work

The following are the scope for the future research work in the development of porous burners.

- Detailed life cycle analysis and kitchen performance test of newly developed PRB for medium scale cooking application.
- Using the concept of partially stabilized combustion, the design of the domestic scale cook stove can be explored.
- With improved LPG operated medium scale PRB for cooking stove
- Detailed performance assessment for developed biogas PRB.
- For further improvement in thermal efficiency of newly developed PRBs, optimization of operational and geometrical parameters (for self-aspiration) can be done with help of a numeral tool.

References

Abnisa F., Daud W.M.A., Sahu J.N., (2015), Optimization and characterization studies on bio-oil production from palm shell by pyrolysis using response surface methodology. *Biomass Bioenergy*, vol. 35, pp. 3604–3616.

Anenberg S.C., Tago K., Arunachalam S., Dolwick P., Jang C., West J.J., (2011), Impacts of global, regional, and sectoral black carbon emission reductions on surface air quality and human mortality. *Atmospheric Chemistry and Physics*, vol. 11, pp. 7253-7267.

Arvind, Bekal S., (2018), Experimental Investigation on the Performance of Novel Stove for Use with Vegetable Oil. *Energy and Power*, vol. 8, pp. 46-50.

Avdic F., Adzic M., Durst F., (2010), Small scale porous medium combustion system for heat production in households. *Applied Energy*, vol. 87, pp. 2148-2155.

Avdic F., (2004), Application of the porous medium gas combustion technique to household heating systems with additional energy sources: *PhD Thesis*, University of Erlangen-Nuremberg.

Babkin V.S., Korzhavin A.A., Bunev V.A., (1991), Propagation of premixed gaseous explosion flames in porous media. *Combustion and Flame*, vol. 87, pp. 82-190.

Barra A.J, Ellzey J.L., (2004), Heat recirculation and heat transfer in porous burners. *Combustion and Flame*, vol. 137, pp. 230-241.

Bingue J.P., Saveliev A.V., Fridman A.A., Kennedy L.A., (2002), Hydrogen production in ultra- rich filtration combustion of methane and hydrogen sulfide. *International Journal of Hydrogen Energy*, vol. 27, pp. 643-649.

Center for Energy Studies, Institute of Engineering (CES/IOE), (2001), A study report on the efficiency measurement of biogas, kerosene and LPG stoves, Tribhuvan University, Pulchowk, Lalitpur.

Chaelek A., Grare U.M., Jugjai S., (2019), Self-aspirating/air-preheating porous medium gas burner. *Applied Thermal Engineering*, vol. 153, pp. 181-189.

Chandra A., Tiwari G.N., Srivastava V.K. Yadav Y.P., (1991a), Performance evaluation of Biogas burners. *Energy Conversion and Management*, vol. 32, pp. 353-58.

Chandra A., Tiwari G.N., Yadav Y.P., (1991b), Hydrodynamical modelling of a biogas burner. *Energy Conversion and Management*, vol. 32, pp. 395-401.

Chen Y.K., Matthews R.D., Howell J.R., (1987), Effect of radiation on the structure of premixed flame within a highly porous inert medium. American Society of Mechanical Engineers, *Heat Transfer Division, (Publication) HTD*, vol. 81, pp. 35-41.

Colorado A., Avila D., McDonell V., (2015), An Experimental Study of the Stability Limits and Emissions of a Surface-Stabilized Combustion Burner using Biogas and Natural Gas. *9th U.S. National Combustion Meeting*, Central States Section of the Combustion Institute Cincinnati, Ohio.

Decker T.J., (2017), A modeling tool for household biogas burner flame port design. *Master of Science Thesis*, Colorado State University Fort Collins, Colorado.

Deshaies B., Joulin G., (1980), Asymptotic study of an excess-enthalpy flame. *Combustion Science and Technology*, vol. 22, pp. 281-285.

Devi S., Sahoo N., Muthukmar P., (2019), Combustion of biogas in Porous Radiant Burner: Low emission combustion. *Energy Procedia*, vol. 158, pp. 1116-1121.

Dillon J., (1999), Combustion in porous media. Los Alamos National Lab., Ae104c Final report, California Institute of Technology, June 8.

Dinesha P., Kumar S., Rosen M.A., (2019), Performance and emission analysis of a domestic wick stove using biofuel feedstock derived from waste cooking oil and sesame oil. *Renewable Energy*, vol. 136, pp. 342-351.

Echigo R., (1982), Effective energy conversion method between gas enthalpy and thermal radiation and application to industrial furnaces. *International Heat Transfer Conference Digital Library*. Begel House Inc.

Echigo R., Yoshizawa Y., Hanamura K., Tomimura T., (1986) Analytical and experimental studies on radiative propagation in porous media with internal heat generation. *International Heat Transfer Conference Digital Library*. Begel House Inc.

Energy Statistics (Twenty Sixth Issue), (2019), Central Statistics Office Ministry of Statistics and Programme Implementation, Government of India, New Delhi.

Echigo R., Zhdanok S.A., (1993), Superadiabatic combustion in a porous medium. *International Journal of Heat and Mass Transfer*, vol. 36, pp. 3201-3209.

Employment – Unemployment Survey Volume I & II, Government of India ministry of Labour & employment Labour bureau Chandigarh, 2013-2014.

Fulford D., (1996), Biogas stove design - A short course, Kingdom Bioenergy Ltd.

Fuse T., Araki Y., Kobayashi N., Hasatani M., (2003), Combustion characteristics in oil-vaporizing sustained by radiant heat reflux enhanced with higher porous ceramics. *Fuel*, vol. 82, pp. 1411-1417.

Gao H., Qu Z., Tao W., He Y. Zhou J., (2011), Experimental Study of Biogas Combustion in a Two-Layer Packed Bed Burner. *Energy & Fuels*, vol. 25, pp. 2887-2895.

Gao H.B., Qu Z.G., Tao W.Q., He Y.L, (2013), Experimental investigation of methane/(Ar, N_2, CO_2)–air mixture combustion in a two-layer packed bed burner. *Experimental Thermal and Fluid Science*, vol. 44, pp. 599-606.

Global Alliance for Clean Cook stoves, India Cook stoves and Fuels Market Assessment, Dalberg Global Development Advisors, February 2013.

Hardesty D.R., Weinberg F.J., (1973), Burners producing large excess enthalpies. *Combustion Science and Technology*, vol. 8, pp. 201-214. Hanamura K.

Hayashi T.C., Malico I., Pereira J.C.F., (2004), Three-dimensional modelling of a two-layer porous burner for household applications. *Computers & structures*, vol. 82, pp. 1543-1550.

Herrera B., Cacua K., Villalba L.O., (2015), Combustion stability and thermal efficiency in a porous media burner for LPG cooking in the food industry using Al_2O_3 particles coming from grinding wastes. *Applied Thermal Engineering*, vol. 91, pp. 1127-1133.

Hsu P.F., Evans W.D., Howell J.R., (1993), Experimental and numerical study of premixed combustion within nonhomogeneous porous ceramics. *Combustion Science and Technology*; vol. 90, pp. 149-172.

Howell J.R., Hall M.J., Ellzey J.L., (1996), Combustion of hydrocarbon fuels within porous inert media. *Progress in Energy and Combustion Science*, vol. 22, pp. 121-145.

IEA, Energy balance for India, (2014)

Indian Standard, Oil pressure stoves-offset burner type-specification, (first revision), IS 10109:2002.

Indian Standard (BIS), Biogas Stove-Specification, (second revision), IS 8749:2002, New Delhi

Indian Standard, Domestic gas stoves for use with Liquefied Petroleum Gases, (fifth revision): IS 4246:2002, New Delhi

Indian Standard, Commercial burners using LPG at inlet pressure up to 147.1 kN/m^2 (1 500 gf/cm^2)-specification, IS 14612:1999, New Delhi

India Fact Sheet, National Family Health Survey (NFHS-4), Ministry of Health and Family Welfare, 2015-16.

India Clean Cooking Forum, (2018), Strategizing Renewable Energy for Cooking, United States Agency for International Development (USAID), Clean Energy Access Network.

Ismail A.K., Abdullah M.Z., Zubair M., Ahmad Z.A., Jamaludin A.R., Mustafa K.F, Abdullah M.N., (2013), Application of porous medium burner with micro cogeneration system. *Energy*, vol. 50, pp. 131-142.

Itodo I.N., Agyo G.E., Yusuf P., (2007), Performance evaluation of a biogas stove for cooking in Nigeria. *Journal of Energy in Southern Africa*, vol. 18, pp. 14-18.

Jadhav M.P., Sudhakar D.S.S., (2015), Analysis of Burner for Biogas by Computational Fluid Dynamics and Optimization of Design by Genetic Algorithm. *International Journal for Research in Emerging Science and Technology*, vol. 2, pp. 39-44.

Janvekar A.A., Abas A., Ahmad Z.A., Juntakan T., Abdullah M.Z., (2019), Effect of Ultra-low Vegetable Oil Droplets on Microporous Media Burner Under Surface and Submerged Flames. *Arabian Journal for Science and Engineering*, vol. 44, pp. 5921-5935.

Jambhulkar G., Nitnaware V., Pal M., Fuke N., Khandelwal P., Sonule P., Narnawre S., Katekar V.P., (2015), Performance evaluation of cooking stove working on spent cooking oil. *International journal of emerging science and engineering (IJESE)*, vol. 3, pp. 26-31.

Jugjai S., Wongpanit N., Laoketkan T., Nokkaew S., (2002), The combustion of liquid fuels using a porous medium. *Experimental Thermal and Fluid Science*, vol. 26, pp. 15-23.

Jugjai S., Polmart N., (2003), Enhancement of evaporation and combustion of liquid fuels through porous media. *Experimental Thermal and Fluid Science*, vol. 27, pp. 901-909.

Jugjai S., Phothiya C., (2007), Liquid fuels-fired porous combustor-heater. *Fuel*, vol. 86, pp. 1062-1068.

Jugjai S., Sanitjai S., (1996), Parametric studies of thermal efficiency in a proposed porous radiant recirculated burner (PRRB): a design concept for the future burner. *RERIC International Energy Journal*, vol. 18, pp. 97-111.

Jugjai S., Rungsimuntuchart N., (2002), High efficiency heat-recirculating domestic gas burners. *Experimental Thermal and Fluid Science*, vol. 26, pp. 581-592.

Kakati S., Mahanta P., Kakoty S.K., (2007), Performance analysis of pressurized kerosene stove with porous medium inserts. Journal of Scientific and Industrial Research, vol. 66, pp. 565-569.

Kakati S., Mahanta P., (2017), Experimental evaluation of performance of pressure stove by using plant oil and kerosene blends. *International conference on computational and experimental methods in mechanical engineering (ICCEMME)*, 8-9th December, pp. 27-33.

Keramiotis C., Founti M.A., (2013), An experimental investigation of stability and operation of a biogas fueled porous burner. *Fuel*, vol. 103, pp. 278-284.

Keramiotis C., Katoufa M., Vourliotakis G., Hatziapostolou A., Founti M.A., (2015), Experimental investigation of a radiant porous burner performance with simulated natural gas, biogas and synthesis gas fuel blends, *Fuel*, vol. 158, pp. 835-842.

Kebede, Kiflu A., (2014), Design of Biogas stove for injera baking application. *International Journal of Novel Research in Engineering and Science*, vol. 1, pp. 6-21.

Keown A.J., Martin J.D., Petty J.W., Scott D.F., (2015), Financial management: principals and applications 2015;10th ed. USA: Prentice Hall.

Khanna V., Goel R., Ellzey J.L., (1994), Measurements of emissions and radiation for methane combustion within a porous medium burner. *Combustion Science and Technology*, vol. 99, pp. 133-142.

Khan M.Y., Kumar M., Mittal A., (2010), Performance of wick stove fueled with used frying oil-kerosene blends. *International conference on advances in mechanical engineering*, National Institute of Technology, Surat, Gujarat, India.

Khan M.Y., Sharma S., Ahmed S., (2011), Performance of wick stove fueled with karanja oil-kerosene blends. *National conference on recent advances in mechanical engineering (RAME-11)*, March 2011.

Khullar V., (2018), Demand for Grants 2018-19 Analysis, Petroleum and Natural Gas, PRS Legislative Research.

Khandelwal K.C., Gupta V., (2009), Popular Summary of the Test Reports on Biogas Stoves and Lamps prepared by testing institutes in China, India and the Netherlands. *SNV Netherlands Development Organisation*.

Kline S.J., McClintock F.A., (1953), Describing uncertainties in single sample experiments. Mechanical engineering, vol. 75 pp. 3-8.

Koseki H., Sato M., (2002), Experimental investigation of flashback during start-up in practical premixed combustion. *Applied energy*, vol. 73, pp. 237-259.

Kratzeisen M., Stumpf E., Mueller J., (2007), Development of a Plant Oil Pressure Stove, Tropentag, *Conference on international agricultural research for development*, Witzenhausen. October 9-11.

Kratzeisen M., Muller J., (2009), Effect of fatty acid composition of soybean oil on deposit and performance of plant oil pressure stoves. *Renewable Energy*, vol. 34, pp. 2461-2466.

Kurchania A.K., Panwar N.L., Pagar S.D., (2010), Design and performance evaluation of biogas stove for community cooking application. *International Journal of Sustainable Energy*, vol. 29, pp. 116-123.

Kurchania A.K., Panwar N.L., Pagar S.D., (2011), Development of domestic biogas stove. *Biomass Conversion and Biorefinery*, vol. 1, pp. 99-103.

Lapirattanakun A., Charoensuk J., (2017), Development of porous media burner operating on waste vegetable oil. *Applied thermal engineering*, vol. 110, pp. 190-201.

Leonardi S.A., Viskanta R., Gore J.P., (2002), Radiation and thermal performance measurements of a metal fiber burner. *Journal of Quantitative Spectroscopy and Radiative Transfer*, vol. 73, pp. 491-501.

Leonardi S.A., Viskanta R., Gore J.P., (2003), Analytical and experimental study of combustion and heat transfer in submerged flame metal fiber burners/heaters. *Journal of heat transfer*, vol. 125, pp. 118-125.

Lok Sabha. (2018). Answer to Unstarred Question 3826, March 19, 2018. New Delhi: Government of India.

Mahin D.B., (1992), Biogas in developing countries, Bioenergy system report to USAID, Washington.

Makmool U., Tia S., Valikul P., Fungtammasan B., Jugjai S., (2006), Performance and diagnostic by PIV of LPG cooking burners in Thailand. *The 20th Conference of Mechanical Engineering Network of Thailand*, Nakhon Ratchasima, Thailand.

Malico I., Mujeebu M.A., (2015), Potential of Porous Media Combustion Technology for Household Applications. International Journal on Advances of Thermofluids Research, vol. 1, pp. 50-69.

Mathis W.M., Ellzey J.L., (2003), Flame stabilization, operating range, and emissions for a methane/air porous burner. *Combustion Science and Technology*, vol. 175, pp. 825-839.

Min D.K., Shin H.D., (1991), Laminar premixed flame stabilized inside a honeycomb ceramic *International Journal of Heat and Mass Transfer*, vol. 34, pp. 341-356.

Ministry of New and Renewable Energy (MNRE), (2017), Annual Report 2016-2017.

Mishra S.C., Muthukumar P., Sinha G.S., Sharma M., Mishra N.K., (2016), Self-aspirated pressurized kerosene cooking stove with a Porous Radiant Burner. *Patent Application No: 201631037245*.

Mital R., Gore J.P., Viskanta R., (1997), A study of the structure of submerged reaction zone in porous ceramic radiant burners. *Combustion and flame*, vol. 111, pp. 175-184.

Mjaanes H.P., Chan L., Mastorakos E., (2005), Hydrogen production from rich combustion in porous media. *International Journal of Hydrogen Energy*, vol. 30, pp. 579-592.

Mishra S.C., Muthukumar P., Pantangi V.K., (2013), Porous Radiant burner for domestic LPG cooking device with improved thermal efficiency and reduced emissions of CO and NOx. *Patent Application No: 73/KOL/2013*.

Mishra S.C., Muthukumar P., Mishra N.K., (2015), Self-aspirated LPG domestic cooking stove with a two-layer porous radiant burner. *Patent Application No: 543/KOL/2015*.

Mishra S.C., Muthukumar P., Mishra N.K., Panigrahi S., (2015a), Medium-scale self-aspirated improved air entrainment LPG Cooking stove with a two-layer porous radiant burner. *Patent Application No: 201631037245, 2015*.

Mishra N.K., (2015), Development of Self-Aspirated Two-Layer Porous Radiant Burners for LPG Cooking Applications, *Ph.D thesis*, Department of Mechanical Engineering, IIT, Guwahati.

Mishra N.K., Muthukumar P., (2018), Development and testing of energy efficient and environment friendly porous radiant burner operating on liquefied petroleum gas. *Applied Thermal Engineering*, vol. 129, pp. 482-489.

Mishra N.K., Mishra S.C., Muthukumar P., (2015), Performance characterization of a medium-scale liquefied petroleum gas cooking stove with a two-layer porous radiant burner. *Applied Thermal Engineering*, vol. 89, pp. 44-50.

Mujeebu M.A., Abdullah M.Z., Abu Bakar M.Z., Mohamad A.A., Muhad R.M.N., Abdullah M.K., (2009a), Combustion in porous media and its applications-A comprehensive survey. *Journal of environmental management*, vol. 90, pp. 2287-2312.

Mujeebu M.A., Abdullah M.Z., Abu Bakar M.Z., Mohamad A.A., Abdullah M.K., (2009b), Applications of porous media combustion technology-A review. *Applied energy*, vol. 86, pp. 1365-1375.

Mujeebu M.A., Abdullah M.Z., Mohamad A.A., Abu Bakar M.Z., (2010), Trends in modeling of porous media combustion. *Progress in Energy and Combustion science*, vol. 36, pp. 627-650.

Mujeebu M.A., Abdullah M.Z., Mohamad A.A., (2011a), Development of energy efficient porous medium burners on surface and submerged combustion modes. *Energy*, vol. 36, pp. 5132-5139.

Mujeebu M.A., Abdullah M.Z., Bakar M.Z.A., Mohamad A.A., (2011b), A mesoscale premixed LPG burner with surface combustion in porous ceramic foam. *Energy Sources, Part A: Recovery, Utilization, and Environmental Effects*, vol. 34, pp. 9-18.

Mujeebu M.A., Abdullah M.Z., Abu Bakar M.Z., Mohamad A.A., (2011c), Development of premixed burner based on stabilized combustion within discrete porous medium. *Journal of Porous Media*, vol. 14, pp. 909-917.

Mujeebu M.A., Abdullah M.Z., Zuber M., (2013), Experiment and simulation to develop clean porous medium surface combustor using LPG, Journal of Thermal Science & Technology, vol. 33, pp. 55-61.

Murthy M.S., Agiwal S.A., Bharambe M.A., Mishra A., Raina A., (2011), Modified kerosene stove for burning high percentage non edible straight vegetable oil blends. *IEEE conference on clean energy and technology (CET)*, vol. 1, pp. 145-150.

Mustafa K.F., Abdullah S., Abdullah M.Z., Sopian K., (2015), Experimental analysis of a porous burner operating on kerosene–vegetable cooking oil blends for thermo-photovoltaic power generation. *Energy conversion and management*, vol. 96, pp. 544–560.

Mustafa K.F., Abdullah S., Abdullah M.Z., Sopian K., (2016), Comparative assessment of a porous burner using vegetable cooking oil–kerosene fuel blends for thermoelectric and thermophotovoltaic power generation. *Fuel*, vol. 180, pp. 137-147.

Muthukumar P., Sinha G.S., Kaushik L.K., Sharma M., Priya N.S., Kanagaraj S., (2018), Self-Aspirated Pressurized Kerosene Cooking Stove with a Porous Burner with Nanoparticles blended. *Patent Application No: 201831003156 (TEMP/E-1/3419/2018-KOL)*.

Muthukumar P., Anand P., Sachdeva P., (2011), Performance analysis of porous radiant burners used in LPG cooking stove. *International Journal of Energy and Environment*, vol. 2, pp. 367-374.

Muthukumar P., Shyamkumar P.I., (2013), Development of novel porous radiant burners for LPG cooking applications. *Fuel*, vol. 112, pp. 562-566.

Natarajana R., Karthikeyana N.S., Agarwaal A., Sathiyanarayanan K., (2008), Use of vegetable oil as fuel to improve the efficiency of cooking stove. *Renewable Energy*, vol. 33, pp. 2423-2427.

Norbury J., Byrne H., (1996), The effects of radiation on combustion in porous media. *Mathematical and Computer Modelling*, vol. 24, pp. 89-94.

NSS, Energy Sources of Indian Households for Cooking and Lighting, (2011-12), 68th Round, Ministry of Statistics and Programme Implementation, Government of India.

Namoco Jr. C.S., Comaling V.C., Buna Jr. C.C., (2017), Utilization of used cooking oil as an alternative cooking fuel resource. *ARPN Journal of engineering and applied sciences*, vol. 12, pp. 435-442.

Nagaraju Y., Gopal L., (2013), Development and performance assessment of a pressurized cook stove using a blend of pongamia oil and kerosene. *International journal of scientific research*, vol. 2, pp. 99-100.

Naik B.K., Muthukumar P., (2019), Experimental investigation and parametric studies on structured packing chamber based liquid desiccant dehumidification and regeneration systems. *Building and Environment*, vol. 149, pp. 330-348.

NSS 68th Round, Report No. 567: Energy Sources of Indian Households for Cooking and Lighting, 2011-12.

Obada D.O., Obi A.I., Dauda M., Anafi F.O., (2014), Design and Construction of a Biogas Burner. *Palestine Technical University Research Journal*, vol. 2, pp. 35-42.

Parikh J.K., Sharma A., Singh C., Neelakantan S., (2016), Providing Clean Cooking Fuel in India: Challenges and solutions, International Institute for Sustainable Development.

Patnaik S., Tripathi S., (2017), Access to Clean Cooking Energy in India, Council on Energy, Environment and Water (CEEW).

Patnaik S., Tripathi S., Jain A., (2018), A Roadmap for Access to Clean Cooking Energy in India. Asian Journal of Public Affairs.

Pickenacker O., Pickenacker K., Wawrzinek K., Trimis D., Pritzkow W., (1999), Innovative ceramic materials for porous medium burners, *Interceram*, vol. 48, pp. 326-329.

Pande M.Y., Patil S., Desale K., Rajput G., Warke K., Patil A., (2017), Experimental investigation on pressure stove with different blends of fuel. *IOSR Journal of mechanical and civil engineering (IOSR-JMCE)*, vol. 14, pp. 61-68.

Panigrahy S., Mishra N.K., Mishra S.C., Muthukumar P., (2016a), Numerical and experimental analyses of LPG (liquefied petroleum gas) combustion in a domestic cooking stove with a porous radiant burner. *Energy*, vol. 95, pp. 404-414.

Panigrahy S., Mishra S.C., (2016b), Analysis of combustion of liquefied petroleum gas in a porous radiant burner. *International Journal of Heat and Mass Transfer*, vol. 95, pp. 488-498.

Pantangi V.K., Karuna Kumar A.S.S.R., Mishra S.C., Sahoo N., (2007), Performance analysis of domestic LPG cooking stoves with porous media. *International Energy Journal*, vol. 8, pp. 139-144.

Pantangi V.K., Mishra S.C., Muthukumar P., Reddy R., (2011), Studies on porous radiant burners for LPG (liquefied petroleum gas) cooking applications. *Energy*, vol. 36, pp. 6074-6080.

Petroleum Planning & Analysis Cell (PPAC), (2019), LPG profile (Data on LPG Marketing), Ministry of Petroleum and Natural Gas, Government of India.

Indian petroleum natural gas statistics, 2017-18, Ministry of Petroleum and Natural Gas, Economic & Statistics Division.

Pradhan P., Mishra P.C., (2018), Performance evaluation of novel surface flame self-aspirated porous radiant burners for cooking applications. *Sadhana*, 43:173.

Sathe S.B., Kulkarni M.R., Peck R.E., Tong T.W., (1991), An experimental and theoretical study of porous radiant burner performance. *Symposium (International) on Combustion*, vol. 23, pp. 1011-1018.

Sharma M., Mishra S.C., Acharjee P., (2009), Thermal efficiency study of conventional kerosene pressure stoves equipped with porous radiant inserts. *International Energy Journal*, vol. 10, pp. 247-254.

Sharma M., Mishra S.C., Mahanta P., (2011), An experimental investigation on efficiency improvement of a conventional kerosene pressure stove. *International Journal of Energy for a Clean Environment*, vol. 12, pp. 79-93.

Sharma M., Mahanta P., Mishra S.C., (2016a), Usability of porous burner in kerosene pressure stove: An experimental investigation aided by energy and exergy analyses. *Energy*, vol. 103, pp. 251-260.

Sharma M., Mishra S.C., Mahanta P., (2016b), Effect of burner configuration and operating parameters on the performance of kerosene pressure stove with submerged porous medium combustion. *Applied Thermal Engineering*, vol. 107, pp. 516-523.

Sinha G.S., (2017), Development and Performance Analysis of Self-Aspirated Porous Radiant Burners for Kerosene Pressure Stove, *Ph.D. Thesis*, Department of Mechanical Engineering, IIT Guwahati.

Sinha G.S., Muthukumar P., (2019), Study of effects of various parameter on thermal efficiency of porous burner with kerosene pressure stove. *IOP Conf. Series: Journal of Physics: Conf. Series*, vol. 1240, p. 012136.

Steen B., (1999), A systematic approach to environmental priority strategies in product development (EPS). Version 2000 – general system characteristics. CPM, Chalmers University of Technology, CPM report.

Steen B., (1999) A systematic approach to environmental priority strategies in product development (EPS). Version 2000 – models and data of the default method. CPM, Chalmers University of Technology, CPM report.

Smith K.R., Uma R., Kishore V.V.N., Zhang J., Joshi V., Khalil M.A.K, (2000), Greenhouse Implications of Household Stoves: An Analysis for India. *Annual Review of Energy and the Environment*, vol. 25, pp. 741-63.

Shiroff S., (2007), Protos the plant-oil cooker: A BOP model for cleaner cooking. *Bosch und Siemens*, Hausgeräte Gruppe.

Singh R.N., (2011), Straight vegetable oil: an alternative fuel for cooking, lighting and irrigation pump. *The IIOAB Journal*, vol. 2, pp. 44–49.

Suhartono, Putri T.A., Fauziah L., (2017a), Performance evaluation of a pressurized cooking stove using vegetable cooking oils as fuel. *International journal on advanced science, engineering and information technology*, vol. 7, pp. 1255-1261.

Suhartono, Suharto, Ahyati A.E., (2017b), The properties of vegetable cooking oil as a fuel and its utilization in a modified pressurized cooking stove. *IOP Conference series: earth and environmental science*, vol. 105, p. 012047.

Shetty D., Sahu D., Kumar R., Bekal S., (2015), Performance and emission characteristics of pongamia oil-kerosene blend used in commercial kerosene stove. *Energy and power*, vol. 5, pp. 19-27.

Stumpf E., Mühlbauer W., (2002), Plant-oil cooking stove for developing countries. *Boiling Point, No 48*, pp. 37-38.

Syamsuri, Suheni, Yustia W.M., (2015), Performance analysis of biogas stoves with variations of flame burner for the capacity of biogas 1 m^3/day. *ARPN Journal of Engineering and Applied Sciences*, vol. 10, pp. 10349-1053.

Takeno T., Sato K., (1979), An excess enthalpy flame theory. *Combustion Science and Technology*, vol. 20, pp. 73-84.

Takeno T., Sato K., Hase K., (1981), A theoretical study on an excess enthalpy flame. *Symposium (International) on Combustion*, vol. 18, pp. 1465-472.

Takeno T., Hase K., (1983), Effects of solid length and heat loss on an excess enthalpy flame. *Combustion Science and Technology*, vol. 31, pp. 207-215.

Takeno T., Murayama M., (1986), One-dimensional flame with extended reaction zone. *Progress in Aerospace Sciences*, vol. 105, pp. 246-262.

Thambi S., Bhatacharya A., Fricko O., (2018), India's Energy and Emissions Outlook: Results from India Energy Model, NITI Ayog, Government of India.

Thumann A., Mehta D.P., (1991), Handbook of energy engineering 1991; 2nd ed. USA: Prentice Hall.

Tumwesige V., Fulford D., Davidson G.C., (2014), Biogas appliances in Sub-Sahara Africa. *Biomass & Bioenergy*, vol. 70, pp. 40-50.

Varun V.S., Pramod B.V.N., Shetty D., (2018), Performance and Emission Characteristics of Commercial Kerosene Stoves using Waste Cooking Oil-Kerosene Blends. *IOP Conference Series: Materials Science and Engineering*, vol. 377, p. 012213.

Venkataraman C., Sagar A.D., Habib G., Lam N., Smith K.R., (2010), The Indian National Initiative for Advanced Biomass Cook stoves: The benefits of clean combustion. *Energy for Sustainable Development*, vol. 14, pp. 63-72.

Viskanta R., (1995), Interaction of combustion and heat transfer in porous inert media. 8th *International Symposium on Transport Phenomena in combustion*, San Francisco.

Vijaykant S., Agrawal A.K., (2007), Liquid fuel combustion within silicon-carbide coated carbon foam. *Experimental Thermal and Fluid Science*, vol. 32, pp. 117-125.

Wagutu A.W., Thoruwa T.F.N., Chhabra S.C., Lang'at-Thoruwa C.C., Mahunnah R.L.A., (2010), Performance of a domestic cooking wick stove using fatty acid methyl esters (FAME) from oil plants in Kenya. *Biomass and bioenergy*, vol. 34, pp. 1250-1256.

Weinberg F.J., (1971), Combustion temperatures: the future?. *Nature*, vol. 233, pp. 239-241.

Woetzel J., Madgavkar A., Gupta R., Manyika J., Ellingrud K., Gupta S., Krishnan M., (2015), The power of parity: Advancing women's equality in India, McKinsey Global Institute.

Wood S., Harris A.T., (2008), Porous burners for lean-burn applications. *Progress in Energy and Combustion Science*, vol. 34, pp. 667-684.

Wua C.Y., Chen K.H., Yang S.Y., (2014), Experimental study of porous metal burners for domestic stove applications. *Energy Conversion and Management*, vol. 77, 380-388.

Yoksenakul W., Jugjai S., (2011), Design and development of a SPMB (self-aspirating, porous medium burner) with a submerged flame. *Energy*, vol. 36, pp. 3092-3100.

Yoshizawa Y., Sasaki K., Echigo R., (1988), Analytical study of the structure of radiation controlled flame. *International Journal of Heat and Mass Transfer*, vol. 31, pp. 311-319.

Zhang T.W., Dornfeld D.A., (2007), Energy Use per Worker-Hour: Evaluating the Contribution of Labor to Manufacturing Energy Use. *14th CIRP International Conference on Life Cycle Engineering*, Tokyo, Japan.

APPENDIX – I

Properties of Fuels

1. LPG (http://www.gasindia.in)

Particulars	Value
Chemical Formula	Propane (C_3H_8) - 60% and Butane (C_4H_{10}) - 40%
Ignition temperature (°C)	488-502
Max. flame temperature (°C)	1985
Higher calorific value (kJ/kg)	49540
Lower calorific value (kJ/kg)	45605.6
Density (kg/m^3)	1.9

2. Biogas

Particulars	Value
Chemical Formula	Methane (CH_4) - 43-56% and Carbon dioxide (CO_2) - 34-38%
Auto ignition temperature (°C)	650
Lower calorific value (kJ/kg)	17000
Density (kg/m^3)	1.2

APPENDIX – II

Life Cycle energy inventory (energy and emission) of LPG

1. *Energy flow diagram for LPG*

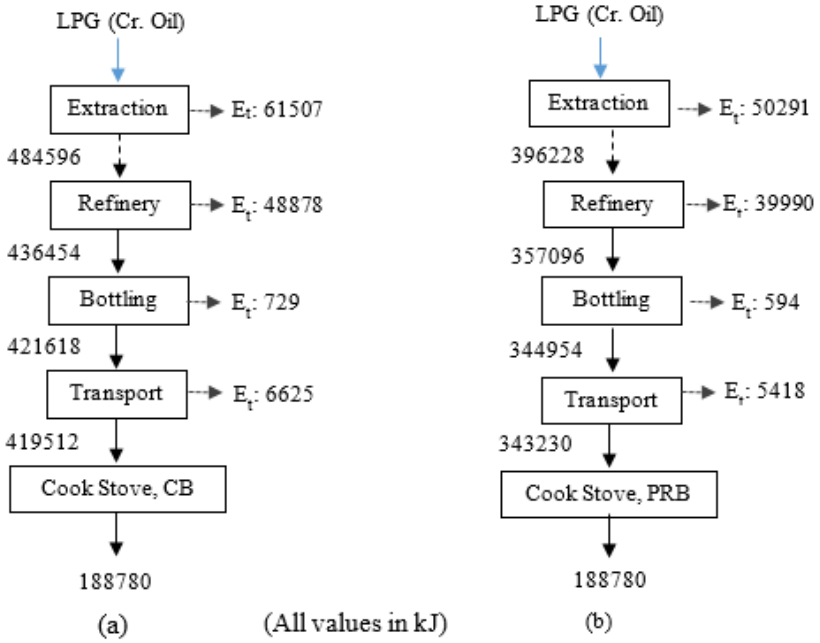

5 kW input power of stove

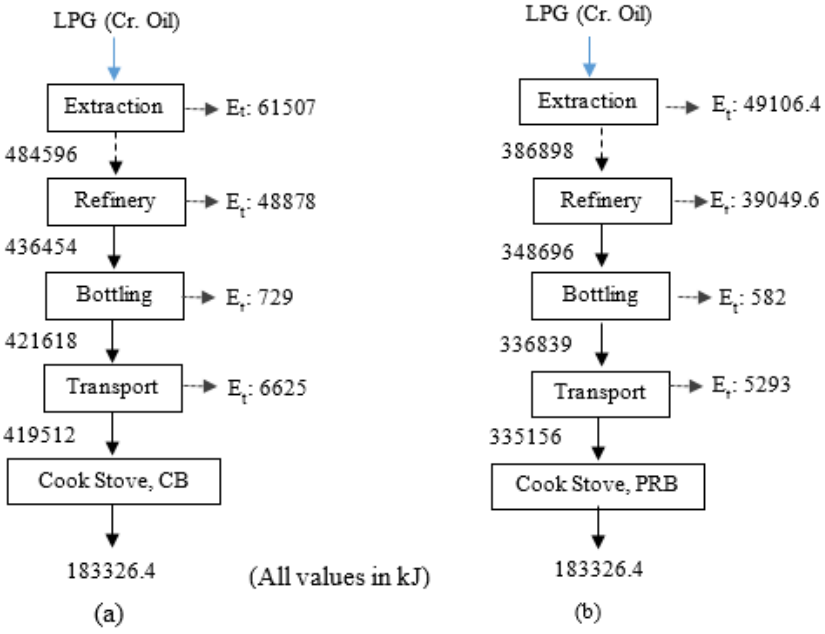

6 kW input power of stove

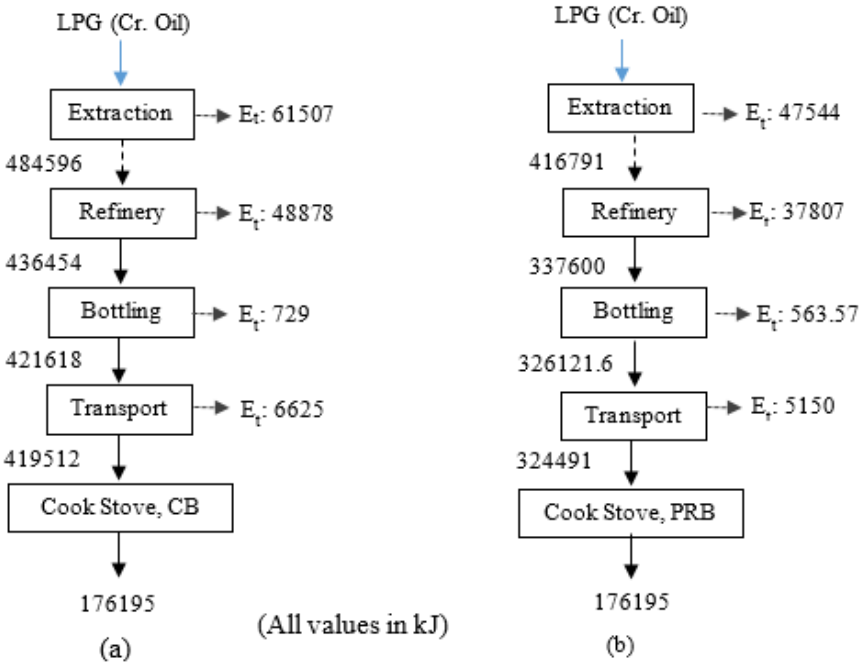

7 kW input power of stove

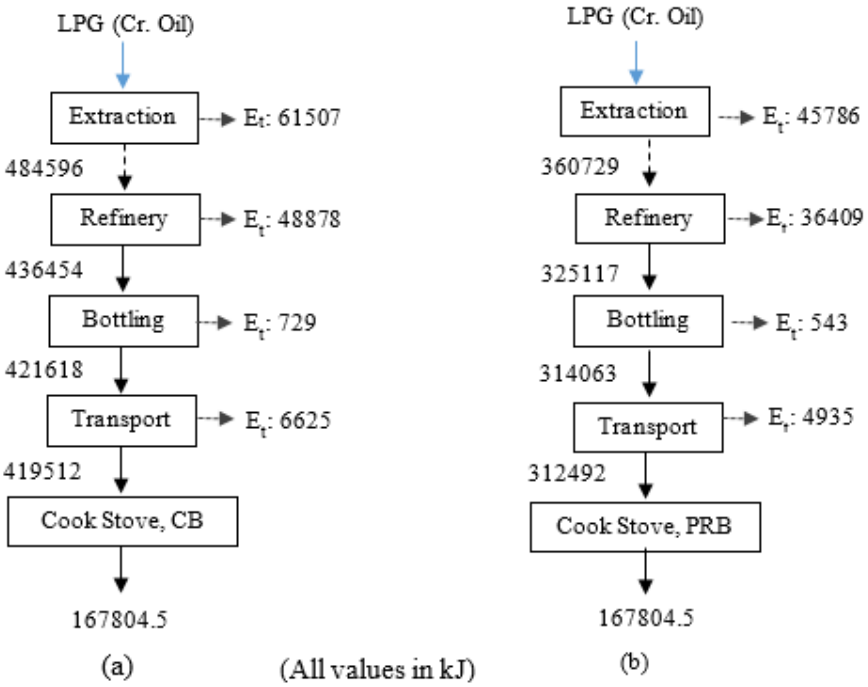

8 kW input power of stove

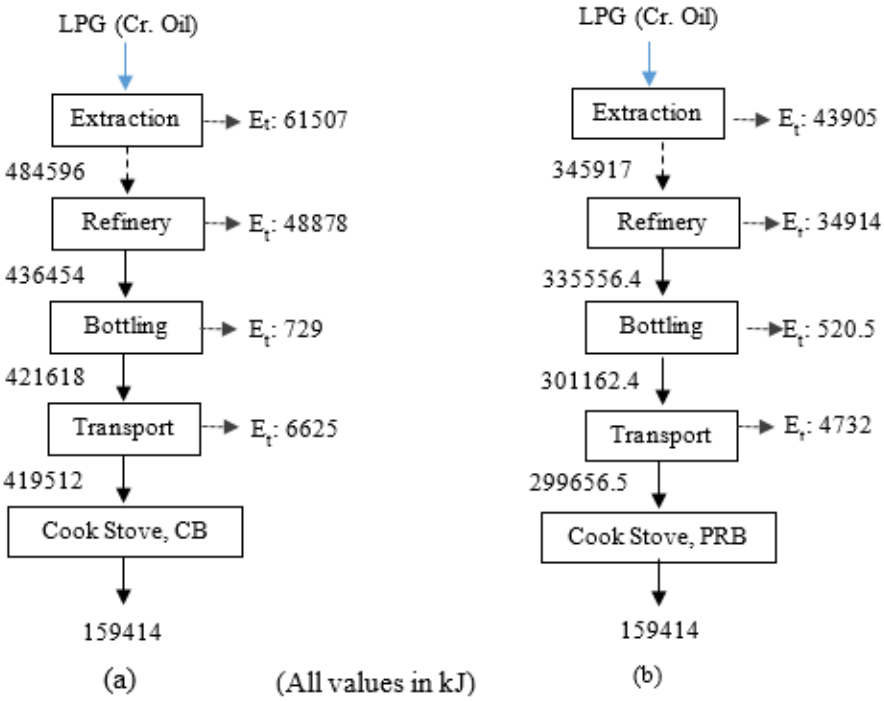

9 kW input power of stove

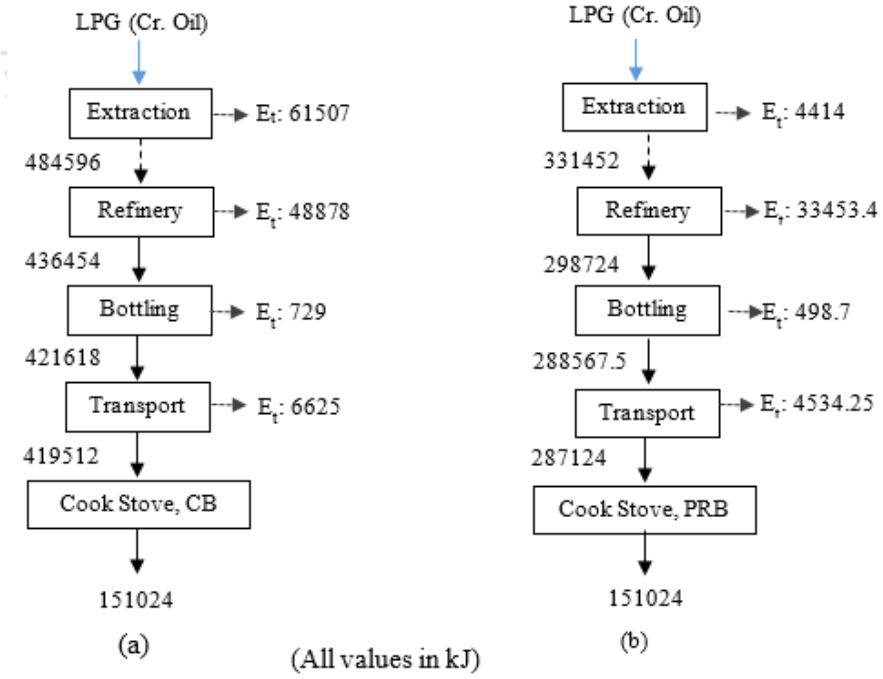

10 kW input power of stove

2. *Distribution of environmental impacts from LPG life cycle*

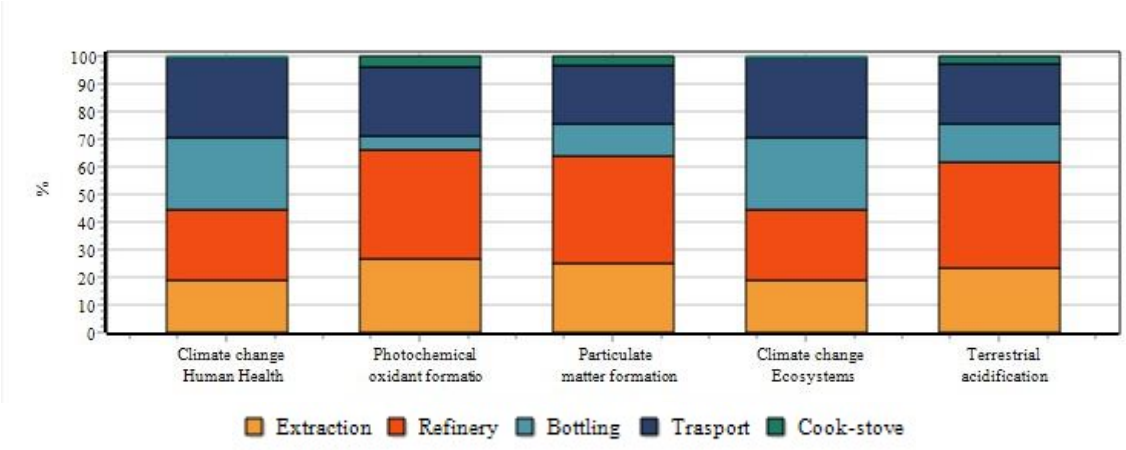

Distribution of environmental impacts from LPG life cycle with CB at 5 kW input operating power

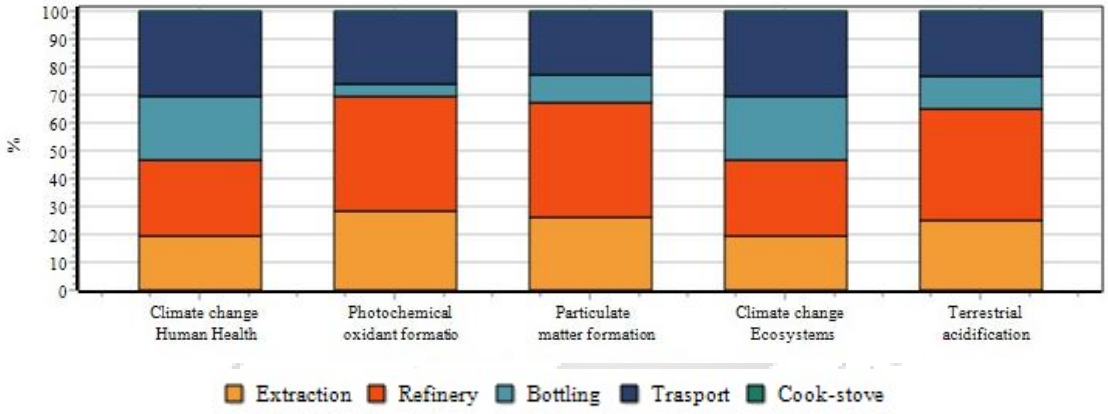

Distribution of environmental impacts from LPG life cycle with PRB at 5 kW input operating power

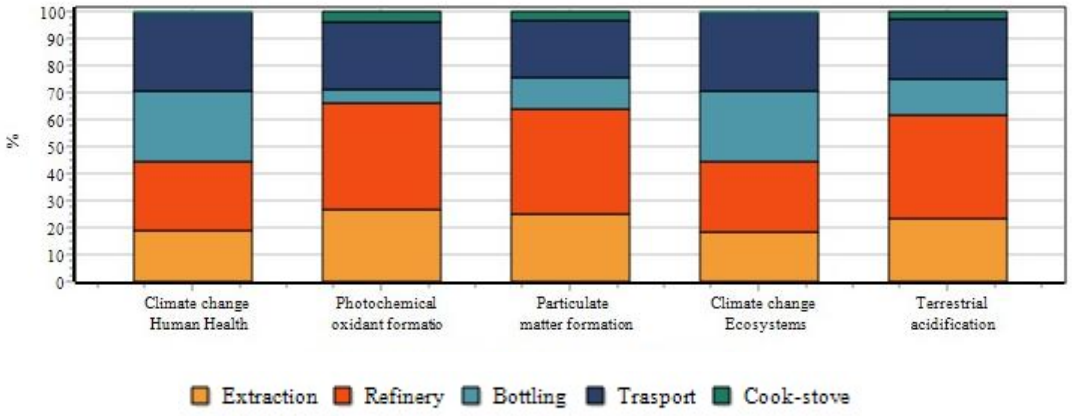

Distribution of environmental impacts from LPG life cycle with CB at 6 kW input operating power

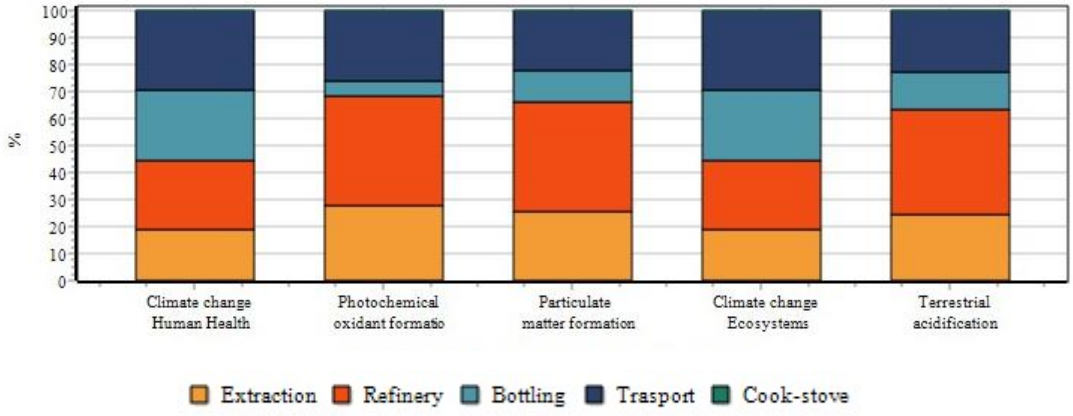

Distribution of environmental impacts from LPG life cycle with PRB at 6 kW input operating power

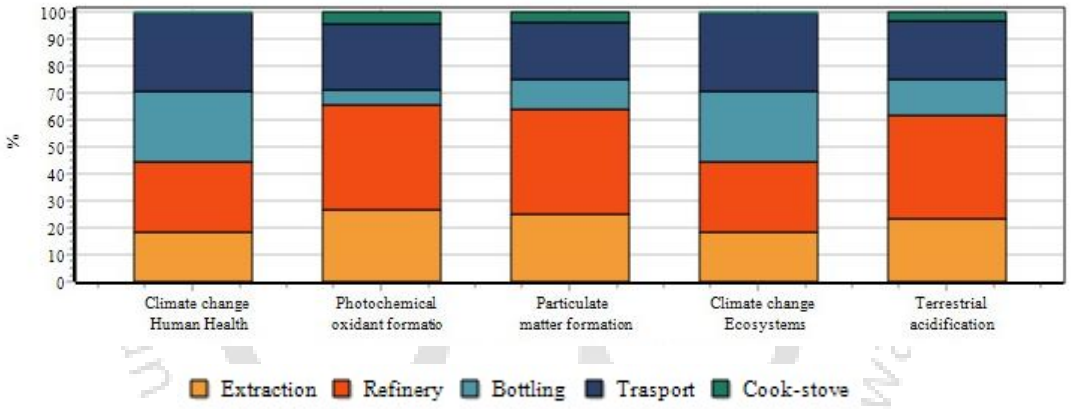

Distribution of environmental impacts from LPG life cycle with CB at 7 kW input operating power

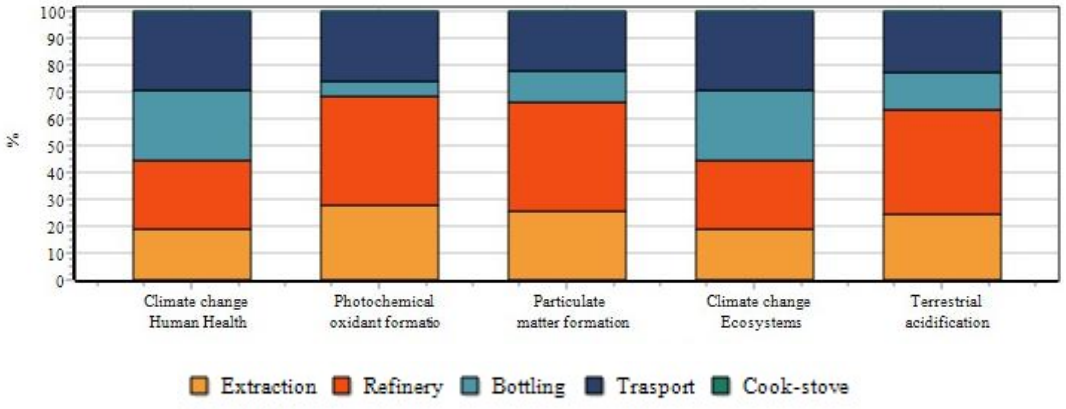

Distribution of environmental impacts from LPG life cycle with PRB at 7 kW input operating power.

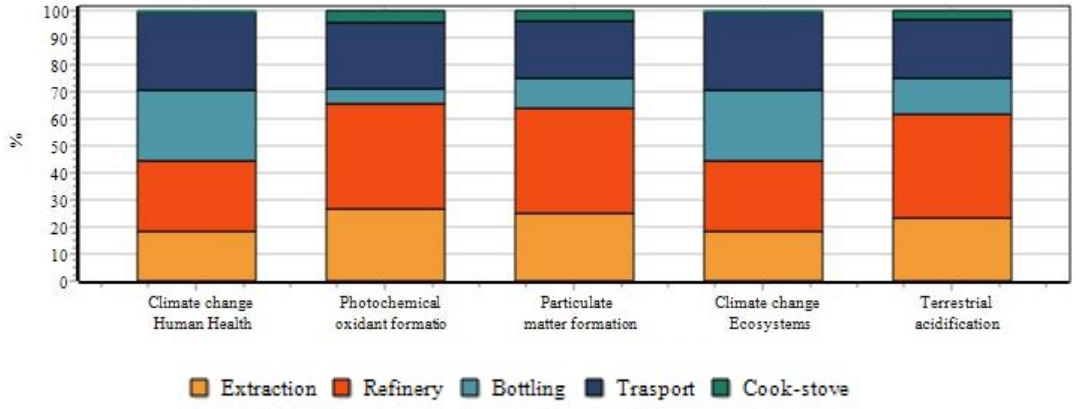

Distribution of environmental impacts from LPG life cycle with CB at 8 kW input operating power

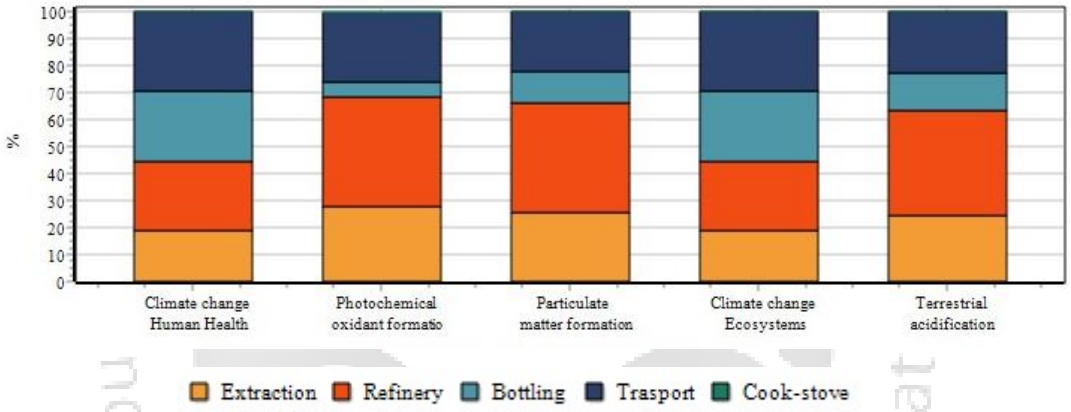

Distribution of environmental impacts from LPG life cycle with PRB at 8 kW input operating power

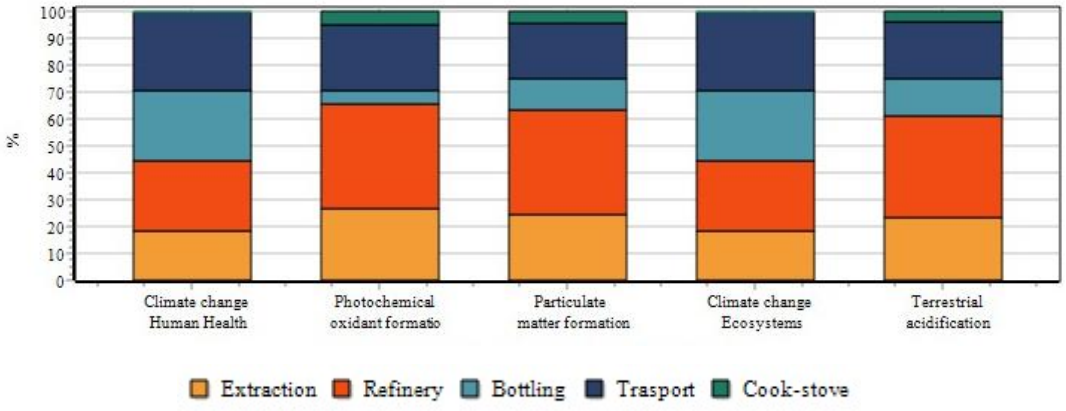

Distribution of environmental impacts from LPG life cycle with CB at 9 kW input operating power

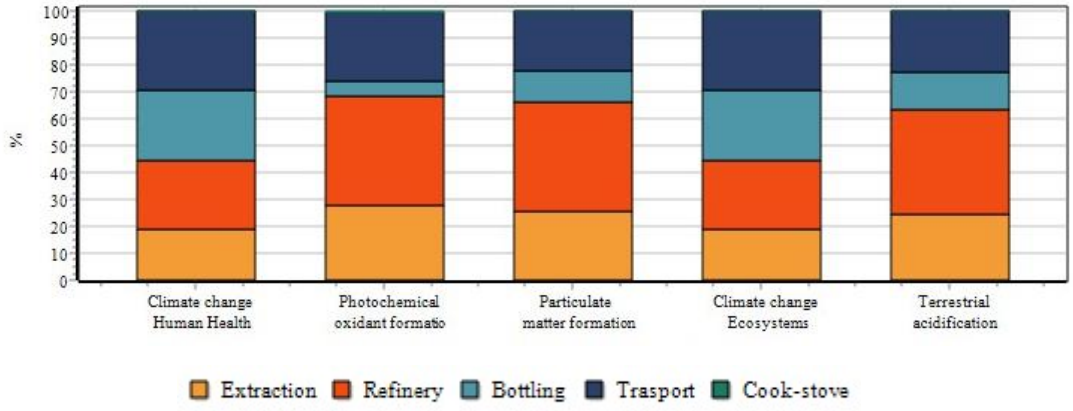

Distribution of environmental impacts from LPG life cycle with PRB at 9 kW input operating power

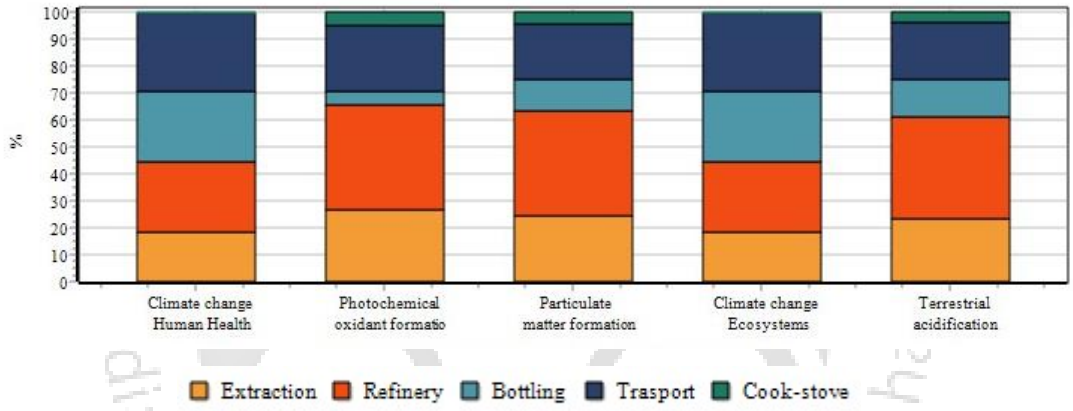

Distribution of environmental impacts from LPG life cycle with CB at 10 kW input operating power

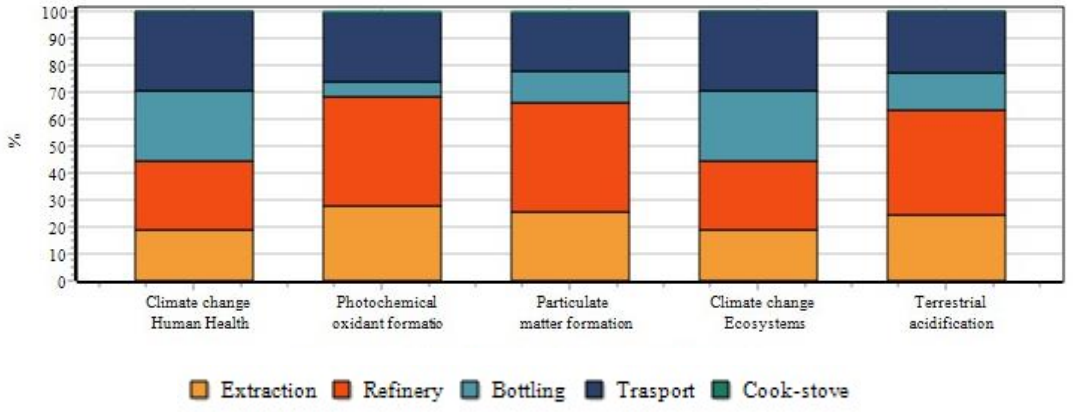

Distribution of environmental impacts from LPG life cycle with PRB at 10 kW input operating power

APPENDIX – III

Uncertainty Analysis

Estimation of uncertainty in the estimated quantities (η_{rad} and η_{th}) have performed according to the procedure described by Klein and McClintock (1953). The expression for error associated with the calculation of η_{rad} (Eq. I) and η_{th} (Eq. II) are given below.

$$\eta_{th} = \frac{(m_p \times C_p + m_w \times C_w) \times (T_2 - T_1)}{m \times LCV_{fuel}} \quad \ldots (I)$$

$$\eta_{rad} = \frac{\varepsilon\sigma(T_{surf}^4 - T_{surr}^4)A_{BS}}{m \times LCV_{fuel}} \quad \ldots. (II)$$

$$\delta\eta_{rad} = \sqrt{(\frac{\delta\eta_{rad}}{\delta T_{surf}}\Delta T_{surf})^2 + (\frac{\delta\eta_{rad}}{\delta T_{surr}}\Delta T_{surr})^2 + (\frac{\delta\eta_{rad}}{\delta A_{BS}}\Delta A_{BS})^2 + (\frac{\delta\eta_{rad}}{\delta m}\Delta m)^2}$$

$$\delta\eta_{rad} = \sqrt{(E_1)^2 + (E_2)^2 + (E_3)^2 + (E_4)^2}$$

$$\delta\eta_{th} = \sqrt{(\frac{\delta\eta_{th}}{\delta m_p}\Delta m_p)^2 + (\frac{\delta\eta_{th}}{\delta m_w}\Delta m_w)^2 + (\frac{\delta\eta_{th}}{\delta(\Delta T)}\Delta(\Delta T))^2 + (\frac{\delta\eta_{th}}{\delta m}\Delta m)^2}$$

$$\delta\eta_{th} = \sqrt{(E_5)^2 + (E_6)^2 + (E_7)^2 + (E_8)^2}$$

The efficiencies have been estimated for various combination of parameters. Maximum uncertainties obtained for the following sets of parameters. The maximum relative uncertainty of radiation efficiency ($\frac{\delta\eta_{rad}}{\eta_{rad}}$) is 2.9% for m = 60 g, T_{surf} = 1032 K, T_{surr} = 300 K and A_{BS} = 0.00348 m^2.

Uncertainty analysis for radiation efficiency (η_{rad})

Surface Temperature (E_1)	Surrounding Temperature (E_2)	Burner surface area (E_3)	Fuel weight (E_4)	$\delta\eta_{rad}$	$\frac{\delta\eta_{rad}}{\eta_{rad}}$
2.61×10^{-4}	6.39×10^{-6}	2.105×10^{-3}	-3.204×10^{-4}	$\pm 2.2\times10^{-3}$	± 2.9%

Similarly, maximum relative uncertainty of thermal efficiency ($\frac{\delta\eta_{th}}{\eta_{th}}$) is 1.26% for m_p = 0.92 kg, m_w = 9.4 kg, ΔT = 62°C, and m = 60 g. Details of the uncertainties are given in the Table below

Uncertainty analysis for thermal efficiency (η_{th})

Pan mass (E_5)	Water mass (E_6)	Boiling water temp. (E_7)	Fuel weight (E_8)	$\delta\eta_{th}$	$\frac{\delta\eta_{th}}{\eta_{th}}$
6.39×10^{-6}	2.985×10^{-5}	4.62×10^{-3}	-1.3776×10^{-3}	$\pm 4.8\times10^{-3}$	± 1.26%

APPENDIX – IV

Details of pan size and mass of water for Water Boiling Test (WBT)

1. Domestic LPG stoves (IS 4246: 2002)

Gas Rate at STP (l/h)	*Pan Diameter (External), mm ±5%*	*Pan Height (External), mm*	*Total Pan Mass with lid, g ±10%*	*Mass of water in pan, kg*
Up to 40	180	100	356	2.0
41-50	205	110	451	2.8
51-60	220	120	519	3.7
61-70	245	130	632	4.8
71-80	260	140	750	6.1
81-95	285	155	853	7.7
96-107	295	165	920	9.4

2. Commercial LPG Burner (IS 14612: 1999)

Gas burning rate, kg/h	*Pan Diameter (External), mm ±5%*	*Pan Height (External), mm*	*Total Pan Mass with lid, g ±10%*	*Mass of water in pan, kg*
1	380	205	2.56	16.5
1.5	420	220	3.07	24.0
2.25	495	265	4.52	37.0
3.5	595	320	8.45	58.0

3. Biogas Stove (IS 8749: 2002)

Gas Rate at STP (l/h)	*Pan Diameter (External), mm ±5%*	*Pan Height (External), mm*	*Total Pan Mass with lid, g ±10%*	*Mass of water in pan, kg*
Up to 240	180	100	356	2.0
246-300	205	110	451	2.8
306-360	220	120	519	3.7
366-420	245	130	632	4.8
426-480	260	140	750	6.1
486-570	285	155	853	7.7
576-692	295	165	920	-
698-810	320	175	1100	-

4. Oil Pressure Stoves (IS 10109: 2002)

Consumption Rate at STP (g/h)	*Pan Diameter (External), mm ±5%*	*Pan Height (External), mm*	*Total Pan Mass with lid, g ±10%*	*Mass of water in pan, kg*
151-180	245	130	632	4.8
181-200	260	140	750	6.1
201-240	285	155	853	7.7
241-270	295	165	920	9.4
271-300	320	175	1.100	11.4
301-330	340	185	1.200	12.5
331-360	350	195	1.310	14.0
361-390	370	200	1.420	16.0
391-420	380	210	1.530	18.0
421-450	400	215	1.640	20.0
451-480	410	225	1.750	22.0
481-510	420	230	1.860	24.0
511-540	435	240	2.000	26.5
541-570	450	245	2.130	29.0
571-600	460	250	2.240	31.0
601-630	470	255	2.320	33.0
631-660	480	260	2.440	35.0
661-700	490	265	2.520	38.0
701-750	500	270	2.650	41.0
751-800	510	275	2.720	44.0
801-850	530	280	3.050	47.0
851-900	540	285	3.190	50.0
901-950	550	290	3.330	53.0
951-1000	560	300	3.480	57.0

APPENDIX – V

Technical Specifications of the Instruments Used in the Experiments

1. Pressure gauge

Make	Warre instruments
Dial size	100 mm
Range	0-2 bar
Readability	0.05 bar
Housing Materials	300 Series SS
Accuracy	±0.05% full scale
Temperature Limits	0 °C to 120 °C

2. Pressure regulators

Make	Norgren
Model	R73G-2GK-RMN
Fluid	Compressed air
Maximum pressure	10 bar

3. Compressor

Make	Ingersoll Rand
Type	Reciprocating
Maximum Pressure	12 kg/cm2
Free air delivery	400-450 lpm
Type	2 stage
Tank capacity	250 liters
Accessories	Precise Pressure regulator, air filter

4. Weighing balance

Make	SARTORIUS COMBICS LITE
Model	CLWP1 – 30ED-I
Capacity	30kg
Platform size	400X300mm
Readability	1g
Power Supply	90 to 260V AC & DC
Indicator	18mm LCD 7 segment backlit

5. Thermocouples

Make	Emerson Process Management Pvt. Ltd.
Type:	metal sheathed K-type
Junction	Grounded
Range	20ºC to 1400 ºC

6. Mass flow meters

Type	Coriolis mass flow meter
Make	Emerson Process Management Pvt. Ltd.
Model	CMF010P323NQB2E222
Flow range	0 to 50 g/min
Flow accuracy	± 0.35% of full scale
Sensitivity	0.001g
Temperature range	-10 to 100 °C
Operating pressure range	0 to 150 bar

7. Portable gas analyzer

Make	Testo
Model	340
O_2	0-25 Vol%
Resolution	0.01 Vol%
Accuracy	±0.2Vol.%
CO	0-10000ppm
Accuracy	±10ppm (0-200 ppm)
Resolution	1 ppm
NO	0-3000 ppm
Accuracy	±5ppm (0-99 ppm)
Resolution	1 ppm
NO_2	0-500ppm
Accuracy	± 10ppm (0-199)
Resolution	0.1 ppm

8. Data Acquisition Unit (DAQ)

Make	Agilent technologies
Model	34970A
Scan rate	60 to 250 channels/second
Scan intervals	0 to 99 hours; 1 ms time step
Accuracy	6 digits of resolution with 0.004%

List of Publications

Patents

1. Muthukumar P, Sinha GS, **Kaushik LK,** Sharma M, Priya NS, Kanagaraj S. Self-Aspirated Pressurized Kerosene Cooking Stove with a Porous Radiant Burner with Nanoparticles blended. ***Application No: 201831003156 (TEMP/E-1/3419/2018-KOL), 2018*.**

Journal Papers

1. **Kaushik LK,** Muthukumar P. Life cycle Assessment (LCA) and Techno-economic Assessment (TEA) of medium scale (5-10 kW) LPG cooking stove with two-layer porous radiant burner. ***Applied Thermal Engineering*, 133 (2018) 316-326.**

2. **Kaushik LK**, Muthukmar P. Performance Assessment of a Porous Radiant Cook Stove Fueled with Blend of Waste Vegetable Oil (WVO) and Kerosene**.** ***Energy Procedia***, 158 (2019) 2391-2396.

3. **Kaushik LK**, Muthukmar P. Thermal and Economic Performance Assessments of Waste Cooking Oil /Kerosene blend Operated Pressure Cook-stove with Porous Radiant Burner, ***Energy*** (Revised manuscript submitted in ***June 2019***)

Conferences

1. **Kaushik LK**, Muthukmar P. Assessment of Energy Saving Potential in Self Aspirated LPG Stove with Porous Radiant Burner. ***ISHMT Digital Library, 2017.***

2. **Kaushik LK**, Deb S, Muthukumar P. Life cycle and techno-economic assessments of domestic and commercial LPG cook-stove with porous radiant burner. ***Proceedings of the International Conference on Sustainable Energy and Environmental Challenges (SEEC)***, pp. 437-440, 2018.

3. **Kaushik LK**, Deb S, Muthukumar P. Energy Saving and Techno-economic Assessment of Self Aspirated Domestic LPG Stove with Porous Radiant Burner**.** ***Int. Conf. Mech., Materials and Renewable Energy***, 377 (2018) 012194.

4. Kaushik LK, Muthukmar P. Experimental Analysis of a Porous Radiant Pressurized Cook Stove Using a Blend of Waste Cooking Oil (WCO) and Kerosene. ***2018 International Conference and Utility Exhibition on Green Energy for Sustainable Development (ICUE), IEEE***, 1-6

5. Kaushik LK, Arun Kumar M, Muthukumar P. Performance Analysis of a Bio-gas operated Porous Radiant Burner for Domestic Cooking Application. ***11th International Exergy, Energy and Environment Symposium (IEEES-11)***, July 14-18, 2019, Chennai, India. (*Selected for Special Issue at Environmental Science and Pollution Research Journal*)

6. Kaushik LK, Sinha GS, Muthukumar P. Assessment of Waste Cooking Oil combustion in a Porous Kerosene Pressure Cook-stove (PKPCs), Accepted for Presentation at ***25th National and 3rd International ISHMT-ASTFE Heat and Mass Transfer Conference (IHMTC-2019)***, December 28-31, 2019, IIT Roorkee, Roorkee, India.